Transcriptomic Approach for the Identification of Genes and Signals Playing a Role in Swarming Motility of *Sinorhizobium meliloti*: Connection with Biofilm Formation and Symbiosis

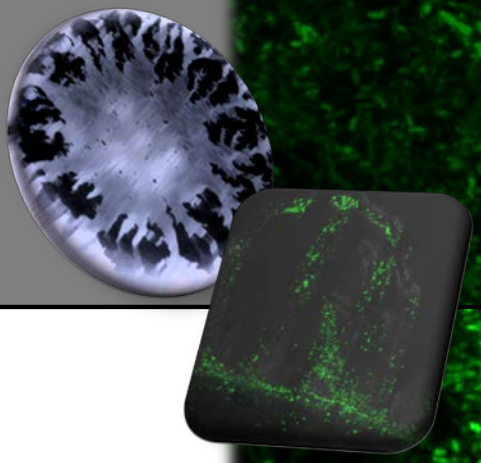

Doctoral Thesis

Carol V. Amaya Gómez

2013

Universidad de Granada
Programa Oficial de Postgrado en Micobiología

Editor: Editorial de la Universidad de Granada
Autor: Carol Viviana Amaya Gómez
D.L.: GR 1921-2013
ISBN: 978-84-9028-605-0

Universidad de Granada

Transcriptomic Approach for the Identification of Genes and Signals Playing a Role in Swarming Motility of *Sinorhizobium meliloti*: Connection with Biofilm Formation and Symbiosis

Carol Viviana Amaya Gómez

Postgrado oficial en Microbiología

Tesis Doctoral 2013

Transcriptomic Approach for the Identification of Genes and Signals Playing a Role in Swarming Motility of *Sinorhizobium meliloti*: Connection with Biofilm Formation and Symbiosis

Aproximación Transcriptómica para la Identificación de Genes y Señales con un Papel en la Motilidad Swarming de *Sinorhizobium meliloti*: Conexión con Formación de Biopelículas y Simbiosis

Memoria de Tesis Doctoral presentada por la licenciada en Microbiología Carol Viviana Amaya Gómez para optar al título de Doctor

Fdo. Carol Viviana Amaya Gómez

VºBº
De la Directora de Tesis

Fdo. Dr. María José Soto Misffut
Dra. en Ciencias Biológicas
Científico Titular del CSIC

María José Soto Misffut, Científico Titular de la Agencia Estatal Consejo Superior de Investigaciones Científicas (CSIC),

Informa:

Que el trabajo de investigación titulado "Transcriptomic Approach for the Identification of Genes and Signals Playing a Role in Swarming Motility of *Sinorhizobium meliloti*: Connection with Biofilm Formation and Symbiosis", ("Aproximación Transcriptómica para la Identificación de Genes y Señales con un Papel en la Motilidad Swarming de *Sinorhizobium meliloti*: Conexión con Formación de Biopelículas y Simbiosis"), realizado por la licenciada Carol Viviana Amaya Gómez bajo mi dirección, se considera ya finalizado y puede ser presentado para su exposición y defensa como Tesis Doctoral en la Universidad de Granada.

Granada, Enero 2013.

Fdo. Dr. María José Soto Misffut

Esta Tesis Doctoral ha sido realizada en el Grupo Interacciones Planta-Bacteria perteneciente al Departamento de Microbiología del Suelo y Sistemas Simbióticos de la Estación Experimental del Zaidín, gracias a una Beca Predoctoral de formación de personal investigador (FPI), adscrita al proyecto de investigación del Plan Nacional Ref. BIO2007-62988, concedida por el Ministerio de Educación y Ciencia.

Parte de los resultados de este trabajo han sido presentados en los siguientes congresos y publicaciones, o están en preparación:

Congresos

Bernabéu-Roda, Lydia M., Amaya-Gómez, Carol-V., Nogales, Joaquina., Escobar-Medina, Antonia., Cuéllar, Virginia., Olivares, José., Soto María J. 2012. Genetic characterization of surface motility in *Sinorhizobium meliloti*. 10th European Nitrogen Fixation Conference. Munich, Alemania.

Nogales, Joquina., Domínguez-Ferreras, Ana., Amaya-Gómez, Carol-V., Cuellar, Virginia., SanJuán, Juan., Olivares, José., Soto, María J. 2010. Transcriptome profiling of a *Sinorhizobium meliloti fadD* mutant reveals the role of rhizobactin 1021 biosynthesis and regulation genes in the control of swarming. 9th European Nitrogen Fixation Conference. Ginebra, Suiza.

Nogales, J., Domínguez-Ferreras, A., Amaya-Gómez, Carol-V., Cuellar, V., San Juán, J., Olivares, J., Soto, MJ. 2010. XIII National Meeting of the Spanish society of Nitrogen Fixation and II Portuguese-Spanish Congress on Nitrogen Fixation. Zaragoza, España.

Nogales, J., Domínguez-Ferreras, A., Amaya-Gómez, Carol-V., Cuellar, V., San Júan, J., Olivares, José., Soto, MJ. 2009. Análisis Transcriptómico del Swarming dependiente del gen *fadD* en *Sinorhizobium meliloti*. III Reunión del Grupo especializado de Microbiología de Plantas. Granada, España

Publicaciones

Nogales,J., Dominguez-Ferreras, A., Amaya-Gómez, C-V., Van Dillewijn,P., Cuellar, V., Sanjuán,J., José Olivares,J. and Soto, MJ. 2010. Transcriptome profiling of a *Sinorhizobium meliloti fadD* mutant reveals the role of rhizobactin 1021 biosynthesis and regulation genes in the control of swarming. BMC Genomics. 11:157.

Carol V Amaya-Gómez [1,2], Ann M. Hirsh[2], and María J. Soto [1]. First evidence for interlinked control of surface motility and biofilm formation in *Sinorhizobium meliloti*. Sometido a Environmental Microbiology.

Carol V Amaya-Gómez[1,2], Lijiang Song [2], Joaquina Nogales[1], Gregory Challis[2] and Soto, María J[1]. Role of siderophore Rhizobactin 1021 (Rhb1021) in *Sinorhizobium meliloti* surface-associated behaviors. En preparación.

La doctoranda Dª Carol Viviana Amaya Gómez y la directora de la tesis Dª María José Soto Misffut, garantizamos al firmar esta tesis doctoral, que el trabajo ha sido realizado por el doctorando bajo la dirección de la directora de la tesis y hasta donde nuestro conocimiento alcanza, en la realización del trabajo, se han respetado los derechos de otros autores a ser citados, cuando se han utilizado sus resultados o publicaciones.

Granada, enero de 2013.

María José Soto Misffut	Carol Viviana Amaya Gómez
Director de la Tesis	Doctorando
Fdo.:	Fdo.:

A Mis padres
y Hermanos.

Símbolos y abreviaturas

ADN	Ácido desoxirribonucleíco
AHLs	Acil homoserina lactonas
Ap	Ampicilina
ARN	Ácido ribunocleíco
BM	Medio Bromfield
Bv	Biovariedad
CAS	Chromo azurol S
cDNA	DNA complementario
CFUs	Unidades formadoras de colonia
CLSM	Microcopia de escaneo láser confocal
cm	Centímetros
COSY	Espectroscopía de correlación
CV	Cristal violeta
di-GMPc	Diguanilato cíclico
DMSO	Dimetilsulfóxido
dNTPs	Desoxinucleótidos trifosfato
EDTA	Ácido etilendiaminotetraacético
EPSs	Exopolisacáridos
Et al.	Y colaboradores
EIC	Cromatograma de iones extraídos
FBN	Fijación biológica de nitrógeno
Fig.	Figura
g	Gramos
GFP	Proteína verde fluorescente
h	Horas
HMBC	Correlación heteronuclear a varios enlaces
HPLC	Cromatografía líquida de alto rendimiento
HR	Respuesta de hipersensibilidad
HRMS	Espectrometría de masas de alta resolución
HSQC	Espectroscopia de coherencia cuántica única heteronuclear
HTDMA	Hexadeciltrimetilamonio
IDM	Medio deficiente en hierro

Kb	Kilobase
Km	Kanamicina
KPS	Polisacáridos capsulares
l	Litros
LC-MS	Cromatografía líquida-espectrometría de masas
LPS	Lipopolisacáridos
M	Molar
Mb	Mega base
mg	Miligramos
min	Minutos
ml	Mililitros
MM	Medio mínimo
mm	Milímetros
mM	Milimolar
mRNA	RNA mensajero
N_2	Nitrógeno molecular
$NADP^+/H$	Nicotinamida adenín dinucleótido fosfato
NF	Factores de Nodulación
ng	Nanogramo
nM	Nanómetro
OD	Densidad óptica
ORF	Marco de lectura abierto
p/v	Peso/volumen
pb	Pares de bases
PBS	Solución de tampón fosfato
PCD	Muerte celular programada
PCR	Reacción de cadena de polimerasa
PVC	Cloruro de polivinilo
pSym	Plásmido simbiótico
QS	Quórum sensing
RDM	*Rhizobium* defined medium
Rhb1021	Rizobactina 1021
Rhbdec	Molécula súper producida por 1021rhbG
rpm	Revoluciones por minuto
seg	Segundos

SDS	Dodecíl sulfato sódico
Sm	Sulfato de estreptomicina
sp	Especie
Sp	Sulfato de espectinomicina
SPI	Isla de patogénesis
TBE	Tampón tris-borato-EDTA
Tc	Tetraciclina
Tris	Tris-hidroximetil-aminometano
TTSS	Sistemas de secreción tipo III
TY	Medio de Triptina y extracto de levadura
V	Voltios
Wt	Silvestre
X-gal	Ácido 5-bromo-4-cloro-3-indol-β-galactósido
X-gluc	Ácido 5-bromo-4-cloro-3-indol-β-D-glucorónido
ºC	Grados centígrados
µg	Microgramos
µl	Microlitros
µm	Micrómetros
µM	Micromolar

Symbols and abbreviations

AHLs	Acyl-homoserine lactones
Ap	Ampicillin
BM	Bromfield media
Bv	Biovar
CAS	Chrome azurol S
cDNA	Complementary DNA
CFUs	Colony forming units
CLSM	Confocal laser scanning microscopy
cm	Centimeters
COSY	Correlation spectroscopy
CV	Crystal violet
DMSO	Dimethyl sulfoxide
DNA	Deoxyribonucleic acid
EDTA	Ethylenediaminetetraacetic acid
EIC	Extracted ion chromatogram
EPSs	Exopolysaccharides
Et al.	And co-workers
Fig.	Figure
g	Grams
GFP	Green fluorescent protein
h	Hours
HMBC	Heteronuclear multiple bond correlation
HPLC	High-performance liquid chromatography
HRMS	High Resolution Mass Spectrometry
HSQC	Heteronuclear single quantum coherence spectroscopy
HTDMA	Hexadecyltrimethylammonium
IDM	Iron-deficient media
Kb	Kilobase
Km	Kanamyicin
KPS	Capsular polysaccharides
l	Liters
LC-MS	Liquid Chromatography- Mass Spectrometry
LPS	Lipopolysaccharides
M	Molar

Mb	Megabase
mg	Milligrams
min	Minutes
ml	Milliliters
MM	Minimal media
mm	Millimeters
mM	Millimolar
mRNA	Messenger RNA
N_2	Molecular nitrogen
$NADP^+/H$	Nicotinamide adenine dinucleotide phosphate
NF	Nodulation Factor
ng	Nanogram
nM	Nanometres
OD	Optical density
ORF	Open reading frame
pb	Base pairs
PBS	Phosphate buffer solution
PCD	Program cell death
PCR	Polymerase chain reaction
PVC	Polyvinyl chloride
pSym	Symbiotic plasmid
QS	Quorum sensing
RDM	*Rhizobium* defined medium
Rhb1021	Rhizobactin 1021
Rhbdec	1021rhbG overproduced molecule
RNA	Ribonucleic acid
rpm	Revolutions per minute
SDS	Sodium dodecyl sulfate
seg	Seconds
Sm	Streptomycin Sulfate
sp	Species
Sp	Spectinomycin sulfate
SPI	pathogenesis island
TBE	Tris-borate-EDTA buffer
Tc	Tetracycline

Tris	Tris(hydroxymethyl)aminomethane
TTSS	Type III secretion systems
TY	Triptone-yeast extract medium
V	Volts
Wt	Wild type
X-gal	5-bromo-4-chloro-3-indolyl-β-galactoside acid
X-gluc	5-bromo-4-chloro-3-indolyl-β-D-glucuronide acid
ºC	Celsius degrees
µg	Micrograms
µl	Microliters
µm	Micrometers
µM	Micromoles

Tabla de Contenidos /Contents

Resumen

Las bacterias del suelo conocidas como *Rhizobium* establecen simbiosis mutualista con plantas leguminosas. El éxito de la asociación depende de los mecanismos que *Rhizobium* utiliza para colonizar, invadir y establecer la infección crónica en su hospedador. Swarming y formación de biopelículas son dos fenómenos multicelulares ligados a superficie que han sido relacionados con la capacidad infectiva e invasiva de bacterias patógenas. El swarming es un tipo de translocación bacteriana que conlleva un proceso de diferenciación celular y que se caracteriza por el movimiento rápido y coordinado de toda una población sobre una superficie semisólida. Las biopelículas son comunidades de células bacterianas embebidas en una matriz de polisacáridos, adheridas entre sí y a una superficie. Los escasos estudios que se han realizado sobre estos dos fenómenos en bacterias beneficiosas como *Rhizobium* sugieren que al igual que en bacterias patógenas, componentes esenciales en motilidad swarming y/o formación de biopelículas, o factores que se expresan durante estos procesos, pueden ser importantes en la interacción con su hospedador. Se sabe que en *Sinorhizobium meliloti*, el endosimbionte de alfalfa, una mutación en el gen *fadD* que codifica una acil-CoA sintetasa específica de ácidos grasos de cadena larga promueve la motilidad swarming. El mutante en *fadD* además de presentar swarming condicional se encuentra afectado en sus propiedades simbióticas, siendo menos infectivo y competitivo por la nodulación que la cepa silvestre GR4 (Soto et al., 2002). Estos resultados sugieren que en *S. meliloti* componentes implicados en este tipo de motilidad también podrían determinar su capacidad infectiva. Con el objetivo de identificar nuevos genes bacterianos que puedan tener un papel en la interacción con la planta, hemos abordado la identificación de determinantes genéticos implicados en el swarming de la bacteria modelo *S. meliloti* mediante aproximación transcriptómica. Algunos de los genes así identificados se han sometido a una investigación más profunda, analizando su papel en la formación de biopelículas y en el establecimiento de simbiosis con plantas de alfalfa.

Como primer acercamiento a la identificación de los mecanismos moleculares propios del swarming en *Rhizobium*, en el capítulo 1 de este

trabajo se realizó un análisis transcriptómico en el que se comparó la expresión génica global del mutante en el gen *fadD* de *S. meliloti* Rm1021 crecido en condiciones inductoras de swarming (medio mínimo (MM) semisólido), con la mostrada tras crecimiento en condiciones no inductoras (MM líquido y MM sólido). Este análisis trascriptómico reveló que la expresión génica de células que crecen sobre una superficie es muy distinta de aquéllas que crecen en un medio líquido. Se observó la expresión diferencial de más de mil genes, entre ellos, genes implicados en metabolismo del carbono, proteínas y energía, genes relacionados con la síntesis de macromoléculas, genes de motilidad y quimiotaxis, genes relacionados con la captación y metabolismo del hierro, y genes relacionados con respuesta a estrés. Estos resultados han evidenciado que el crecimiento sobre una superficie desencadena grandes cambios en la fisiología celular de *S. meliloti*. Adicionalmente se observó que el crecimiento en condiciones específicas de swarming provoca la inducción de genes relacionados con la captación y metabolismo de hierro. Se ha demostrado que los niveles de hierro presentes en el medio, el plásmido simbiótico pSymA y concretamente, los genes implicados en la biosíntesis del sideróforo rizobactina 1021 (Rhb1021) desempeñan un papel clave en el control de la motilidad swarming de *S. meliloti* Rm1021 pero no en el mutante *fadD*. La presencia en el medio de altas concentraciones de hierro inhibe la motilidad swarming de la cepa silvestre Rm1021 pero no la de un mutante en el regulador global de respuesta a hierro RirA ni la del mutante en *fadD*. Estos resultados forman parte de una publicación aparecida en el año 2010 en la revista BMC Genomics (Nogales et al., 2010).

Estudios realizados en diversas bacterias han revelado que la motilidad swarming y la formación de biopelículas son fenómenos multicelulares estrechamente relacionados. En bacterias como *Pseudomonas aeruginosa*, estos comportamientos sociales parecen estar inversamente regulados por una ruta genética común (Caiazza et al., 2007). Se ha descrito la capacidad de *S. meliloti* de formar biopelículas tanto en superficies bióticas como abióticas, identificándose factores como los flagelos, el EPS II o el componente oligosacarídico del factor Nod, que desempeñan un papel importante en este proceso (Fujishige et al., 2006; Fujishige et al., 2008; Rinaudi and González, 2009). Con objeto de identificar una posible conexión de este fenómeno con la motilidad swarming, en el capítulo 2 decidimos analizar la capacidad de

formación de biopelículas de cepas de *S. meliloti* con distinto comportamiento en cuanto a motilidad en superficie. Existen evidencias que demuestran que la regulación del swarming en la cepa de referencia Rm1021 y en la cepa GR4 aislada de suelos de Granada, ocurre de manera diferente. Aunque una mutación en el gen *fadD* promueve motilidad en superficie en ambas cepas, condiciones inductoras del swarming en Rm1021 no permiten el movimiento en superficie de la cepa GR4 (Nogales et al., 2010; Soto et al., 2002). Por ello, se ha analizado la capacidad de formación de biopelículas de estas dos cepas silvestres Rm1021 y GR4, así como de sus correspondientes mutantes *fadD*. Adicionalmente se ha evaluado el fenotipo de formación de biopelículas de dos mutantes derivados de Rm1021 con alteraciones en motilidad en superficie: un mutante *rirA* que produce el sideróforo Rhb1021 de manera constitutiva y muestra swarming incluso en altas concentraciones de Fe en el medio, y un mutante *rhbA* deficiente en la síntesis de Rhb1021 e incapaz de desplazarse en superficie. Por otra parte, dada la participación del hierro como señal reguladora del swarming de Rm1021, se ha estudiado la importancia de la concentración de este compuesto en el establecimiento de biopelículas. La capacidad de formación de biopelículas de las distintas cepas se ha evaluado haciendo uso de superficies abióticas como cloruro de polivinilo (PVC) y vidrio, y bióticas, concretamente la superficie de raíces de alfalfa. La cepa GR4 ha manifestado una mayor capacidad de formación de biopelículas que Rm1021 en superficie de vidrio y en raíces de alfalfa, no detectándose diferencias en PVC, superficie sobre la que *S. meliloti*,en general, es bastante ineficiente formando biopelículas. Hemos comprobado que los niveles de hierro en el medio afectan a la estructura de la biopelícula formada por cepas silvestres de *S. meliloti*: mientras bajas concentraciones de hierro llevaron a la formación de biopelículas de estructura homogénea o plana, la presencia de altas concentraciones de dicho compuesto indujo la formación de biopelículas más estructuradas con torres y valles, tanto en Rm1021 como en GR4. Independientemente de la concentración de hierro en el medio y de la superficie evaluada, los mutantes en *fadD*, *rhbA* o *rirA* mostraron un fenotipo alterado en formación de biopelículas con respecto a su cepa parental. FadD, RirA y la concentración de hierro en el medio parecen regular de manera inversa swarming y formación de biopelículas. En conjunto estos resultados han puesto de manifiesto que genes y señales (Fe en el medio) que participan en el control del swarming también juegan un papel esencial en la formación

de biopelículas de *S. meliloti*. Además mutantes en dichos genes mostraron ser menos efectivos en la colonización de raíces de alfalfa, lo que sugiere que la identificación de factores determinantes del swarming puede ser utilizada como estrategia alternativa en la identificación de genes bacterianos importantes en la colonización de las plantas.

Mutaciones en los genes *rhb,* abolen la producción de Rhb1021 y el desplazamiento en superficie en *S. meliloti* Rm1021 (Nogales et al., 2012; Nogales et al., 2010). Por otra parte se ha observado que un mutante en *rhbA* es incapaz de formar biopelículas gruesas. Estos resultados sugieren que la producción de Rhb1021 es clave para la motilidad en superficie y la formación de biopelículas de *S. meliloti* Rm1021. En el capítulo 3 de este trabajo, hemos abordado el estudio de las posibles funciones que la Rhb1021 puede desempeñar en ambos procesos. Para ello, se ha llevado a cabo el aislamiento de rizobactina 1021 desde el sobrenadante del mutante *rirA* que presenta una producción desregulada del sideróforo. El ensayo de colapso de gota efectuado con Rhb1021 purificada, evidenció que este sideróforo presenta actividad surfactante, la cual, puede tener un impacto tanto en motilidad en superficie como en formación de biopelículas. Con el propósito de confirmar que el papel de Rhb1021 en los dos fenotipos asociados a superficie se encontraba ligado a la actividad surfactante de la molécula, se obtuvieron y caracterizaron 2 mutantes afectados en dos genes (*rhbD* y *rhbG*) que según predicciones *in silico* prodrían estar implicados en la incorporación del ác. graso que forma parte de la estructura de Rhb1021 y que le confiere propiedades anfifílicas. El mutante *rhbD* resultó ser incapaz de producir sideróforo y su comportamiento en superficie (motilidad y formación de biofilm) fue similar al de un mutante *rhbA*. Nuestros resultados encajan con la función asignada por otros autores a RhbD. Por el contrario, los datos derivados de la caracterización del mutante *rhbG* claramente demuestran que contrariamente a lo propuesto por otros autores Lynch et al. (2001) y (Challis, 2005), *SMa2339* (*rhbG*) no es responsable de incorporar el radical de ác. graso a la molécula de Rhb1021, y por el momento, su función sigue siendo desconocida. Además, a diferencia de los demás genes que pertenecen al operón *rhbA-F*, *rhbG* no es esencial para la síntesis del sideróforo ni para la motilidad en superficie de *S. meliloti,* aunque interviene en los comportamientos asociados a superficie de la bacteria. La pérdida de función de *rhbG* promueve motilidad en superficie independiente de

flagelos e interfiere en el normal desarrollo de biopelículas, mostrando un patrón similar al de mutantes en *rhbA* o *rhbD*. Mediante análisis de cromatografía líquida y espectrofotometría de masas del sobrenadante de *rhbG*, hemos observado que esta mutación lleva a la acumulación de (2E)-N-[3-(acetilamino)propil]-N-hidroxidec-2-enamida y a un descenso en la producción del sideróforo Rhb1021. Finalmente, mediante aproximación transcriptómica, hemos investigado la posible función de Rhb1021 como molécula señal, comparando la expresión génica global de células de 1021rhbD con la de células de Rm1021 crecidas en medio semisólido. Si bien no se detectaron grandes cambios en expresión génica, este análisis desveló que bien la Rhb1021 o alguno de sus intermediarios son necesarios para activar la transcripción de los genes *rhb* y *rhtA*.

Como último objetivo de este trabajo de investigación, se ha estudiado qué influencia tienen en el establecimiento de la simbiosis, los distintos genes identificados en este trabajo que participan en el control de la motilidad en superficie y capacidad de formación de biopelículas de *S. meliloti*: genes *rhb, rhtA*, y *rirA* (Capítulo 4). Aunque está descrito que ninguno de ellos es esencial para el desarrollo de nódulos fijadores de N (Chao et al., 2005; Lynch et al., 2001; Viguier et al., 2005), su participación en fenómenos multicelulares asociados a superficie, podría ser indicativo de su función en etapas tempranas de la interacción con la planta. El análisis de la capacidad de adhesión del mutante en *rhtA* ha permitido observar que este mutante tiene un fenotipo similar al descrito para el mutante en biosíntesis del sideróforo *rhbA* y el mutante en *rirA* en el capítulo 2*,* mostrándose incapaz de adherirse tan eficientemente a las raíces de alfalfa como la cepa silvestre. El estudio de la capacidad infectiva y competitiva de estas cepas ha permitido observar que éstas manifiestan alteraciones en su fenotipo simbiótico. Estos defectos fueron más evidentes en las cepas que muestran un fenotipo de motilidad en superficie incrementado (*rhtA* y *rirA*) que en aquéllas que están impedidas en el desplazamiento en superficie (*rhbA*). Curiosamente, el mutante *rirA* ha presentado severos defectos en infectividad (retraso y reducción número de nódulos), competitividad e incluso en la capacidad de fijación de nitrógeno.

Los resultados obtenidos en este trabajo de Tesis Doctoral validan la estrategia consistente en caracterizar las bases moleculares que rigen el

movimiento en superficie de *S. meliloti* para la identificación de nuevos genes bacterianos importantes en la colonización de plantas.

Introducción General

1. Motilidad bacteriana

La persistencia de las bacterias en el medio natural a lo largo de la evolución ha dependido de cómo éstas han logrado llevar a cabo la regulación de los mecanismos adaptativos que les permiten lidiar con los cambios constantes en disponibilidad de nutrientes y estreses tanto químicos como físicos. Como parte de esta evolución, las bacterias han desarrollado la capacidad de quimiotaxis y movimiento. La capacidad de moverse confiere a las bacterias numerosas ventajas entre las que se encuentran: mayor eficiencia en adquisición de nutrientes, poder evitar el efecto de sustancias tóxicas, acceder a mejores nichos, o facilitar la dispersión bacteriana en el medio ambiente. Los flagelos y pili tipo IV son las estrucutras bacterianas responsables de la capacidad de translocación de estos organismos, siendo estos últimos los mejor estudiados. El flagelo es un filamento largo (10-15 micras) y delgado (14 nm de diámetro) en el que se distinguen 3 estructuras fundamentales: i) cuerpo basal que ancla el flagelo a la envoltura de la bacteria y que contiene el motor que provocará la rotación del flagelo, ii) gancho, codo o articulación, un cilindro curvado y flexible que transfomará el movimiento de rotación en ondas, y iii) el filamento, un tubo hueco constituido por hasta 20.000 subunidades de una proteína mayoritaria denominada flagelina (Fig. 1). La detección de estímulos y el control sobre el movimiento de los flagelos puede ser crucial para la supervivencia bacteriana. No obstante, el coste energético que implica la síntesis y ensamblaje de flagelos es muy alto (2-3% de la energía total de la que dispone la célula) y por ello estos procesos están bajo un estricto control de regulación génica.

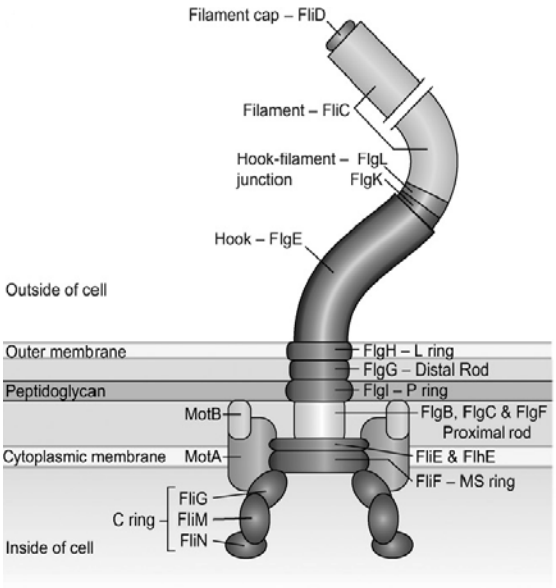

Figura 1. Componentes de un flagelo. Figura tomada de Copeland and Weibel (2009)

En enterobacterias, más de 50 genes están implicados en el ensamblaje de flagelos, motilidad y quimiotaxis. Estos genes a cuyo conjunto se conoce como regulón flagelar están distribuidos en el genoma en cuatro regiones separadas. La biosíntesis de los flagelos es un proceso muy complejo que requiere la regulación coordinada y temporal de decenas de genes a través de un control transcripcional de tipo jerárquico (Smith and Hoover, 2009). La regulación temporal de los genes flagelares pretende asegurar que los componentes estructurales del flagelo se vayan sintetizando a medida que se vayan necesitando. En el ensamblaje del flagelo primero ha de generarse el cuerpo basal, seguido del gancho y finalmente el filamento. La expresión secuencial de los genes del regulón flagelar se consigue mediante una cascada reguladora que controla la expresión de varios grupos de genes flagelares. Esta cascada además responde a determinados puntos de chequeo en la biosíntesis del flagelo de forma que se coordina la expresión génica con el proceso de ensamblaje. De acuerdo al orden secuencial de su expresión los genes del regulón flagelar de enterobacterias se distribuyen en 3 clases. La clase I se compone de los genes *flhD* y *flhC*, que se transcriben como un operón bicistrónico y que codifican las subunidades del activador transcripcional global $FlhD_4C_2$ que regula la expresión de los genes de la clase II. Entre los genes de la clase II se incluyen los genes que codifican proteínas del cuerpo basal del flagelo, componentes de un sistema de secreción tipo III (TTSS) específico para flagelina, proteínas del gancho flagelar, así como las proteínas reguladoras FliA y FlgM. FliA codifica el factor σ^{28} necesario para la transcripción de los genes de la clase III, mientras FliM codifica un factor anti-sigma. La última clase está constituida por los genes que codifican la flagelina *(fliC)*, motor del flagelo (*mot*) y genes de quimiotaxis (*che*) (Patrick and Kearns, 2012).

Dependiendo de las propiedades hidrofílicas del medio se ha descrito que las bacterias pueden emplear al menos cinco tipos distintos de motilidad (Henrichsen, 1972). En medios líquidos las bacterias emplean la motilidad tipo swimming, y sobre superficies pueden moverse por medio de swarming, sliding, twitching o gliding (Fig. 2). El swimming es un movimiento dependiente de flagelos que se caracteriza por un patrón de movimiento bacteriano desorganizado, y se da en medios acuosos y en superficies con una capa densa de

fluido sobre ella. Gliding es un tipo de motilidad bacteriana muy estudiado en mixobacterias que no requiere la presencia de flagelos o pili pero implica componentes de adhesión focal. Estos componentes anclan la bacteria al substrato y posiblemente actúan como motor. El twitching es un tipo de motilidad sobre superficies presentado por células individuales que tiene lugar como consecuencia de la extensión y retracción de pili tipo IV. El swarming es un tipo de translocación bacteriana dependiente de flagelos y se caracteriza por el movimiento rápido y coordinado de toda una población sobre una superficie. El sliding, a diferencia del swarming, es un movimiento independiente de flagelos que se produce por las fuerzas de expansión de una colonia en crecimiento en combinación con la reducción de tensiones superficiales por la excreción de agentes surfactantes (Henrichsen, 1972; Kearns, 2010).

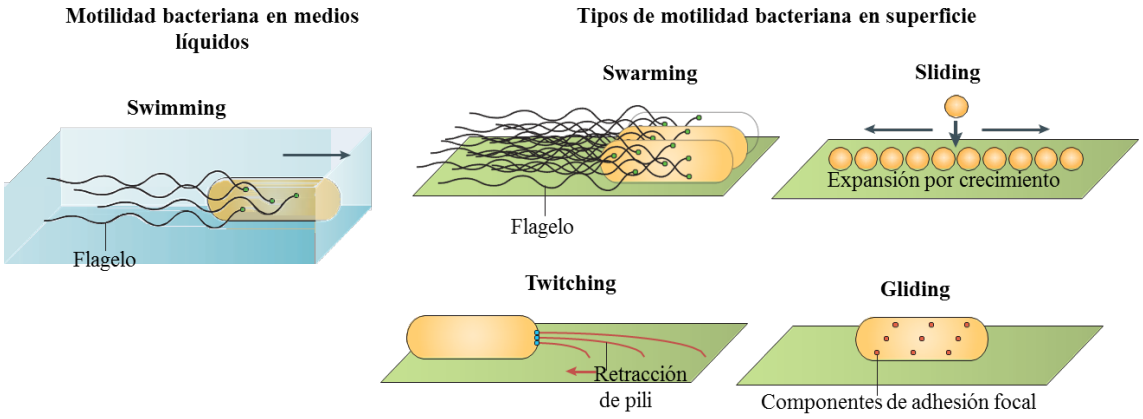

Figura 2. Tipos de motilidad bacteriana. Figura adaptada de Kearns (2010).

2. Generalidades del swarming

El swarming es un tipo de translocación bacteriana caracterizada por el movimiento rápido y coordinado de toda una población sobre una superficie e impulsado por la rotación flagelar (Henrichsen, 1972; Kearns, 2010). Este tipo de motilidad conlleva generalmente la diferenciación a una célula alargada e hiperflagelada "célula swarmer", es dependiente de flagelos, se da en presencia de una capa delgada de fluido sobre la superficie y suele requerir la producción de compuestos surfactantes. Son estímulos críticos la densidad celular, el contacto

con la superficie y señales fisiológicas, además del alineamiento celular y la producción de factores de migración, los que facilitan la translocación de la población bacteriana. Muchos géneros flagelados típicamente hacen swarming como por ejemplo: *Proteus*, *Vibrio*, *Bacillus y Clostridium* y con un comportamiento menos contundente se observa en *Serratia, Salmonella, Rhizobium, Sinorhizobium, Escherichia, Rhodospirillum*, *Azospirillum*, *Aeromonas*, y *Yersinia* (Allison et al., 1994; Bernier et al., 2011; Fraser and Hughes, 1999; Kearns, 2010).

Las células bacterianas son capaces de producir y detectar señales moleculares, permitiendo a toda una población iniciar una acción concertada una vez se ha alcanzado una concentración crítica (lo que corresponde con una densidad poblacional particular). Este fenómeno es conocido como Quorum Sensing (QS). En bacterias Gram negativas, las moléculas señales de quórum más frecuentemente utilizadas son las N-acil homoserina lactonas (AHLs). La densidad celular es crucial para que se inicie y se mantenga la motilidad tipo swarming. Se ha descrito que las señales QS están involucradas en la producción de biosurfactantes (agentes que reducen la tensión superficial) y diferenciación a célula "swarmer" (Daniels et al., 2004). Los trabajos que existen sobre el papel de estas señales en swarming demuestran que en cada bacteria actúan de diferente manera y que pueden cumplir otras funciones (Verstraeten et al., 2008). Se ha visto, por ejemplo, que el control por QS sobre el swarming de *Pseudomonas aeruginosa* está condicionado por los nutrientes presentes en el medio (Shrout et al., 2006). Mutantes de esta bacteria defectuosos en QS son incapaces de presentar swarming cuando crecen sobre la superficie de un medio de agar cuya fuente de carbono es succinato; sin embargo, cuando el medio contiene glutamato, estos mutantes no muestran defectos en este tipo de motilidad. En *Rhizobium etli* las AHLs que contienen en su estructura un ácido graso de cadena larga cumplen una función doble, actúan como moléculas de QS y además actúan como agentes surfactantes (Daniels et al., 2006).

2.1. Diferenciación celular asociada al swarming

Se sabe que entre las especies bacterianas existe cierta versatilidad en cuanto al número de flagelos, su localización y su organización. La razón de estas variaciones aún se desconoce. Se ha descrito que el tamaño de las células "swarmer" y número de flagelos suele ser diferente entre las especies de bacterias en las que ha descrito este tipo de motilidad.

Las células "swarmer" de microorganismos como *Proteus mirabilis y Vibrio parahaemolyticus*, se caracterizan por ser elongadas y presentar un aumento en el número de flagelos (Fig 3). Las células "swarmer" de *B. subtilis* no exhiben cambios en el tamaño de la célula, y sin embargo el número de flagelos se ve incrementado (Fig. 3). Por el contrario en algunas especies, no existe ni elongación, ni hiperflagelación de las células "swarmer". Takahashi et al. (2008) demostraron que las células "swarmer" de *P. aeruginosa* PAO1 presentan el tamaño de una célula normal y no son hiperflageladas.

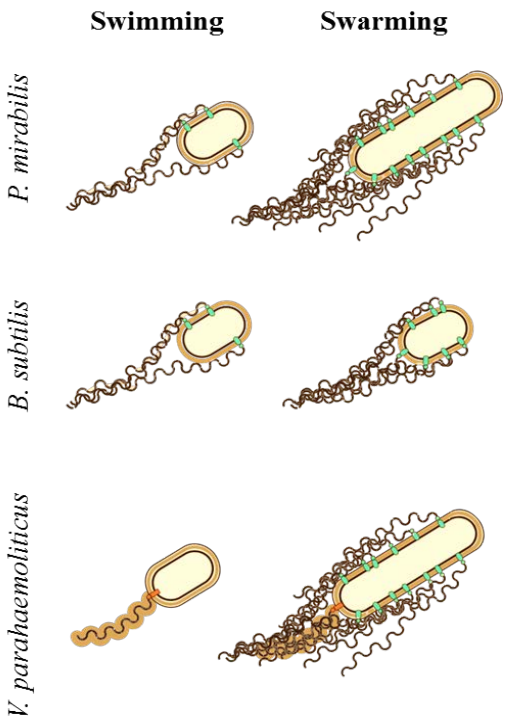

Figura 3. Células swimming y swarmer de *P. mirabilis*, *B. subtilis* y *V. parahaemolitycus*. Figura adaptada de Patrick et al. (2012).

Los reguladores máster flagelares parecen definir el número de flagelos, a través del control que ejercen sobre el nivel de expresión de los genes implicados en el ensamblaje y componentes del cuerpo basal flagelar (Patrick et al., 2012). En enterobacterias se ha visto que el regulador máster flagelar FlhDC, integra múltiples señales medioambientales. En *Serratia liquefaciens,* por ejemplo, la sobrexpresión artificial de *flhDC* induce la aparición de células "swarmer" en condiciones no inductoras del proceso (Eberl et al., 1999). En células "swarmer" de *P. mirabilis* hay una expresión de 30 veces

más de *flhDC* viéndose implicadas varias proteínas, como la proteína reguladora en respuesta a leucina (Lrp), cuatro proteínas Umo (encargadas de la regulación del operón máster) y WosA un regulador positivo de *flhDC* (Pearson et al., 2010). Se ha visto que para que se lleve a cabo la diferenciación a célula "swarmer" es necesario que la bacteria detecte la superficie, estímulo que parece controlar los reguladores máster flagelares. McCarter et al. (1988) demostraron que el flagelo polar de *V. parahaemolyticus* actúa como un mecanosensor. La inhibición de la rotación del flagelo polar induce la expresión y ensamblaje de los flagelos laterales llevando a la diferenciación de células que muestran motilidad swarming. Rather (2005) extiende este concepto a *P. mirabilis*, especie en la cual las células planctónicas se diferencian en células que presentan motilidad swarming cuando están sobre una superficie y la rotación del flagelo es inhibida por el sustrato. Las células "swarmer" de *P. mirabilis* se diferencian en células planctónicas en cuanto son transferidas a medio líquido probablemente como resultado de la pérdida del estímulo que produce la superficie.

2.2. Expresión génica en células que muestran motilidad swarming

Diversos estudios de expresión génica global y mutagénesis al azar en diferentes bacterias han permitido la identificación de genes esenciales para el swarming. Las células "swarmer" de *Salmonella typhimurium*, *Escherichia coli* y *P. aeruginosa* presentan alteraciones sustanciales en rutas metabólicas y en la expresión génica indicando que la diferenciación a célula "swarmer" representa más que un fenotipo en motilidad (Inoue et al., 2007; Kim and Surette, 2004; Overhage et al., 2007; Wang et al., 2004b). En *E. coli*, más del 50% de los genes del genoma parecen estar implicados en swarming (Inoue et al., 2007). Se ha demostrado que, junto a las funciones flagelares, un gran número de genes implicados en distintas actividades metabólicas, adquisición de hierro, proteínas reguladoras, chaperonas, y componentes de la superficie celular, son importantes para este tipo de migración multicelular.

En *P. aeruginosa* incluso se ha visto que existen diferencias en expresión génica entre las células que se encuentran dentro de la colonia "swarmer".

Tremblay and Deziel (2010) demostraron que en general la población de células localizadas en el borde de la colonia "swarmer" presenta una represión de los genes asociados con virulencia y una activación de los genes implicados en el metabolismo energético, sugiriendo que estas células, con mayor motilidad, buscan la colonización de superficies. Contrariamente, observaron que las células presentes en el centro de la colonia "swarmer" parecen estar en un estado de vida sésil simulando el estado de células pertenecientes a una biopelícula.

2.3. Producción de agentes surfactantes

Los surfactantes (surface-active agents) son moléculas anfipáticas, es decir, que poseen tanto grupos polares como grupos apolares. Dicha propiedad lleva a que los biosurfactantes se acumulen en las superficies y reduzcan la tensión superficial entre el sustrato y las células bacterianas facilitando el movimiento de las células sobre una superficie. Se ha visto que estas moléculas juegan un papel importante en el swarming, la formación de biopelículas, la señalización y diferenciación, la actividad antimicrobiana y el incremento de la biodisponibilidad de moléculas hidrofóbicas (Abdel-Mawgoud et al., 2010; Ron and Rosenberg, 2001; Xu et al., 2012). La estructura química de las moléculas surfactantes varía mucho entre las distintas especies de microorganismos y su efecto surfactante depende de las propiedades de la superficie. Los biosurfactantes pueden ser de bajo peso molecular como po ej. glicolípidos o lipopéptidos, o de alto peso molecular como polisacáridos anfipáticos, proteínas, lipopolisacáridos, lipoproteínas o mezclas complejas de estos biopolímeros. Entre las estructuras moleculares que componen la molécula surfactante se suelen incluir radicales hidrofóbicos que contienen a) ácidos grasos saturados, insaturados y/o hidroxilados o alcoholes grasos y b) radicales hidrofílicos que consisten en mono-, oligo- o polisacáridos, péptidos o proteínas (Ron and Rosenberg, 2001).

Entre los surfactantes de bajo peso molecular más estudiados que se ha visto que son esenciales para la motilidad bacteriana en superficie se encuentran los lipopéptidos, como la surfactina o serrawetina producidos por *B. subtilis*

(Kinsinger et al., 2003) y *Serratia liquefaciens* (Lindum et al., 1998) respectivamente, y los glicolípidos, como los ramnolípidos producidos por *P. aeruginosa* (Abdel-Mawgoud et al., 2010). Los mutantes en genes implicados en la biosíntesis de surfactantes son incapaces de moverse sobre una superficie, y en general, cuando estas moléculas son purificadas y añadidas de manera exógena, su fenotipo swarming es restaurado (Caiazza et al., 2005; Lindum et al., 1998; Peypoux et al., 1999).

2.4. Swarming y virulencia

En muchas bacterias patógenas el swarming es considerado un factor de virulencia en sí mismo. En *P. mirabilis,* el swarming facilita la colonización, el ascenso por el tracto urinario y la formación de biopelículas en los catéteres. Las mutaciones que afectan el swarming generalmente tienden a reducir la capacidad invasiva de la bacteria. Esto se debe a que el swarming, además de contribuir a una rápida colonización del nicho ecológico, conlleva la expresión acoplada de factores de virulencia (Allison et al., 1994). Se ha descrito que durante el proceso de diferenciación a célula "swarmer" en *P. mirabilis* más de 50 genes ven alterada su expresión entre los que se encuentran factores de virulencia como ureasa, hemolisina o metaloproteasa. En general se ha señalado que el swarming es un proceso de adaptación que lleva a un incremento en la producción de factores de virulencia en distintos microorganismos. Por ejemplo, en las células "swarmer" de *P. aeruginosa* y *S. typhimurium* se ha observado la sobrexpresión de genes que codifican para factores de virulencia como los sistemas de secreción tipo III y los sistemas de captación, transporte y metabolismo del hierro (Overhage et al., 2008; Wang et al., 2004b). Otra característica intrínseca de las células "swarmer" de distintas especies es que presentan una mayor resistencia a antibióticos.

3. Formación de biopelículas

3.1. Etapas en la formación de biopelículas

Las biopelículas son comunidades de microorganismos que crecen embebidos en una matriz de sustancias extracelulares poliméricas y adheridas a una superficie inerte o un tejido vivo (Hall-Stoodley et al., 2004).

A lo largo del proceso de formación de biopelículas generalmente se distinguen 5 etapas: 1) El proceso comienza cuando células planctónicas libres entran en contacto con la superficie y se adhieren de manera reversible a ésta. 2) Una vez la bacteria se ha adherido a la superficie, comienza a dividirse y las células hijas se extienden alrededor del sitio de unión formando una microcolonia donde la adhesión a la superficie es irreversible. La figura 4 muestra el proceso de formación de una microcolonia. 3) En una etapa posterior, la bacteria comienza a secretar distintos compuestos de naturaleza polisacarídica como exopolisacáridos (EPSs), proteínas, ácidos nucleicos y lípidos que constituyen la matriz de la biopelícula. 4) Las microcolonias son embebidas completamente en la matriz de polisacáridos dando lugar a una biopelícula madura. 5) Finalmente, el proceso concluye con la liberación de algunas células móviles que van a colonizar nuevas superficies (Hall-Stoodley et al., 2004). En la figura 5 se puede observar un esquema de las etapas de formación de una biopelícula en bacterias.

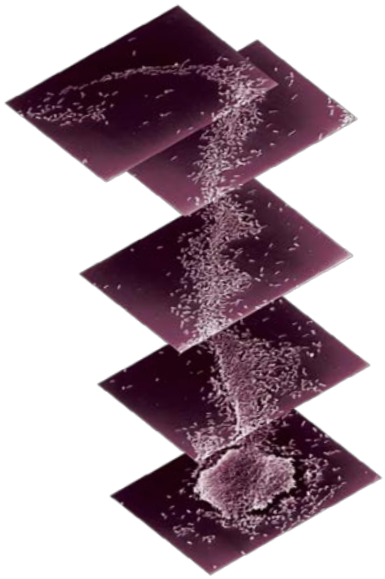

Figura 4. Proceso de formación de una microcolonia en *P. aeruginosa*. Figura tomada de Hall-Stoodley et al. (2004).

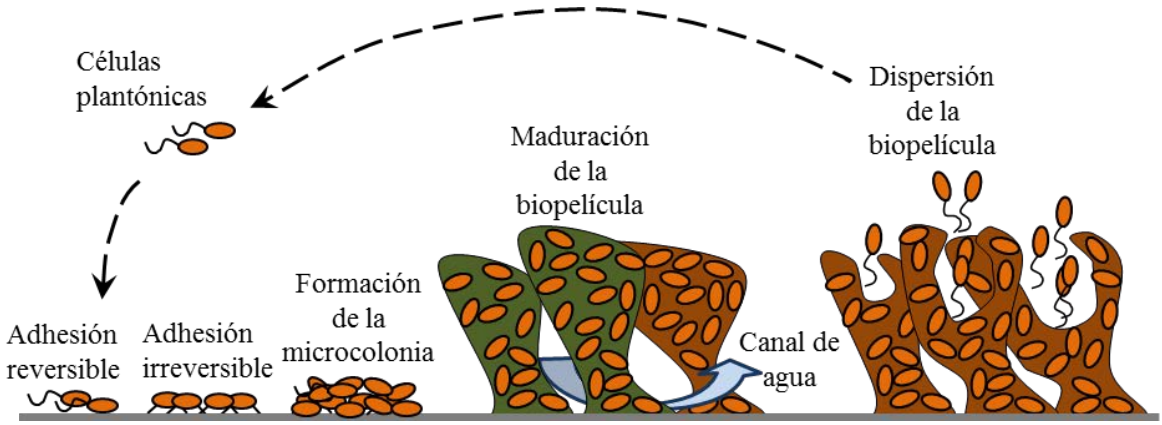

Figura 5. Esquema general representando las principales etapas del proceso de formación de biopelículas en bacterias. Modificado de Hirsch et al. (2009).

3.2. Biopelículas: Estructuras complejas

La habilidad de los procariotas de adaptar la estructura de las biopelículas en respuesta a las condiciones ambientales les proporciona flexibilidad y rápida adaptación. Se ha observado que la estructura de la biopelícula depende de muchos factores, entre ellos: condiciones hidrodinámicas, condiciones nutricionales, motilidad bacteriana, comunicación intercelular, producción de EPSs y proteínas de superficie, y composición de la matriz de la biopelícula (Flemming and Wingender, 2010). Las condiciones nutricionales son determinantes en el fenotipo de motilidad que los microorganismos adoptan y en la composición de la matriz polisacarídica en la que están embebidas las células dentro de la biopelícula. A la matriz polisacarídica se le atribuyen distintas funciones, entre ellas: proveer de estabilidad mecánica a la biopelícula, mediar la adhesión a la superficie de toda la comunidad celular, dar forma a una red de estructuras tridimensionales interconectadas, y transitoriamente, inmovilizar las células que forman parte de la biopelícula. Además, esta matriz funciona como un escudo que protege la comunidad bacteriana frente a predadores como protozoos y fagos líticos, la desecación, rayos UV, agentes antimicrobianos y respuesta inmune (Flemming and Wingender, 2010). Gracias a la retención de enzimas extracelulares en la matriz de la biopelícula se genera un sistema digestivo externo versátil en donde hay un secuestro de nutrientes particulares y

nutrientes disueltos en la fase acuosa, y utilización de éstos, como nutrientes y fuente de energía. La matriz de la biopelícula además actúa como centro de reciclaje manteniendo disponibles todos los componentes procedentes de las células lisadas.

El uso de Microscopía Láser Confocal (CLSM) y programas de análisis de imágenes ha permitido observar *in vivo* cómo se organizan las células adheridas a una superficie. La superposición de las imágenes en los ejes "*x*", "*y*", "*z*" permite el estudio de la estructura de la biopelícula entre distintas cepas y distintas condiciones. Las secciones ortogonales "*xz*" o "*yz*" muestran el grosor de la biopelícula y permiten ver la disposición homogénea o heterogénea de las células. En general se puede decir que existen biopelículas planas y biopelículas estructuradas. Una biopelícula plana es de grosor uniforme y no se observan microcolonias definidas. Sin embargo, en una biopelícula estructurada se observan grupos organizados de células de estructura tridimensional (microcolonias). Dependiendo del microorganismo, se describe que las microcolonias presentan estructuras en forma de hongos, torres, penachos, o crestas. En una biopelícula estructurada, las microcolonias están embebidas en una gruesa matriz polisacarídica estando separadas por canales que permiten el fluido de agua y nutrientes (Heydorn et al., 2000). En la figura 6 se pueden observar algunos ejemplos de imágenes del CLSM mostrando diferentes tipos de biopelículas.

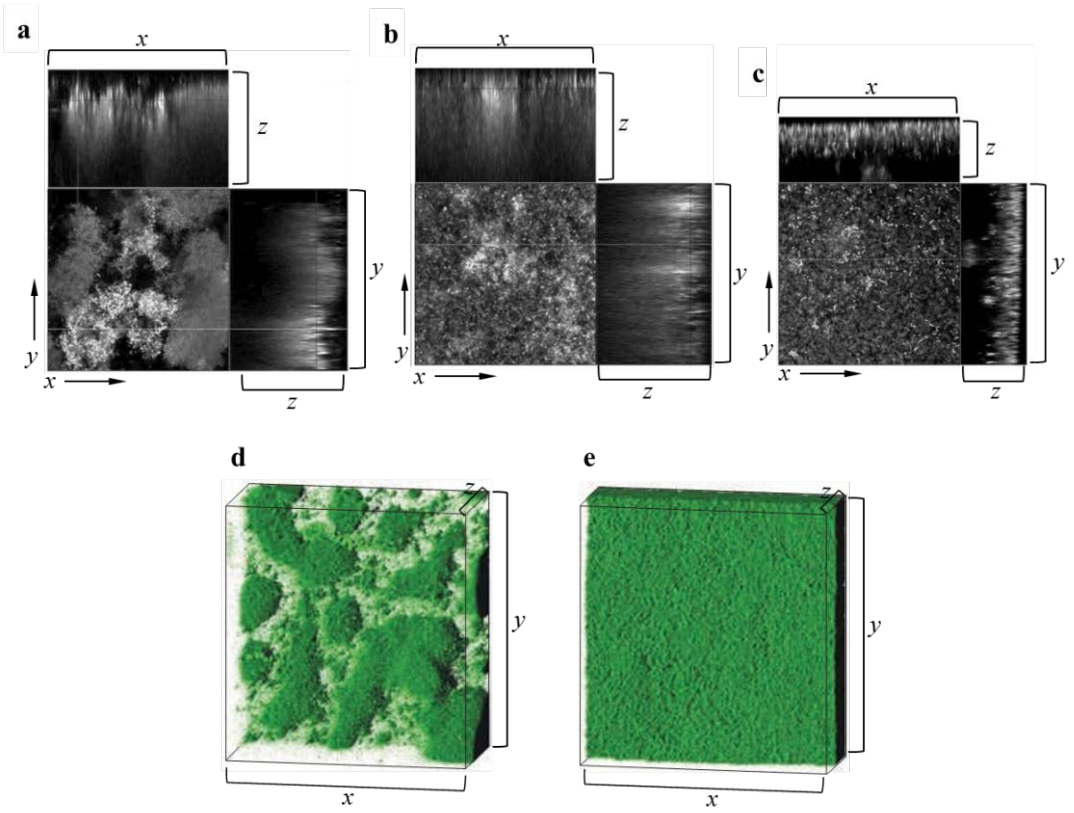

Figura 6. Diferentes estructuras de biopelículas. a, b y c imágenes de CLSM (planos *xy*, *xz*, *yz*) mostrando los diferentes tipos de biopelículas maduras observadas en un estudio de distintas cepas de *Streptococcus pneumoniae*. a) biopelícula formada por distintas microcolonias y canales de agua profundos, b) biopelícula de grosor similar, de microcolonias y canales de agua no definidos, c) biopelícula plana formada por agregados de muy pocas células, figura adaptada de Allegrucci and Sauer (2007). Imágenes tridimensionales de: d) biopelícula estructurada con microcolonias en forma de hongo formada por una cepa superproductora de alginato de *P. aeruginosa*, b) biopelícula plana formada por la cepa silvestre de *P. aeruginosa* PAO1 (no mucosa), figura adaptada de Flemming and Wingender (2010).

4. Motilidad y formación de biopelículas

La regulación génica dependiente de las señales ambientales que lleva a la formación de biopelículas o desencadena que la bacteria se mueva es muy compleja; ambos procesos requieren componentes similares en etapas determinadas y bajo condiciones específicas. En la etapa de inicio de formación de biopelículas las bacterias requieren pili y flagelos y la motilidad en superficie parece ser crucial en la determinación de la estructura última de la biopelícula ya que puede favorecer o no la formación de microcolonias (Shrout et al., 2006). Por otra parte, en la etapa final del ciclo de formación de biopelículas la motilidad

permite la dispersión de las células de la biopelícula. Recientemente Houry et al. (2012) han descrito que aún después de que la biopelícula ha madurado, entre un 0.1% y un 1% de las células mantienen la habilidad de moverse por medio de motilidad tipo swimming. Se cree que esta habilidad permite a las células abrir poros dentro de la biopelícula madura facilitando el intercambio de nutrientes y macromoléculas con el medio exterior.

En microorganismos como *V. chlolerae*, *V. parahaemolyticus Variovorax paradoxus* y *P. aeruginosa* se ha demostrado la existencia de una ruta genética común que regula de manera inversa la motilidad swarming y la formación de biopelículas, (Ferreira et al., 2008; Liu et al., 2010; Overhage et al., 2007; Pehl et al., 2012; Pratt et al., 2009; Shrout et al., 2006). Se ha comprobado que los niveles intracelulares del segundo mesajero diguanilato cíclico (di-GMPc) regulan comportamientos de poblaciones celulares como formación de biopelículas, motilidad y virulencia en respuesta a señales extracelulares. Altas concentraciones de di-GMPc están asociadas a un estado de vida sésil y llevan a una disminución de la motilidad, mientras bajas concentraciones causan el efecto contrario, promueven la motilidad y disminuyen la formación de biopelículas (Verstraeten et al., 2008). Ferreira et al. (2008) observaron que la proteína de membrana citoplasmática ScrC, que contiene los dominios GGDEF y EAL, característicos de enzimas con actividad diguanilato ciclasa y fosfodiesterasa que participan en la síntesis o degradación de di-GMPc respectivamente en *V. parahaemolyticus,* controla la decisión de la célula de optar por un estado de alta motilidad swarming o formar parte de una biopelícula. Otro ejemplo es el de la fosfodiesterasa CdgJ de *V. chlolerae*, la cual contiene el dominio EAL que le permite degradadar di-GMPc y regular de manera inversa motilidad y formación de biopelículas (Liu et al., 2010). En *V. chlolerae* también se ha descrito que el regulador de respuesta de los niveles de fosfato PhoB, el cual regula la expresión del operón *acgAB* implicado en la síntesis de las enzimas metabólicas del di-GMPc, regula positivamente la motilidad y negativamente la formación de biopelículas (Pratt et al., 2009). El gen *bifA* de *P. aeruginosa* codifica una fosfodiesterasa degradadora de di-GMPc. Un mutante delecionado de *bifA* muestra mayores niveles de di-GMPc que la cepa silvestre, un incremento en la

capacidad de formación de biopelículas y es incapaz de desplazarse por medio de motilidad tipo swarming (Kuchma et al., 2007). Además de esta regulación a través de los niveles de di-GMPc, se ha visto que las bacterias cuentan con otros mecanismos implicados en la regulación coordinada de ambos procesos. Por ejemplo, Pehl et al. (2012) identificaron al menos 8 genes en *V. paradoxus* EPS, cuya interrupción con un transposón Tn*5* llevaba a un fenotipo de mayor formación de biopelículas y una reducción de la motilidad tipo swarming. Los autores sugieren que este microorganismo responde a su ambiente por medio de la expresión coordinada de genes implicados en la producción de exopolisacáridos y formación de pili tipo IV entre otros. La mutación de *sadB* de *P. aeruginosa* PA14 impide que las células adheridas de manera reversible a la superficie, logren efectuar la adhesión irreversible, lo que imposibilita la formación de microcolonias (Caiazza et al., 2007). Además el swarming en un mutante *sadB* se ve incrementado, lo que demuestra que SadB actúa como un efector negativo de este tipo de motilidad. Caiazza et al. (2007) defienden que SadB regula de manera inversas estos procesos modulando las reversiones flagelares en condiciones de alta viscosidad, e influyendo en la producción del exopolisacárido Pel, el cual forma parte de la matriz de la biopelícula. SadB parece actuar sobre la tasa de reversión flagelar a través del sistema de quimiotaxis CheIV.

Como se ha descrito anteriormente, la producción de agentes surfactantes es esencial para la motilidad en superficie de numerosos microorganismos. Existen algunos trabajos en los que se ha descrito que los agentes biosurfactantes que facilitan el desplazamiento en superficie de un microorganismo también están relacionados con su capacidad de formación de biopelículas. En algunas bacterias se ha descrito una relación inversa entre la producción de biosurfactantes y la capacidad de formar biopelículas, como el efecto producido por los lipopéptidos surfactina, serrawetina o putisolvina (Kuiper et al., 2004; Mireles et al., 2001). Mireles et al. (2001) demostraron que los mutantes afectados en la producción de surfactina de *S. enterica* serovar Thyphymurium o *B. subtilis*, o serrawetina de *Serratia marcescens*, se ven afectados en el desplazamiento tipo swarming. Contrariamente a lo descrito para *P. aeruginosa*, estos mutantes en producción de surfactina o serawetina

muestran una mayor eficiencia en la formación de biopelículas. La acción surfactante de estas moléculas parece dificultar la formación de biopelículas. La adición exógena de surfactina inhibe la formación de biopelículas de los mutantes en la producción de surfactina de *S. enterica y* serrawetina de *S. marcescens* en pocillos de placas de cloruro de polivinilo, y la formación de biopelículas de *S. enterica*, *E. coli*, *P. mirabilis* y *P. aeruginosa* en catéteres uretrales (Mireles et al., 2001). En *P. aeruginosa*, el aumento en la producción de ramnolípidos generado por la baja disponibilidad de hierro lleva a un aumento en la motilidad tipo twitching y a la formación de biopelículas desestructuradas, finas y planas (Glick et al., 2010). Adicionalmente, se ha descrito que los ramnolípidos son esenciales en distintas etapas de la formación de biopelículas. Se ha observado que estas moléculas son requeridas para el proceso de iniciación de la formación de la microcolonia, facilitan la migración de las bacterias para que se forme el sombrero de las estructuras en forma hongo, mantienen la estructura de la biopelícula dejando canales libres de células entre las microcolonias y además son necesarias en la etapa de dispersión de la biopelícula (Pamp and Tolker-Nielsen, 2007).

Las múltiples rutas de control génico que inducen swarming o la formación de biopelículas, hacen evidente la compleja regulación de las señales que desencadenan cada proceso. En condiciones de laboratorio se ha visto que cada especie bacteriana posee demandas específicas de nutrientes, condiciones físicas y químicas para que se observe swarming. Algunas bacterias como *B. subtilis*, hacen swarming en una gran variedad de medios ricos, sin embargo, bacterias como *S. enterica* y *Y. enterocolítica* requieren la adición de suplementos particulares como glucosa (Kearns, 2010). El swarming es promovido por altas tasas de crecimiento, lo que puede explicar la exigencia por parte de algunas bacterias de medios ricos en nutrientes. En algunas especies, mientras una alta disponibilidad de nutrientes lleva a la formación de biopelículas, en otras la inhibe. *E. coli* K-12, por ejemplo, forma biopelículas en medios completos pero en medios mínimos, es capaz de formarlas únicamente si estos son suplementados con aminoácidos. Contrariamente, *E. coli* O157:H7 forma biopelículas únicamente en condiciones de baja disponibilidad de nutrientes. Sin embargo, otros

microrganismos como *P. aeruginosa* y *P. fluorescens,* considerados potenciales formadores de biopelículas, establecen biopelículas bajo la mayoría de condiciones nutricionales que permiten el crecimiento celular (Davey and O'toole, 2000). En *P. aeruginosa*, el tipo de motilidad usado a lo largo del proceso de formación de biopelículas depende de las condiciones prevalentes en el medio y la superficie. Aunque existen controversias en cuanto a qué tipo de motilidad en superficie (swarming o twitching) está implicado en la formación de biopelículas en esta bacteria, se está de acuerdo en que aquellas condiciones que favorecen la motilidad llevan a la formación de biopelículas de estructura plana (Klausen et al., 2003a; Klausen et al., 2003b; Shrout et al., 2006).

4.1. Importancia del hierro en motilidad y formación de biopelículas

El hierro es un elemento esencial para las bacterias ya que es requerido en el mantenimiento celular, funciona como cofactor de muchas enzimas, y es importante en el metabolismo del ARN y el ADN. Sin embargo, su exceso puede ser tóxico debido a que promueve la generación de radicales libres a través de la reacción de Fenton, radicales que pueden dañar el ADN, las proteínas y la membrana celular de la bacteria (Touati, 2000). En condiciones aerobias el hierro soluble (Fe^{2+}) es escaso y la mayoría del hierro presente se encuentra en su forma insoluble como Fe^{3+}. Es por esto que las bacterias han tenido que desarrollar mecanismos sofisticados y versátiles de adquisición de hierro que promuevan la entrada de Fe^{3+} y su conversión en hierro Fe^{2+}. Uno de los mecanismos que las bacterias utilizan para la captura de Fe^{3+} del medio implica la secreción y captura de sideróforos (del griego “transportadores de hierro”). Los sideróforos son moléculas quelantes de hierro de bajo peso molecular (< 1.000 Da). Debido a su tamaño, éstos no pueden penetrar libremente a través de las porinas presentes en la membrana extracelular de las bacterias Gram negativas y requieren de receptores de membrana externa y de sistemas de entrada y transporte (Sandy and Butler, 2009). La producción de sideróforos se encuentra regulada por la disponibilidad de hierro en el medio. Bajas concentraciones de este compuesto incitan a su producción y, contrariamente, altas concentraciones la bloquean.

La disponibilidad de hierro parece ser una de las señales más extendidas entre diversos géneros bacterianos para la regulación de la motilidad en superficie y la formación de biopelículas. Por ejemplo, en *P. aeruginosa* PAO1 y *Burkholderia cenocepacia* se ha visto que bajas concentraciones de hierro estimulan un estado de motilidad activa y colonización, mientras que altas concentraciones de este compuesto inducen la agregación de las células y la formación de biopelículas (Berlutti et al., 2005). Contrariamente, en bacterias como *Staphylococcus aureus* Newman (Johnson et al., 2008), *Acinetobacter baumannii* (Gaddy and Actis, 2009) y *Streptococcus mutans* (Yoshida, 2005) se conoce que condiciones de limitación de hierro inducen la formación de biopelículas. Puesto que la disponibilidad de hierro está ligada a la producción de sideróforos, no es sorprendente que en algunas bacterias se haya observado que la producción de sideróforos puede ser clave en estos procesos asociados a superficie. Se han caracterizado sideróforos como la pioverdina o la pioquelina, producidas por varias especies de *Pseudomonas,* y la enterobactina producida por *E. coli,* que son requeridos para la motilidad en superficie y la formación de biopelículas (Alché Ramírez et al., 2007; Banin et al., 2005; Inoue et al., 2007; May and Okabe, 2011). Mutantes en *P. putida* KT2440 en *ppsD,* gen implicado en la síntesis del sideróforo, o en el receptor de membrana del sideróforo FpvA son incapaces de desplazarse sobre una superficie semisólida (Alché Ramírez et al., 2007). En medio mínimo definido con bajas concentraciones de hierro, se ve estimulada la motilidad tipo twitching y se induce la formación de biopelículas planas en *P. aeruginosa* (Patriquin et al., 2008). Banin et al. (2005) han estudiado la importancia del hierro como señal en la formación de biopelículas de *P. aeruginosa* caracterizando el fenotipo de formación de biopelículas de mutantes incapaces de producir los sideróforos pioverdina y pioquelina. Se ha demostrado que para la formación normal de biopelículas maduras con estructuras de hongo se requiere la presencia de un sistema de captura de hierro funcional (producción de pioverdina o pioquelina). Los autores sugieren que la señal que regula la formación de biopelículas estructuradas en *P. aeruginosa* es el transporte activo del hierro quelado o los niveles intracelulares de este compuesto. El sideróforo enterobactina, producido por *E. coli*, es otro ejemplo de sideróforo que ha sido identificado como relevante para la motilidad en superficie y la formación de

biopelículas. En *E. coli* K-12, se observó que las condiciones específicas de swarming llevan a la inducción de los genes de biosíntesis y transporte de enterobactina (Inoue et al., 2007). Recientemente May and Okabe (2011) estudiaron la formación de biopelículas de una cepa de *E. coli* delecionada del 17.6% del genoma de la cepa parental, capaz de formar biopelículas maduras. En este estudio se observó que el gen de biosíntesis de enterobactina *entB* está implicado en la formación de biopelículas de esta bacteria, y que la superproducción de este sideróforo promueve la formación de biopelículas y su maduración.

5. Simbiosis *Rhizobium*-leguminosa

En suelos desprovistos de nitrógeno los denominados "rizobios clásicos" son capaces de fijar nitrógeno atmosférico al establecer simbiosis mutualista con plantas leguminosas. Los rizobios están relacionados filogenéticamente con numerosos microorganismos patógenos de animales y de plantas, y se acumulan evidencias que sugieren que este microorganismo utiliza mecanismos similares a los usados por bacterias patógenas en la invasión de hospedadores eucariotas. Es por ello que la simbiosis *Rhizobium*-leguminosa es utilizada como modelo de estudio de las bases moleculares que rigen las interacciones bacteria-planta. En esta asociación, la bacteria induce en la planta el desarrollo de un nuevo órgano, al que se denomina nódulo, dentro del cual se produce la fijación biológica del nitrógeno atmosférico (FBN) (Masson-Boivin et al., 2009; Oldroyd et al., 2011). La formación del nódulo implica un reconocimiento específico entre los componentes procariótico y eucariótico de la asociación, la invasión de las células de la planta por la bacteria y otros muchos cambios en la estructura y bioquímica de ambos organismos (Oldroyd et al., 2011).

El preludio a la infección de las raíces de leguminosas por *Rhizobium* se caracteriza por el crecimiento de la bacteria en la rizosfera, estimulado por una serie de compuestos exudados por la planta. Determinados flavonoides (derivados de 2-fenil-1,4-benzopirona) presentes en los exudados de las leguminosas hospedadoras inducen la expresión en la bacteria de un conjunto de genes

esenciales en el proceso de nodulación: genes *nod*, *nol* y *noe*. El resultado es la aparición de una serie de proteínas (25 aproximadamente) que participan en la síntesis y secreción de una molécula señal: el factor Nod (FN) o lipoquitooligosacárido. Todas las especies de *Rhizobium* producen FN con la misma estructura básica: un esqueleto oligosacarídico de quitina resultante de la unión de 4-5 restos de N-acetilglucosamina, el cual se encuentra sustituido en su extremo no reductor por un ácido graso. Cada especie de *Rhizobium* produce un FN o un espectro de FN con características particulares basadas en una serie de decoraciones que pueden aparecer en el esqueleto de quitina, así como en la longitud y grado de saturación del ácido graso. Los genes *nodABC* codifican las proteínas requeridas para la síntesis del esqueleto del FN. Los productos del resto de los genes *nod* y los genes *noe* y *nol* se encargan de hacer las modificaciones de los FN, tales como la adición de residuos fucosil, sulfiril, acetil, metil, carbamoil o arabinosil y cambios en la cadena del ácido graso, responsables de la especificidad de hospedador (Jones et al., 2007). Los FN son la llave que abre la puerta de entrada en el hospedador específico de *Rhizobium* (Peck et al., 2006). Por sí solos y en cantidades muy pequeñas (nM), son capaces de desencadenar en la planta una serie de respuestas requeridas para iniciar el proceso de infección bacteriana (deformación de pelos radicales, formación de canales de pre-infección y control de respuestas defensivas de la planta), así como para la organogénesis del nódulo (división de células del córtex y expresión de nodulinas, proteínas vegetales específicas de la simbiosis).

Una vez iniciado el diálogo molecular entre las contrapartes, las bacterias colonizan la superficie de la raíz y se adhieren a las células de la epidermis y mayoritariamente a los pelos radicales. Se cree que los rizobios se acumulan y adhieren en la superficie de la raíz en forma de biopelículas (Hirsch et al., 2009). Los rizobios deben atravesar la epidermis y corteza de la raíz para poder acceder al primordio nodular (nódulo inmaduro) donde las bacterias son liberadas al citoplasma de las células vegetales para llevar a cabo la fijación biológica de nitrógeno (FBN) (Fig. 7). *Rhizobium* puede llegar al nódulo a través de canales de infección, por medio de “cracks” o fisuras en la epidermis ocasionadas por la emergencia de raíces laterales, o a través de los espacios intercelulares (Oldroyd

et al., 2011). La manera más común de entrada es a través de la formación de canales de infección iniciados en pelos radicales en crecimiento. Para ello, las células de *Rhizobium* se adhieren a los pelos radicales de manera polar, esto es, el extremo de la célula bacteriana contacta con el pelo radical induciendo una curvatura del pelo radical en la que los rizobios quedan atrapados. Es en este momento cuando tiene lugar la infección propiamente dicha, que comienza con una hidrólisis muy localizada de la pared celular de la planta y la invaginación de la membrana plasmática del pelo radical dando lugar a una estructura tubular conocida como canal o cordón de infección. A través del canal de infección, las bacterias penetran en el interior de la raíz. El canal de infección, con las bacterias en su interior, progresa ramificándose y atravesando las distintas capas de células de la raíz dirigiéndose hacia el primordio nodular. A medida que el canal de infección se va formando, las paredes de la células vegetales son degradadas, se cree que por enzimas pectinolíticas y celulolíticas secretadas por la planta hospedadora, la bacteria o ambos simbiontes (Robledo et al., 2008). Simultáneamente a la formación y avance del canal de infección, determinadas células del córtex de la raíz comienzan a dividirse dando lugar a un pequeño tumor conocido como primordio nodular (van Brussel et al., 1992). Cuando el canal de infección alcanza las células del primordio, las bacterias son liberadas al citoplasma de estas células vegetales, en un proceso similar al de la endocitosis, en el que la bacteria queda rodeada por una porción de membrana de la célula vegetal que recibe el nombre de membrana peribacteroidal. El proceso finaliza con la diferenciación de las bacterias en su forma pleiomórfica endosimbiótica de bacteroides, responsables de la fijación de nitrógeno, y la diferenciación del primordio nodular en nódulo maduro. La planta hospedadora ejerce el control en la supervivencia de la bacteria dentro del simbiosoma, y no sólo debe proveer de nutrientes a la bacteria sino que también debe proporcionar el ambiente microaeróbico necesario para la fijación de N_2 y algunas de las especificaciones necesarias que forman parte del programa de diferenciación de la bacteria. Ver figura 7.

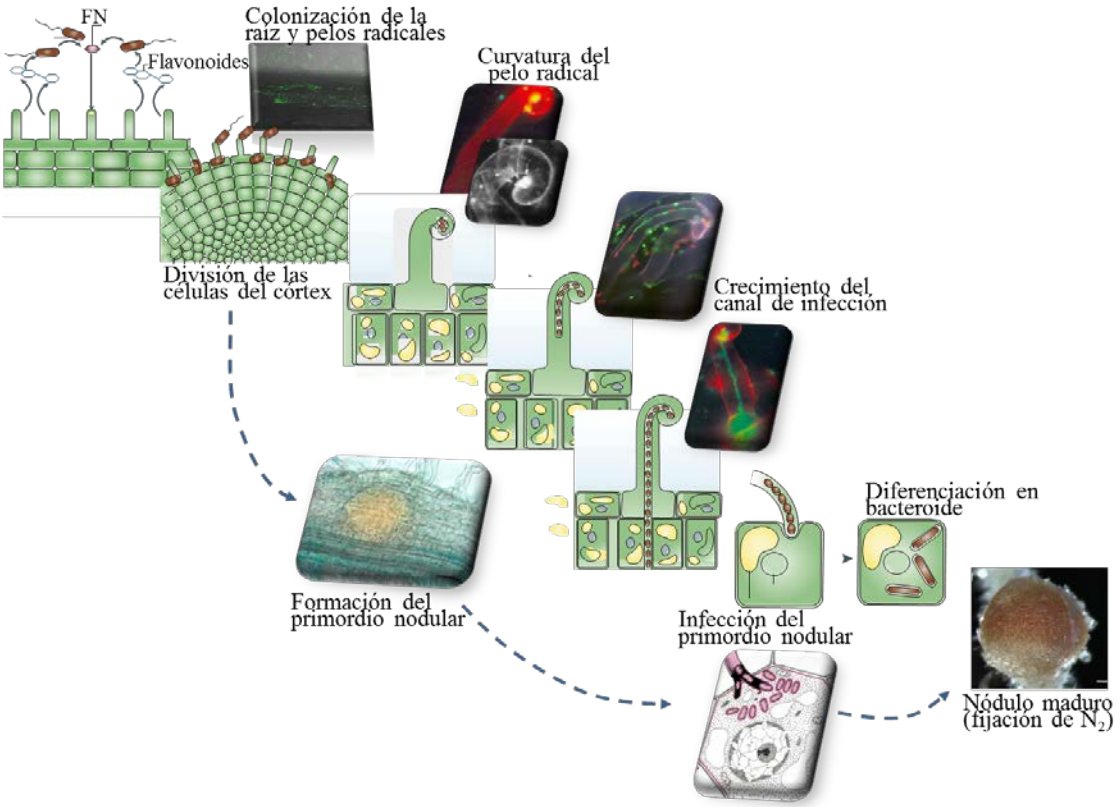

Figura 7. Proceso de formación del nódulo en la simbiosis *Rhizobium*-leguminosa. Modificado de (Jones et al., 2007). FN, Factores Nod.

6. *Sinorhizobium meliloti*: aspectos relevantes de la motilidad de esta bacteria

El microorganismo objeto de estudio de este trabajo *Sinorhizobium meliloti*, es una α-proteobacteria perteneciente a la familia Rhizobiaceae y al género *Sinorhizobium* (*Ensifer*) (Lindström et al., 2010). Este microorganismo es un bacilo Gram negativo, aerobio, cuyo tamaño oscila entre 0.5-1 µm de ancho y 1.2-3 µm de largo. Posee entre 6 a 8 flagelos periticos que rotan en una única dirección a distintas velocidades, permitiendo a la célula bacteriana cambiar de dirección. Su genoma que fue el primero de los rizobios en ser secuenciado, tiene un tamaño de 6.7 millones de pares de bases (pb) y está compuesto por tres replicones (Galibert et al., 2001). El elemento de mayor tamaño es el cromosoma de 3.65 Mb (Mb) (Capela et al., 2001), y los otros dos elementos son conocidos como los megaplásmidos pSymA y pSymB, de 1.35 Mb y 1.68 Mb, respectivamente

(Barnett et al., 2001; Finan et al., 2001), en los que se localizan la mayoría de los genes requeridos para el establecimiento de la interacción simbiótica.

En el elemento cromosómico se albergan casi todos los genes constitutivos de subsistencia celular, los genes "housekeeping", tales como los genes implicados en metabolismo de ácidos nucleicos y proteínas, los genes que participan en procesos metabólicos celulares como el transporte y degradación de péptidos y aminoácidos, y los genes relacionados con el metabolismo de azúcares. Además aquí se localizan los genes implicados en los procesos de motilidad, quimiotaxis, y los genes de respuesta a estrés (Capela et al., 2001). El replicón más pequeño es pSymA, en el que se localizan la mayoría de los genes de nodulación (*nod*) y fijación de N (*nif*, *fix*) (Barnett et al., 2001). Casi el 20 % de los marcos de lectura abierta (ORFs) presentes en el megaplásmido pSymB codifican para sistemas de captura de nutrientes. Aunque los genes que participan en la biosíntesis de los exopolisacáridos se localizan en el pSymB, la mayoría de los reguladores transcripcionales de la síntesis de polisacáridos se encuentran en el cromosoma (Finan et al., 2001).

Distintos aspectos de la motilidad y quimiotaxis de *S. meliloti* difieren con respecto al paradigma de enterobacterias (Schmitt, 2002). En *E. coli*, los filamentos del flagelo se componen de un solo tipo de flagelina mientras que en *S. meliloti* los filamentos flagelares son complejos estando compuestos por cuatro subunidades de flagelina estrechamente relacionadas FlaA, FlaB, FlaC, y FlaD, codificadas por 4 genes ligados pero que se transcriben de manera independiente. Las uniones entre subunidades de flagelina confieren a los filamentos una conformación helicoidal. En enterobacterias los flagelos son flexibles y para responder a los estímulos quimiotácticos las células cambian el sentido de rotación de los flagelos. En *S. meliloti* los flagelos son rígidos, giran únicamente en el sentido de las agujas del reloj y la orientación del movimiento está determinada controlando la velocidad de rotación flagelar. Mientras que en el procesamiento de las señales quimiotácticas en *E. coli* participa un único regulador de respuesta, CheY y la fosfatasa CheZ, en el procesamiento de la señalización quimiotáctica en *S. meliloti* participan dos reguladores de respuesta

diferentes, CheY1 y CheY2, y no existe una fosfatasa CheZ. Otra diferencia en motilidad entre enterobacterias y *S. meliloti* es la organización de los genes implicados en este proceso. En *S. meliloti*, la mayoría de genes implicados en motilidad, están organizados en una región continua del cromosoma de 56 Kb. Al igual que en enterobacterias, en *S. meliloti* la regulación transcripcional de estos genes ocurre de manera jerárquica y se han organizado en tres clases principales. La clase IA consta de los genes reguladores máster *visN* y *visR* los cuales codifican subunidades similares al activador transcripcional LuxR, que conforman el activador transcripcional global heterodimérico (o heterotetramérico) VisNR; la clase IB situada en la cascada debajo de la clase IA pero por encima de la clase II, incluye el gen *rem* (regulador of exponential growth motility), que codifica un activador transcripcional de los genes de la clase II responsable de limitar la expresión de estos genes a la fase exponencial de crecimiento; otra diferencia con el paradigma de enterobacterias es la subdivisión de la clase II en las clases IIA (*orf38* y *fliM*) y IIB (*motA* y *motBC*) dependiendo de si controlan la expresión de genes de la clase III (*fla* y *che*) o no (Rotter et al., 2006; Sourjik et al., 2000).

Al igual que en otras bacterias, con el propósito de evitar gastos de energía innecesarios, en *S. meliloti* la expresión de los genes flagelares parece estar sujeta a un estricto control. Distintos análisis de expresión génica global de *S. meliloti* han demostrado que la expresión de los genes flagelares y de motilidad es rápidamente reprimida en respuesta a cambios ambientales como por ejemplo: estrés osmótico, pH ácido y hambre de hierro y fosfato (Domínguez-Ferreras et al., 2006; Hellweg et al., 2009; Krol and Becker, 2004). Por otra parte se ha observado una corregulación inversa entre motilidad y la producción de EPSs, la cual esta mediada por distintos sistemas de regulación. El sistema de QS ExpR/Sin controla la expresión de un gran número de genes, entre ellos, algunos de los genes implicados en la producción de EPS I o succinoglicano, EPS II o galactoglucano y genes de motilidad (Gurich and González, 2009; Hoang et al., 2004). En condiciones de baja densidad celular, la inducción de la expresión de genes relacionados con motilidad requiere la participación del regulador transcripcional ExpR. Cuando incrementa la densidad poblacional, ExpR junto

con acil-homoserina lactonas (AHLs) producidas por la AHL sintasa SinI, inhibe la transcripción del operón *visNR*, provocando la reducción en la expresión de los genes que pertenecen al regulón flagelar. El sistema de regulación ExoR/ExoS/ChvI implicado en la regulación de la síntesis de EPS I, además reprime la expresión de los genes de motilidad a través de VisNR y Rem (Hoang et al., 2008). Distintos mutantes en este sistema superproducen EPS I y además son aflagelados. Mutantes que carecen de CbrA, una putativa histidínquinasa asociada con un dominio sensor PAS e inicialmente descrito como un regulador del proceso de simbiosis, superproducen EPS I y algunos genes de motilidad se encuentran reprimidos, entre ellos *visNR* (Gibson et al., 2007). La proteína reguladora MucR, la cual juega un papel esencial en la producción de EPS, reprime la expresión de *rem* (Bahlawane et al., 2008). Finalmente, el sistema EmmABC formado por la proteína reguladora EmmA y el sistema de dos componmentes EmmBC, se ha visto que también esta implicado en la regulación de la producción de EPS y motilidad (Morris and González, 2009).

7. Papel de motilidad y quimiotaxis en la simbiosis *Rhizobium*-leguminosa

Al igual que en otras bacterias móviles, la quimiotaxis permite a *Rhizobium* detectar los cambios en el ambiente exterior y responder a los estímulos de incremento de nutrientes o presencia de sustancias tóxicas, y acercarse o alejarse de ellos. La transducción de la cascada de señalización de quimiotaxis controla la velocidad (*S. meliloti*) o sentido (*E. coli*) de la rotación flagelar, dirigiendo el movimiento de la célula. Aunque en *S. meliloti* se han estudiado ampliamente los genes que están implicados tanto en motilidad como en quimiotaxis, su contribución al establecimiento de la simbiosis no se ha investigado rigurosamente utilizando cepas mutantes genéticamente bien definidas. De manera general, se cree que la capacidad de *Rhizobium* de responder quimiotácticamente a exudados de raíces de leguminosas, podría facilitar el establecimiento de la simbiosis al dirigir la bacteria hacia el sitio adecuado para iniciar el proceso de infección. De acuerdo con esta hipótesis, distintas referencias bibliográficas describen el comportamiento quimiotáctico de diferentes especies de *Rhizobium* hacia exudados radicales (Caetano-Anollés et al., 1988;

Dharmatilake and Bauer, 1992). Estudios clásicos realizados con cepas mutantes de *Rhizobium* no quimiotácticas o no móviles, pero no caracterizadas genéticamente, mostraban que estas cepas eran menos competitivas y menos eficientes en la nodulación que las cepas silvestres, sugiriendo que si bien motilidad y quimiotaxis no eran esenciales para la nodulación y fijación de nitrógeno, sí que parecían contribuir a las etapas iniciales de la interacción bacteria-planta (Ames and Bergman, 1981; Caetano-Anollés et al., 1988; Soby and Bergman, 1983). Más recientemente en en *Rhizobium leguminosarum* bv. viciae se ha demostrado que dos proteínas de quimiotaxis aceptoras de grupos metilo (MCP) y el cluster de quimiotaxis *che1*, son importantes en la eficiencia de nodulación de plantas de guisante y en la capacidad competitiva de la bacteria (Miller et al., 2007; Yost et al., 1998). Mutantes en *fliP* o en *flhG* de *S. meliloti* (no móviles y aflagelados) muestran un retraso en la formación de nódulos fijadores de nitrógeno (Fujishige et al., 2006b).

Una vez se ha iniciado el proceso de infección, en general se admite que la motilidad ya no es necesaria para el desarrollo de los bacteroides, o en el proceso de fijación de nitrógeno. De acuerdo con esta idea, un análisis transcriptómico, reveló una menor expresión de genes flagelares y de quimiotaxis en células de *S. meliloti* y *R. leguminosarum* aisladas de nódulos maduros que en células en vida libre (Becker et al., 2004; Yost et al., 2004). De hecho, la represión de genes de motilidad de *S. meliloti* mediada por el sistema de QS ExpR/Sin, es esencial para que se logre llevar a cabo una invasión efectiva de los nódulos (Gurich and González, 2009). Un mutante s*inI* de *S. meliloti* induce menor número de nódulos por planta que la cepa silvestre. Además, la proporción de nódulos rosados (fijadores de N) frente a nódulos blancos (no fijadores de N) desarrollados en plantas inoculadas con el mutante, es menor que en plantas inoculadas con la cepa silvestre, un mutante *expR* o un doble mutante *expRsinI*. Gurich y González (2009) demostraron que la incapacidad del mutante *sinI* de reprimir la síntesis de flagelos era la causa de su defecto simbiótico, ya que un mutante *sinI* incapaz de producir flagelos recuperaba completamente la capacidad de establecer una simbiosis efectiva. Aún no se conoce cómo los flagelos podrían interferir con el desarrollo de la interacción simbiótica. Entre las posibles explicaciones podrían

estar que los flagelos interfieran con el movimiento de las bacterias en el interior de los canales de infección, o bien que desencadenen respuestas de defensa en la planta (Gurich and González, 2009).

Si poco se conoce sobre el papel de la motilidad en general de los rizobios en el establecimiento de la simbiosis mutualista, mucho menor es el conocimiento sobre la función específica de determinados tipos de motilidad en superficie recientemente identificados en distintos rizobios (ver apdo. 8). Así se desconoce qué relevancia tiene la motilidad swarming en la interacción con la planta hospedadora. No obstante, el hecho de que algunas de las mutaciones que alteran el movimiento swarming en *S. meliloti* y *R. etli*, provoquen defectos simbióticos sugiere que componentes esenciales en este tipo de motilidad y/o factores que se co-regulan durante el proceso de diferenciación a célula "swarmer" pueden ser relevantes en la interacción simbiótica. Por otro lado, el movimiento tipo sliding, podría permitir a los rizobios colonizar superficies en aquellas condiciones que reprimen la expresión de genes flagelares, como por ej. en condiciones de alta densidad celular o durante el proceso de invasión. Un movimiento colectivo tipo sliding se ha propuesto como mecanismo que contribuiría a la colonización de los canales de infección (Fournier et al., 2008).

8. Swarming en *Rhizobium*

La motilidad tipo swarming en rizobios se ha descrito en *S. meliloti, R. etli* y *R. leguminosarum* (Braeken et al., 2008; Soto et al., 2002; Tambalo et al., 2010). Daniels et al. (2004) describieron la existencia de swarming en una cepa silvestre de *R. etli*. Los mismos autores observaron que mutaciones en el sistema de QS *cinIR* de esta bacteria abolen la puesta en marcha de la motilidad swarming. Más adelante estos mismos autores demostraron que las AHLs de *R. etli*, las cuales se caracterizan por un ácido graso de cadena larga, además de actuar como señal de QS, actúan como biosurfactantes facilitando la translocación bacteriana sobre la superficie (Daniels et al., 2006). Braeken et al. (2008) realizaron una mutagénesis al azar con minitransposón Tn*5* con el fin de identificar los determinantes del swarming en *R. etli*. El análisis de las secuencias de los transposantes afectados

en swarming desveló que los defectos en este tipo de motilidad no sólo son consecuencia de mutaciones en genes relacionados con motilidad, quimiotaxis o flagelos. Obtuvieron mutantes afectados en genes relacionados con QS, composición y transporte de polisacáridos, y metabolismo de aminoácidos y poliaminas. Además, en algunos de estos mutantes se vio afectada la nodulación y la fijación de nitrógeno.

Tambalo et al. (2010) caracterizaron el swarming de las cepas 3841 y VF39SM de *R. leguminosarum* bv. viciae. Se observó que para el swarming de este rizobio son parámetros cruciales la densidad celular, la fuente de carbono y la temperatura de incubación. Los autores defienden que en la capa de matriz extracelular que rodea la colonia "swarmer" de *R. leguminosarum* bv. viciae no se detectó la presencia de moléculas surfactantes. La cepa VF39SM mostró una mayor eficiencia en motilidad tipo swarming en comparación con la cepa 3841. VF39SM además de iniciar el desplazamiento en superficie antes que 3841, fue capaz de colonizar casi en su totalidad la superficie de agar de la placa de Petri. El borde de la colonia "swarmer" de VF39SM se caracterizó por la presencia de células hiperflageladas, mientras que en el centro de la colonia se detectaron colonias similares a aquéllas en estado vegetativo. Mientras que el número de flagelos en VF39SM se vio incrementado en cinco veces respecto a las células vegetativas (2 flagelos por célula), las células "swarmer" de 3841 mostraron un promedio de 3 flagelos por célula. Los autores señalan que la hiperflagelación de VF39SM debe contribuir a su mejor fenotipo en swarming. Adicionalmente, se demostró que las células "swarmer" de *R. leguminosarum* bv. viciae VF39SM y 3841 presentan una mayor resistencia a antibióticos.

Soto et al. (2002) fueron los primeros en desvelar la existencia de swarming en *Rhizobium.* Estos autores describieron el swarming de un mutante de *S. meliloti,* el mutante QS77 derivado de la cepa GR4. En QS77, la mutación en el gen *fadD*, que codifica una acil-CoA sintetasa específica de ácidos grasos de cadena larga, resulta en la aparición de swarming y en defectos en nodulación. La colonia de QS77 se mueve extendiéndose sobre la superficie del medio mostrando un patrón dendrítico. Las células "swarmer" son casi el doble de largas que las de

la cepa silvestre y son hiperflageladas, presentando aproximadamente seis veces mayor número de flagelos. El swarming de este mutante se ve influenciado por: a) la concentración y tipo de agar, b) la densidad poblacional, c) la fuente de nitrógeno, d) la fuente de carbono y e) la viscosidad del medio de crecimiento. QS77 además, muestra alteraciones en expresión génica tales como menor expresión del gen simbiótico *nodC* en distintas condiciones de crecimiento, o la sobre-expresión de genes flagelares (*flaA*) en repuesta al crecimiento en condiciones inductoras de swarming. A pesar de que el mutante *fadD* es capaz de inducir nódulos fijadores de nitrógeno en plantas de alfalfa, se muestra menos infectivo y competitivo que la cepa silvestre. Estos resultados llevaron a sugerir que compuestos de naturaleza lipídica relacionados con la actividad FadD podrían actuar como señales capaces de controlar "swarming" y la capacidad simbiótica de la bacteria. Una aproximación genética llevada a cabo en nuestro grupo en la que se aislaron y caracterizaron transposantes derivados de mutantes *fadD* de *S. meliloti* que mostraban alteraciones en motilidad en superficie con respecto a la cepa parental, ha permitido poner de manifiesto que el swarming de *S. meliloti* dependiente de una mutación en *fadD* requiere la participación de genes flagelares, quimiotaxis, genes de respuesta a estreses ambientales, reguladores que afectan la producción de exopolisacáridos y otros genes de función desconocida (Amaya-Gómez., 2009; Bernabéu-Roda, 2010).

Investigaciones realizadas en el grupo de la Dra. Soto revelan que la capacidad de desplazarse en la superficie de medios semisólidos es distinta dependiendo de la cepa de *S. meliloti* de la que se trate. Así mientras la cepa GR4 se comporta como no móvil en la superficie de medio mínimo semisólido, las cepas de referencia Rm1021 y Rm2011 sí muestran desplazamiento en estas condiciones, lo que sugiere la existencia de mecanismos de control distintos (Nogales et al. 2010; Nogales et al. 2012). Estudios enfocados a aclarar el papel del regulador transcripcional ExpR perteneciente al sistema QS de *S. meliloti*, han demostrado que la cepa Rm1021 es capaz de desplazarse en una superficie utilizando al menos dos tipos de motilidad: un movimiento independiente de la acción flagelar que es promovido por la producción de altos niveles de exopolisacáridos (EPS I y EPS II), y motilidad swarming, absolutamente

dependiente de flagelos (Nogales et al. 2012). Puesto que la secuencia *expR* de la cepa Rm1021/Rm2011 se encuentra interrumpida por una secuencia de inserción, de estos estudios se deduce que ExpR aunque promueve motilidad en superficie a través de la producción de EPS II, no es esencial para la motilidad swarming. Posteriormente Gao y colaboradores (Gao et al. 2012) han descrito y caracterizado un tipo de movimiento en superficie mostrado por una cepa *expR*$^+$ de *S. meliloti* que por su dependencia de actividad flagelar ha sido catalogado de swarming. Se trata de un desplazamiento coordinado que se pone de manifiesto en la superficie de medio LB diluido y con bajo porcentaje de agar, y que es estimulado sólo por determinadas AHLs ($C_{16:1}$ y 3-oxo- $C_{16:1}$ HL) de manera dependiente de ExpR. Estos estudios reflejan la complejidad de un fenotipo hasta ahora poco estudiado en los rizobios como es la motilidad en superficie.

9. Formación de biopelículas en *Rhizobium*

Una estrategia común usada por lasbacterias para establecerse en la rizosfera o en las raíces de las plantas, es la formación de biopelículas. La formación de una comunidad de células adheridas a una superficie facilita la comunicación entre los microorganismos que forman asociaciones (beneficiosas o patogénicas) con la planta, promueve la capacidad de virulencia, y protege las bacterias frente a las respuestas defensivas de las plantas (Danhorn and Fuqua, 2007). Tanto en asociaciones beneficiosas como patogénicas con plantas, la adhesión de las bacterias a las raíces es el primer paso necesario para llevar a cabo el proceso de infección y colonización. En el caso de la simbiosis *Rhizobium*-leguminosa, aunque los FN pueden inducir la formación de nódulos en la planta hospedadora, si la bacteria no se adhiere, los nódulos nunca llegan a ser infectados, ya que la adhesión es una etapa crítica para la formación de canales de infección que permiten a la bacteria alcanzar el primordio nodular (nódulo inmaduro)(Hirsch et al., 2009). La observación directa de los rizobios adheridos a las raíces y pelos radicales ha puesto de manifiesto que estos se organizan asemejando la organización de las células en una biopelícula (Fujishige et al., 2006c). Se ha propuesto que las células de *Rhizobium* migran a través del canal de infección como filamentos de biopelículas (Ramey, 2004). *Rhizobium* es capaz

de adherirse a las raíces de plantas leguminosas y no leguminosas. La habilidad especial de *Rhizobium* de adherirse a la raíz de leguminosas con respecto a otras bacterias tiene dos ventajas: el aumento en el número de rizobios en la rizosfera y una mayor probabilidad de infección de la planta (Danhorn and Fuqua, 2007; Rodríguez-Navarro et al., 2007). A pesar de que la adhesión es una etapa que parece ser esencial para el éxito de la simbiosis, sólo existen unos cuantos trabajos en donde se ha profundizado en su estudio. Aún no se ha descrito un mutante de *Rhizobium* cuya habilidad de adhesión haya sido completamente abolida. No obstante, se ha observado que mutantes con dificultades de adhesión (formación de biopelículas) muestran una reducción en su capacidad de formación de nódulos (Hirsch et al., 2009). La identificación y caracterización de componentes de *Rhizobium* implicados en la formación de biopelículas, así como su importancia en el establecimiento de la simbiosis comenzó hace menos de una década. Como primera aproximación en la identificación de señales medioambientales y determinantes genéticos que afectan de manera cuantitativa la capacidad de *Rhizobium* de formar biopelículas *in vitro* se está utilizando una modificación del ensayo en placas de micropocillos inicialmente desarrollado por O'Toole y colaboradores (1999). Además la microscopía láser confocal (CLSM) de células marcadas con proteínas autofluorescentes, permite monitorizar el proceso de desarrollo de biopelículas en superficies como el vidrio o raíces vegetales, siendo posible analizar su estructura tridimensional.

La formación de biopelículas de *Rhizobium* sobre superficies bióticas y abióticas fue descrita por primera vez para *S. meliloti* (Fujishige et al., 2006b; Fujishige et al., 2006c). A pesar de que se ha visto que *S. meliloti* no es un buen formador de biopelículas en placas de PVC, el uso de esta metodología ha permitido caracterizar diferentes factores de esta bacteria implicados en el establecimiento de biopelículas. Se ha visto que mientras el aumento en la concentración de nutrientes como sacarosa, fosfato y calcio favorecen el incremento en la formación de biopelículas, temperaturas o pHs subóptimos, y el estrés osmótico tienen un impacto negativo en este proceso (Rinaudi et al., 2006). *R. leguminosarum* bv. viciae es mejor formador de biopelículas que *S. meliloti* en placas de PVC y vidrio. Sobre estas superficies *R. leguminosarum* es capaz de

formar biopelículas tridimensionales y organizadas en forma de panal de abejas (Russo et al., 2006; Williams et al., 2008). Además, a diferencia de *S. meliloti*, este microorganismo forma biopelículas en la interfase líquido-aire en cultivos crecidos en medio mínimo y en agitación. Al igual que en *S. meliloti*, las condiciones de limitación de nutrientes promueven la formación de biopelículas en *R. leguminosarum*. A pesar de que las raíces de las plantas son consideradas como un ambiente rico en nutrientes, se ha visto que ambas especies son capaces de establecer biopelículas sobre ellas. Se ha propuesto que factores producidos por la planta podrían compensar el efecto inhibidor causado por los nutrientes en la formación de biopelículas de *Rhizobium* (Rinaudi and Giordano, 2010).

Se cree que el proceso de adhesión de *Rhizobium* a la raíz ocurre en dos etapas; la primera es descrita como una etapa de acoplamiento de las células a la superficie "docking" o unión no específica, y la segunda como una etapa de adhesión irreversible o "locking" (Hirsch et al., 2009). Durante el docking las células se adhieren débilmente y de manera reversible por medio de las lectinas de la planta y las ricadhesinas y flagelos de la bacteria. Con posterioridad a esta débil adhesión se produce el locking, una unión fuerte e irreversible de las bacterias a la raíz favorecido por los polisacáridos de superficie, fibrillas de celulosa, pili y otras proteínas (Hirsch et al., 2009; Robledo et al., 2012; Rodríguez-Navarro et al., 2007).

Las lectinas se definen como proteínas que de manera reversible y no enzimática se unen a carbohidratos específicos (Komath et al., 2006). De manera general se acepta que las lectinas de la planta funcionan como receptores de los polisacáridos de superficie de la bacteria. Laus et al. (2006) observaron que existe una clara interacción entre las lectinas de plantas de guisante y el radical glucomanano que forma parte de un polisacárido específico producido por *R. leguminosarum* bv. viciae (compuesto en un 95% por glucosa, manosa y pequeñas cantidades de ramnosa) localizado exclusivamente en uno de los polos de la célula bacteriana. En este estudio se observó que a pesar de que un mutante incapaz de sintetizar el radical de glucomanano de este polisacárido lograba

inducir nódulos fijadores de nitrógeno, era menos competitivo que la cepa silvestre, llevando a los autores a concluir que la adhesión de las células de *Rhizobium* se ve incrementada por la unión de las lectinas a polisacáridos específicos de la bacteria. Se han llevado a cabo experimentos en los que se han transferido lectinas de una especie de leguminosa a otra (van Rhijn et al., 2001) y se ha demostrado que si estas plantas son inoculadas con un *Rhizobium* diferente al hospedador habitual, pero específico de la leguminosa cuya lectina ha sido transferida, esté es capaz de inducir nódulos fijadores de nitrógeno en este nuevo hospedador. Rhijn et al. (2001) proponen que la lectina afín facilita la adhesión de *Rhizobium* a la superficie de la raíz, lo que permite la acumulación del FN por encima de los niveles requeridos habitualmente, y por ello es posible que se lleve a cabo la formación de nódulos fijadores de nitrógeno.

Las ricadhesinas (rhizobial calcium-binding surface proteins) median la unión polar de células individuales a los pelos radicales. Uniéndose al calcio y a uno de los polos de la bacteria y éstos a su vez a los pelos radicales de la planta, las ricadhesinas llevan a la aglutinación de células independientes (Gage, 2004). Es poco lo que se conoce sobre estas proteínas en *Rhizobium* y aún menos sobre sus receptores en las plantas. Aunque ha sido posible purificar la ricadhesina producida por *R. leguminosarum* bv. viciae, no se ha descrito cuál es el gen que la codifica (Laus et al., 2006). Smit et al. (1991) observaron que en condiciones de crecimiento con limitación de calcio (Ca^{2+}), las células de *R. leguminosarum* muestran una reducción en la capacidad de adhesión a la superficie de los pelos radicales de plantas de guisante. En estas condiciones no fue posible aislar ricadhesinas de la membrana celular. Se observó que estas proteínas eran expulsadas al medio de crecimiento. Aparentemente el ion calcio parece estar implicado en el anclaje de las ricadhesinas a la superficie celular de la bacteria y no a la unión de las ricadhesinas a la superficie de la planta (Smit et al., 1991).

Los flagelos también han sido relacionados con el docking de *Rhizobium* a la raíz. Aunque se asume un papel de la motilidad o flagelos de *Rhizobium* en la formación de biopelículas sobre raíces y pelos radicales de las plantas, lo cierto es que su contribución en la formación de biopelículas aún no se ha investigado en

profundidad. Se ha demostrado que la capacidad de formación de biopelículas de mutantes aflagelados de *S. meliloti* (mutantes *fliP* y *flgH*) en placas de PVC se ve disminuida. En condiciones axénicas estos mutantes aunque son capaces de formar nódulos fijadores de nitrógeno, muestran un retraso en la formación de nódulos (Fujishige et al., 2006b). Hirsch et al. (2009) proponen que los flagelos facilitan la unión reversible de *Rhizobium* a la raíz; sin embargo, aún no esta claro si el defecto simbiótico causado por la ausencia de flagelos se debe a la incapacidad de movimiento, a los defectos en la formación de biopelículas, o a ambos. Existen algunos ejemplos adicionales de mutantes con alteraciones tanto en motilidad como en formación de biopelículas; sin embargo, los fenotipos pleiotrópicos desarrollados por la mayoría de las cepas dificultan el establecer una conexión directa entre formación de biopelículas y motilidad. Tal es el caso de los mutantes de *S. meliloti exoR95* y *exoS96* mencionados anteriormente. Otro ejemplo es el del mutante *rosR* de *R. leguminosarum* vb trifolii, que muestra un descenso significativo en motilidad y un fenotipo alterado en formación de biopelículas en superficies de plástico. Estos mutantes forman nódulos no fijadores en trébol y además muestran un grave defecto en competitividad por la nodulación, fenotipos que podrían ser explicados por una disminución en la producción de EPSs (Janczarek et al., 2010). De igual manera, se ha observado que mutantes *fabF2/F1* de *R. leguminosarum* vb. viciae, que muestran alteraciones en LPS y diferentes fenotipos asociados con modificaciones en la envoltura celular, son no móviles y las células se organizan de distinta manera dentro de las biopelículas (Vanderlinde et al., 2009). Recientemente, en *S. meliloti*, un incremento en motilidad se ha correlacionado con un incremento en dispersión de la biopelícula como consecuencia de la reducción de los niveles intracelulares de di-GMPc causados por la expresión de BdcA de *E. coli*; una proteína que une di-GMPc (Ma et al., 2011). No obstante, los cambios en los niveles de di-GMPc pueden afectar otros mecanismos celulares, y debido a esto, los defectos en formación de biopelículas no pueden ser atribuidos únicamente al incremento en motilidad.

Los polisacáridos bacterianos de superficie tales como EPSs, lipopolisacáridos (LPSs), polisacáridos capsulares (KPSs) y β-1-2 glucanos, junto

con las fibrillas de celulosa, pili e incluso FN, parecen mediar la adhesión firme de las bacterias a los pelos radicales y anclar las bacterias a la superficie de la raíz. La pérdida de función de diversos genes implicados en la producción de EPS (Bomfeti et al., 2011), LPS (Carlson et al., 2010), β-1-2-glucanos o KPS (Fraysse et al., 2003; Skorupska et al., 2006) provoca una disminución de la capacidad de adhesión de los rizobios a la raíz y una reducción de la capacidad de colonización e infección de nódulos.

Mutantes defectivos en la producción de EPSs generalmente muestran menor capacidad de formación de biopelículas, mientras que cepas súperproductoras de EPSs muestran una mayor capacidad de adherencia y formación de biopelículas que a pesar de ser más gruesas, son menos estables que las de la cepa parental (Fujishige et al., 2006c; Rinaudi and Giordano, 2010; Rinaudi and González, 2009; Wells et al., 2007). *S. meliloti* produce dos tipos de EPSs; EPS I o succinoglicano y EPS II o galactoglucano. Un mutante *exoY* de *S. meliloti*, defectivo en la producción de EPS I, es incapaz de formar biopelículas maduras. Por otra parte, mutantes *exoR95* y *exoS96*, súperproductores de EPS I, son mejores formadores de biopelículas en PVC, aunque estas biopelículas se desprenden fácilmente de la superficie al llevarse a cabo el lavado de los pocillos (Fujishige et al., 2006b; Wells et al., 2007). La mayor capacidad de formación de biopelículas mostrada por estos mutantes, sin embargo, no puede ser únicamente atribuída a la súperproducción de EPS I ya que estos mutantes exhiben fenotipos pleiotrópicos como la ausencia de flagelos, componentes que son importantes para el establecimiento de biopelículas en distintas bacterias. En cuanto al EPS II, Rinaudi and González (2009) mostraron evidencias de que la producción de la fracción de bajo peso molecular de este polisacárido es esencial para que *S. meliloti* pueda desarrollar biopelículas estructuradas sobre las raíces de las plantas. Los EPSs también han sido relacionados en la formación de biopelículas de otros *Rhizobium* como *R. leguminosarum* bv. viciae, *Mesorhizobium tianshanense* el simbionte de *Glycyrrhiza uralensis*, y en el simbionte de soja *Bradyrhizobium japonicum* (Pérez-Giménez et al., 2009; Russo et al., 2006; Wang et al., 2008). De manera general se cree que al igual que para otras bacterias, en *Rhizobium* los EPSs son importantes para estabilizar la estructura tridimensional

del biofilm o al servir como andamios de otras moléculas que mantienen la biopelícula unida.

En cuanto a los LPSs, se ha visto que en *S. meliloti* una mutación en *lpsB* (codifica la glicosiltransferasa I responsable de la biosíntesis del esqueleto de los LPSs), o en *bacA*, la cual genera defectos en distribución de los ácidos grasos que forman parte del lípido A, conlleva una disminución en la formación de biopelículas en placas de micropocillos de PVC, siendo ésta más evidente en el caso del mutante en *bacA* (Fujishige, 2006). El mutante en *bacA*, además, muestra una reducción tanto en la frecuencia de formación de microcolonias en forma de torre como en el tamaño de éstas.

Los genes relacionados con β-1,2-glucanos en *S. meliloti* son los genes *ndvA* y *ndvB*. El gen *ndvB* codifica la proteína de membrana citoplasmática que se encarga de la síntesis de β-glucanos cíclicos desde UDP-glucosa, y *ndvA* codifica la proteína de transporte de unión a ATP responsable de la secreción de los β-glucanos al espacio intercelular. Mutaciones en alguno de estos genes causan una reducción en adhesión de las células de *S. meliloti* a la raíz de la planta. El mutante *ndvB* además muestra una reducción del 41% en la formación de biopelículas en una superficie de plástico (Fujishige, 2006). Es importante mencionar que además de su importancia en la etapa de adhesión, se ha visto que los EPSs, LPS, KPS y β-1-2-glucanos son requeridos en etapas posteriores de la simbiosis, atribuyéndoles varias posibles funciones: i) actuar como molécula señal induciendo procesos específicos de la simbiosis o bloqueando respuestas defensivas de la planta, ii) actuar a modo de barrera que protege a la bacteria de mecanismos de defensa del vegetal, o iii) permitir la adaptación de la bacteria a los distintos ambientes con los que se encontrará a lo largo del proceso infectivo (Soto et al., 2009; Soto et al., 2006).

El otro polisacárido que se ha visto que juega un papel importante en la formación de biopelículas por *Rhizobium* o microorganismos muy relacionados es la celulosa. Es poco lo que se conoce sobre la producción de celulosa y su papel en la simbiosis. En el caso de algunas de las especies para las que se ha descrito

la producción de celulosa, se ha propuesto que este polisacárido es requerido para lograr una infección óptima de los pelos radicales largos y para la formación de agregados o "caps" a pH 6.5 y 7.5 tras la adhesión inicial de la bacteria a los pelos radicales (Mateos et al., 1995; Smit et al., 1992). Recientemente, Robledo et al. (2012) han demostrado que alteraciones en los niveles de endoglucanasa CelC2 en una cepa silvestre de *R. leguminosarum* bv. trifolii ocasionan una reducción de la capacidad de formación de biopelículas tanto en superficies abióticas como *in planta*. Los autores proponen que CelC2 modula la longitud de las fibrillas de celulosa que median la adhesión firme de las células de *Rhizobium* y que la celulosa es un componente esencial de la arquitectura de la matriz polisacarídica de la biopelícula.

Las señales de QS han sido relacionadas con numerosos procesos en *Rhizobium* entre los que se encuentra la formación de biopelículas. En cepas de *S. meliloti* con un *expR* funcional, la formación de biopelículas es controlada por el sistema de QS ExpR/Sin a través de la producción de EPS II. Rinaudi and González (2009) sugieren que la fracción de bajo peso molecular del EPSII puede controlar la formación de biopelículas tanto *in vivo* como *in vitro*. Se ha postulado que el EPSII provee la matriz que permite que se desarrollen biopelículas altamente organizadas. Por el contrario, en *R. leguminosarum*, la interrupción del sistema de QS CinIR o de *expR* lleva a un incremento en la formación de biopelículas (Edwards et al., 2009). Dos estudios diferentes sugieren que las señales de QS en *Mesorhizobium* regulan positivamente la formación de biopelículas en *M. huakuii* (Wang et al., 2004a) y en *M. tianshanense* (Wang et al., 2008). En *R. etli* se ha visto que las señales de QS participan la dispersión de biopelículas ya formadas (Daniels et al., 2004).

Además de los flagelos/motilidad, los EPSs, y las señales de QS, se ha visto que algunos factores específicos de *Rhizobium* participan en la formación de biopelículas. Mutantes delecionados en el plásmido pSym de *R. leguminosarum* bv. viciae muestran una reducción en la capacidad de formación de biopelículas sugiriendo que factores codificados en este plásmido son necesarios en el establecimiento de biopelículas de esta bacteria (Fujishige et al., 2006a). En

Rhizobium, los genes *nod* y sus productos (los FN) son esenciales para el desarrollo de nódulos fijadores de nitrógeno en leguminosas. Fujishige et al. (2008) han demostrado que los FN además de ser requeridos en el proceso de simbiosis también son requeridos en el establecimiento de biopelículas maduras. Mutantes en los genes *nod* son incapaces de formar biopelículas tridimensionales tanto en superficies abióticas como bióticas. Se ha propuesto que además de su función como morfógenos, el esqueleto del FN funciona como una adhesina que mantiene las células de *Rhizobium* unidas confiriendo a la bacteria mayor resistencia a la desecación y/o a las respuestas defensivas de la planta.

Objetivos

Las bacterias del suelo conocidas globalmente como *Rhizobium* establecen simbiosis mutualista con plantas leguminosas. El éxito de la asociación depende, entre otros, de los mecanismos que *Rhizobium* utiliza para colonizar, invadir y establecer la infección crónica en su hospedador. Swarming y formación de biopelículas son dos fenómenos multicelulares ligados a superficie que han sido relacionados con la capacidad infectiva e invasiva de bacterias patógenas. Los escasos estudios que se han realizado sobre estos dos fenómenos en bacterias beneficiosas como *Rhizobium* sugieren que al igual que en bacterias patógenas, componentes esenciales en motilidad swarming y/o formación de biopelículas, o factores que se expresan durante estos procesos, pueden ser importantes en la interacción con su hospedador.

El **Objetivo General** de este trabajo ha sido el de identificar nuevos genes bacterianos que pueden ser importantes en la colonización de las plantas, a través de la identificación y caracterización de determinantes genéticos implicados en el swarming en la bacteria modelo *Sinorhizobium meliloti* y estudiar su posible conexión con formación de biopelículas. Para ello se han abordado los siguientes **objetivos específicos:**

1. Determinar el patrón de expresión génica global de *S. meliloti* durante el swarming.
2. Estudiar el efecto sobre formación de biopelículas desarrolladas por *S. meliloti* de distintos factores que influyen en la motilidad swarming de esta bacteria.
3. Investigar el papel específico que desempeña el sideróforo rizobactina 1021 durante el swarming y formación de biopelículas de *S. meliloti* Rm1021.
4. Analizar el fenotipo simbiótico de mutantes identificados en este estudio afectados en swarming y en formación de biopelículas.

Materiales y Métodos Generales

1. Técnicas microbiológicas

1.1. Cepas y plásmidos utilizados

Las cepas de *S. meliloti* y *E. coli*, así como los plásmidos empleados en este trabajo, junto con sus características más relevantes se describen en las tablas 1 y 2.

Tabla 1. Cepas utilizadas en este trabajo

Bacteria	Características relevantes	Referencias
Escherichia coli		
DH5α	*sup*E44, Δ*lac*U169, *f*80, *Lac*ZΔM, 5*hsd*R171, *rec*A1, *end*A1, *gyr*A96, *thi*-1, *rel*A1	Bethesda Research Laboratory
S17-1	*thi*, *pro*, *recA*, *hsdR*, *hsdM*, RP4-2-2Tc::Mu, Km::Tn*7*, Tp^r,Sm^r	(Simon et al., 1983)
Sinorhizobium meliloti		
Rm1021	Cepa silvestre, Nod$^+$, Fix$^+$, SU47 *expR102*::ISR*m*2011-1;Sm^r.	(Meade and Signer, 1977)
GR4	Cepa silvestre, Nod$^+$, Fix$^+$	(Casadesus and Olivares, 1979)
1021FDCSS	Rm1021 (Δ*fadD*::SmSp); Sm^r Sp^r	(Amaya-Gómez., 2009)
GR4FDCSS	GR4 (Δ*fadD*::SmSp); Sm^r, Sp^r	(Amaya-Gómez., 2009)
QS77	GR4 (*fadD*::Tn*5*), Km^r	(Soto et al., 2002)
1021FDC5	Rm1021 (Δ*fadD*::Km), Sm^r, Km^r	Este trabajo
1021rhbA	Rm1021 (*rhbA*::Tn*5lac*); Sm^r Nm^r	(Nogales et al., 2012)
1021rhbD	Rm1021 (Δ*rhbD*); Sm^r	Este trabajo
1021rhbG	Rm1021 (Δ*SMa2339*); Sm^r	Este trabajo
Rm2011	SU47 *expR102*::IS*Rm*2011-1; Sm^r	(Casse et al., 1979)
2011FDC	Rm2011 (Δ*fadD*::SmSp); Sm^r, Sp^r	Este trabajo
SmA818	Rm2011 curado de pSymA; Sm^r	(Oresnik et al., 2000)
A818FDC	SmA818 (Δ*fadD*::SmSp); Sm^r, Sp^r	Este trabajo
2011rhbA62	Rm2011 (*rhbA*::Tn*5lac*); Sm^r, Rif^r, Nm^r	(Lynch et al., 2001)
2011rhbAFDC	2011rhbA62 (Δ*fadD*::SmSp); Sm^r, Sp^r,Rifr, Nm^r	Este trabajo

2011rhbE11	Rm2011 (*rhbE*::Tn*5lac*); Sm^r, Rif^r, Nm^r	(Lynch et al., 2001)
2011rhbEFDC	2011rhbE11 (Δ*fadD*::SmSp); Sm^r, Sp^r, Rif^r, Nm^r	Este trabajo
2011rhrA26	Rm2011 (*rhrA*::Tn*5lac*); Sm^r, Rif^r, Nm^r	(Lynch et al., 2001)
2011rhrAFDC	2011rhrA26 (Δ*fadD*::SmSp); Sm^r, Sp^r, Rif^r, Nm^r	Este trabajo
2011rhtA1	Rm2011 (*rhtA*::Tn*5*); Sm^r, Rif^r, Nm^r	(Lynch et al., 2001)
2011rhtAFDC	2011rhtA1 (Δ*fadD*::SmSp); Sm^r, Sp^r, Rif^r,Nm^r	Este trabajo
G212rirA	Rm1021 (*lac*-, *rirA*::Km); Sm^r, Km^r	O'Connell, M. (Osterås et al., 1995)
G212rirAFDC	G212rirA (Δ*fadD*::SmSp); Sm^r, Km^r	Este trabajo
GR4-*gfp*	GR4 (pHC60); Tc^r	Este trabajo
GR4FDCSS-*gfp*	GR4FDCSS (pHC60); Sm^r Sp^r Tc^r	Este trabajo
Rm1021-gfp	Rm1021 (pHC60); Sm^r Tc^r	Este trabajo
1021FDCSS-*gfp*	1021FDCSS (pHC60),); Sm^r Sp^r Tc^r	Este trabajo
1021rhbA-*gfp*	1021rhbA3 (pHC60),); Sm^r Nm^r Tc^r	Este trabajo
1021rhbG-*gfp*	1021rhbG (pHC60); Sm^r Tc^r	Este trabajo
1021rhbD-*gfp*	1021rhbD (pHC60); Sm^r Tc^r	Este trabajo
G212rirA-*gfp*	G212::rirA (pHC60),); Sm^r Km^r Tc^r	Este trabajo
1021(pGus3)	Rm1021(pGus3); Sm^r Km^r	(Amaya-Gómez., 2009)
2011(pGus3)	Rm2011(pGus3); Sm^r Km^r	Este trabajo

Tabla 2. Plásmidos utilizados en este trabajo

Plasmidos	Características relevantes	Referencias
pGEM-T easy	Vector de clonación para fragmentos de PCR; Ap^r	Promega
pBSKS(+)	Vector de clonación; Ap^r	Stratagene
pCR®-XL-TOPO®	Vector de clonación para productos de PCR; Km^r	Invitrogen®
pHP45Ω Km	Plásmido portador de un cassette de Sm/Sp; Ap^r, Sm^r, Sp^r	(Fellay et al., 1987)
pHP45Ω Km	Plásmido portador de un cassette de Km; Ap^r, Km^r	(Schäfer et al., 1994)
pK18mobsacB	Plasmido suicida; Km^r	(Schäfer et al., 1994)

pBBRD4	Derivado de pBBR1MCS-3 que contiene el gen *fadD* de *S. meliloti* GR4; Tc^r	(Soto et al., 2002)
pBSDIL12	Derivado de pBSKS que contiene el gen *fadD* de *S. meliloti* GR4; Ap^r	Este trabajo
pBS12.6Km	Derivado de pBSDIL12 que contiene el gen *fadD* delecionado, e interrumpido con un cassette de Km; Ap^r, Km^r	Este trabajo
pK18fadDCKm	Derivado de pK18*mobsacB* portador de la versión mutada del gen *fadD* de pBS12.6Km; Km^r	Este trabajo
pK18fadDCSS	Derivado de pK18fadDCKm en el que el cassette de Km que interrumpía el gen *fadD* fue substituído por un cassette Sm/Sp; Km^r, Sm^r, Sp^r	Este trabajo
pGrhbD	Derivado de pGEm-T easy portador de la versión mutada del gen *rhbD*; Ap^r	Este trabajo
pKrhbD	Derivado de pK18*mobsacB* portador de la deleción mutada del gen *rhbD*; Km^r.	Este trabajo
pGrhbG	Derivado de pGEM-T easy portador de la versión mutada del gen *SMa2339*; Ap^r	Este trabajo
pKrhbG	Derivado del pK18*mobsacB* portador de la deleción del gen *SMa2339*; Km^r	Este trabajo
pGus3	Plásmido con la fusión entre el promotor del gen *nfeD* y el gen *gusA* del pBI100. Km^r	(Garcia-Rodriguez and Toro, 2000)
pHC60	Plásmido estable en *Rhizobium* que expresa constitutivamente GFP; Tc^r	(Cheng and Walker, 1998)

1.2. Medios de cultivo

1.2.1. Medios de cultivo para *E. coli*

Para el cultivo de *E. coli*, se utilizó habitualmente el medio Luria-Bertani (**LB**), (Miller, 1972), cuya composición es la siguiente:

NaCl.....5 g

Triptona.....10 g

Extracto de levadura.....5 g

Agar (para medio sólido).....15 g

Agua desionizada.....1000 ml

El medio se esterilizó en autoclave a 120 ºC durante 20 min.

1.2.2. Medios de cultivo para rizobios

El medio completo utilizado para el crecimiento de *S. meliloti* fue el medio Triptona-extracto de levadura (**TY**) (Beringer, 1974), cuya composición es la siguiente:

Triptona.....5 g
Extracto de levadura.....3 g
$CaCl_2.2H_2O$.....0,9 g
Agar (medio sólido).....15 g
Agua desionizada.....1000 ml

El medio se esterilizó en autoclave a 120 ºC durante 20 min.

Como medio mínimo (**MM**) para *Rhizobium* se ha empleado el de Robertsen et al. (1981), modificado según se especifica a continuación:

K_2HPO_4.....0,3 g
KH_2PO_4.....0,3 g
$MgSO_4.7H_2O$.....0,15 g
$CaCl_2.2H_2O$.....0,05 g
$FeCl_3$.....0,006 g
NaCl.....0,05 g
Glutamato sódico.....1,1 g
Manitol.....10 g
Solución de vitaminas*.....1 ml
Agar purificado PRONADISA (medio sólido)...13 g
Agua destilada.....1000 ml

Para los ensayos de swarming se usó una concentración del 0.6% de agar purificado PRONADISA, o agar noble DiftcoTM. Se ajustó a un pH de 6.8-7.2, y se esterilizó en autoclave a 120 ºC durante 20 min.

*La solución concentrada de vitaminas (1000x) consta de:

Biotina..... 0.2 g
Clorhidrato de tiamina..... 0.1g
Pantotenato sódico.....0.1g
Agua destilada.....1000 ml

Se esterilizó por filtración y se adicionó 1 ml/litro al MM autoclavado.

Para los ensayos de swimming se utilizó el medio Bromfield (**BM**).

Triptona……..0.4g
Extracto de levadura……0.1g
$CaCl_2$……0.1g
Agar Bacteriológico……3g
Agua destilada……1000 ml

Como medio para la inducción de producción del sideróforo rizobactina 1021 y sus intermediarios de biosíntesis se ha empleado el Iron Deficient Media (**IDM**) de Müller and Raymond (1984) con algunas modificaciones:

Para la preparación del IDM se utilizaron recipientes plásticos descontaminados de hierro lavando con HCL 6M.

Soluciones stock de elementos traza
Tiamina……20 mg/ml H_20
$ZnSO_4$. $7H_2O$……20 mg/ml H_20
$CuSO_4$……0,5 mg/ml H_20
$MnSO_4$. H_2O……3.5 mg/ml H_20

Soluciones stock de otros compuestos
$CaCl_2$……0,5 g/50 ml H_20
Extracto de levadura……0,25 g/50 ml H_20
Sacarosa……22,24 g/50 ml H_20

Receta para 1L de IDM

K_2SO_4……2 g
K_2HPO_4……3 g
NaCl……1 g
NH_4Cl……5 g

La solución debe ser agitada durante una noche con 50 g de Chelex-100 (forma sódica). Para evitar evaporación de la solución, el vaso de precipitado se cubrió con papel parafilm.

A continuación la resina de Chelex se retiró mediante filtración con un círculo de papel Whatman y se añadieron los elementos traza en las siguientes concentraciones.

Por litro de IDM se deben añadir:
100µl del stock de tiamina
100µl del stock de $ZnSO_4.7H_2O$
10µl del stock de $CuSO_4$
10µl del stock de $MnSO_4.H_2O$
80mg de $MgSO_4.7H_2O$

Finalmente el medio fue autoclavado y justo antes de ser utilizado se añadieron por cada 50 ml de medio, 500 µl de cada solución de stock de $CaCl_2$, extracto de levadura y sacarosa.

1.3. Antibióticos

La adición de antibióticos a los medios de cultivo se realizó a partir de soluciones concentradas (100X) de los mismos en agua desionizada y posterior esterilización con unidades de filtración Minisart® NML (Sartorius) de 0.2 µm de tamaño de poro. En el caso de la solución de tetraciclina no fue necesaria la esterilización por filtración ya que se empleó metanol para disolverla. La concentración final de los distintos antibióticos utilizados en este trabajo se indica en la tabla 3.3.

Tabla 3. Antibióticos

Antibiótico	Concentración (µg/ml)	
	E. coli	*S. meliloti*
Ampicilina (Ap)	200	-
Espectinomicina (Spc)	100	100
Sulfato de estreptomicina (Sm)	50	200
Sulfato de kanamicina (Km)	50	200
Sulfato de neomicina (Nm)	-	100
Tetraciclina (Tc)	10	10

1.4. Conservación de cepas bacterianas

Para la conservación prolongada de las distintas cepas se utilizaron criotubos que contenían alícuotas de cultivos en fase logarítmica adicionados con glicerol estéril a una concentración final del 20%. Los criotubos se almacenaron a una temperatura de -80 ºC.

1.5. Conjugaciones biparentales

Esta técnica se utilizó cuando fue necesaria la transferencia de un plásmido entre cepas bacterianas. Las conjugaciones se realizaron mezclando un cultivo en fase logarítmica de crecimiento del donador (O.D. 600 nm entre 0.6 y 0.7 para *E. coli* S17-1), con otro en fase exponencial tardía del receptor (O.D. 600 nm superior a 1), en proporción 1:1. Donador y receptor se precipitaron y se lavaron varias veces con medio líquido (el mismo usado para el crecimiento del cultivo) para eliminar restos de antibióticos. Finalmente, la mezcla se resuspendió en un pequeño volumen (30 µl) y se depositó sobre un filtro Millipore estéril de 0.45 µm de poro y 2.5 cm de diámetro, previamente colocado sobre una placa de medio TY sólido. La mezcla se incubó de este modo durante 16-20h a 28°C. Transcurrido este tiempo la mezcla de conjugación se resuspendió en medio líquido estéril, se lavó y se sembró sobre placas de medio selectivo.

1.6. Ensayos de motilidad swarming

Para mantener la reproducibilidad del comportamiento en swarming todos los cultivos líquidos rutinariamente partieron del stock de glicerol. Las cepas de

S. meliloti se crecieron en agitación a 30 ºC en medio TY líquido hasta una O.D. 600 nm de 0.9 -1. Después de la incubación, las células se recogieron por centrifugación, se lavaron dos veces con MM y se resuspendieron en este mismo medio en una décima parte del volumen inicial. Alícuotas de 2 µl de esta suspensión, se colocaron sobre la superficie de placas de Petri preparadas con 20 ml de MM conteniendo agar al 0.6% y secadas durante 15 min a temperatura ambiente. Tras la colocación de las gotas, éstas se dejaron secar a temperatura ambiente durante 10 min. Las placas se incubaron en posición invertida durante 24 h.

Para facilitar la comparación de las colonias swarming de los mutantes construidos con respecto a la cepa parental, se procedió a medir la longitud de cada uno de los lados del teórico rectángulo que engloba a la colonia (en centímetros) y se realizó la media de esos valores. A los resultados obtenidos de un mínimo de tres experimentos independientes (con al menos 2 réplicas técnicas), se les aplicó el error típico con un nivel de confianza del 95%.

1.7. Ensayos de motilidad swimming

Las cepas de *S. meliloti* se crecieron en agitación a 30 ºC en medio TY líquido hasta una O.D. 600 nm de 0.9 -1. Después de la incubación, alícuotas de 3 µl del cultivo se colocaron sobre la superficie de placas de Petri preparadas con 25 ml de BM 0.3% de agar, secadas a temperatura ambiente tapadas. Tras la colocación de las gotas las placas se incubaron boca arriba durante 48h.

Para facilitar la comparación de las colonias swimming de los mutantes construidos con respecto a la cepa parental, se procedió a medir el diámetro del halo de dispersión de la colonia a las 48h de incubación y se calculó la media. A los resultados obtenidos de un mínimo de tres experimentos independientes (con al menos 2 réplicas técnicas), se les aplicó el error típico.

1.8. Ensayos de formación de biopelículas

1.8.1. Formación de biopelículas en placas multipocillo de cloruro de polivinilo (PVC)

Para la medida de formación de biopelículas en placas multipocillo se siguió el procedimiento descrito por O'Toole et al. (1999) y más recientemente por Fujishige et al. (2006) con algunas modificaciones. Este ensayo se basa en la capacidad de adhesión de células bacterianas a la superficie de placas de 96 multipocillos de PVC (Falcon 3911, Becton Dickinson, Franklin Lakes, NY).

1. Las cepas de *S. meliloti* fueron crecidas en MM adicionado con antibióticos hasta una O.D. 600 nm de 1.5-2.
2. Los cultivos fueron lavados 2 veces con MM sin hierro.
3. Las células se resuspendieron bien en MM con una concentración de 22 µM $FeCl_3$ (MM de uso rutinario) o 220 µM de $FeCl_3$ si se deseaba evaluar la formación de biopelículas en MM en presencia de altas concentraciones de hierro.
4. 150 µl de una dilución a O.D. 600 nm de 0.2 se puso en cada micropocillo. Las placas fueron cubiertas con tapas Falcon 3913, Becton Dickinson, Franklin Lakes, NY e incubadas a 30 ºC durante 48 h, sin agitación en una cámara húmeda para evitar la evaporación del medio. La cámara húmeda consintió en un recipiente de plástico con tapa dentro del cual se mantuvo un papel humedecido con agua.
5. Antes de proceder con la tinción de la biopelícula, se verificó que al final del experimento las cepas a estudiar presentaban la misma densidad óptica. Para ello se leyó la O.D. 590 nm de los cultivos crecidos en los pocillos haciendo uso del lector de placas de micropocillos Elisa SunriseTM (Tecan Group Ltd, Männedorf, Switzerland).
6. Por aspiración con el kitasato, el medio de cultivo y las células que no se habían adherido a las paredes de los pocillos fueron retirados.
7. Cada pocillo fue teñido con 180 µl de una solución de cristal violeta (CV) al 0.1% durante 20 min y posteriormente lavado con 180 µl de agua destilada estéril tres veces, dejando el agua de cada lavado durante 5 min.

8. La placa se dejo secar durante al menos 1h a temperatura ambiente en la campana de extracción de gases.
9. Tras desteñir los pocillos con 180 µl de una solución 80% etanol/20% acetona, la biomasa adherida fue cuantificada midiendo la O.D. 550 nm en el lector de placas SunriseTM.

El análisis de los datos obtenidos se realizó de al menos 60 pocillos provenientes de tres experimentos independientes. Los datos fueron sometidos a la prueba de Levene para evaluar la igualdad de varianzas con el programa SPS 15.0 para Windows (SPSS Inc., Chicago, iL, USA). La diferencia estadística entre la media de los datos fue evaluada por medio de la prueba *t* Student asumiendo varianzas desiguales (Prueba de Welch). Cuando el test de Welch mostró que la diferencia entre la media de los datos tenía una probabilidad $P < 0.01$ la media de los datos comparados se consideró como distinta.

1.8.2. Formación de biopelículas en superficie de vidrio

Esta técnica permite la observación in vivo de la estructura de la biopelícula formada sobre una superficie de vidrio a lo largo del tiempo, para ello se siguió el protocolo descrito por O'Toole et al. (1999) y más recientemente por Rinaudi and González (2009).

1. Las cepas de *S. meliloti* marcadas con la GFP (Green Fluorescence Protein) fueron crecidas de igual manera que para el ensayo de observación de biopelículas en superficie de placas de microtitulación de PVC (sección 1.8.1).
2. 500 µl de la dilución de células lavadas a O.D. 600 nm de 0.2 fueron puestos en cada pocillo de las chambered cover glass slides con 1 µm de borosilicato en la base (Lab-Tek no. 155411; Nunc).
3. Las placas de vidrio fueron incubadas a 30 ºC, en una cámara húmeda y sin agitación. La cámara húmeda consintió en una palca de Petri que guardaba la placa de vidrio, dispuesta dentro de un recipiente de plástico con tapa que contenía en el fondo un papel humedecido con agua.

4. Transcurrido el tiempo de incubación (de 3 a 10 días), el medio de cultivo fue aspirado y las células no adheridas fueron retiradas lavando cada pocillo con 500 µl de agua estéril.
5. La arquitectura tridimensional de la biopelícula formada fue observada por medio de microscopía laser confocal (CLSM). Al observar al microscopio la biopelícula fue estudiada haciendo fotografías de varios segmentos de la superficie con los objetivos 4x, 40x y 100x.
6. El análisis de las imágenes se realizó con el programa EZ-C1 free viewer de Nikon.

1.8.3. Formación de biopelículas en raíces de plantas

La esterilización de las semillas de alfalfa fue llevada a cabo como se describe más adelante en la sección 3.1. Para el crecimiento de las plantas se utilizó la solución mineral libre de nitrógeno descrita por Rigaud and Puppo (1975), la cual se describe posteriormente en la sección 3.2. La solidificación de esta solución se llevó a cabo adicionando agarosa al 0.8%. En cada placa cuadrada de 12.5 cm x 12.5 cm se sirvieron 45ml de la solución para plantas con agarosa. Para evitar la adhesión de las raíces, sobre la superficie de agar se dispuso un papel de filtro Whatman cuadrado que se humedeció con 2 ml de agua estéril. Por placa se pusieron 15 semillas recién germinadas de aproximadamente 1 cm de largo y fueron inoculadas como se describe a continuación.

1. Las cepas marcadas con la GFP de *S. meliloti* fueron crecidas en placas de medio TY adicionado con los correspondientes antibióticos para cada cepa.
2. Para la inoculación de las raíces se tomó masa celular de cada cepa y se resuspendió en TY hasta O.D. 600 nm de 0.1. Esta suspensión celular se lavo una vez con agua destilada estéril y de aquí se hicieron diluciones seriadas 1/10 hasta obtener una dilución de 1×10^4 células/ml.
3. Cada plántula se inoculó bañando la raíz desde el ápice hacia arriba con 30µl de la dilución celular que contenía 1×10^4 células/ml. Diluciones seriadas del inóculo fueron sembradas en placas de medio TY adicionadas con el

correspondiente antibiótico de cada cepa, para llevar el control del número de CFUs con el que las plántulas habían sido inoculadas.

4. Las placas fueron selladas con papel parafilm dejando el borde superior de la placa descubierta. Para evitar la incidencia de la luz sobre la raíz, la parte inferior de la placa fue cubierta con un sobre de papel oscuro. La incubación de las plantas se llevó a cabo en cámaras con una emisión de intensidad lumínica de 500 μeinstein x m^{-2} x s^{-1}(λ = 400 – 700 nm), fotoperiodo 15/9 horas luz/oscuridad, temperatura de 24/18 ºC - día/noche y humedad relativa de un 50%.

5. A los tiempos determinados, de 1 a 3 días al menos 10 raíces por cepa fueron lavadas y observadas al microscopio. Para llevar a cabo el lavado, el papel sobre el que crecieron las plantas fue colocado sobre una rejilla de plástico y sujetado con una goma. La rejilla fue sumergida en un recipiente de plástico con agua y agitada vigorosamente de manera que todas aquellas células bacterias que no estaban firmemente adheridas a la raíz fueran retiradas. Este proceso fue repetido tres veces utilizando agua limpia en cada repetición.

6. Para la observación al microscopio las plántulas fueron puestas sobre un portaobjeto, de tal manera que la cara superior de la raíz, es decir la opuesta a la que estaba en contacto directo con el papel, fuera la cara objeto de observación.

7. La raíz fue cubierta con un cubre objeto y estudiada en el microscopio invertido de fluorescencia con el objetivo de 20x.

8. La distribución de las bacterias a lo largo de la raíz fue registrada y por medio de CLSM se hicieron fotos representativas de esta distribución. Las imágenes en el CLSM fueron tomadas con el objetivo 20x multi-inmersión.

1.9. Curvas de crecimiento

Las curvas de crecimiento se realizaron en placas multipocillo de poliestireno de 9x7.5 cm. Generalmente, se utilizó un medio mínimo (MM) y un medio rico (TY) sin antibióticos para poder hacer comparaciones entre las distintas cepas.

En cada pocillo se aplicó 350 µl de un inóculo conteniendo 5 $\times 10^7$ células/ml de medio de cada una de las cepas. Para ello, se hicieron precultivos en TY adicionando los correspondientes antibióticos. Cuando estos cultivos alcanzaron una O.D. 600 nm aproximada de 1 se lavaron dos veces con MM para eliminar los restos de TY y se diluyeron en medio pasivo (MM o TY) hasta obtener aproximadamente 5 $\times 10^7$ células/ml. En cada experimento se llevaron tres réplicas de cada cepa. La turbidez de los cultivos se determinó a intervalos regulares de tiempo (cada dos horas) durante dos días, en un Microbiology Reader Bioscreen C a 28ºC y a una longitud de onda comprendida entre 420-580 nm.

Alternativamente, las curvas de crecimiento se determinaron en tubos de vidrio con 3 ml de TY o MM sin antibióticos. Se partió de una densidad celular inicial de 5 × 10^7 células/ml, diluyendo de un preinóculo de TY crecido con antibióticos hasta O.D. 600 nm = 1. En el caso de la curva realizada con MM fue necesario lavar dos veces y después diluir el cultivo. La turbidez de los cultivos se determinó a intervalos regulares de tiempo en un espectofotómetro a una O.D. 600 nm.

2. Técnicas de biología molecular

2.1. Aislamiento de ADN plasmídico

Según requerimientos, compatibilidades y necesidades se han utilizado 2 métodos distintos:

2.1.1. Mini preparación mediante lisis alcalina

Se llevó a cabo el protocolo descrito por Sambrook y colaboradores (1989) que consistió en:

1. Inocular la bacteria portadora del plásmido en 3 ml de medio suplementado con los correspondientes antibióticos e incubar a temperatura óptima (37ºC para *E. coli*, o 30 ºC para *S. meliloti*) durante 12-15 horas.
2. Centrifugar las células en tubos de microfuga (12.000 rpm, 3 min). Retirar el sobrenadante.
3. En el caso de *S. meliloti*, resuspender el sedimento en 200 µl de sarkosyl 0,1% en TE, para eliminar restos de polisacáridos. Centrifugar las células (12.000 rpm, 3 min). Eliminar el sobrenadante.
4. Resuspender el sedimento en 100 µl de solución I. Dejar 5 min a temperatura ambiente.
5. Añadir 200 µl de solución II. Mezclar por inversión rápida unas 3 veces. Dejar en hielo 5 min.
6. Añadir 150 µl de solución III fría. Mezclar suavemente por inversión manual varias veces. Dejar en hielo 5 min.
7. Centrifugar durante 5 min a 12.000 rpm.
8. Recoger el sobrenadante y adicionar 1 volumen (400 µl, aproximadamente) de una mezcla de fenol/cloroformo (1:1).
9. Agitar con vórtex y centrifugar 5 min a 12.000 rpm.
10. Recoger en un nuevo tubo la fase superior acuosa que contiene el ADN.
11. Añadir 2,5 volúmenes (1ml) de etanol al 100% pre enfriado a -20ºC. Mezclar por inversión y dejar a – 80ºC al menos 30 min.
12. Centrifugar 15 min a 12.000 rpm.
13. Retirar el sobrenadante.
14. Añadir 200 µl de etanol 70% frío y centrifugar 3 min a 12.000 rpm. Eliminar el sobrenadante
15. Secar el precipitado al vacío, 5-10 min, aproximadamente.
16. Resuspender el precipitado en 20 - 40 µl de tampón TE o H_2O milli-Q. Conservar a -20ºC.

SOLUCIONES:

Solución I:

Glucosa 50 mM

EDTA 10 mM

Tris-HCl 25 mM pH 8
Lisozima, 4mg/ml

Solución II:
NaOH 0,2 M
SDS 1%

Solución III:
Acetato potásico 5 M (60 ml)
Ácido acético glacial (11,5 ml)
H_2O (28,5 ml); pH 4,5.
Tampón TE:
Tris 10 mM
EDTA 1 mM, pH 8,0

Mezcla fenol:cloroformo (1:1): El cloroformo es una mezcla de alcohol isoamílico: cloroformo (1:24). El fenol contiene fenol al 100% (1:1), 0,1% 8-hidroxiquinoleína en Tris-HCl 0,1 M (pH 8,0).

2.1.2. Mini preparación de ADN plasmídico con el kit Genelute plasmid (SIGMA)

Este método se utilizó cuando se requería una mayor calidad de la preparación de ADN (ej., para secuenciación). Se procedió, siguiendo las indicaciones del fabricante, como se describe a continuación:

1. Inocular la cepa en 3 ml de medio LB líquido suplementado con los correspondientes antibióticos e incubar a 37 ºC durante 12-15 horas.
2. Resuspender las células en 200 µl de solución de resuspensión.
3. Añadir 200 µl de solución de lisis. Mezclar por inversión y dejar aclarar durante 5 min.
4. Añadir 350 µl de solución de neutralización (S3). Mezclar por inversión de 5 a 6 veces.

5. Centrifugar 10 min a 12.000 rpm para separar los restos celulares.
6. Para acondicionar la columna, añadir 500µl de la solución de preparación de columna a una columna previamente colocada sobre un tubo recolector.
7. Centrifugar 1 minuto a 12.000 g, y eliminar el filtrado.
8. Transferir el lisado a la columna.
9. Centrifugar 1 minuto y eliminar el filtrado.
10. Lavar la columna con 500µl de la solución opcional de lavado de columna, centrifugar 1 minuto a 12.000 rpm, eliminar el filtrado.
11. Lavar de nuevo con 750 µl de solución de lavado de columna, centrifugar durante 1 minuto y eliminar el filtrado.
12. Centrifugar 1 minuto para secar bien la columna.
13. Transferir la columna a un nuevo tubo, añadir 50-75 µl de solución de elución y centrifugar 1 minuto para recoger el ADN.

2.2. Aislamiento de ADN genómico total

Para la obtención de ADN genómico total de *S. meliloti* se utilizó un método especialmente diseñado para *Rhizobium* en el departamento de Genética de la Universidad de Biefeld (Alemania), y que consistió en los siguientes pasos:

1. Crecer la cepa de *S. meliloti* en 3 ml de TY líquido adicionado de los correspondientes antibióticos hasta alcanzar una fase logarítmica media.
2. Repartir 1.5 ml del cultivo en tubos eppendorf y centrifugar durante 2 min a 12.000 rpm.
3. Resuspender el sedimento en 200 µl de sarkosyl 0,1% en TE (ver soluciones en apartado 2.2.1.1), para eliminar restos de polisacáridos. Centrifugar las células (12.000 rpm, 3 min) y eliminar el sobrenadante.
4. Resuspender las células en 1 ml NaCl 1 M y dejar la suspensión al menos 30 min a 4 ºC, agitando de vez en cuando.
5. Centrifugar (12.000 rpm, 3 min), y eliminar el sobrenadante.
6. Resuspender el sedimento de células en 250 µl de una solución de sacarosa 20% en TE.

7. Añadir 250 µl de una solución en TE que contiene lisozima (5 mg/ml) y RNasa (1 mg/ml), agitar por inversión e incubar 30 min a 37 ºC.
8. Adicionar 100 µl de una solución en TE que contiene sarkosyl 5% y pronasa (10 mg/ml) e incubar 1 hora a 37ºC.
9. Añadir 70 µl de acetato sódico 3M pH 5,2, 200 µl de mezcla fenol-cloroformo (ver soluciones en apartado 2.2.1.1), y 200 µl de fenol (kirby mix). Agitar en vórtex durante 2-3 min.
10. Centrifugar (12.000 rpm, 5 min) y recoger la fase superior acuosa en otro tubo.
11. Añadir 300 µl de cloroformo, agitar y centrifugar (12.000 rpm, 3 min).
12. Recoger la fase superior en otro tubo eppendorf, añadir 700 µl de isopropanol, agitar, y mantener a -80ºC al menos 30 min.
13. Centrifugar 15 min a 12.000 rpm, y eliminar sobrenadante.
14. Añadir 300 µl de etanol 70%, centrifugar 3 min.
15. Eliminar sobrenadante y secar al vacío 5-10 min aproximadamente.
16. Resuspender en 100 µl de TE pH 8 diluido 1/10, e incubar 30 min a 65ºC.

2.3. Aislamiento de ARN total de *S. meliloti*

Para la obtención de ARN total de *S. meliloti* se utilizó el RNase-free DNase kit de Quiagen. Se tomaron 12 alícuotas de 1.5 ml de cada cepa o condición a evaluar. Las células fueron centrifugadas y tras retirar el sobrenadante, lavadas con una solución de sarkosyl al 0.1% en tampón TE. A continuación el pellet celular fue congelado en nitrógeno líquido y guardado a –80 ºC. Cuando se deseaba recoger células “swarmer”, se añadieron 2 ml de MM en la superficie de la placa del medio semisólido. Haciendo uso de una espátula de vidrio las células “swarmer” fueron desprendidas de la superficie y recogidas para luego proceder con el lavado y su congelación en nitrógeno líquido.

1. En el momento de su uso se descongelaron en hielo 4 viales de células por cada cepa u condición y se añadieron 100 µl de una solución de lizosima 4mg/ml en tampón TE, se mezcló mediante vórtex y se incubó a temperatura ambiente durante 5 min.

2. A la muestra se añadieron 350 µl de tampón RTL al que previamente se le habían adicionado 10 µl/ml de β-mercaptoetanol. Se mezcló por inversión manual y se centrifugó 5 min a 13.000 rpm para eliminar los restos celulares.
3. En el sobrenadante se añadieron 250 µl de etanol absoluto y se mezcló por inversión manual.
4. Por cada columna de purificación se pasaron 2 viales, centrifugando 30 seg a 13.000 rpm y eliminando el sobrenadante cada vez.
5. A continuación se lavó cada columna con 750 µl de solución RW1 y se centrifugó a 13.000 rpm durante 30 seg.
6. Tras cambiar las columnas a nuevos tubos de recolección, se lavó la columna dos veces añadiendo 500 µl de buffer RPE y centrifugando a 13.000 rpm durante 30 seg.
7. Los restos de solución fueron eliminados centrifugando las columnas a 13.000 durante 2 min.
8. La columna de purificación se colocó en un nuevo tubo de microfuga y se añadieron 30 µl de H_2O libre de RNAsa. Se incubó durante 1 min a temperatura ambiente para hidratar la resina y se centrifugó 1 min a 13.000 rpm. Este paso se repitió, y se mezcló el ARN procedente de las dos extracciones realizadas para cada muestra hasta obtener un volumen final de 60 µl.
9. Al volumen total obtenido (120 µl) se añadieron 14 µl de solución buffer RDD (RNaase free DNAse set, Quiagen) y 6 µl de DNasa. La mezcla se incubó durante dos horas a 28 ºC.
10. A continuación a los 140 µl de solución que contenían el ARN se añadieron 490 µl de la solución RTL con β-mercaptoetanol, 350 µl de etanol absoluto y se mezcló por inversión.
11. La solución se pasó por una columna RNeasy para retener el ARN (13.000 rpm durante 30 seg) y se continuó con su lavado.
12. La columna se lavó con 350 µl de solución RW1 y se centrifugó a 13.000 rpm durante 30 seg.
13. La columna se lavó dos veces añadiendo 500 µl de buffer RPE centrifugando a 13.000 rpm durante 30 seg.
14. Los restos de solución fueron eliminados centrifugando las columnas a 13.000 durante 2 min.

14. Finalmente, se añadieron 25 µl de agua RNase free sobre la resina de la columna. Esta se dejó hidratar por un minuto a temperatura ambiente y se centrifugo durante 30 seg a 13.000 rpm. Este paso se repitió dos veces para obtener un volumen final de ARN de 50 µl.

2.4. Concentración de muestras de ARN total *de S. meliloti*

Las muestras de ARN se concentraron utilizando columnas Microcon -30 (Amicon, Millipore). Primero se añadieron 500 µl de agua libre de RNasa a la muestra de ARN. A continuación se pasó la mezcla por la columna centrifugando a 14.000 xg hasta que sobre la membrana quedaron unos 35 µl (6-8 min). La muestra concentrada se recuperó invirtiendo la columna sobre un nuevo microtubo y centrifugando a 1.000 xg durante 2 min.

2.5. Estimación de la concentración de ADN y ARN

Se ha seguido el método espectofotométrico descrito por Sambrook ((Maniatis et al., 1989). La absorbancia (O.D.260 nm y O.D.280 nm) de las soluciones de ADN o ARN en agua o en TE se terminaron usando como blanco agua o TE, respectivamente. La concentración se calculó respecto a los valores estándar de O.D. 260 nm = 1 para soluciones con 50 µg/ml de ADN de cadena doble. En el caso de muestras de ARN se determinó su concentración a través de valores estándar de O.D. 260 nm = 1 en soluciones con 40 µg/ml de ARN en espectofotómetro NanoDrop ND-1000 (NanoDrop Technologies, Inc.). Para estimar la pureza de muestras de ADN se tomó la relación O.D. 260 nm/O.D. 280 nm, considerándose valores inferiores a 1.8 como indicadores de contaminación por proteínas o fenol. Para muestras de ADN muy impuras o de baja concentración, se empleó el método de comparación de fluorescencia en gel de agarosa bajo luz UV frente a marcadores de ADN de concentración conocida, también descrito por Sambrook. En el caso de muestras de ARN se rechazaron aquellas muestras cuya relación O.D. 260 nm/O.D. 280 nm mostró valores inferiores a 2.0 por falta de pureza.

2.6. Manipulación enzimática del ADN

2.6.1. Digestión total de ADN con endonucleasas de restricción.

La digestión total de ADN con enzimas de restricción se llevó a cabo en las condiciones óptimas para cada enzima, siguiendo las indicaciones, en cuanto a temperatura y tampón, recomendadas por el proveedor (Roche®, Alemania). Las digestiones con más de una enzima de restricción se realizaron simultáneamente usando el tampón y la temperatura recomendadas por el proveedor.

2.6.2. Electroforesis de ADN en geles de agarosa

La separación de fragmentos de restricción se realizó mediante electroforesis horizontal en geles de agarosa 0.8% sumergidos en tampón de electroforesis TBE (Tris 50 mM; EDTA-Na_2 2,5 mM; BO_3H_2 50 mM; pH 8.2). El voltaje usual de trabajo fue 90 V en cubetas de electroforesis Wide mini-sub® cell GT o Mini-sub® cell GT (BioRad). Como tampón de carga se utilizó una mezcla de sacarosa al 40% y azul de bromofenol al .25%, ambos preparados en agua destilada.

2.6.3. Revelado de geles y fotografía

Las muestras de ADN presentes en los geles de agarosa se visualizaron tras la inmersión de los geles en agua destilada que contenía una solución de GelRedTM (Biotium) (100 µl/L), durante 30-40 min. Posteriormente se observaron con luz UV (260 nm) en un transiluminador. Para la visualización e impresión se ha utilizado una videocámara acoplada a un sistema de impresión de imágenes (Gelprinter Vm509) y el analizador de imágenes Quantity One de BioRad.

2.6.4. Estimación del tamaño molecular de los fragmentos de ADN

La determinación del tamaño molecular de los fragmentos de restricción se ha efectuado mediante la construcción de gráficas en las que se representa el

logaritmo de tamaño molecular relativo de moléculas patrón de ADN frente a la movilidad relativa (Rf) de las mismas en el gel de agarosa. Como marcadores de tamaño molecular se han utilizado los fragmentos de restricción del ADN del fago lambda resultantes de la digestión con *Hind*III (Marcador II), o *Eco*RI/*Hind*III (Marcador III), ambos de Roche. También se ha utilizado el marcador de 100 pb GeneRuler (Fermentas).

2.6.5. Purificación de fragmentos de ADN a partir de geles de agarosa

Para aislar fragmentos de ADN de la agarosa se utilizó el método de electroelución descrito por (Sambrook and Fritsch, 1989), en el que se hace uso de membranas de diálisis. La membrana de diálisis utilizada fue de Spectra/por (SPECTRUM Medical Industries) con tamaño de poro de 12.000 a 14.000 Da. Las membranas se prepararon sumergiéndolas en un volumen abundante de tampón conteniendo bicarbonato sódico 2% (p/v) y EDTA 1 mM, y llevándolas a ebullición durante 10 min. Posteriormente, las membranas se lavaron con agua desionizada y se añadió un poco de etanol 100% para su conservación a 4ºC. Previo a su uso, las membranas se enjuagaron con agua desionizada. El proceso de electroelución se llevó a cabo con los siguientes pasos:

1. Cortar del gel de agarosa el fragmento que contiene el ADN de interés, e introducirlo en el tubo de diálisis sellado previamente en uno de sus extremos con una pinza.
2. Añadir 500 µl de TBE (ver apartado 2.5) y cerrar el otro extremo del tubo con una segunda pinza, intentando no dejar grandes burbujas de aire.
3. Colocar la bolsa de diálisis en una cubeta de electroforesis, y aplicar un voltaje de 120 voltios durante 20 min.
4. Invertir la polaridad durante 1 minuto y comprobar con el uso de luz UV que no queda ADN en el fragmento de agarosa.
5. Recoger la solución de TBE con el ADN y colocarla en un tubo eppendorf.
6. Precipitar el ADN añadiendo 50 µl de acetato sódico 3 M pH 5,2, y 2 volúmenes de etanol 100% (1 ml).
7. Agitar por inversión y dejar 20 min a -80ºC

8. Centrifugar 15 min a 12.000 rpm y eliminar el sobrenadante.
9. lavar con etanol 70% (200µl). Secar el precipitado al vacío. Resuspender en 20 µl de agua Milli-Q o TE (ver soluciones en apartado 2.1.1).

2.6.6. Ligación de fragmentos de restricción en vectores de clonación

1.- En un tubo eppendorf, adicionar:

- x µl de ADN vector*
- y µl de ADN inserto*
- 1 µl de ADN ligasa del fago T4 (1 unidad/□)
- 2 µl de tampón de la ligasa (concentrado 10x)
- H_2O milli-Q, completar hasta 20 µl.

2. Mezclar suavemente e incubar a temperatura 15 ºC durante toda la noche.

*Se ha de mantener la proporción vector:inserto en relación (molar) 1:3. La cantidad x+y debe ser de unos 200 ng.

2.7. Preparación de células competentes de *E. coli*

La preparación de células competentes de *E. coli* se ha realizado esencialmente según la técnica descrita por Lederberg and Cohen (1974).

1. Inocular la cepa de *E. coli* en 3ml de LB líquido e incubar a 37 ºC 12-15 h.
2. Diluir 1 ml del cultivo anterior en 100 ml de LB líquido preparado previamente en un matraz de 250 ml. Incubar a 37 ºC hasta alcanzar una O.D. 600 nm de 0.5 (aproximadamente 2 horas).
3. Dejar en hielo 10 min.
4. Centrifugar a 6.000 xg, 10 min a 4ºC y eliminar el sobrenadante.
5. Resuspender las células en 1 volumen de una solución $MgCl_2$ 0,1 M estéril y preenfriada a 4 ºC.
6. Centrifugar a 3.000 xg, 5 min a 4 ºC y eliminar el sobrenadante.
7. Resuspender el precipitado de células en 1/2 volumen de una solución de $CaCl_2$ 0.1 M estéril y preenfriada a 4 ºC.

8. Dejar las células en hielo durante al menos 30 min.
9. Centrifugar a 3.000 xg, 5 min a 4 ºC, y retirar cuidadosamente el sobrenadante.
10. Finalmente, resuspender suavemente las células en 1/10 volumen de una solución estéril de $CaCl_2$ 0,1 M conteniendo glicerol al 20% (p/v) preenfriada a 4 ºC.
11. Repartir las células en alícuotas de 200 µl en tubos eppendorf preenfriados en hielo.
12. Conservar a -80ºC. La competencia de las células se mantuvo de esta forma durante varios meses

2.8. Transformación de células competentes de *E. coli*

Para la transformación de células competentes con ADN plasmídico se siguió la técnica descrita por Rodriguez and Tait (1983), modificada como se indica a continuación:

1. Descongelar las alícuotas de 200 µl de células competentes guardadas a una temperatura de -80ºC, manteniéndolas en hielo (10-15 min).
2. Añadir 50-100 ng del ADN con el que se pretende transformar. Mezclar mediante agitación suave e incubar en hielo al menos 30 min.
3. Dar un choque térmico 5 min a 37ºC y rápidamente pasar a hielo y dejar otros 5 min.
4. Añadir 1 ml de LB e incubar durante 1:15-1:30 horas a 37 ºC.
5. Sembrar en placas de LB con los correspondientes antibióticos*, diferentes volúmenes de la transformación e incubar a 37ºC durante una noche.

*Si se lleva a cabo una selección por color se puede adicionar a cada placa 40 µl de una solución de 5-bromo-4-cloro-3-indolil-β-D-galactopiranósido (X-Gal), o 40 µl de una solución de 5-bromo-4–cloro–3– indolil-β-D-ácido glucurónico (X-gluc), preparados ambos a una concentración de 20 mg/ml en dimetilformamida.

2.9. Experimentos de hibridación ADN-ADN

2.9.1. Transferencia de ADN a filtros de nylon

Se llevó a cabo de acuerdo a la metodología descrita por Southern (1975). Para ello:

1. Realizar una electroforesis en agarosa al 0.8%. La concentración de agarosa puede variar según el tamaño de los fragmentos que se quieran separar. Es conveniente emplear un voltaje bajo cuando se quiera transferir ADN total digerido con alguna enzima de restricción.
2. Tinción del gel con GelRedTM (Biotium) y fotografía del mismo.
3. Depurinación ácida del ADN: sumergir el gel en HCl 0.25 M hasta viraje del azul de bromofenol a amarillo (20 min). Lavar con agua destilada 3 veces.
4. Desnaturalización alcalina del ADN: sumergir el gel durante 20 min en una solución NaOH 0.5 M, NaCl 1.5 M. Repetir el proceso. Lavar el gel con agua destilada.
5. Neutralización del ADN: sumergir el gel en una solución Tris-HCl 0.5 M, NaCl 1.5 M (pH: 7.4) durante 15 min dos veces. Retirar la solución y lavar con agua destilada.
6. Humedecer una membrana de nylon (Roche®), cargada positivamente, en SSC 10x durante al menos 5 min. El tamaño de la membrana debe ser igual al del gel. Recortar también dos piezas de papel Whatman 3 mm del mismo tamaño y otra de mayor tamaño que el gel, y saturarlas en tampón SSC 10x.
7. Sobre una superficie regular, habitualmente un cristal, construir una unidad de transferencia compuesta, de abajo hacia arriba, por una pieza de papel Whatman 3 mm, cuyos extremos, a modo de mecha se sumergen en un reservorio de tampón de transferencia SSC 10x, el gel, el filtro de nylon y las dos piezas restantes de papel Whatman 3 mm. Colocar un marco de plástico que bordee todo el sistema y, a continuación, cubrir con papel absorbente. Sobre todo el conjunto se coloca una placa de vidrio y, sobre ésta, un peso de aprox. 0,5-1 Kg para mantener el sistema ligeramente comprimido. Comprobar que el sistema está perfectamente horizontal, y dejar la transferencia toda la noche. Finalizado el

proceso, lavar la membrana con SSC 2x durante 5 min. Dejar secar la membrana a temperatura ambiente durante 30 min y finalmente fijar el ADN a la membrana mediante calentamiento en vacío, a 120ºC durante 30 min.

SOLUCIONES:
SSC 20x:
175.3 g de NaCl
8.2 g de citrato sódico
800 ml de H_2O destilada. Ajustar el pH a 7,0 y completar hasta 1 litro.

2.9.2. Marcaje de sondas de ADN no radioactivas

El marcaje de sondas de ADN se ha realizado empleando el sistema no radioactivo comercializado por Roche®, siguiendo las recomendaciones del proveedor. Esta técnica consiste en la síntesis parcial de ADN a partir del ADN molde que se quiere usar como sonda. Para ello, se utiliza el ADN molde desnaturalizado por calor (100 ºC, 10 min) y enfriado en agua/hielo durante 2 min, una mezcla de hexanucleótidos, el fragmento Klenow de la ADN polimerasa I de *E. coli* y una mezcla de dNTPs que incluye dUTP marcado con digoxigenina, nucleótido que se puede detectar mediante reacción inmunológica específica. La cantidad de ADN molde que se empleó fue de entre 100-500 ng, en un volumen final de 20 µl, preferiblemente linearizado mediante la digestión con una enzima de restricción. El tiempo de incubación fue de unas 20 horas, y la temperatura de 37 ºC.

2.9.3. Hibridación ADN-ADN con sondas de ADN no radioactivas

El proceso de hibridación utilizando ADN homólogo como sonda se efectuó de la siguiente manera:

1. Prehibridación: mantener la membrana de nylon inmersa en 30 ml de solución de prehibridación durante al menos 2 horas, a 42ºC.

2. Hibridación: tras eliminar la solución de prehibridación, adicionar nueva solución de prehibridación con el ADN sonda (100 mg/ml solución) previamente desnaturalizado por calor (100ºC, 10 min) y enfriado en agua/hielo durante otros 2 min. Incubar durante al menos 6 horas a 42ºC.

3. Tras la hibridación, se realizaron los siguientes lavados: 2 x 5 min en 100 ml de SSC 2x; SDS 0,1% a temperatura ambiente; 2 x 15 min en 100 ml de SSC 0.1x; SDS 0.1% a 68 ºC.

4. Lavar 1-5 min en tampón I.

5. Incubar 30 min en tampón II.

6. Detección inmunológica: incubar durante 30 min con anticuerpos anti-digoxigenina conjugados con fosfatasa alcalina (Roche) diluidos 1:10.000 en tampón II.

7. Lavar (2 x 15 min) con tampón de lavado, formado por tampón I + Tween 20 al 0,1%.

8. Incubar 5 min con tampón III.

9. Incubar la membrana 5 min en 10 ml de CSPD (Roche) (1:100 en tampón III), evitando incidencia de la luz.

10. Envolver la membrana en plástico transparente e incubar a 37 ºC durante 15 min.

11. Exponer la membrana a una película autorradiográfica (Kodak X-Omat®). El tiempo de exposición (30 min a 6 h) varía en función de la concentración de ADN, el porcentaje de homología entre los ADNs sonda y problema y la eficiencia del marcaje.

12. Para el revelado de las películas se emplearon el revelador y el fijador de TETENAL® a las diluciones y tiempos recomendados por las casas comerciales.

SOLUCIONES:

Solución de prehibridación:
SSC 5x
formamida 50%
Reactivo de bloqueo 2% (p/v) (Roche)
N-lauryl-sarcosina 0.1%

SDS 0,02%

Tampón I:
Tris-HCl 100 mM (pH 7.5)
NaCl 150 mM

Tampón II:
Tampón I
Reactivo de bloqueo 1%

Tampón III:
Tris-HCl 100 mM (pH 9.5)
NaCl 100 mM

2.10. Amplificación de ADN mediante la reacción en cadena de la polimerasa (PCR)

La amplificación de fragmentos de ADN mediante la técnica de PCR se llevó a cabo preparando una mezcla de reacción con tampón de PCR (10x), Cl_2Mg 1.5 mM, dNTPs 0.3 mM, 50 pmoles de cada cebador, 10-50 ng de ADN molde y 2 unidades de Taq (Biotherm) en un volumen final de 50 µl. Para el proceso se utilizó un termociclador Thermo (Electron Corporation) con un programa básico que consistió en un ciclo de desnaturalización a 94 ºC de 5 min, 30 ciclos de tres pasos cada uno: desnaturalización (94 ºC, 1 min), apareamiento del cebador (55-58 ºC dependiendo de la secuencia del cebador, 1 min) y extensión (72 ºC, 1-4 min según la longitud del fragmento a amplificar) y finalmente un último ciclo de extensión (72ºC, 10 min). Los cebadores empleados en este trabajo se describen en la Tabla 3.4.

Tabla 3.4. Cebadores empleados para PCR

Primer	Sequencia (5´ to 3´)*
Universal	GTAAAACGACGGCCAGT
Reverso	GAAACAGCTATGACCATG
rhbGA1	AAAAAGCTTAGGTCTACGCCAATTTCAGC (*Hind*III)
rhbGB2	GGAGATCGACATGAGAAAGGAGCGAAAG
rhbGC3	CTTTCGCTCCTTTCTCATGTCGATCTCC
rhbGD4	AAAAAGCTTCGATAGACGTTACCGTCACG (*Hind*III)
rhbD1	ATAAAGCTTAGAACATCGTGGTCGAGATC (*Hind*III)
rhbD2	TTGTCGGGAAGGTCGAAGCTGATCGTCC
rhbD3	GGACGATCAGCTTCGACCTTCCCGACAA
rhbD4	TAAGGATCCGGTGCCAACGTCTTGATCTG (*Bam*HI)

Los sitios de restricción usados en clonación están subrayados y las enzimas se indican entre paréntesis.

2.11. Mutagénesis in vitro por deleción mediante PCR solapante

Las versiones delecionadas de los distintos genes se han obtenido fusionando, mediante reacción de PCR, dos amplicones solapantes, correspondientes al ADN que flanquea a izquierda y derecha la deleción, metodología basada en Ho et al. (1989) y Griffitts and Long (2008).

Para la amplificación de las regiones de ADN que flanquean a derecha o izquierda la deleción deseada, se llevó a cabo una reacción de PCR utilizando 10 ng de ADN genómico de 1021 como ADN molde, tampón PCR Accutherm (10x), 0.2 unidades de Accutherm (polimerasa usada en lugar de Taq polimerasa Biotherm) para evitar generar mutaciones no deseadas aguas arriba o abajo del gen por errores de la polimerasa, 50 pmoles de los cebadores correspondientes al fragmento a amplificar (tabla 3.4) y completando con agua desionizada hasta un volumen de 50 µl.

Dicho proceso se llevó a cabo mediante un termociclador Thermo (Electron Corporation) con un programa básico consistente en un ciclo de desnaturalización a 94ºC durante 5 min, 30 ciclos de tres pasos cada uno: desnaturalización (94ºC, 30 seg), apareamiento del cebador (57-60ºC dependiendo de la secuencia de los cebadores, 30 seg) y extensión (68º C, 30 seg-2 min según la longitud del fragmento a amplificar).

Para obtener el producto de fusión, se realizó una segunda reacción de PCR utilizando 2 ng de cada uno de los flancos obtenidos previamente. El producto de fusión tiene un tamaño que oscila entre 1.4-1.5 kb con aproximadamente 700 pb correspondientes a cada flanco.

2.12. Secuenciación automática de ADN de doble cadena

Las reacciones de secuenciación se realizaron en un termociclador Perkin Elmer 9.600, utilizando el producto comercial Abi Prism (Perkin-Elmer) y la polimerasa Amplitaq FS, por el Servicio de Secuenciación del Instituto de Parasitología y Biomedicina López-Neyra y el de la Estación Experimental del Zaidín, CSIC, Granada. La determinación de la secuencia se realizó mediante el sistema de terminadores marcados con fluorocromos. Al ADN a secuenciar (0.4-1 □g) se le adicionó el cebador específico (6.4 picomoles) y agua Milli Q hasta un volumen final de 12 □.

Los cebadores empleados para la secuenciación de las versiones delecionadas de los genes, han sido los descritos en la tabla 3.4.

2.13. Análisis informático de secuencias de ADN y proteínas

Los análisis de las secuencias de ADN y proteínas, búsqueda de sitios de restricción, diseño y análisis de oligonucleótidos, localización de posibles marcos abiertos de lectura (ORFs), etc., se han realizado con el programa informático Vector NTI®. La búsqueda de homologías a nivel de ADN y proteína con secuencias conocidas presentes en los bancos de datos se realizó con el programa BLAST (Altschul et al., 1998) disponible en el servidor NCBI (http://www.ncbi.nlm.nih.gov/). Los datos sobre el genoma de *S. meliloti* 1021 se consultaron en http://sequence. toulouse.inra.fr/.

2.14. Experimentos de microarrays

2.14.1. Reversotranscripción del ARN

1. Se tomaron 15 µg de ARN total de *S. meliloti* concentrado y se llevaron a un volumen final de 13 µl con agua libre de RNAsa. Se añadieron 2 µl de una mezcla de hexanucleótidos (5 µg/µl) y se incubó a 70 ºC durante 10 min.
2. A continuación se dejó enfriar en hielo durante 5 min y se añadieron 6 µl de solución 5xRT (Stratagene), 3 µl de solución 0.1 M de DTT (Stratagene), 0.5 µl de inhibidor de RNasa (40 U/µl), 1.5 µl de reverso transcriptasa (Superscript II, Stratagene) y 0.6 µl de una solución madre de dNTPs que incluía dUTP amino modificado (25 mM dATP, 25 mM dCTP, 25 mM dGTP, 5 mM dTTP, y 20 mM aa-dUTP). Los componentes de la reacción se mezclaron y se mantuvieron durante una hora a 42 ºC. Transcurrido este tiempo se añadió 1 µl más de reverso transcriptasa (Superscript II, Stratagene) y se dejó transcurrir la reacción durante otra hora hasta la obtención de la muestra final de ADNc.

2.14.2. Hidrólisis de ARN

1. Se adicionaron a la muestra 15 µl de NaOH 0.2 M, se mezcló bien y se incubó a 70 ºC durante 10 min.
2. A continuación se neutralizó el pH añadiendo 15 µl de HCL 0.2 M y se procedió a limpiar el cDNA ulitizando columnas CyScribe GFX (Amsterdam Biosciences). Para ello se mezcló la muestra con 450 µl de tampón de captura, esta fue puesta en columna CyScribe GFX y se centrifugó a 13.000 rpm durante 30 seg.
3. La columna se lavó dos veces con 600 µl de etanol al 80% y se centrifugó una vez más a 13.000 rpm durante 10 seg para eliminar restos de líquido.
4. La columna fue colocada en un nuevo tubo contenedor, se añadieron 60 µl de $NaCO_3$ 0.1 M a pH y se incubó a temperatura ambiente durante 5 min. Para recuperar el cDNA se centrifugó a 13.000 rpm durante 1 min. A continuación se procedió con el marcaje del cDNA.

2.14.3. Marcaje del cDNA

El cDNA se marcó utilizando como fluoróforo Cy3 para la muestra o condiciones control y Cy5 para la muestra o condición problema. Tanto los fluoróforos como las muestras marcadas se mantuvieron protegidos de la luz a lo largo de todo el proceso.

1. Los fluoróforos de Amersham se disolvieron en 10 µl de DMSO (es importante que el DMSO no contenga agua) y se separaron 10 alícuotas de 1 µl del fluoróforo que se desecaron en "Speed-vac" y se conservaron a -20 ºC en bolsas selladas con un paquete de sílica gel para evitar su hidratación.
2. Para llevar a cabo la reacción de marcaje, se transfirió la muestra a un microtubo con una alícuota del fluoróforo correspondiente y se resuspendió pipeteando. Alternativamente se puede añadir 1 µl del fluoróforo recién resuspendido en DMSO y pipetear hasta obtener una suspensión homogénea. Se dejaron transcurrir 2 horas manteniendo la suspensión a temperatura ambiente en oscuridad.
3. A continuación se procedió a neutralizar los fluoróforos que pudieran haber quedado libres añadiendo 4.5 µl de hidroxilamina 4 M, mezclando suavemente y dejando la mezcla 15 min más a temperatura ambiente en oscuridad.
4. Las muestras marcadas con Cy3 y Cy5 que constituían una sonda se mezclaron en este momento y se purificaron juntas utilizando el CyScribe GFX Purification Kit (Amersham Biosciences) según las instrucciones del fabricante. La muestra marcada con Cy5 se mezcló con 600 µl de solución de captura y luego se añadió la muestra marcada con Cy3.
5. Tras pipetear repetidas veces para obtener una mezcla homogénea, está se aplicó a una columna CyScribe GFX. Se centrifugó a 13.000 rpm durante 30 seg para eliminar restos de líquido.
6. LA columna fue lavada tres veces con 600 µl de buffer de lavado, centrifugando durante 30 seg a a 13.000 rpm.
7. La columna se centrifugó 30 seg más para eliminar los restos de líquido.

8. La columna fue colocada en un nuevo microtubo oscuro y se añadieron 60 µl de solución de elución. Se incubó a temperatura ambiente durante 5 min y luego se centrifugó a 13.000 rpm durante 1 min para recuperar el cDNA marcado. El cDNA marcado de esta forma puede mantenerse a -20 ºC hasta el momento de su utilización.

2.14.4. Procesamiento del microarray previo a la hibridación

Los Sm6koligo o los Sm14koligo microarray que se han utilizado son cristales QMT con grupos epoxi a los que se unen los oligonucleótidos. Cada Sm6koligo microarray contiene 6212 oligonucleótidos de 70 de monómeros de bases que representan todos los ORFs contemplados en la anotación de *S. meliloti* Rm1021 (Rüberg et al., 2003). Recientemente se han dispuesto los Sm14koligo microarrays, los cuales contienen 6208 oligonucleótidos de 70 monómeros de bases que representan todos los ORFs y además 8080 oligonucleótidos de 50 a 70 monómeros de bases que representan las regiones intergénicas contempladas en la anotación de *S. meliloti* Rm1021. Estos cristales deben ser procesados antes de la hibridación para bloquear los grupos epoxi libres, para ello:

1. Los cristales se lavaron durante 5 min a temperatura ambiente en solución 1 (250 µl de Triton X100 en 250 ml de agua MilliQ, disolver calentando 5 min a 80 ºC y dejar enfriar a temperatura ambiente antes de usar).
2. A continuación esto fueron lavados dos veces durante 2 min a temperatura ambiente en solución 2 (50 µl de HCl 37% en 500 ml de agua MilliQ).
3. Los cristales se mantuvieron durante 10 min a temperatura ambiente en solución 3 (25ml de 1mM KCl 1 M en 225 ml de agua MilliQ) y se aclararon 1 min en agua MilliQ a temperatura ambiente.
4. Finalmente, los cristales fueron transferidos a la solución de bloqueo (150 ml de agua MilliQ, 40 µl de HCl 37% y 50 ml de 4xQMT blocking solution) que se preparó en el momento y se precalentó a 50ºC antes de su uso. Los cristales se mantuvieron en la solución de bloqueo a 50 ºC durante 15 min en un contenedor de cristal, se aclararon 1 min en agua MilliQ a temperatura ambiente y se secaron por centrifugación a 1.200 rpm durante 3 min.

2.14.5. Hibridación de los microarrays

Las muestras de cDNA marcado se desecaron utilizando un "Speed-vac" y se resuspendieron en 45 µl de DIG Easy Hyb pipeteando varias veces y se incubó a 65ºC durante 5-10 min. Los cristales pretratados según las instrucciones del apartado 3.2.19.4. se colocaron a 42ºC en las cámaras de hibridación para evitar las posibles precipitaciones debidas a gradientes térmicos. La sonda se aplicó como una gota sobre el cristal y se colocó el cubre objetos de modo que no quedaran burbujas. La incubación se llevó a cabo en un incubador Thermomixer confort (Thermomixer confort, Eppendorf) a 42 ºC durante 14-18 h.

2.14.6. Procesamiento del microarray tras la hibridación

Transcurrido el tiempo de hibridación, los cristales se lavaron primero con una solución 2x SSC y SDS al 0.1% (p/v) durante 1 min a temperatura ambiente, otras dos veces con una solución 0.2x SSC durante 1 min a temperatura ambiente y finalmente una vez con una solución 0.1x SSC preenfriada a 18 ºC durante 1 min. Por último, los cristales se secaron por centrifugación a 1.200 rpm durante 5 min a 4ºC y se dejaron a temperatura ambiente un mínimo de 20 min más antes de escanearlos. Durante todo el proceso los cristales se mantuvieron en oscuridad en la medida de lo posible.

2.14.7. Adquisición de la imagen y tratamiento de los datos

Se utilizó un escáner confocal (ScanArray4000) para la obtención de las imágenes correspondientes a la utilización de los láseres de 555 nm y 647 nm para detección de la fluorescencia de Cy3 y Cy5, respectivamente. Para la obtención de los datos se utilizó el programa ImaGene 5.5. (Biodiscovery Inc. Los Angeles, Calif., USA) que determinó la intensidad de los distintos puntos impresos en el cristal así como la intensidad del fondo asociado a cada punto y la calidad del punto (según su forma, tamaño, intensidad respecto al fondo). Se obtuvo el valor del $\log_2$ de la relación entre las intensidades detectadas de cada fluoróforo para cada punto (M) mediante la formula $Mi=\log_2 (RiGi)$ siendo Ri=Ichli-

Bgchli y Gi = Ich2i-Bgch2i donde Ichli o Ich2i es la intensidad de un punto en el canal 1 o el 2, respectivamente. También se calculó la intensidad media para cada punto (A) según la formula Ai= $\log_2$ (RiGi) 0.5. Cada experimento se llevó a cabo por triplicado. Para la normalización de los datos y el análisis estadístico de las réplicas se utilizó el programa EMMA1.1 (Dondrup et al., 2003) con el que se obtuvieron los correspondientes valores de M y A una vez normalizados y promediados en las réplicas con una calidad aceptable (n) junto con el valor de fidelidad de estos datos (p) según una *t* de Student. Se consideraron como diferencialmente expresados aquellos genes para los que n ≥ 5, P ≤ 0.05, A ≥ 9 y M ≥ 1 o M ≤ -1 (es decir, si su expresión variaba cuatro veces como mínimo entre ambas condiciones experimentales) en al menos 2 de los 16 experimentos que se llevaron a cabo.

2.15. RT- qPCR (Reverse transcription quantitative real-time PCR)

2.15.1. Síntesis de cDNA para RT-qPCR

La síntesis de cDNA para RT-qPCR se realizó desde las muestras de ARN total (adquirido tal y como se describe en la sección 2.3.) siguiendo el protocolo que se describe a continuación:

1. Se mezclaron 1 µg de ARN total, 1 µl de una solución conteniendo 100 ng/µl de una mezcla de oligonucleótidos (Random Primers, Roche), 1 µl de una mezcla 10 mM de dNTP y se completó el volumen hasta 12 µl con agua milliQ.
2. La muestra fue incubada a 65 ºC durante 5 min y transferida inmediatamente a hielo.
3. Se añadieron 5 µl de tampón de síntesis 5x (First-strand, Invitrogen), 2 µl de 0.1 M DTT y 1 µl de inhibidor de ARNasa (40 U/µl, Protector RNAse inhibitor. Roche)
4. La mezcla se incubó a 25 ºC durante 2 min, se añadió 1 µl de reverso transcriptasa (Superscript II reverse transcriptase, 200 U/µl, Invitrogen) y se incubó a 25 ºC durante 10 min para la unión de los cebadores y, posteriormente, 50 min a 42 ºC para la síntesis de cDNA.

5. Finalmente para inactivar el enzima y parar la reacción se sometió a la mezcla a 65 ºC durante 10 min.

2.15.2. Reacción de amplificación para la cuantificación de la expresión génica relativa. RT- qPCR

La amplificación de los fragmentos de cDNA para la cuantificación de los niveles de ARN mensajero se realizó utilizando Platinum Taq ADN polimerasa de invitrogen. Las reacciones de amplificación se realizaron en un termociclador IQ de BIORAD. La mezcla para la reacción contenía: 1 µg de ARN reverso transcrito (cDNA), 0.2 µm de los primers específicos del gen a estudiar, 0.2 mM de mezcla de dNTPs, 1.5 mM de $MgCl_2$, solución de SYBR Green I 0.1x platinum Taq ADN polimerasa (1-2.5 U). El programa estándar de amplificación consistió en un ciclo de desnaturalización inicial a 95 ºC durante 3 min, precedido de 35 ciclos de amplificación y cuantificación de 30 seg a 95 ºC, 45 seg, a 55 ºC y 45 seg a 72 ºC. A continuación se llevaron a cabo 1 ciclo de 1 min a 95 ºC, otro ciclo de 1 min a 70 ºC y 90 ciclos de 10 seg a 55 ºC. Terminada la reacción se realizó un análisis de la curva de Melting o curva de fusión para la determinación de la formación de productos específicos. En la tabla 3.5. se pueden observar los primers utilizados en RT-qPCR en este trabajo.

Tabla 5. Cebadores empleados en RT-qPCR

Gen	Forward Primer (5' to 3')	Reverse Primer (5' to 3')
SMc03224 (*16S*)	TCTACGGAATAACGCAGG	GTGTCTCAGTCCCAATGT
SMc03015 (*visN*)	TCCTTGATGCTGCTCTTC	CTCGGTCAGTTCGCATTC
SMc03046 (*rem*)	CGAAAGCCACATCAGCAAGC	ATTCCAGTCGATGCAGTAGCC
SMc03027 (*flgB*)	GAAAGCGTGCTTCAGAAC	CTGACTTCGGTCACATGC
SMc03037 (*flaA*)	CGATTATGTCAAGGTCCA	GCAATGGTGATGTCGATC
SMc03040 (*flaC*)	CCGACGGCAGCGTTACG	ATCCGCATTCACCGCCTTG
SMc01513 (*hmuS*)	ACATCAAGCAAGGACACG	CACTTGTCGAAGAACTGC
SMc02726 (*shmR*)	CGACAATGATCTCAGAGC	CGAAATCATAGTCCAGCG
SMc02085 (*exbB*)	CTTCCGCATGATCTTTCG	AGTTCCAGCGTCTTCACG
SMa2402 (*rhbB*)	TGAACATCAACGTCGCTG	GGAGTAGAGACTGCTTGC
SMa2414 (*rhtA*)	CATCATCACGAAGAAGGG	TCGCTGTTATAGGTGACC
SMa2339 (*rhbG*)	TCGGACCTTTCTCAGGTG	ACATCAGATGCAGAAGGG
SMa2412 (*rhrA*)	CTCCTGACGAATTATGCG	TATCTTGAGCAAGCACCG
SMa1077 (*nex18*)	GTCAATTCAAGACGCTGG	GGTTTCAGCAGGTTTTCG
SMb20934 (*exsF*)	ATCGCTACTCTCGATCTC	TCGTTCAGGCAAGTCAAG

3. Ensayos con plantas

3.1. Esterilización y germinación de semillas de alfalfa

Las semillas de alfalfa (Medicago sativa L, cultivar Aragón) se esterilizaron en superficie de acuerdo al siguiente protocolo descrito por (Olivares et al., 1980):

1. Sumergir las semillas de alfalfa, en $HgCl_2$ al 2.5% durante 9 min y medio.
2. Lavar 5-6 veces con abundante agua desionizada estéril. Dejar en imbibición durante 2 horas.
3. Lavar 2-3 veces con abundante agua desionizada estéril.
4. Colocarlas las semillas bien separadas y en condiciones asépticas en placas Petri que contienen papel de filtro humedecido con agua desionizada estéril.
5. Germinar en oscuridad a 28ºC durante aproximadamente 24 horas.

3.2. Solución nutritiva para el cultivo de plantas

Se ha empleado la solución mineral libre de nitrógeno descrita por Rigaud and Puppo (1975), cuya composición se describe a continuación:

Macroelementos (por litro de agua):

KH_2PO_4, 68 mg

K_2HPO_4, 44 mg

$SO_4Mg.7H_2O$,123 mg

K_2SO_4, 174 mg

SO_4Ca, 173 mg

Ácido ethilendiaminotetraacético hierro (III) sal de sodio (EDTA iron (III) sodium salt), 25 mg

Microelementos (por litro de agua):

$MoO_4Na2.2H_2O$, 0,11 mg

BO_3H_3, 2,85 mg

$SO_4Mn.4H_2O$, 0,37 mg

$SO_4Zn.7H_2O$, 0,55 mg

$SO_4Cu.5H_2O$, 0,2 mg.

El pH de la solución se ajustó a 7.5. La solución se esterilizó en autoclave a 120ºC durante 20 min.

3.3. Cultivo axénico de plantas en placa: medida del grado de infectividad

La esterilización de las semillas de alfalfa fue llevada acabo como se describió en la sección 3.1. Para el crecimiento de las plantas se utilizó la solución mineral libre de nitrógeno descrita por Rigaud and Puppo (1975), descrita anteriormente en la sección 3.2. La solidificación de esta solución se llevó a cabo adicionando agarosa al 0.8%. En cada placa cuadrada de 12.5 cm x 12.5 cm se sirvieron 45ml de la solución para plantas con agarosa. Para evitar la adhesión de las raíces al agar, sobre la superficie de agar se dispuso un papel de filtro Whatman cuadrado que se humedeció con 2 ml de agua estéril. Por placa se pusieron 15 semillas recién germinadas de aproximadamente 1 cm de largo y fueron inoculadas como se describe a continuación.

1. Las células de *S. meliloti* fueron crecidas en placas de medio TY adicionado con los correspondientes antibióticos para cada cepa.
2. Para la inoculación de las raíces se tomó masa celular de cada cepa y se resuspendió en TY hasta O.D. 600 nm de 0.1. Esta suspensión celular se lavo una vez con agua destilada estéril y de aquí se hicieron diluciones seriadas 1/10 hasta obtener una dilución de 1 x 10^4 células/ml aproximadamente.
3. Cada plántula se inoculó bañando la raíz desde el ápice hacia arriba, con 30µl de la dilución celular que contenía 1 x 10^4 células/ml. Diluciones seriadas del inóculo fueron sembradas en placas de medio TY adicionadas con el correspondiente antibiótico de cada cepa, para llevar el control del número de CFUs con el que las plántulas habían sido inoculadas.

4. Las placas fueron selladas con parafilm dejando el borde superior de la placa descubierta. Para evitar la incidencia de la luz sobre la raíz, la parte inferior de la placa fue cubierta con un sobre de papel oscuro.
5. La incubación de las plantas se llevó a cabo en cámaras con: una emisión de intensidad lumínica de 500 µeinstein x m^{-2} x s^{-1}(λ = 400 – 700 nm), fotoperiodo 15/9 horas luz/oscuridad, temperatura de 24/18ºC - día/noche y humedad relativa de un 50%.

Tras la inoculación se registró diariamente el número de plantas noduladas y el número de nódulos formados en cada planta. Se consideró que una planta estaba nodulada cuando en sus raíces existía al menos un nódulo visible. El seguimiento de la nodulación se continuó hasta que todas las plantas estuvieron noduladas. La infectividad de la cepa se considera en función del tiempo de nodulación y del número de nódulos que forma.

3.4. Cultivo axénico de plantas en jarras Leonard: medida del grado de competitividad

El cultivo de plantas se llevó a cabo utilizando jarras Leonard (Leonard, 1943). Para ello, se rellenó el recipiente superior con vermiculita y el inferior con la solución mineral para plantas descrita en la sección 3.2. Las jarras fueron esterilizadas mediante autoclavado a 120 ºC durante 20 min. En cada jarra se sembraron 12 semillas de alfalfa germinadas según se describe en la sección 3.1. Antes de ser inoculadas, las plántulas fueron incubadas durante un día en la cámara de plantas con una emisión de intensidad lumínica de 500 µeinstein x m^{-2} x s^{-1}(λ = 400 – 700 nm), fotoperiodo 15/9 horas luz/oscuridad, temperatura de 24/18ºC - día/noche y humedad relativa de un 50%.

La determinación del número de nódulos que una cepa es capaz de formar en presencia de otra se hizo utilizando cepas marcadas con el gen informador *gusA* (β-glucuronidasa). Cada planta fue inoculada con 1 ml de una suspensión de 1 x 10^2 células/ml que contenía en proporción 1:1 una mezcla de la cepa

silvestre o la cepa de estudio con la cepa silvestre marcada con el plásmido pGUS3. Una vez inoculadas, las jarras se cubrieron con una capa de perlita estéril para evitar la posible contaminación ambiental y reflejar la luz, evitando el calentamiento excesivo de las semillas que pudiera alterar el desarrollo de las mismas. La unión entre el componente superior e inferior de la jarra se selló con papel parafilm. Las jarras fueron envueltas en papel opaco oscuro para evitar la incidencia de la luz sobre las raíces y fueron llevadas de nuevo a la cámara de plantas.

15 días después de la inoculación se cortaron las raíces, se aclararon con agua destilada entre 10 – 15 minutos y se mantuvieron surmergidas en 5mL de una solución de X-Gluc (21mg/40mL) en tampón fosfato sódico 50mM pH 7 y SDS al 1%, durante 14-16 horas a 37ºC en oscuridad. Pasado este tiempo, los nódulos que contenían la cepa silvestre marcada con pGUS3 o estaban ocupados por ambas cepas aparecieron teñidos de azul, mientras que aquellos ocupados exclusivamente por la cepa de interés permanecieron blancos. Se pudo establecer así la relación entre la capacidad de ocupación de los nódulos de la cepa de estudio y su parental.

3.5. Recuento unidades formadoras de colonia (UFCs) adheridas a raíces

Para llevar a cabo la medida de la capacidad de adhesión de las distintas cepas de *S. meliloti* a las raíces de alfalfa, se llevó a cabo el siguiente procedimiento:

1. La esterilización de las semillas de alfalfa fue llevada a cabo como se describió en la sección 3.1. Para el crecimiento de las plantas se utilizaron 45 ml de la solución mineral libre de nitrógeno descrita por Rigaud and Puppo (1975), adicionada con agarosa al 0.8% preparada como se describe en la sección 3.2.
2. Por placa se dispusieron 17 semillas recién germinadas de aproximadamente 1 cm de largo. Las placas fueron selladas con papel parafilm

dejando el borde superior descubierto. La parte inferior de la placa fue cubierta con un sobre de papel opaco para evitar la incidencia de la luz sobre la raíz.

3. Antes de ser inoculadas, las plántulas fueron incubadas durante una noche en una cámara de cultivo de plantas, bajo las siguientes condiciones: 500 μeinstein.m^{-2}.s^{-1} (longitud de onda: 400-700 nm) de intensidad luminosa, fotoperíodo de 16/8 horas luz/oscuridad, 24/17ºC de temperatura día/noche y 50% de humedad relativa.

4. Las células de *S. meliloti* fueron crecidas en placas de medio TY adicionado con los correspondientes antibióticos para cada cepa. Para la inoculación de las raíces se tomó masa celular de cada cepa y se resuspendió en TY hasta O.D. 600 nm de 0.1.

5. Esta suspensión celular se lavó una vez con agua destilada estéril y de aquí se hicieron diluciones seriadas 1/10 hasta obtener una dilución de 1 x 10^6 células/ml aproximadamente.

6. Cada raíz fue inoculada con 30 μl de esta dilución celular bañando la raíz con el inóculo, empezando desde ápice hacia arriba. Diluciones seriadas del inóculo fueron sembradas en placas de medio TY adicionadas con el correspondiente antibiótico para cada cepa, para llevar el control del número de CFUs con el que las plántulas habían sido inoculadas.

7. Las placas fueron nuevamente selladas, guardadas en los sobres e incubadas en la cámara de plantas.

8. A los tiempos determinados para llevar a cabo el recuento de UFCs por mg de raíz, las raíces fueron lavadas con agua tres veces. Para ello, 15 raíces fueron puestas en un falcón de 50 ml con en 20 ml de agua estéril que fue agitado por inversión.

9. El exceso de humedad fue retirado secando la raíz en un papel Whatman estéril. 15 raíces fueron repartidas en 5 tubos epperdorf de 1.5 ml con 1ml de tampón TE estéril (10mM Tris-HCl, pH 7.5; 1mM EDTA) previamente tarados (3 raíces por eppendorf).

10. El tubo eppendorf conteniendo las tres raíces fue pesado de nuevo, para luego calcular el peso de las raíces.

11. A continuación los tubos fueron sometidos a sonicación mediante ultrasonidos. Se aplicaron 2 pulsos de 1min con un intervalo de 1min de espera entre ellos, para disociar las células adheridas a las raíces.
12. Se realizaron diluciones seriadas del contenido de los tubos y se sembraron en placas de TY más el correspondiente antibiótico. A los 2-3 días se llevó acabo el recuento del número UFCs. La eficiencia de cada cepa en la colonización y adhesión a las raíces se estimó en función de las UFCs referidas al peso de la raíz.

4. Técnicas químicas

4.1. Ensayo CAS (Chrome Azurol S) para la detección de sideróforos

4.1.1. Ensayo CAS del sobrenadante de cultivos celulares

La detección de la producción de sideróforos mediante el ensayo CAS líquido se realizó siguiendo el procedimiento descrito por Schwyn and Neilands (1987).

1. Se prepararon las siguientes soluciones

Solución 1 (stock): 50 ml de una solución 2 mM de CAS.
Solución 2 (stock): 50 ml de una solución 1mM de $FeCl_3.6H_2O$, 10 mM HCL.
Solución 3: Disolver 2.15 g de PIPERAZINE en 15 ml de H_2O destilada y ajustar el pH a 5.6 por adición de aproximadamente 6.25 ml de HCl concentrado.
Solución 4 (stock): 50 ml de 5-ácido sulfosalicílico 0.2 mM.

2. Disolver 0.01 g de bromuro de Hexadeciltrimetilammonio (HTDMA) en 25 ml de agua en un vaso de precipitado con un volumen de 50 ml. El compuesto debe ser disuelto con agitación lenta para evitar la formación de espuma.
3. A continuación sin dejar de agitar la solución de HTDMA, añadir en el siguiente orden las soluciones preparadas anteriormente:

3750 µl de la solución 1

750 µl de la solución 2

15 ml de la solución 3

1ml de la solución 4

Finalmente ajustar el volumen de la solución a 50 ml con H_2O destilada. La solución debe ser conservada en oscuridad y puede utilizarse por un tiempo aproximado de 24 h.

4. Para llevar a cabo la detección de producción del sideróforo rizobactina 1021, las cepas derivadas de Rm1021 fueron crecidas en MM hasta una O.D. 600 nm entre 1.2 y 1.5.

5. Se centrifugo 1 ml del cultivo durante 3 min a 12.000 rpm para retirar el pellet celular.

6. 500 µl del sobrenadante se mezclaron con 500 µl de la solución CAS. Esta solución se incubó durante 30 min a temperatura ambiente en oscuridad.

7. Tras la incubación la pérdida del color azul del complejo Fe-CAS-HTDMA se midió a 630 nm comparando la absorbancia de las muestras a evaluar, frente a la absorbancia de un blanco de MM tratado de igual manera. El ratio de producción del sideróforo se obtuvo dividiendo la absorbancia de la muestra entre la absorbancia del blanco. Para ajustar la absorbancia del espectrofotómetro se utilizó una cubeta vacía.

4.1.2. Ensayo CAS-agar (CASDA)

La detección de la producción de sideróforos mediante el ensayo CAS-agar se realizó siguiendo el procedimiento descrito por Schwyn and Neilands (1987) con algunas modificaciones. 500 ml de CAS-agar fueron preparados como se describe a continuación.

1. Disolver 30.25 mg de CAS (Fluka Chemicals) en 25 ml de H_2O destilada y mezclar con 5 ml de una solución de $FeCl_3.6H_2O$ 1 mM, 10 mM HCL.

2. Disolver 36.45 mg de HDTMA en 20 ml de H_2O destilada y mezclar con la solución anterior. Esta solución debe ser de color azul oscuro. Autoclavar a 120 ºC durante 20 min.

3. Por otra parte, disolver 15.12 g de Pipes, 6 g de una solución de NaOH al 50 % w/v en 400 ml de agua destilada (pH aproximadamente 5.4). Ajustar el pH

de esta solución a 6.8 con NaOH al 50 % w/v, adicionar 3 g agar purificado (0.6% del volumen final del medio CAS-agar en lugar de 1.3%) y llevar a un volumen de 450 ml. Esta solución debe ser autoclavada.

4. Mezclar las dos soluciones autoclavadas, y añadir 5ml de 5-ácido sulfosalicílico 0.2 M estilizado por filtración.

5. Servir 20 ml del medio CAS-agar en una placa de Petri. Dejar secar a temperatura ambiente y abrir un agujero de 5 mm de diámetro en el centro de la placa ayudándose de la parte trasera de una punta de micropipeta de 1000 µl.

6. Inocular el pocillo con 35 µl del sobrenadante de un cultivo crecido en MM hasta una O.D. 600 nm entre 1.2-1.5. Incubar durante al menos 8 h a 37 ºC en oscuridad.

4.1.3. Detección de la producción de sideróforos en colonias swarming

Para la detección de la producción de sideróforos en colonia swarming se modificó el protocolo del CAS-agar de (Schwyn and Neilands, 1987) como se describe a continuación:

1. Se realizó el ensayo swarming como se especifica en la sección 1.6.
2. Se prepararó el CAS-agar como se específica en la sección 4.1.2.
3. 24 h después del crecimiento de la colonia swarming el CAS-agar se vertió encima de la colonia.
4. Una vez solidificado el CAS-agar la placa fue incubada durante una noche a 37 ºC en oscuridad.

4.2. Purificación del sideróforo rizobactina 1021 de *S. meliloti*

Este protocolo fue desarrollado en la Universidad de Warwick (Coventry, Inglaterra), con ayuda del Profesor Gregory L. Challis y el Doctor Lijiang Song.

1. Se creció un preinóculo de G212rirA hasta una O.D. 600 nm de 1.5-1.8 en TY adicionado con los correspondientes antibióticos.
2. 3 ml del preinóculo crecido en TY fueron lavados dos veces con IDM.
3. 5 ml de IDM adicionado con 10 µM de $FeCl_3.6\ H_2O$ dispuestos en falcones de 50 ml, fueron inoculados con 100 µl del preinóculo de G212rirA lavado con IDM. Este cultivo se creció durante 4 días a 30 ºC (O.D. 600 nm = 1). De esta forma se crecieron aproximadamente 250 ml de cultivo.
4. Los 250 ml de cultivo se repartieron en falcones de 50ml. El sobrenadante fue recogido por centrifugación a 4000 rpm, durante 45 min, congelado en nitrógeno liquido y liofilizado a -70ºC, 100 µB, durante 2 noches.
5. La muestra de sobrenadante seca fue resuspendida en 4ml de una solución 80% metanol/20% agua destilada.
6. Para la purificación del sideróforo fue necesario correr dos programas de cromatografía líquida HPLC (High-performance liquid chromatography). En los ambos la mezcla de solventes que se utilizó fue la siguiente:

A: Agua para HPLC con ácido fórmico al 0.1%
D: Metanol para HPLC con metanol al 0.1%

Se utilizó un HPLC de fase reversa Agilent 1100 Semi-preparative, equipado con una columna 21 × 100 mm, C18, 5 µm, una bomba binaria y un detector de diodos.

Para recolectar la primera fracción de solvente que contenía el pico de m/z 531.2 se utilizaron los siguientes parámetros:

Parámetros de la cromatografía líquida
Tiempo total de ejecución: 50min
Tiempo total de funcionamiento de la bomba: 50min
Tasa de flujo: 5 ml/min
Temperatura: 25 ºC

Mezcla del solvente:

A: 65%

B: 0%

C: 0%

D: 35%

Tabla 6. Tiempos de disolución de la cromatografía líquida del primer HPLC de purificación de rizobactina 1021.

Tiempo	Función	Valor	
0	Mezcla de solvente	65% de A	35% de D
5min	Mezcla de solvente	65% de A	35% de D
30min	Mezcla de solvente	0% de A	100% de D
35min	Mezcla de solvente	0% de A	100% de D
40min	Mezcla de solvente	65% de A	35% de D

7 Se recogieron todas las fracciones mostrando picos altos de saturación y se analizaron con el espectrofotómetro de masas. La fracción cuyo tiempo de retención fue de 27.3 min y 28.3- 28.6 min mostró contener m/z 531.2. Hasta inyectar el total del volumen de la disolución metanol/agua del sobrenadante, se corrieron numerosos HPLC y se recolectaron las fracciones que contenían el pico correspondiente a m/z 531.2.

8. Las fracciones recolectadas fueron mezcladas y el metanol proveniente del HPLC fue eliminado haciendo uso de un rota vapor. La muestra seca se disolvió en 1 ml de agua y se congeló en nitrógeno líquido para luego ser liofilizada.

9. Para correr el segundo HPLC la muestra obtenida se disolvió en 2 ml de una solución que contenía 60% agua destilada/40% metanol. Los precipitados de sales presentes en la muestra fueron eliminados mediante centrifugación a 13000 rpm, durante 10 min a 4°C.

10. El segundo HPLC se corrió utilizando los siguientes parámetros:

Parámetros de la cromatografía líquida

Tiempo total de ejecución: 50min

Tiempo total de funcionamiento de la bomba: 50min

Tasa de flujo: 5 ml/min

Temperatura: 25 °C

Mezlca del solvente:

A: 30%

B: 0%

C: 0%

D: 70%

Tabla 7. Tiempos de disolución de la cromatografía líquida del segundo HPLC de purificación de rizobactina 1021.

Tiempo	Función	Valor	
0	Mezcla de solvente	65% de A	35% de D
5min	Mezcla de solvente	30% de A	70% de D
30min	Mezcla de solvente	0% de A	100% de D
35min	Mezcla de solvente	0% de A	100% de D
40min	Mezcla de solvente	30% de A	70% de D

11. El espectrofotómetro de masas mostró que el pico correspondiente a m/z 531.2 era el que tenía un tiempo de retención de 14.8 min y 17.8 min. Las fracciones recolectadas fueron mezcladas y secadas en un rota vapor.

12. La muestra seca fue lavada dos veces con 1 ml de agua y secada de nuevo en el rota vapor.

13. La muestra obtenida se disolvió en 2 ml de agua destilada, se congeló en nitrógeno líquido y se liofilizó.

14. Finalmente, para realizar el análisis en NMR la muestra fue disuelta en DMSO.

17. La rizobactina obtenida se diluyó en DMSO al 99% y se conservó a -20 ºC hasta su utilización.

4.3. Purificación de la molécula súper producida por 1021rhbG

Este protocolo fue desarrollado en la Universidad de Warwick (Coventry, Inglaterra), con ayuda del Profesor Gregory L. Challis y el Doctor Lijiang Song.

1. Se creció un preinóculo de 1021rhbG hasta una O.D. 600 nm de 1.5-1.8 en TY adicionado con los correspondientes antibióticos.

2. 1 ml del preinóculo crecido en TY fue lavado dos veces con IDM.
3. 10 falcones de 50 ml conteniendo 5 ml de IDM fueron inoculados con 100 µl del preinóculo de 1021rhbG lavado con IDM. Estos cultivos fueron incubados durante 2 días a 30ºC. Cuando los cultivos alcanzaron una O.D. 600 nm de 0.5-0.6, se adicionó ácido cítrico a una concentración final de 500 µm y se incubaron durante dos días más a 30 ºC hasta que alcanzaron una O.D. 600 nm de 1-1.2.
4. Los 100 ml de cultivo se repartieron en falcón de 50 ml y fueron centrifugados a 4000 rpm durante 45 min. El sobrenadante fue congelado en nitrógeno liquido y liofilizado a -70ºC, 100 µB durante 2 noches.
5. La muestra de sobrenadante seca fue resuspendida en 4ml de una solución 80% metanol/20% agua destilada.
6. Para la purificación de la molécula con m/z 307.2 fue necesario correr dos programas de HPLC. En ambos la mezcla de solventes que se utilizó fue la siguiente:

A: Agua para HPLC con ácido fórmico al 0.1%
D: Metanol para HPLC con metanol al 0.1%

Se utilizó un HPLC Agilent 1200 Series preparative, equipado con una bomba binaria y un detector de diodos.

Para recolectar la fracción de solvente que contenía la molécula m/z 307.2 se utilizó el siguiente programa:

Parámetros de la cromatografía líquida
Tiempo total de ejecución: 50 min
Tiempo total de funcionamiento de la bomba: 50 min
Tasa de flujo: 5 ml/min
Temperatura: 25 ºC

Mezcla del solvente:
A: 65%
B: 0%
C: 0%

D: 35%

Tabla 8. Tiempos de disolución de la cromatografía líquida, del primer HPLC de purificación de la molécula súper producida por 1021rhbG

Tiempo	Función	Valor	
0	Mezcla de solvente	65% de A	35% de D
5min	Mezcla de solvente	65% de A	35% de D
30min	Mezcla de solvente	0% de A	100% de D
35min	Mezcla de solvente	0% de A	100% de D
40min	Mezcla de solvente	65% de A	35% de D

7. Se recogieron todas las fracciones mostrando picos altos de saturación y se analizaron con el espectrofotómetro de masas. La fracción cuyo tiempo de retención era de entre 27.3 min y 29 min mostró contener la molécula con m/z 307.2. Hasta inyectar el total del volumen obtenido de la mezcla metanol/agua proveniente del sobrenadante, se corrieron numerosos HPLC y se recolectaron las fracciones que contenían m/z 307.2.

8. Las fracciones recogidas fueron mezcladas y a continuación el metanol proveniente del HPLC fue eliminado haciendo uso de un rota vapor. La muestra seca se disolvió en 1 ml de agua, se congeló en nitrógeno líquido y se liofilizó.

9. Para correr el segundo HPLC la muestra se disolvió en 2 ml de una solución que contenía 60% agua destilada/40% de metanol. Los parámetros utilizados para correr el segundo HPLC son los siguientes:

Parámetros de la cromatografía líquida

Tiempo total de ejecución: 50 min

Tiempo total de funcionamiento de la bomba: 50min

Tasa de flujo: 5 ml/min

Temperatura: 25 ºC

Mezlca del solvente:

A: 30%

B: 0%

C: 0%

D: 70%

Tabla 9. Tiempos de disolución de la cromatografía líquida del segundo HPLC de purificación de la molécula súper producida por 1021rhbG

Tiempo	Función	Valor	
0	Mezcla de solvente	65% de A	35% de D
5min	Mezcla de solvente	30% de A	70% de D
30min	Mezcla de solvente	0% de A	100% de D
35min	Mezcla de solvente	0% de A	100% de D
40min	Mezcla de solvente	30% de A	70% de D

10. El espectrofotómetro de masas mostró que el pico correspondiente a m/z 307.2 era el pico con tiempo de retención de entre 17.8 min y 18.5 min. Las fracciones recolectadas fueron mezcladas y secadas en un rota vapor.

11. La muestra seca fue lavada dos veces con 1 ml de agua y secada de nuevo en el rota vapor.

12. Se añadieron 2 ml de agua destilada a la muestra seca para luego congelarla en nitrógeno líquido y liofilizarla.

13. Para el correr el tercer HPLC la muestra conteniendo la molécula superproducida por 1021rhbG fue disuelta en una solución que contenía 0.1% TFA, 50% agua/metanol. Para llevar a cabo el tercer HPLC se siguieron los mismos parámetros descritos en la tabla 3.9.

14. Se recogió la fracción con tiempo de retención de 17.8 min y 18.5 min. El metanol en la muestra se retiró haciendo uso del rota vapor.

15. Finalmente para realizar el análisis en NMR compuesto fue disuelto en DMSO.

Bibliografía

Abdel-Mawgoud, A., F. Lépine, and E. Déziel. 2010. Rhamnolipids: diversity of structures, microbial origins and roles. Applied Microbiology and Biotechnology 86: 1323–1336.

Alché Ramírez, J. d. D. et al. 2007. Temperature and pyoverdine-mediated iron acquisition control surface motility of *Pseudomonas putida*. Environmental Microbiology 9: 1842–1850.

Allegrucci, M., and K. Sauer. 2007. Characterization of colony morphology variants isolated from *Streptococcus pneumoniae* biofilms. Journal of Bacteriology 189: 2030-2038.

Allison, C., L. Emody, N. Coleman, and C. Hughes. 1994. The role of swarm cell differentiation and multicellular migration in the uropathogenicity of *Proteus mirabilis*. Journal of Infectious Diseases 169: 1155-1158.

Amaya-Gómez., C. V. 2009. Identificación de determinantes genéticos del swarming en *S. meliloti*. Trabajo de Investigación Tutelada, Universidad de Granada, Trabajo de Investigación Tutelada.

Ames, P., and K. Bergman. 1981. Competitive advantage provided by bacterial motility in the formation of nodules by *Rhizobium meliloti*. Journal of Bacteriology 148: 728-729.

Bahlawane, C., M. McIntosh, E. Krol, and A. Becker. 2008. *Sinorhizobium meliloti* regulator MucR couples exopolysaccharide synthesis and motility. Molecular plant-microbe interactions : MPMI 21: 1498–1509.

Banin, E., M. L. Vasil, and E. P. Greenberg. 2005. Iron and *Pseudomonas aeruginosa* biofilm formation. Proceedings of the National Academy of Sciences of the United States of America 102: 11076-11081.

Barnett, M. J. et al. 2001. Nucleotide sequence and predicted functions of the entire *Sinorhizobium meliloti* pSymA megaplasmid. Proceedings of the National Academy of Sciences 98: 9883–9888.

Becker, A. et al. 2004. Global Changes in Gene Expression in *Sinorhizobium meliloti* 1021 under Microoxic and Symbiotic Conditions. Molecular Plant-Microbe Interactions 17: 292-303.

Beringer, J. E. 1974. R factor transfer in *Rhizobium Leguminosarum* Journal of General Microbiology 84: 188-198.

Berlutti, F. et al. 2005. Iron availability influences aggregation, biofilm, adhesion and invasion of *Pseudomonas aeruginosa* and *Burkholderia cenocepacia*. International journal of immunopathology and pharmacology 18: 661–670.

Bernabéu-Roda, L. 2010. Identificación y caracterización inicial de genes que participan en el control del swarming de *Sinorhizobium meliloti*: papel en formación de biopelículas y establecimiento de simbiosis. Trabajo de investigación Tutelada, Universidad de Granada, Trabajo de Investigación Tutelada.

Bernier, S. P., D.-G. Ha, W. Khan, J. H. Merritt, and G. A. O'Toole. 2011. Modulation of *Pseudomonas aeruginosa* surface-associated group behaviors by individual amino acids through c-di-GMP signaling. Research in Microbiology 162: 680-688.

Bomfeti, C. A. et al. 2011. Exopolysaccharides produced by the symbiotic nitrogen-fixing bacteria of leguminosae. Revista Brasileira de Ciência do Solo 35: 657-671.

Braeken, K. et al. 2008. Genetic determinants of swarming in *Rhizobium etli*. Microbial Ecology 55: 54–64.

Caetano-Anollés, G., D. K. Crist-Estes, and W. D. Bauer. 1988. Chemotaxis of *Rhizobium meliloti* to the plant flavone luteolin requires functional nodulation genes. Journal of Bacteriology 170: 3164–3169.

Caiazza, N. C., J. H. Merritt, K. M. Brothers, and G. A. O'Toole. 2007. Inverse regulation of biofilm formation and swarming motility by *Pseudomonas aeruginosa* PA14. Journal of Bacteriology 189: 3603-3612.

Caiazza, N. C., R. M. Q. Shanks, and G. A. O'Toole. 2005. Rhamnolipids modulate swarming motility patterns of *Pseudomonas aeruginosa*. Journal of Bacteriology 187: 7351–7361.

Capela, D. et al. 2001. Analysis of the chromosome sequence of the legume symbiont *Sinorhizobium meliloti* strain 1021. Proceedings of the National Academy of Sciences 98: 9877–9882.

Carlson, R. W., L. S. Forsberg, and E. L. Kannenberg. 2010. Lipopolysaccharides in *Rhizobium*-Legume symbioses. In: X. Wang and P. J. Quinn (eds.). Subcellular Biochemistry No. 53. p 339–386. Springer Netherlands.

Casadesus, J., and J. Olivares. 1979. Rough and fine linkage mapping of the *Rhizobium meliloti* chromosome. Molecular & General Genetics 174: 203-209.

Casse, F., C. Boucher, J. S. Julliot, M. Michel, and J. Denarie. 1979. Identification and characterization of large plasmids in *Rhizobium meliloti* using agarose gel electrophoresis. Journal of General Microbiology 113: 229–242.

Cheng, H. P., and G. C. Walker. 1998. Succinoglycan is required for initiation and elongation of infection threads during nodulation of alfalfa by *Rhizobium meliloti*. Journal of Bacteriology 180: 5183-5191.

Copeland, M. F., and D. B. Weibel. 2009. Bacterial swarming: a model system for studying dynamic self-assembly. Soft Matter 5: 1174–1187.

Danhorn, T., and C. Fuqua. 2007. Biofilm formation by plant-associated bacteria Annu. Rev. Microbiol. Annual Review of Microbiology No. 61. p 401-422. Annual Reviews, Palo Alto.

Daniels, R. et al. 2006. Quorum signal molecules as biosurfactants affecting swarming in *Rhizobium etli*. Proceedings of the National Academy of Sciences 103: 14965-14970.

Daniels, R., J. Vanderleyden, and J. Michiels. 2004. Quorum sensing and swarming migration in bacteria. Fems Microbiology Reviews 28: 261-289.

Davey, M. E., and G. A. O'toole. 2000. Microbial Biofilms: From ecology to molecular genetics. Microbiology and Molecular Biology Reviews 64: 847-867.

Dharmatilake, A. J., and W. D. Bauer. 1992. Chemotaxis of *Rhizobium meliloti* towards nodulation gene-inducing compounds from alfalfa roots. Applied and Environmental Microbiology 58: 1153–1158.

Domínguez-Ferreras, A. et al. 2006. Transcriptome profiling reveals the importance of plasmid pSymB for osmoadaptation of *Sinorhizobium meliloti*. Journal of Bacteriology 188: 7617–7625.

Dondrup, M. et al. 2003. EMMA: a platform for consistent storage and efficient analysis of microarray data. Journal of Biotechnology 106: 135–146.

Eberl, L., S. Molin, and M. Givskov. 1999. Surface motility of *Serratia liquefaciens* MG1. Journal of Bacteriology 181: 1703–1712.

Edwards, A. et al. 2009. The *cin* and *rai* quorum-sensing regulatory systems in *Rhizobium leguminosarum* are coordinated by ExpR and CinS, a small regulatory protein coexpressed with CinI. Journal of Bacteriology 191: 3059–3067.

Fellay, R., J. Frey, and H. Krisch. 1987. Interposon mutagenesis of soil and water bacteria: a family of DNA fragments designed for in vitro insertional mutagenesis of Gram-negative bacteria. Gene 52: 147–154.

Ferreira, R. B. R., L. C. M. Antunes, E. P. Greenberg, and L. L. McCarter. 2008. *Vibrio parahaemolyticus* ScrC modulates cyclic dimeric GMP regulation of gene expression relevant to growth on surfaces. Journal of Bacteriology 190: 851–860.

Finan, T. M. et al. 2001. The complete sequence of the 1,683-kb pSymB megaplasmid from the N2-fixing endosymbiont *Sinorhizobium meliloti*. Proceedings of the National Academy of Sciences 98: 9889–9894.

Flemming, H.-C., and J. Wingender. 2010. The biofilm matrix. Nat Rev Micro 8: 623-633.

Fournier, J. et al. 2008. Mechanism of Infection thread elongation in root hairs of *Medicago truncatula* and dynamic Interplay with associated rhizobial colonization. Plant Physiology 148: 1985-1995.

Fraser, G. M., and C. Hughes. 1999. Swarming motility. Current Opinion in Microbiology 2: 630–635.

Fraysse, N., F. Couderc, and V. Poinsot. 2003. Surface polysaccharide involvement in establishing the *Rrhizobium*–legume symbiosis. European Journal of Biochemistry 270: 1365–1380.

Fujishige, N., L. Rinaudi, W. Giordano, and A. Hirsch. 2006a. Superficial liaisons: colonization of roots and abiotic surfaces by rhizobia. Biology of Plant-Microbe Interactions 5: 292–299.

Fujishige, N. A. 2006. Molecular analysis of biofilm formation by Rhizobium species. University of California, Los Angeles.

Fujishige, N. A., N. N. Kapadia, P. L. De Hoff, and A. M. Hirsch. 2006b. Investigations of *Rhizobium* biofilm formation. FEMS Microbiology Ecology 56: 195-206.

Fujishige, N. A., N. N. Kapadia, and A. M. Hirsch. 2006c. A feeling for the micro-organism: structure on a small scale. Biofilms on plant roots. Botanical Journal of the Linnean Society 150: 79-88.

Fujishige, N. A. et al. 2008. *Rhizobium* common nod genes are required for biofilm formation. Molecular Microbiology 67: 504-515.

Gaddy, J. A., and L. A. Actis. 2009. Regulation of *Acinetobacter baumannii* biofilm formation. Future microbiology 4: 273.

Gage, D. J. 2004. Infection and invasion of roots by symbiotic, nitrogen-fixing rhizobia during nodulation of temperate Legumes. Microbiol. Mol. Biol. Rev. 68: 280-300.

Galibert, F. et al. 2001. The composite genome of the legume symbiont *Sinorhizobium meliloti*. Science 293: 668-672.

Garcia-Rodriguez, F. M., and N. Toro. 2000. *Sinorhizobium meliloti nfe* (nodulation formation efficiency) genes exhibit temporal and spatial expression patterns similar to those of genes involved in symbiotic nitrogen fixation. Mol Plant Microbe Interact 13: 583–591.

Gibson, K. E., M. J. Barnett, C. J. Toman, S. R. Long, and G. C. Walker. 2007. The symbiosis regulator CbrA mdulates a complex regulatory network affecting the flagellar apparatus and cell envelope proteins. Journal of Bacteriology 189: 3591–3602.

Glick, R. et al. 2010. Increase in rhamnolipid synthesis under iron-limiting conditions influences surface motility and biofilm formation in *Pseudomonas aeruginosa*. Journal of Bacteriology 192: 2973-2980.

Griffitts, J. S., and S. R. Long. 2008. A symbiotic mutant of *Sinorhizobium meliloti* reveals a novel genetic pathway involving succinoglycan biosynthetic functions. Molecular Microbiology 67: 1292–1306.

Gurich, N., and J. E. González. 2009. Role of quorum sensing in *Sinorhizobium meliloti*-alfalfa symbiosis. Journal of Bacteriology 191: 4372–4382.

Hall-Stoodley, L., J. W. Costerton, and P. Stoodley. 2004. Bacterial biofilms: from the natural environment to infectious diseases. Nat Rev Micro 2: 95-108.

Hellweg, C., A. Puhler, and S. Weidner. 2009. The time course of the transcriptomic response of *Sinorhizobium meliloti* 1021 following a shift to acidic pH. BMC Microbiology 9: 37.

Henrichsen, J. 1972. Bacterial surface translocation: a survey and a classification. Bacteriological Reviews 36: 478–503.

Heydorn, A. et al. 2000. Quantification of biofilm structures by the novel computer program COMSTAT. Microbiology 146: 2395–2407.

Hirsch, A., M. Lum, and N. Fujishige. 2009. Microbial Encounters of a Symbiotic Kind: Attaching to Roots and Other Surfaces

Ho, S. N., H. D. Hunt, R. M. Horton, J. K. Pullen, and L. R. Pease. 1989. Site-directed mutagenesis by overlap extension using the polymerase chain reaction. Gene 77: 51–59.

Root Hairs. In: A. Emons and T. Ketelaar (eds.). Plant Cell Monographs No. 12. p 295–314. Springer Berlin / Heidelberg.

Hoang, H. H., A. Becker, and J. E. González. 2004. The LuxR homolog ExpR, in combination with the Sin quorum sensing system, plays a central role in *Sinorhizobium meliloti* gene expression. Journal of Bacteriology 186: 5460–5472.

Hoang, H. H., N. Gurich, and J. E. González. 2008. Regulation of motility by the ExpR/Sin quorum-sensing System in *Sinorhizobium meliloti*. Journal of Bacteriology 190: 861–871.

Houry, A. et al. 2012. Bacterial swimmers that infiltrate and take over the biofilm matrix. Proceedings of the National Academy of Sciences 109: 13088–13093.

Inoue, T. et al. 2007. Genome-wide screening of genes required for swarming motility in *Escherichia coli* K-12. Journal of Bacteriology 189: 950–957.

Janczarek, M., J. Kutkowska, T. Piersiak, and A. Skorupska. 2010. *Rhizobium leguminosarum* bv. trifolii *rosR* is required for interaction with clover, biofilm formation and adaptation to the environment. BMC Microbiology 10: 284.

Johnson, M., A. Cockayne, and J. A. Morrissey. 2008. Iron-regulated biofilm formation in *Staphylococcus aureus* Newman requires *ica* and the secreted protein Emp. Infection and Immunity 76: 1756–1765.

Jones, K. M., H. Kobayashi, B. W. Davies, M. E. Taga, and G. C. Walker. 2007. How rhizobial symbionts invade plants: the *Sinorhizobium*-Medicago model. Nat. Rev. Microbiol. 5: 619-633.

Kearns, D. B. 2010. A field guide to bacterial swarming motility. Nat Rev Micro 8: 634-644.

Kim, W., and M. G. Surette. 2004. Metabolic differentiation in actively swarming *Salmonella*. Molecular Microbiology 54: 702–714.

Kinsinger, R. F., M. C. Shirk, and R. Fall. 2003. Rapid surface motility in *Bacillus subtilis* is dependent on extracellular surfactin and potassium ion. Journal of Bacteriology 185: 5627–5631.

Klausen, M., A. Aaes-Jorgensen, S. Molin, and T. Tolker-Nielsen. 2003a. Involvement of bacterial migration in the development of complex multicellular structures in *Pseudomonas aeruginosa* biofilms. Molecular Microbiology 50: 61–68.

Klausen, M. et al. 2003b. Biofilm formation by *Pseudomonas aeruginosa* wild type, flagella and type IV pili mutants. Molecular Microbiology 48: 1511-1524.

Komath, S. S., M. Kavitha, and M. J. Swamy. 2006. Beyond carbohydrate binding: new directions in plant lectin research. Organic & Biomolecular Chemistry 4: 973–988.

Krol, E., and A. Becker. 2004. Global transcriptional analysis of the phosphate starvation response in *Sinorhizobium meliloti* strains 1021 and 2011. Molecular Genetics and Genomics 272: 1–17.

Kuchma, S. L. et al. 2007. BifA, a cyclic-di-GMP phosphodiesterase, inversely regulates biofilm formation and swarming motility by *Pseudomonas aeruginosa* PA14. Journal of Bacteriology 189: 8165-8178.

Kuiper, I. et al. 2004. Characterization of two *Pseudomonas putida* lipopeptide biosurfactants, putisolvin I and II, which inhibit biofilm formation and break down existing biofilms. Molecular Microbiology 51: 97–13.

Laus, M. C. et al. 2006. A novel polar surface polysaccharide from *Rhizobium leguminosarum* binds host plant lectin. Molecular Microbiology 59: 1704–1713.

Lederberg, E. M., and S. N. Cohen. 1974. Transformation of *Salmonella typhimurium* by plasmid deoxyribonucleic Acid. Journal of Bacteriology 119: 1072–1074.

Leonard, L. T. 1943. A simple assembly for use in the testing of cultures of rhizobia. Journal of Bacteriology 45: 523–527.

Lindström, K., M. Murwira, A. Willems, and N. Altier. 2010. The biodiversity of beneficial microbe-host mutualism: the case of rhizobia. Research in Microbiology 161: 453–463.

Lindum, P. W. et al. 1998. N -acyl-l-homoserine lactone autoinducers control production of an extracellular lipopeptide biosurfactant required for swarming motility of *Serratia liquefaciens* MG1. Journal of Bacteriology 180: 6384–6388.

Liu, X., S. Beyhan, B. Lim, R. G. Linington, and F. H. Yildiz. 2010. Identification and characterization of a phosphodiesterase that inversely regulates motility and biofilm formation in vibrio cholerae. Journal of Bacteriology 192: 4541–4552.

Lynch, D. et al. 2001. Genetic organization of the region encoding regulation, biosynthesis, and transport of rhizobactin 1021, a siderophore produced by *Sinorhizobium meliloti*. Journal of Bacteriology 183: 2576-2585.

Ma, Q., G. Zhang, and T. Wood. 2011. *Escherichia coli* BdcA controls biofilm dispersal in *Pseudomonas aeruginosa* and *Rhizobium meliloti*. BMC Research Notes 4: 447.

Maniatis, T., E. F. Fritsch, and J. Sambrook. 1989. Molecular cloning : a laboratory manual / J. Sambrook, E.F. Fritsch, T. Maniatis. New York : Cold Spring Harbor Laboratory Press.

Masson-Boivin, C., E. Giraud, X. Perret, and J. Batut. 2009. Establishing nitrogen-fixing symbiosis with legumes: How many *Rhizobium* recipes? Trends in Microbiology 17: 458-466.

Mateos, P. F. et al. 1995. Direct in siut identification of cellulose microfibrils associated with *Rhizobium leguminosarum* biovar *trifolii* attached to the root epidermis of white clover. Canadian Journal of Microbiology 41: 202–207.

May, T., and S. Okabe. 2011. Enterobactin is required for biofilm development in reduced-genome *Escherichia coli*. Environmental Microbiology 13: 3149–3162.

McCarter, L., M. Hilmen, and M. Silverman. 1988. Flagellar dynamometer controls swarmer cell differentiation of *V. parahaemolyticus*. Cell 54: 345-351.

Meade, H. M., and E. R. Signer. 1977. Genetic mapping of *Rhizobium meliloti*. Proceedings of the National Academy of Sciences of the United States of America 74: 2076-2078.

Miller, J. H. 1972. Experiments in molecular genetics. New York : Cold Spring Harbor Laboratory.

Miller, L. D., C. K. Yost, M. F. Hynes, and G. Alexandre. 2007. The major chemotaxis gene cluster of *Rhizobium leguminosarum* bv. *viciae* is essential for competitive nodulation. Molecular Microbiology 63: 348–362.

Mireles, J. R., A. Toguchi, and R. M. Harshey. 2001. *Salmonella enterica* Serovar Typhimurium swarming mutants with altered biofilm-forming abilities: surfactin inhibits biofilm formation. Journal of Bacteriology 183: 5848–5854.

Morris, J., and J. E. González. 2009. The novel genes emmABC Are associated with exopolysaccharide production, motility, stress Adaptation, and symbiosis in *Sinorhizobium meliloti*. Journal of Bacteriology 191: 5890–5900.

Müller, G., and K. N. Raymond. 1984. Specificity and mechanism of ferrioxamine-mediated iron transport in *Streptomyces pilosus*. Journal of Bacteriology 160: 304–312.

Nogales, J., L. Bernabéu-Roda, V. Cuéllar, and M. J. Soto. 2012. ExpR is not required for swarming but promotes sliding in *Sinorhizobium meliloti*. Journal of Bacteriology.

Oldroyd, G. E., J. D. Murray, P. S. Poole, and J. A. Downie. 2011. The rules of engagement in the legume-rhizobial symbiosis. Annu. Rev. Genet. 45: 119–144.

O'Toole, G. A. et al. 1999. Genetic approaches to study of biofilms. Methods in enzymology 310: 91–109.

Olivares, J., J. Casadesus, and E. J. Bedmar. 1980. Method for testing degree of infectivity of *Rhizobium melioti* strains. Applied and Environmental Microbiology 39: 967-970.

Oresnik, I. J., S.-L. Liu, C. K. Yost, and M. F. Hynes. 2000. Megaplasmid pRme2011a of *Sinorhizobium meliloti* is not required for viability. Journal of Bacteriology 182: 3582–3586.

Osterås, M., B. T. Driscoll, and T. M. Finan. 1995. Molecular and expression analysis of the *Rhizobium meliloti* phosphoenolpyruvate carboxykinase (pckA) gene. Journal of Bacteriology 177: 1452-1460.

Overhage, J., M. Bains, M. D. Brazas, and R. E. W. Hancock. 2008. Swarming of *Pseudomonas aeruginosa* is a complex adaptation leading to increased production of virulence factors and antibiotic resistance. Journal of Bacteriology 190: 2671-2679.

Overhage, J., S. Lewenza, A. K. Marr, and R. E. W. Hancock. 2007. Identification of genes involved in swarming motility using a *Pseudomonas aeruginosa* PAO1 Mini-Tn5-lux mutant library. Journal of Bacteriology 189: 2164–2169.

Pamp, S. J., and T. Tolker-Nielsen. 2007. Multiple roles of biosurfactants in structural biofilm development by *Pseudomonas aeruginosa*. Journal of Bacteriology 189: 2531-2539.

Patrick, J. E., Kearns, and D. B. 2012. Swarming motility and the control of master regulators of flagellar biosynthesis, Blackwell, Oxford, ROYAUME-UNI.

Patrick, J. E., and D. B. Kearns. 2012. Swarming motility and the control of master regulators of flagellar biosynthesis. Molecular Microbiology 83: 14–23.

Patriquin, G. M. et al. 2008. Influence of quorum sensing and iron on twitching motility and biofilm formation in *Pseudomonas aeruginosa*. Journal of Bacteriology 190: 662-671.

Pearson, M. M., D. A. Rasko, S. N. Smith, and H. L. T. Mobley. 2010. Transcriptome of swarming *Proteus mirabilis*. Infection and Immunity 78: 2834–2845.

Peck, M. C., R. F. Fisher, and S. R. Long. 2006. Diverse flavonoids stimulate NodD1 binding to *nod* gene promoters in *Sinorhizobium meliloti*. J. Bacteriol. 188: 5417-5427.

Pehl, M. J. et al. 2012. Genes that influence swarming motility and biofilm formation in Variovorax paradoxus EPS. PLoS ONE 7: e31832.

Pérez-Giménez, J. et al. 2009. Soybean lectin enhances biofilm formation by *Bradyrhizobium japonicum* in the absence of plants. International Journal of Microbiology 2009.

Peypoux, F., J. M. Bonmatin, and J. Wallach. 1999. Recent trends in the biochemistry of surfactin. Applied Microbiology and Biotechnology 51: 553□563.

Pratt, J. T., E. McDonough, and A. Camilli. 2009. PhoB regulates motility, biofilms, and cyclic di-GMP in *Vibrio cholerae*. Journal of Bacteriology 191: 6632–6642.

Ramey, B. E. 2004. Biofilm formation in plant-microbe associations. Current Opinion in Microbiology 7: 602.

Rather, P. N. 2005. Swarmer cell differentiation in *Proteus mirabilis*. Environmental Microbiology 7: 1065–1073.

Rhijn, V. et al. 2001. Sugar-binding activity of pea lectin enhances heterologous infection of transgenic alfalfa plants by *Rhizobium leguminosarum* biovar *viciae*. American Society of Plant Biologists, Rockville, MD, ETATS-UNIS.

Rigaud, J., and A. Puppo. 1975. Indole-3-acetic acid catabolism by soybean bacteroids. Journal of General Microbiology 88: 223–228.

Rinaudi, L. et al. 2006. Effects of nutritional and environmental conditions on *Sinorhizobium meliloti* biofilm formation. Research in Microbiology 157: 867-875.

Rinaudi, L. V., and W. Giordano. 2010. An integrated view of biofilm formation in rhizobia. FEMS microbiology letters 304: 1–11.

Rinaudi, L. V., and J. E. González. 2009. The low-molecular-weight fraction of exopolysaccharide II from *Sinorhizobium meliloti* is a crucial determinant of biofilm formation. Journal of Bacteriology 191: 7216-7224.

Robertsen, B. K., P. Aman, A. G. Darvill, M. McNeil, and P. Albersheim. 1981. The structure of acidic extracellular polysaccharides secreted by *Rhizobium leguminosarum* and *Rhizobium trifolii*. Plant Physiology 67: 389-400.

Robledo, M. et al. 2008. Rhizobium cellulase CelC2 is essential for primary symbiotic infection of legume host roots. Proceedings of the National Academy of Sciences 105: 7064–7069.

Robledo, M. et al. 2012. Role of Rhizobium endoglucanase CelC2 in cellulose biosynthesis and biofilm formation on plant roots and abiotic surfaces. Microb Cell Fact 11: 125.

Rodríguez-Navarro, D. N., M. S. Dardanelli, and J. E. Ruíz-Saínz. 2007. Attachment of bacteria to the roots of higher plants. FEMS microbiology letters 272: 127–136.

Rodriguez, R. L., and R. C. Tait. 1983. Recombinant DNA techniques: An introduction. Addison-Wesley (Reading, Mass.).

Ron, E. Z., and E. Rosenberg. 2001. Natural roles of biosurfactants. Environmental Microbiology 3: 229–236.

Rotter, C., S. Mühlbacher, D. Salamon, R. Schmitt, and B. Scharf. 2006. Rem, a new transcriptional activator of motility and chemotaxis in *Sinorhizobium meliloti*. Journal of Bacteriology 188: 6932–6942.

Rüberg, S. et al. 2003. Construction and validation of a *Sinorhizobium meliloti* whole genome DNA microarray: genome-wide profiling of osmoadaptive gene expression. Journal of Biotechnology 106: 255-268.

Russo, D. M. et al. 2006. Proteins exported via the PrsD-PrsE type I secretion system and the acidic exopolysaccharide are involved in biofilm formation by *Rhizobium leguminosarum*. Journal of Bacteriology 188: 4474-4486.

Sambrook, J., and E. Fritsch. 1989. Maniatis: T Molecular clonning: A laboratory manual. Cold Spring Harbor Laboratory Press 2: Cold Spring Harbor N.Y.

Sandy, M., and A. Butler. 2009. Microbial iron acquisition: marine and terrestrial siderophores. Chemical Reviews 109: 4580–4595.

Schäfer, A. et al. 1994. Small mobilizable multi-purpose cloning vectors derived from the *Escherichia coli* plasmids pK18 and pK19: selection of defined deletions in the chromosome of *Corynebacterium glutamicum*. Gene 145: 69-73.

Schmitt, R. 2002. Sinorhizobial chemotaxis: a departure from the enterobacterial paradigm. Microbiology 148: 627-631.

Schwyn, B., and J. B. Neilands. 1987. Universal chemical assay for the detection and determination of siderophores. Analytical Biochemistry 160: 47–56.

Shrout, J. D. et al. 2006. The impact of quorum sensing and swarming motility on *Pseudomonas aeruginosa* biofilm formation is nutritionally conditional. Molecular Microbiology 62: 1264-1277.

Simon, R., U. Priefer, and A. Puhler. 1983. A broad host range mobilization system for In vivo genetic engineering: Transposon mutagenesis in Gram negative bacteria. Nat Biotech 1: 784-791.

Skorupska, A., M. Janczarek, M. Marczak, A. Mazur, and J. Krol. 2006. Rhizobial exopolysaccharides: genetic control and symbiotic functions. Microbial Cell Factories 5: 7.

Smit, G., S. Swart, B. J. J. Lugtenberg, and J. W. Kijne. 1992. Molecular mechanisms of attachment of *Rhizobium* bacteria to plant roots. Molecular Microbiology 6: 2897–2903.

Smit, G., D. M. J. Tubbing, J. W. Kijne, and B. J. J. Lugtenberg. 1991. Role of Ca2+ in the activity of rhicadhesin from *Rhizobium leguminosarum* biovar *viciae* , which mediates the first step in attachment of *Rhizobiaceae* cells to plant root hair tips. Archives of Microbiology 155: 278–283.

Smith, T. G., and T. R. Hoover. 2009. Deciphering bacterial flagellar gene regulatory networks in the genomic era. Advances in applied microbiology 67: 258.

Soby, S., and K. Bergman. 1983. Motility and chemotaxis of *Rhizobium meliloti* in soil. Applied and Environmental Microbiology 46: 995–998.

Soto, M. J., A. Domínguez-Ferreras, D. Pérez-Mendoza, J. Sanjuán, and J. Olivares. 2009. Mutualism versus pathogenesis: the give-and-take in plant–bacteria interactions. Cellular Microbiology 11: 381-388.

Soto, M. J., M. Fernández-Pascual, J. Sanjuan, and J. Olivares. 2002. A *fadD* mutant of *Sinorhizobium meliloti* shows multicellular swarming migration and is impaired in nodulation efficiency on alfalfa roots. Molecular Microbiology 43: 371-382.

Soto, M. J., J. Sanjuán, and J. Olivares. 2006. Rhizobia and plant-pathogenic bacteria: common infection weapons. Microbiology 152: 3167–3174.

Sourjik, V., P. Muschler, B. Scharf, and R. Schmitt. 2000. VisN and VisR are global regulators of chemotaxis, flagellar, and motility genes in *Sinorhizobium* (*Rhizobium*) *meliloti*. Journal of Bacteriology 182: 782–788.

Southern, E. M. 1975. Detection of specific sequences among DNA fragments separated by gel electrophoresis. Journal of Molecular Biology 98: 503–517.

Takahashi, C. et al. 2008. Swarming of *Pseudomonas aeruginosa* PAO1 without differentiation into elongated hyperflagellates on hard agar minimal medium. FEMS microbiology letters 280: 169–175.

Tambalo, D. D., C. K. Yost, and M. F. Hynes. 2010. Characterization of swarming motility in *Rhizobium leguminosarum* bv. *viciae*. FEMS microbiology letters 307: 165-174.

Touati, D. 2000. Iron and Oxidative Stress in Bacteria. Archives of Biochemistry and Biophysics 373: 1–6.

Tremblay, J., and E. Deziel. 2010. Gene expression in *Pseudomonas aeruginosa* swarming motility. BMC Genomics 11: 587.

van Brussel, A. A. N. et al. 1992. Induction of pre-infection thread structures in the leguminous host plant by mitogenic lipo-oligosaccharides of *Rhizobium*. Science 257: 70-72.

van Rhijn, P., N. A. Fujishige, P. O. Lim, and A. M. Hirsch. 2001. Sugar-binding activity of pea lectin enhances heterologous infection of transgenic alfalfa plants by *Rhizobium leguminosarum* biovar *viciae*. Plant Physiol 126: 133–144.

Vanderlinde, E. M. et al. 2009. *Rhizobium leguminosarum* biovar viciae 3841, deficient in 27-hydroxyoctacosanoate-modified lipopolysaccharide, is

impaired in desiccation tolerance, biofilm formation and motility. Microbiology 155: 3055-3069.

Verstraeten, N. et al. 2008. Living on a surface: swarming and biofilm formation. Trends in Microbiology 16: 496-506.

Wang, H., Z. Zhong, T. Cai, S. Li, and J. Zhu. 2004a. Heterologous overexpression of quorum-sensing regulators to study cell-density-dependent phenotypes in a symbiotic plant bacterium *Mesorhizobium huakuii*. Archives of Microbiology 182: 520–525.

Wang, P., Z. Zhong, J. Zhou, T. Cai, and J. Zhu. 2008. Exopolysaccharide biosynthesis is important for *Mesorhizobium tianshanense*: plant host interaction. Archives of Microbiology 189: 525–530.

Wang, Q. F., J. G. Frye, M. McClelland, and R. M. Harshey. 2004b. Gene expression patterns during swarming in *Salmonella typhimurium*: genes specific to surface growth and putative new motility and pathogenicity genes. Molecular Microbiology 52: 169-187.

Wells, D. H., E. J. Chen, R. F. Fisher, and S. R. Long. 2007. ExoR is genetically coupled to the ExoS–ChvI two-component system and located in the periplasm of *Sinorhizobium meliloti*. Molecular Microbiology 64: 647–664.

Williams, A. et al. 2008. Glucomannan-mediated attachment of *Rhizobium leguminosarum* to pea root hairs is required for competitive nodule infection. Journal of Bacteriology 190: 4706–4715.

Xu, J., T. G. Platt, and C. Fuqua. 2012. Regulatory linkages between flagella and surfactant during swarming behavior: lubricating the flagellar propeller? Journal of Bacteriology 194: 1283–1286.

Yoshida, A. 2005. LuxS-based signaling affects *Streptococcus mutans* biofilm formation. Applied and Environmental Microbiology 71: 2372.

Yost, C. K., K. L. Del Bel, J. Quandt, and M. F. Hynes. 2004. *Rhizobium leguminosarum* methyl-accepting chemotaxis protein genes are down-regulated in the pea nodule. Archives of Microbiology 182: 505–513.

Yost, C. K., P. Rochepeau, and M. F. Hynes. 1998. *Rhizobium leguminosarum* contains a group of genes that appear to code for methyl-accepting chemotaxis proteins. Microbiology 144: 1945–1956.

Results

Chapter 1: Transcriptome profiling of a *Sinorhizobium meliloti fadD* mutant reveals the role of rhizobactin 1021 biosynthesis and regulation genes in the control of swarming

Transcriptome profiling of a *Sinorhizobium meliloti fadD* mutant reveals the role of rhizobactin 1021 biosynthesis and regulation genes in the control of swarming.

Joaquina Nogales, Ana Domínguez-Ferreras, Carol V Amaya-Gómez, Pieter van Dillewijn, Virginia Cuéllar, Juan Sanjuán, José Olivares, and María J Soto.

Departamento de Microbiología del Suelo y Sistemas Simbióticos, Estación Experimental del Zaidín, CSIC, Profesor Albareda, 1, 18008 Granada, Spain.

Published in BMC Genomics, Volume 11:157, pages 1471-2164, in March 2010.

1.1. Abstract

Background

Swarming is a multicellular phenomenom characterized by the coordinated and rapid movement of bacteria across semisolid surfaces. In *Sinorhizobium meliloti* this type of motility has been described in a *fadD* mutant. To gain insights into the mechanisms underlying the process of swarming in *Rhizobium*, we compared the transcriptome of a *S. meliloti fadD* mutant grown under swarming inducing conditions (semisolid medium) to those of cells grown in non-swarming conditions (broth and solid medium).

Results

More than a thousand genes were identified as differentially expressed in response to growth on agar surfaces including genes for several metabolic activities, iron uptake, chemotaxis, motility and stress-related genes. Under swarming-specific conditions, the most remarkable response was the up-regulation of iron-related genes. We demonstrate that the pSymA plasmid and specifically genes required for the biosynthesis of the siderophore rhizobactin 1021 are essential for swarming of a *S. meliloti* wild-type strain but not in a *fadD* mutant. Moreover, high iron conditions inhibit swarming of the wild-type strain but not in mutants lacking either the iron limitation response regulator RirA or FadD.

Conclusions

The present work represents the first transcriptomic study of *Rhizobium* growth on surfaces including swarming-inducing conditions. The results have revealed major changes in the physiology of *S. meliloti* cells grown on a surface relative to liquid cultures. Moreover, analysis of genes responding to swarming inducing conditions led to the demonstration that iron and genes involved in rhizobactin 1021 synthesis play a role in the surface motility shown by *S. meliloti* which can be circumvented in a *fadD* mutant. This work opens a way to the identification of new traits and regulatory networks involved in swarming by *Rhizobium*.

1.2. Introduction

Swarming is a type of bacterial motility generally dependent on flagella and is characterized by a rapid and co-ordinated population migration across solid surfaces. In contrast to other modes of bacterial surface translocation, swarming involves a complex process of differentiation in which cells usually become hyperflagellated and elongated [1]. Signals and signalling pathways controlling swarm cell differentiation are largely unknown. Extracellular chemical signals such as N-acyl-homoserine lactones (AHL), peptides and amino acids, fatty acids, polyamines, etc, as well as physiological parameters, surface contact and wetness provide stimuli to trigger swarm cell differentiation (reviewed in [1-4]). It is generally believed that the different environmental, cell-to-cell, and intracellular signals may be sensed and transduced by two-component regulatory systems and cytosolic regulators, leading to a complex regulatory network.

Classical genetic studies performed in different bacteria have allowed the identification of several genes essential for swarming. Interestingly, recent genome-scale approaches performed in model bacteria such as *Salmonella typhimurium*, *Escherichia coli* and *Pseudomonas aeruginosa*, indicate that swarmer differentiation represents much more than a motility phenotype as substantial alterations in metabolic pathways and gene expression have been observed [5-9]. In *E. coli*, up to one-fifth of the genes on the genome seem to be involved in swarming [7]. Besides flagellar functions, a large number of genes involved in several metabolic activities, iron acquisition, regulatory proteins, chaperones, and biosynthesis of cell surface components have been demonstrated to be important for this multicellular migration [7,8].

In several pathogenic bacteria, swarming is associated with virulence [1,2]. This could be partially due to the fact that the expression of some virulence determinants seems to be coregulated with swarmer differentiation. Urease, metalloprotease and haemolysin are up-regulated during swarming in the uropathogenic *Proteus mirabilis* [3], whereas phospholipase is induced in the opportunistic pathogen *Serratia liquefaciens* [10]. Global gene expression analysis

performed on swarmer cells has revealed the upregulation of a large number of virulence-related genes in *S. typhimurium* and *P. aeruginosa* such as genes encoding components of a type III secretion system, its effectors, extracellular proteases, and proteins involved in iron transport [6,9]. An interesting aspect related to virulence is the fact that swarmer cells, like biofilm communities, display increased resistance to several antimicrobials when compared to planktonic cells [9,11].

Although swarming has been extensively studied in pathogenic bacteria, this type of surface motility has also been described in beneficial bacteria like rhizobia. These soil bacteria are known for their ability to establish a mutualistic symbiosis with legume plants. A remarkable feature of this interaction is the formation of a new organ, the root nodule, within which endosymbiotic differentiated bacteria fix atmospheric nitrogen to generate nitrogen sources usable by the plant, thus conferring a nutritional advantage to the host. The formation of a nitrogen-fixing nodule is a complex process requiring the coordination of bacterial infection with a root developmental program (for a review see [12,13]). Accumulating evidence suggests that in order to colonize, invade and establish a chronic infection within the host, rhizobia use similar strategies as pathogenic bacteria (reviewed in [14,15]).

The first report of swarming by rhizobia was described for a *fadD* mutant of the alfalfa symbiont *Sinorhizobium meliloti* [16]. In this bacterium, the lack of the *fadD* gene (encoding a long-chain fatty acyl-coenzyme A ligase), results in multicellular swarming behaviour but also defects in nodulation, thereby suggesting that fatty acid-related compounds may act as signals controlling motility and symbiosis. More recently, it has been reported that a wild type strain of *Rhizobium etli*, the bacterial symbiotic partner of common bean plants, can swarm [17]. The finding that mutants in the *cinIR* quorum sensing system of this bacterium were no longer able to move over semisolid surfaces, led to the discovery that AHL carrying a long-chain fatty acid moiety have a dual role in swarming in this rhizobium: as quorum sensing signals and as biosurfactants which promote surface translocation [18]. The characterization of several *R. etli*

mutants defective in swarming has allowed the identification of additional genetic determinants which seem to play a role in this multicellular behaviour, including genes involved in polysaccharide synthesis or export, motility and amino acid and polyamines metabolism [19]. Interestingly, half of the mutants with an altered swarming pattern showed deficiencies in either nodulation or nitrogen fixation. The biological role of swarming in rhizobia remains to be elucidated. However, the fact that some mutations which alter swarming behaviour in *S. meliloti* and *R. etli* result in an impairment in the establishment of the symbiosis, suggests that either components essential for this multicellular motility and/or factors which are co-regulated during swarmer cell differentiation might play a role in the interaction with the host plant.

To gain insights into the adaptation process involved in multicellular swarming motility in rhizobium, global gene expression profiles of *S. meliloti fadD* cells in swarming inducing conditions were determined and compared with the profiles obtained during growth in liquid media as well as on non-swarming hard agar.

1.3. Materials and methods

Bacterial strains and growth conditions

Strains used in this study are listed in table 1.1. *E. coli* strains were grown in Luria-Bertani (LB) medium [50] at 37°C; *S. meliloti* strains were grown at 30°C in TY complex medium [51] or in minimal medium (MM) containing glutamate (6.5 mM), mannitol (55 mM), mineral salts (K_2HPO_4, 1.3 mM; KH_2PO_4 . $3H_2O$, 2.2 mM; $MgSO_4$ $7H_2O$, 0.6 mM; $CaCl_2$ $2H_2O$, 0.34 mM; $FeCl_3$ $6H_2O$, 0.022 mM; NaCl, 0.86 mM) and vitamins (biotin (0.2mg/L); calcium pantothenate (0.1 mg/L)) [52]. Standard MM contains 22 µM $FeCl_3$. When a different concentration or source of iron was required, stock solutions 100-fold concentrated of either $FeCl_3$ or ferric citrate were prepared and added to MM without iron. To test the ability to use oleate as sole carbon source, M9 medium [53] was used in which glucose was replaced with 5 mM oleate. When required, antibiotics were added at the following

final concentrations: for *E. coli*, streptomycin (Sm) 50 μg/ml, spectinomycin (Sp) 100 μg/ml, kanamycin (Km) 50 μg/ml, and ampicillin (Ap) 200 μg/ml; for *S. meliloti*, Sm 200 μg/ml, Km 200 μg/ml, rifampin (Rif) 100 μg/ml, and neomycin sulphate (Nm) 100 μg/ml. To improve reproducibility of behaviour, all liquid cultures of *S. meliloti* were routinely initiated from glycerol stocks.

Table 1.1. Bacterial strains and plasmids used

Strain or plasmid	Relevant characteristics[a]	Reference or source
Escherichia coli		
DH5α	*supE*44, Δ*lacU*169, *f*80, *lacZ*ΔM, *recA*1, *endA*1, *gyrA*96, *thi*1, *relA*1, *5hsdR*171	Bethesda Research Lab®
S17.1	*thi*, *pro*, *recA*, *hsdR*, *hsdM*, Rp4Tc::Mu, Km::Tn*7*; Tp^r, Sm^r, Sp^r	[60]
Sinorhizobium meliloti		
GR4	Wild type	[61]
QS77	GR4 (*fadD*::Tn*5*), Km^r	[16]
Rm1021	SU47 *expR102*::IS*Rm*2011-1, Sm^r	[62]
1021FDC5	Rm1021 (Δ*fadD*::Km), Sm^r Km^r	This work
1021FDCSS	Rm1021 (Δ*fadD*::SmSp), Sm^r Sp^r	This work
Rm2011	SU47 *expR102*::IS*Rm*2011-1, Sm^r	[63]
2011FDC	Rm2011 (Δ*fadD*::SmSp), Sm^r Sp^r	This work
SmA818	Rm2011 pSymA cured, Sm^r	[64]
A818FDC	SmA818 (Δ*fadD*::SmSp), Sm^r Sp^r	This work
2011rhbA62	Rm2011 (*rhbA::*Tn*5lac*), Sm^r Rif^r Nm^r	[30]
2011rhbAFDC	2011rhbA62 (Δ*fadD*::SmSp), Sm^r Sp^r Rif^r Nm^r	This work
2011rhbE11	Rm2011 (*rhbE::*Tn*5lac*), Sm^r Rif^r Nm^r	[30]
2011rhbEFDC	2011rhbE11 (Δ*fadD*::SmSp), Sm^r Sp^r Rif^r Nm^r	This work
2011rhrA26	Rm2011 (*rhrA::*Tn*5lac*), Sm^r Rif^r Nm^r	[30]
2011rhrAFDC	2011rhrA26 (Δ*fadD*::SmSp), Sm^r Sp^r Rif^r Nm^r	This work
2011rhtA1	Rm2011 (*rhtA::*Tn*5*), Sm^r Rif^r Nm^r	[30]
2011rhtAFDC	2011rhtA1 (Δ*fadD*::SmSp), Sm^r Sp^r Rif^r Nm^r	This work
G212rirA	Rm1021 (lac^-, *rirA*::Km), Sm^r Km^r	O'Connell, M.
G212rirAFDC	G212rirA (Δ*fadD*::SmSp), Sm^r Km^r	This work
Plasmids		
pBSKS(+)	Cloning vector; Ap^r	Stratagene
pHP45Ω	Plasmid containing Sm/Sp cassette; Ap^r, Sm^r, Sp^r	[65]
pHP45Ω Km	Plasmid containing Km cassette; Ap^r, Km^r	[66]
pK18mobsacB	Suicide plasmid; Km^r	[54]
pBBRD4	pBBR1MCS-3 derivative containing the *fadD* gene of *S. meliloti* GR4; Tc^r	[16]
pBSDIL12	pBSKS derivative containing the *fadD* gene of *S. meliloti* GR4; Ap^r	This work
pBS12.6Km	pBSDIL12 in which the *fadD* gene has been deleted and interrupted with a Km cassette; Ap^r Km^r	This work
pK18fadDCKm	pK18*mobsacB* carrying the fadD mutated version of pBS12.6Km;	This work
pK18fadDCSS	pK18fadDCKm in which the Km cassette interrupting the *fadD* gene has been substituted by a Sm/Sp cassette	This work

Construction of *S. meliloti fadD* mutants

The *fadD*- strain 1021FDC5 used in the microarray experiments was obtained by allelic exchange. A disrupted version of the *fadD* gene was constructed by deleting an internal fragment and inserting a kanamycin resistance cassette. Firstly, a *Kpn*I/*Xba*I fragment harbouring the *fadD* gene of *S. meliloti* was subcloned from pBBRD4 [16] into pBluescript to give pBSDIL12. After removal of a *Bam*HI site from the polylinker of pBSDIL12, an internal *Bam*HI fragment of 300 bp of the *fadD* gene was replaced with a 2.2 kb *Bam*HI fragment containing the Km^R cassette from pHP45Ω-Km to give pBS12.6Km. This construction was digested with *Kpn*I, treated with T4 DNA polymerase (Roche Biochemicals) to make blunt ends, and then digested with *Xba*I to isolate the Km^R fragment which was then cloned into the suicide vector pK18*mobsacB* previously digested with *Sma*I/*Xba*I, to give pK18fadDCKm. This plasmid was introduced by conjugation into *S. meliloti* 1021 and allele replacement events were selected as described previously [54].

The *fadD*- strain 1021FDCSS was obtained following the same procedure as for 1021FDC5 with the only difference that the Km^R cassette present in pK18fadDCKm was substituted by the Sm^R/Sp^R cassette from pHP45Ω to give pK18fadDCSS. The *fadD* mutation present in 1021FDCSS was transferred into different strain backgrounds by generalized transduction of 1021FDCSS using phage ϕM12 as described previously [55]. All the different *fadD* mutants obtained were confirmed by Southern hybridization with a specific probe.

Swarming and swimming assays

Swarming assays were carried out as described in Soto *et al.* [16]. Briefly, *S. meliloti* cells grown in TY broth to late logarithmic phase (optical density (OD) at 600 nm = 1-1.2) were pelleted, washed twice in MM and resuspended in 0.1 volume of the latter medium. 2-µl aliquots of this bacterial suspension (ca. 2 x 10^7cells) were dispensed onto the surface of swarm plates and allowed to dry for 10 min. Swarm plates were prepared with 20 ml of MM containing 0.6% purified

agar (Pronadisa), and air dried at room temperature for 15 min. Incubation periods of 14 to 20 h at 30ºC, were enough to observe swarming. To complement swarming in rhizobactin-defective mutants, a well was cut in the center of the swarm plate and 100 µl of a concentrated supernatant containing rhizobactin was added. Aliquots of the wild type strain and rhizobactin-defective mutants prepared as described above were placed onto the surface of the swarm plate surrounding the well. Alternatively for this complementation assay, cells were grown in TY broth, pelleted, washed twice in MM and resuspended in 0.1 volume of concentrated supernatant containing rhizobactin. Finally, 2-µl aliquots of this bacterial suspension were assayed for surface motility on swarm plates. Concentrated supernatants containing rhizobactin 1021 were obtained as described by Lynch et al. [30] from wild-type strain Rm2011 grown to stationary phase in either TY broth with 200 µM 2, 2'-dipyridyl or MM broth with 2 µM 2, 2'-dipyridyl. Before its use in swarming assays, the presence of siderophore in the supernatants was checked in iron nutrition bioassays as described by Lynch et al. [30].

Swimming plates were prepared with either Bromfield medium (0.04% tryptone, 0.01% yeast extract, and 0.01% $CaCl_2.2H_2O$) containing 0.3% Bacto agar or with MM containing 0.3% purified agar. Plates were inoculated with 3-µl droplets of rhizobial cultures grown in TY, and incubated at 30ºC for 2 to 5 days.

Determination of bacterial growth curves

Bacterial growth curves of *S. meliloti* 1021FDC5 were determined in liquid, semisolid (0.6% purified agar) and solid (1.3% purified agar) MM. A preinoculum was grown in 20 ml of TY broth to late logarithmic phase ($OD_{600\ nm}$ = 1-1.2). After incubation, cells were pelleted, washed twice in MM and resuspended in 2 ml of the latter medium. For growth curves in liquid MM, Erlenmeyer flasks (250 ml) containing 50 ml of liquid MM were inoculated with 0.5 ml of the rhizobial suspension (the initial inoculum of the culture being approximately 10^8 cells/ml) and incubated at 30ºC with continuous shaking (190 r.p.m.). For growth curves in plates, aliquots of 0.1 ml of the rhizobial suspension were used to sow MM

plates (initial inoculum of approximately 10^9 cells/plate) . This size of inoculum was used to ensure that on semisolid and solid MM plates, the same density of cells per surface area is applied as in standard swarming assays (10^7 cells per 0.2 cm^2). The rhizobial suspension was evenly spread over the surface of semisolid and solid MM plates, allowed to dry for 10 min and then inverted and incubated at 30°C. This sampling on plates was preferred over inoculation with droplets allowing swarmers to migrate out, to minimize heterogeneity among cells. Samples from liquid cultures and plates were collected at different time points for cell count determination. Cells grown on plates were harvested by scraping the surface with 2 ml of sterile liquid MM.

RNA isolation and synthesis of labelled cDNA

For RNA isolation, cells from 18 ml of broth culture or grown on the surface of 3 plates were harvested, washed with sarkosyl 0.1% and cell pellets were immediately frozen in liquid nitrogen and conserved at -80°C until RNA isolation. For microarray hybridization and reverse transcription quantitative real-time PCR(RT-qPCR), RNA was isolated using the Qiagen RNeasy RNA purification kit (Qiagen) following manufacturer's instructions. Residual DNA was removed with RNase-free Dnase I Set (ROCHE). The quality of RNA was checked on 1.4% agarose gel electrophoresis.

Cy3- and Cy5-labelled cDNAs were prepared according to DeRisi *et al.* [56] (http://www.microarrays.org/protocols.html) from 15 µg of total RNA. Three slide hybridizations were performed using the labelled cDNA synthesized from each of the RNA preparations from three independent bacterial cultures.

Microarray hybridization, image acquisition and data analysis

Sm6koligo microarrays were purchased from A. Becker (University of Bielefeld, Bielefeld, Germany). Hybridizations were performed as described previously [21,37]. For image acquisition a GenePix 4100A Scanner (Axon Instruments, Inc., Foster City, CA, USA) was used. Quantifications of mean signal

intensities for each spot were determined using the GenePix Pro 5.0 software (Axon Instruments, Inc.). Normalization and t-statistics were carried out using the EMMA 2.6 microarray data analysis software developed at the Bioinformatics Resource Facility, Center for Biotechnology, Bielefeld University (http://www.genetik.uni-bielefeld.de/EMMA/) [57]. Three independent biological replicates were performed for each experiment. Genes were regarded as differentially expressed if they showed $p \leq 0.05$, $A \geq 7$ and $M \geq 1$ or $M \leq -1$ (A, average signal-to noise; M value is $\log_2$ experiment/control ratio) in any of the experiments performed. Detailed protocols and raw data resulting from the microarray experiments have been deposited in the ArrayExpress database with the accession number E-MEXP-1953.

Reverse transcription quantitative real-time PCR (RT-qPCR).

Total RNA (1 µg) treated with RNase-free Dnase I Set (ROCHE) was reversely transcribed using Superscript II reverse transcriptase (INVITROGEN) and random hexamers (ROCHE) as primers. Quantitative real-time PCR was performed on an iCycler iQ5 (Bio-Rad, Hercules, CA, USA). Each 25 µl reaction contained either 1 µl of the cDNA or a dilution of it (1:10.000, for amplification of the 16S rRNA gene), 200 nM each primer and iQ SyBrGreen Supermix (BioRad). Control PCR reactions of RNA samples no treated with reverse transcriptase were also performed to confirm the absence of contaminating genomic DNA. Samples were initially denatured by heating at 95ºC for 3 minutes followed by a 35-cycle amplification and quantification program (95ºC for 30s, 55ºC for 45s, and 72ºC for 45s). A melting curve was conducted to ensure amplification of a single product. The oligonucleotide sequences for qPCR are listed in table 1.2. The efficiency for each primer pair (E) was determined by running 10-fold serial dilutions (4 dilution series) of Rm1021 genomic DNA as template and generating a standard curve by plotting the log of the dilution factor against the C_T value during amplification of each dilution. Amplification efficiency is calculated using the formula ($E=[10^{(1/a)}-1]x100$) where a is the slope of the standard curve.

The relative expression of each gene was normalized to that of 16S rRNA and the analysis of results was done using the comparative critical threshold ($\Delta\Delta C_T$) method [58].

Table 1.2. Sequences of the oligonucleotides used for quantitative real-time PCR.

Gene	Forward Primer (5' to 3')	Reverse Primer (5' to 3')
SMc03224 (*16S*)	TCTACGGAATAACGCAGG	GTGTCTCAGTCCCAATGT
SMc03015 (*visN*)	TCCTTGATGCTGCTCTTC	CTCGGTCAGTTCGCATTC
SMc03046 (*rem*)	CGAAAGCCACATCAGCAAGC	ATTCCAGTCGATGCAGTAGCC
SMc03027 (*flgB*)	GAAAGCGTGCTTCAGAAC	CTGACTTCGGTCACATGC
SMc03037 (*flaA*)	CGATTATGTCAAGGTCCA	GCAATGGTGATGTCGATC
SMc03040 (*flaC*)	CCGACGGCAGCGTTACG	ATCCGCATTCACCGCCTTG
SMc01513 (*hmuS*)	ACATCAAGCAAGGACACG	CACTTGTCGAAGAACTGC
SMc02085 (*exbB*)	CTTCCGCATGATCTTTCG	AGTTCCAGCGTCTTCACG
SMa2402 (*rhbB*)	TGAACATCAACGTCGCTG	GGAGTAGAGACTGCTTGC
SMa2414 (*rhtA*)	CATCATCACGAAGAAGGG	TCGCTGTTATAGGTGACC
SMa1077 (*nex18*)	GTCAATTCAAGACGCTGG	GGTTTCAGCAGGTTTTCG
SMb20934 (*exsF*)	ATCGCTACTCTCGATCTC	TCGTTCAGGCAAGTCAAG

CAS siderophore assay

The determination of siderophores in liquid cultures was performed using the Chrome azurol S (CAS) assay solution described by Schwyn and Neilands [59]. Supernatants of *S. meliloti* cultures grown in MM containing different concentrations of $FeCl_3$ were mixed 1:1 with the CAS assay solution. After reaching equilibrium, the absorbance was measured at 630 nm.

1.4. Results and Discussion

Construction and characterization of a *S. meliloti* 1021 *fadD* mutant

In *S. meliloti*, swarming motility has been reported for a *fadD* mutant (QS77) of the GR4 strain. Under the same swarming inducing conditions, the wild type strain GR4 has never shown this surface motility [16,20]. In order to identify genes which are expressed during swarm cell differentiation in *S. meliloti*, we performed a transcriptomic analysis of a *fadD* mutant using the Sm6kOligo microarrays [21]. Since these arrays are based on the genome of *S. meliloti* strain

Rm1021 [22], we constructed a *fadD* mutant in this genetic background by site-directed mutagenesis as described in Materials and Methods. The mutant obtained was named 1021FDC5. In contrast to the wild type strains GR4 and Rm1021, 1021FDC5 like QS77 cannot grow on M9 medium plates containing oleate as sole carbon source (data not shown). Introduction of the pBBRD4 construct harbouring the *S. meliloti fadD* gene into 1021FDC5, restored the ability to grow on oleate indicating that like in QS77, the growth phenotype shown by 1021FDC5 is the result of a mutation in the *fadD* gene. Furthermore, as reported for QS77, 1021FDC5 shows conditional swarming motility on semisolid MM plates (Fig. 1.1). It is worth mentioning that whereas GR4, as stated above, has never shown surface motility under our swarming inducing conditions, in approximately 70% of the experiments performed, Rm1021 cells spread over the surface of the plate resembling the movement displayed by the *fadD* mutants (Fig. 1.1). A similar behaviour to that shown by Rm1021 was also observed for the closely related strain Rm2011 (see Fig. 1.6 and 1.7). This suggests that the control of swarming may be different in GR4 and Rm1021/Rm2011, although in all three *S. meliloti* strains a mutation in *fadD* promotes multicellular surface motility (Fig. 1.1 and 1.7). This result was particularly intriguing as it has been published that in *S. meliloti*, ExpR is required for swarming but not for swimming [23,24], and it is known that Rm1021 and Rm2011 are *expR*-deficient strains [25]. We have tried to reproduce swarming in different *S. meliloti* strains under the conditions described by Bahlawane *et al.* [24] without success. In any case, we show here that *expR*-defective strains (Rm1021, Rm2011 and their *fadD*-derivative mutants) can swarm on semisolid MM (Fig. 1.1, 1.6 and 1.7) which suggests that the role of ExpR in swarming needs to be re-evaluated. This and the identification of the molecular bases responsible for the different swarming behaviour shown by GR4 and Rm1021 are currently under investigation in our group [67].

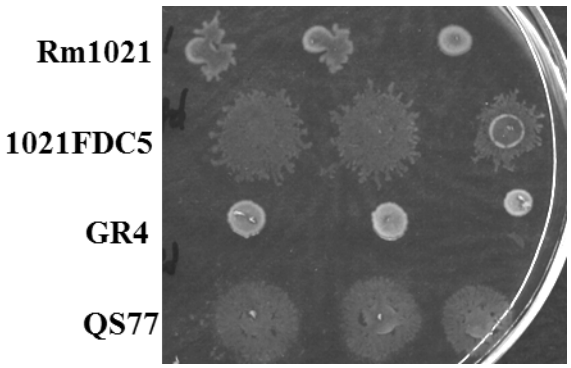

Figure 1.1. Swarming behaviour of *S. meliloti* strains. The swarming motility phenotype of S. meliloti wild-type strains Rm1021 and GR4 and their corresponding *fadD*-derivative mutants 1021FDC5 and QS77 was analyzed by inoculating aliquots (2 µl) of each strain prepared as described in Materials and Methods onto semisolid MM plates containing 0.6% purified agar. Replicates corresponding to the same strain were placed on a row. The picture was taken 48 hours after inoculation and is a representative of at least three independent experiments.

Transcriptome profiling of *S. meliloti* 1021FDC5 in broth and on agar surfaces

In order to identify genes whose expression is altered during swarming in *S. meliloti*, the transcriptome of 1021FDC5 growing in swarming-inducing media (semisolid MM containing 0.6% agar) was compared with the transcriptome of cells growing in non-swarming conditions (solid MM containing 1.3% hard agar and MM broth). We also compared the transcriptomes of 1021FDC5 after growth in broth and solid MM to identify genes which are not specific for swarming but responsive to growth on surfaces. This analysis required, as a first step, the determination of bacterial growth curves in liquid, semisolid and solid MM to ensure that the respective transcriptomes of all strains were obtained in the same growth phase. Figure 1.2 shows that the growth profiles were very similar for all three conditions tested, with cells entering stationary phase at 24 h.

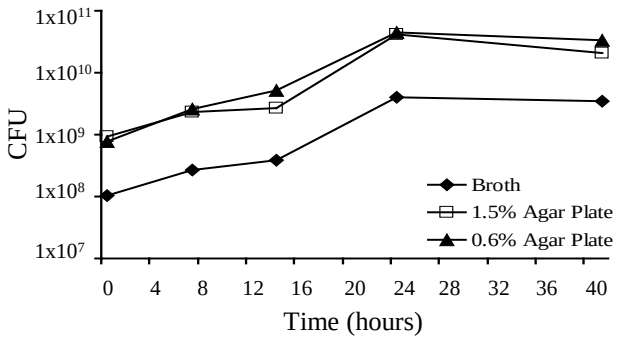

Figure 1.2. Growth curves of *S. meliloti* 1021FDC5 in broth and agar surfaces. Bacterial growth curves were determined in liquid, semisolid (0.6% purified agar) and solid (1.3% purified agar) MM. CFU refers to colony forming units/ml of broth or per plate. Data are representative of at least two replicate experiments.

We studied the different expression profiles at early exponential phase (7 hours) and mid exponential phase (14 hours). These time points were chosen because in our standard swarming assays, 7 hours is the minimum time required to macroscopically observe surface motility whereas after 14 hours, swarming diminishes as recognized by slower cell migration and increased mucoidy. The macroscopic appearance of 1021FDC5 cells growing on solid and semisolid MM is shown in Figure 1.3. After 14 h on solid MM (1.3% agar), 1021FDC5 grows as a homogenous lawn on the plate, indistinguishable from the non-swarming strain GR4. On the other hand, on semisolid MM (0.6%), growth of both, GR4 and 1021FDC5, is not homogenous on the surface of the plate with visible uncolonized areas. However, whereas the borders of colonized areas by GR4 are smooth, in the case of 1021FDC5 these borders show a dendritic morphology indicating that these cells were actively swarming. Therefore, we conclude that this experimental setup is adequate for a transcriptomic study of swarming.

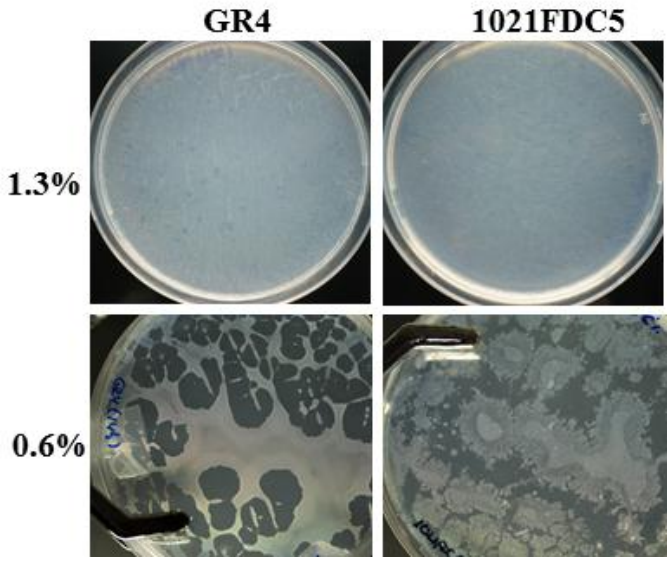

Figure 1.3. Macroscopic appearance of 1021FDC5 cells growing on solid and semisolid MM plates. 100 µl of a suspension containing approximately 10^9 cells of either *S. meliloti* 1021FDC5 (*fadD* mutant) or GR4 (wild type strain which does not show swarming) as control were evenly spread over the surface of solid (1.3% agar) and semisolid (0.6% agar) MM plates. The pictures were taken 14 hours after incubation at 30°C.

An internal control experiment in which Cy3- and Cy5- labeled cDNAs were synthesized from total RNA extracted from liquid cultures of 1021FDC5, led us to consider as differentially expressed only genes showing an M value ($\log_2$ values of the ratio of intensities) of ≥1 or ≤ -1. A total of 1166 genes (19% of the annotated genes in the *S. meliloti* Rm1021 genome) appeared as differentially expressed in any of the six conditions studied (see additional data file 1.1 and table 1.3). More than 35% of the 1166 genes formed part of presumed operons where two or more genes appeared as differentially expressed under our experimental conditions. To facilitate the analysis, genes showing up- or down-regulation in any of the six different comparisons were plotted in a Venn diagram (Fig. 1.4).

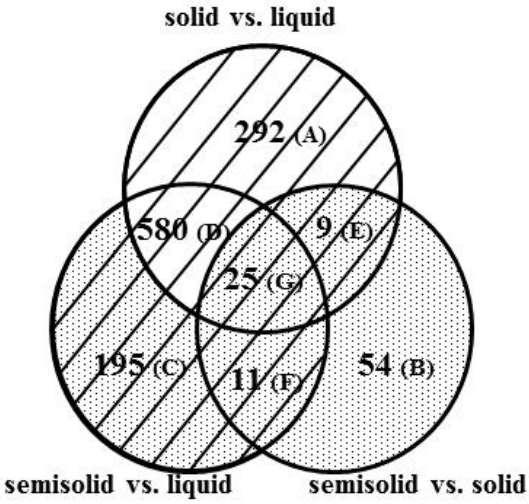

Figure 1.4. Venn diagram of *S. meliloti* differentially regulated genes identified in microarray experiments. The diagram represents the number of differentially expressed genes obtained in six different microarray experiments (based on additional data file 1.1). The transcriptomes of *S. meliloti* 1021FDC5 cells obtained after growth in liquid, solid and semisolid MM were compared. For each of the three combinations, changes in the mRNA levels were monitored after 7 and 14 hours growth. The different subsets have been assigned with letters (A-G). The set of surface responsive genes is indicated with stripes and that of swarming responsive genes with dots.

Most of the genes identified in our study (1112) showed differential expression in response to growth on a surface (i.e. differentially expressed in cells grown in solid or semisolid media vs. broth; striped area in Fig. 1.4) and only 54 genes appeared exclusively in the comparison of the transcriptome of cells grown in semisolid MM with that of cells grown in solid MM. Within the group of surface-responsive genes, more than 50% of the genes (580 + 25) showed differential expression regardless of the concentration of agar used, whereas a smaller number of genes showed differential expression after growth specifically on hard agar or semisolid medium, (292 and 195, respectively). On the other hand, a total of 294 genes were found to be differentially expressed specifically under swarming inducing conditions (dotted area in Fig. 1.4) comprising genes which appeared differentially expressed in the comparison of cells grown in semisolid vs. solid media (99 genes), plus 195 genes which exclusively appeared differentially expressed in cells grown in semisolid vs. liquid media). It is noteworthy that 45 out of the 294 genes differentially expressed under swarming inducing conditions were also found differentially expressed in response to surface growth (subsets E, F, and G of 9, 11, and 25 genes, respectively; Fig. 1.4).

This might suggest that a significant portion of swarming-responsive genes are regulated in response to contact with a surface, a known signal for swarming in other bacteria [1, 4].

Surface responsive genes

The comparison of the transcriptome of cells grown in liquid MM with that of cells grown in solid or semisolid MM sampled at two different time points, led to the identification of 1112 differentially expressed genes (table 1.3 and striped area in Fig. 1.4): 705 genes were up-regulated in response to surface growth, 384 down-regulated, and 23 genes showed variable responses (up- or down-regulated depending on the time point or agar concentration). Most of the surface responsive genes identified in our study (96%) showed a late response, appearing as differentially expressed after 14 hours growth (table 1.3).

Many of the down-regulated genes (31%) encoded proteins of unknown or hypothetical function, which hindered drawing conclusions on down regulated processes. Most noteworthy of the remaining down-regulated genes is that several are involved in nitrogen metabolism and exopolysaccharide production. Among the former are the regulatory genes *glnK* and *ntrBC*, glutamine synthetase genes (*glnII*, *glnT*, SMc01594 and SMc02352), putative glutamate synthase genes (*glxBCD* and *gltD*), the *nirB* nitrite reductase gene, and genes coding for transporters for ammonium (*amtB*), nitrate (*nrtABC* and SMb21114), and amino acids (*aap* genes). The lower expression observed for most of these genes for growth on agar surfaces compared to growth in broth culture could be explained by the down-regulation of the *ntrC* gene coding for the key transcriptional activator of nitrogen catabolic operons [26]. However, the reason why *ntrC* is down-regulated on agar surface conditions compared to broth is presently unknown. Likewise, the expression of some *nif* (*nifA, nifB, nifX*) and *fix* (*fixB, fixI*$_2$, *fixQP*$_3$) genes was diminished in cells grown on solid and semisolid media compared to liquid culture. This could also be a consequence of the lower abundance of the NtrC activator and/or of the higher oxygen concentration in agar-solidified media. The other conspicuous group of down-regulated genes in

response to growth in agar surfaces includes several *exo* genes involved in exopolysaccharide (EPS) production (*exoA*, *exoM*, *exoN*, *exoP*, *exoN2*). The molecular bases for the lower expression of these *exo* genes remain unknown.

Table 1.3. Number of genes differentially expressed in *S. meliloti* 1021FDC5 in response to different growth conditions

Comparison [a]	Up-regulated		Down-regulated	
	7 hours	14 hours	7 hours	14 hours
Semisolid vs liquid (811)	35	580	8	217
Semisolid vs solid (99)	38	18	39	9
Solid vs liquid (906)	7	542	10	354

[a] The total number of genes identified as differentially expressed in each comparison is shown in parenthesis. This number does not coincide with the addition of numbers of the same line because some of the genes appeared as differentially expressed in the two time points analyzed or showed variable responses depending on the time point.

In contrast with the down-regulated genes, the majority (85%) of the genes up-regulated in response to surface growth have known or putative functions. Below we describe some of the most relevant ones:

1) Carbon and energy metabolism. The induction of genes involved in the uptake (*smoEFGK*) and metabolism (*smoS*, *mtlK*, *xylA*) of mannitol as well as those involved in glutamate degradation (*glmS*, *gsh1*, *carA*, *gabT*, *nodM*), the carbon and nitrogen sources provided in our experiments, indicated a higher metabolic rate in response to surface growth. This is in agreement with the up-regulation of genes of the tricarboxylic acid cycle (*lpdA2*, *acnA*, *icd*, *sdhBCD*, *mdh*, *sucABCD*, *pckA*), the Calvin cycle (SMb20194, *ppe*, *cbbXSLAT*), the glycolysis (*cbbA2*, *gap*, *glk*, *pgk*, *eno, pdhAa*, *pgi*), and of the different complexes in the respiratory chain and associated functions: *nuoA1B1C1D1G1IJK1LMN*, *cyoBC*, *fixN1Q1*, *ndh*, *ctaBCDE*, *rrpP*, *ppa, ppk*, *atpABDEFF2GHI* and SMc00410. The higher metabolic rate could also be the cause of the observed induction of phosphate transport systems (*phoTEDC*, *phoU*, *pstABC* and SMc02146).

2) Protein metabolism. As many as 54 genes coding for ribosomal proteins were found to be induced during surface growth. We also observed up-regulation of different genes involved in the ribosome assembly and maturation (*rbfA* and *rhlE*), genes involved in the processing of mRNA, rRNA and tRNA (*rne*, *rnc*, *rnr*, *rnpA* and *pnp*), and different genes related to the translation process (*infB*, *tufA, tufB, fusA1, tsf*, *pth* and *prfB*). Due to the general induction of protein synthesis it was not a surprise to find induction of other related processes such as tRNA and amino acid biosynthesis (16 tRNA synthetases and 46 genes involved in the synthesis of different amino acids showed increased expression during surface growth).

3) Macromolecule synthesis. In agreement with the above mentioned increase in protein synthesis, the induction of several functions related to the transcription process was also observed. This includes the induction of RNA polymerase genes (*rpoA*, *rpoB*, *rpoC* and *rpoZ*), several sigma factors (*rpoH1*, *rpoE4* and *sigA*) and the transcription terminator factor (*rho*). On the other hand, we also detected induction of genes related with DNA synthesis (*dnaN*, *dnaX*, *topA*, and *gyrA*) and related functions (*purA*, *purM*, *purQ*, *guaA*, *guaB*, *pyrB*, SMc01361, *pyrC-pyrE-frk*, *pyrF*, *cyaC*, SMa2357, *ndk*, *prsA*, SMc02218, *typA*).

Our microarray data suggest that during growth on agar surfaces, *S. meliloti* cells stimulate fatty acid biosynthesis over degradation. Thus, genes involved in the initiation (*accA*, *accBC*, *accD*) and elongation (*fabABI2*, *fabF*, *fabG*, *plsX-fabH*, *fabI1*, *fabZ*, SMc04273) of fatty acids during biosynthesis and the acyl carrier protein AcpP were up-regulated during growth on agar media compared to broth, whereas the *fadB* and SMc02229 genes, putatively involved in degradation of fatty acids were down-regulated.

As previously mentioned, we observed repression of several *exo* genes suggesting that in response to growth on agar surfaces, *S. meliloti* produces less succinoglycan. On the contrary, several genes with a role in the synthesis of different surface polysaccharides have been found to be up-regulated. This is the case for the *kdsA*, *kdsB* and *kdtA* genes, involved in the synthesis and transfer of

Kdo (3-deoxy-D-manno-2-octulosonic acid), a component present in capsular polysaccharides (KPS) and lipopolysaccharides (LPS); the *rkpA* gene involved in the biosynthesis of a specific lipid carrier required for KPS synthesis; and the *acpXL* and *lpxD* genes involved in the biosynthesis of the lipid A part of LPS [27]. Genes involved in the transport and modification of cyclic β-glucans such as *ndvA* and *opgC* as well as genes involved in the synthesis of peptidoglycan (*murA*) and lipoproteins (*lgt*) are also up-regulated under surface growth conditions.

4) Motility and chemotaxis. No less than thirty seven genes of the flagellar regulon were up-regulated during growth on a surface, whereas only two chemotaxis genes (*cheW3* and *mcpT*) showed lower expression under these conditions compared to growth in liquid medium. Up-regulated genes included genes for chemotaxis (*cheABR* and *mcpEUX*), the flagellar structure (*flaCD, fliEFLGM*, *fliK*, *flgABCDEFGHIKL*), the flagellar motor (*motABC*), the chaperone-encoding gene *motE*, related genes of yet unknown function (SMc03013, SMc03017, SMc03023, and SMc03045), as well as genes coding for regulatory proteins (*flaF*, *flbT*, *visN* and *rem*) [28,29]. Motility genes were generally more induced than chemotaxis genes in response to growth on a surface. Five genes belonging to the four different classes of the *S. meliloti* flagellar regulon were chosen to validate our microarray data (see below).

5) Iron uptake and metabolism. 19 genes up-regulated in response to growth on surfaces belong to this functional category including genes involved in the synthesis (*rhbBCDEF* and SMa2339) and transport (*rhtA, rhtX*) of the siderophore rhizobactin 1021 [30-32]; several genes coding for proteins involved in the uptake of haem and hydroxamate siderophores (*hmuPS, hmuT, shmR, fhuA1, fhuA2, fhuP*) [33-35]; the *exbB-exbD* genes putatively coding for the inner membrane components of the TonB energy transduction complex required for Fe^{3+}-siderophore acquisition systems [36]; the *fhuF* gene coding for ferrioxamine B reductase [35]; and the putative iron regulator *irr*. Induction of these genes may be related to increased difficulty for iron acquisition during growth on a solid surface because there is a slower diffusion of nutrients than in broth.

6) Stress-related genes. Up-regulation of genes related to oxidative stress was detected in response to surface growth including *sodB*, *katA*, peroxidases (SMb20964 and *cpo*), and glutathione transferases (*gst4* and *gst8*). Noticeable was also the induction of genes related to thermal stress such as those coding for cold shock proteins (*cspA1*, *cspA4*, *cspA2* and *cspA6*) and heat shock proteins (*grpE*, *hslU*, *hslV*, *hslO*, *ibpA*, SMb21295 and SMc01106). The up-regulation of genes involved in DNA repair processes (*radA*, *recF*, *recN* and *ligA*) could be linked to the induction of genes involved in DNA synthesis (see above), whereas the induction of chaperone genes (*groESL1, groESL2, tig, ibpA*, *lon*) could be the consequence of the observed increase in protein synthesis and/or the existence of stress conditions during surface growth. Also noteworthy is the induction of several genes involved in resistance to different toxic compounds. This is the case for *mrcA1*, a gene coding for a probable penicillin-binding 1A transmembrane protein, the *fsr* gene which encodes a putative fosmidomycin resistance transmembrane protein, the *uppP* gene coding for a putative undecaprenyl-diphosphatase which could confer resistance to bacitracin, putative components of a multidrug efflux system (SMc02867 and SMc02868), and the *aqpS-arsC* genes involved in arsenic detoxification.

All together these data suggest the existence of striking differences in the physiology of *S. meliloti* growing in broth compared with agar surfaces and more specifically that cells growing on agar surfaces have a higher metabolic rate than those grown in broth. Similar results were obtained in a transcriptomic study performed in *Salmonella* [6]. As suggested in the work by Wang *et al.* [6], this could be explained if agar surfaces represent a more aerobic environment than liquid cultures. This could also explain the down-regulation we have observed for several low oxygen responsive genes (*nif* and *fix*) during growth on agar-solidified media when compared to broth. On the other hand, the up-regulation of several genes related to oxidative stress, chaperone functions, or genes involved in resistance to different toxic compounds, could indicate that cells growing on solid agar surfaces are subject to stress. However, the observed induction of chemotaxis and motility genes together with the down-regulation of several *exo* genes under surface growth contrast with the response of *S. meliloti* to several

environmental stresses (osmotic stress, phosphate and iron starvation, or acidic pH), in which motility genes are down-regulated while at the same time *exo* genes are up-regulated [21,37,38]. The identification of several regulatory genes in *S. meliloti* which simultaneously affect EPS production and cellular motility, indicates that regulation of these two rhizobial traits are coupled [24,39-41]. In addition to environmental stresses, the results obtained in this work suggest that contact with a surface might be another signal recognized by *S. meliloti* to co-ordinate the regulation of EPS production and motility.

Regulation of genes in response to swarming-specific conditions

In contrast to surface growth, our microarray data revealed that the response of *S. meliloti* to swarming-specific conditions is characterized by the differential expression of a smaller number of genes (294) (dotted area in Fig. 1.4; additional data file 1.2): 99 of these were identified in the comparison semisolid vs. solid, 36 of which also appeared in the comparison semisolid vs broth, plus 195 genes which exclusively appeared in semisolid vs broth. This result is comparable to that found in a similar transcriptomic study performed in *Salmonella* in which a small number of genes (97) were found to show swarming-specific regulation, in contrast with more than a thousand genes found to respond to surface growth [6]. In our study, most of the genes (73%) responding to swarming-specific conditions identified in the comparison semisolid vs. solid showed an early response (7 hours after incubation) (table 1.3). On the contrary, the majority of genes (89%) identified in the semisolid vs. broth comparison, appeared after 14 hours of growth.

207 genes out of the 294 genes were up-regulated under swarming-inducing conditions, only 78 were found to be down-regulated and the remaining 9 showed variable responses. No informative conclusions could be reached from down-regulated functions as, firstly, approximately one fourth of the genes code for hypothetical proteins of unknown function and secondly the remaining down-regulated genes belong to diverse functional categories. Similarly, most of the up-regulated genes belong to genes of unknown function or which display partial or

global homology to genes deposited in databases (66 genes). This suggests that bacterial components with a putative role in swarming in *S. meliloti* have yet to be studied. However, a subset (25 genes) of the up-regulated genes induced under swarming inducing conditions could be assigned to iron uptake and metabolism, including the transcriptional regulator of the iron limitation response *rirA* [42,43], and the putative iron response regulator *irr*. It is also interesting that swarming conditions induce in *S. meliloti* 1021FDC5 the slight up-regulation of genes involved in the resistance to toxic compounds (*mrcA2, uppP, aqpS-arsC*). Increased resistance to antibiotics and to other antimicrobials has been observed in swarmer cells of different bacteria [9,11]. Whether this is also the case for *S. meliloti* swarmer cells will be the subject of further studies.

To gain further insight into some of the genes responding to swarming specific conditions, we focused on the subset of 36 genes (from now on S36) which were identified as differentially expressed in both semisolid vs. solid and semisolid vs. broth (subsets F and G of 11 and 25 genes, respectively in Fig. 1.4) (Table 1.4). Five genes of S36 were chosen to validate our microarray data (see below). The majority of the genes within S36 (27 genes) were up-regulated under swarming-inducing conditions compared to growth in either broth or on hard agar, whereas only one gene (SMb21284) was found to be down-regulated. 36% of the genes belonging to S36 were located on megaplasmid pSymA, percentage which is significantly higher than the 21% expected for an even distribution among *S. meliloti* replicons, suggesting a putative role of this megaplasmid in *S. meliloti* swarming. Interestingly, up to 17 genes present in S36 are related with iron uptake and metabolism. They include SMb21431 and SMb21432 which code for putative components of iron uptake ABC transporters, and 15 out of the 19 iron-related genes identified as up-regulated in response to surface growth (only *rhbD, rhtX, fhuA1, fhuA2* and *irr* were not present in S36).

Table 1.4. Subset S36[a] of *S. meliloti* 1021FDC5 genes differentially expressed in swarming-specific conditions.

Gene	Descriptions	M value[b]			
		SS/L 7h	SS/L 14h	SS/S 7h	SS/S 14h
SMa0520	Transcriptional regulator, RpiR family	1,45	1,90	1,73	1,55
SMa0564	Putative dehydrogenase	-0,45	-1,12	-0,83	2,78
SMa1052	Conserved hypothetical protein	1,01	1,24	0,51	1,56
SMa1077 (*nex18*)[c]	Nex18 Symbiotically induced conserved protein	1,16	0,81	0,44	2,76
SMa1078	Conserved hypothetical protein	1,89	1,74	0,28	1,93
SMa1079 (*tspO*)	TspO Tryptophan rich sensory protein	1,36	0,31	0,59	1,91
SMa1100	Conserved hypothetical protein	1,31	1,61	0,52	1,57
SMa2339	Siderophore biosynthesis protein	0,80	1,33	1,55	-0,17
SMa2402 (*rhbB*) [c]	L-2,4-diaminobutyrate decarboxylase	1,84	0,75	2,58	-0,19
SMa2404 (*rhbC*)	RhbC rhizobactin biosynthesis protein	1,49	1,19	2,65	0,00
SMa2408 (*rhbE*)	RhbE rhizobactin biosynthesis protein	2,38	2,23	3,83	0,03
SMa2410 (*rhbF*)	RhbF rhizobactin biosynthesis protein	2,36	1,34	3,76	-0,11
SMa2414 (*rhtA*) [c]	RhtA rhizobactin transporter	1,43	1,64	2,68	0,05
SMb20005	Putative glutathione S-transferase	2,34	-0,08	0,31	-1,38
SMb20604	ABC transporter, permease	0,18	-4,84	0,20	1,14
SMb20605	ABC transporter, periplasmic solute-binding protein	0,01	-5,55	0,09	1,34
SMb21284	Putative polysaccharide deacetylase	-0,21	-1,55	-0,15	-1,15
SMb21431	Hypothetical protein, possibly C terminus of iron ABC transporter periplasmatic solute-binding protein	-0,34	1,75	1,44	-0,14
SMb21432	Putative iron uptake ABC transporter periplasmic solute-binding protein precursor	-1,07	1,63	2,15	-0,40
SMb21676	Hypothetical protein	0,17	1,92	-0,58	1,96
SMc00402	Hypothetical signal peptide protein	-0,03	1,91	1,42	-0,23
SMc00592	Hypothetical, transmembrane protein	-0,44	1,47	1,30	-0,23
SMc01242	Conserved hypothetical signal peptide protein	0,29	-1,35	0,13	1,04
SMc01417	Hypothetical protein	1,26	0,14	1,12	-0,05
SMc01510 (*hmuV*)	Putative hemin transport system ATP-binding ABC transporter	-0,06	1,48	1,53	-0,12
SMc01512 (*hmuT*)	Putative hemin binding periplasmic transmembrane protein	-0,34	1,49	1,39	0,09
SMc01513 (*hmuS*) [c]	Putative hemin transport protein	-0,93	1,34	2,60	-0,07
SMc01514	Conserved hypothetical protein	-1,14	1,50	2,37	-0,09
SMc01658 (*fhuF*)	Siderophore reductase	-0,39	1,28	2,03	-0,06
SMc01659 (*fhuP*)	Periplasmic component of ferrichrome and ferrioxamine B ABC transporter	-0,41	1,85	2,60	0,12
SMc01747 (*hmuP*)	Hypothetical protein, hemin uptake protein	-0,78	1,29	2,23	0,04
SMc01917 (*nuoE1*)	NADH dehydrogenase I chain E	0,03	1,21	-1,13	-0,14
SMc02084 (*exbD*)	Probable biopolymer transport transmembrane protein	-0,68	1,48	1,16	-0,03
SMc02085 (*exbB*) [c]	Probable biopolymer transport transmembrane protein	-0,54	1,82	1,55	-0,01
SMc02726 (*shmR*)	Hemin-binding outer membrane receptor	-0,11	2,02	2,84	0,30
SMc03167	MFS-type transport protein	1,09	0,62	1,27	0,38

[a] The subset S36 comprises 36 genes showing differential expression in the two transcriptome comparisons aimed to identify swarming responsive genes (i.e. semisolid vs. solid and semisolid vs. broth); [b] $\log_2$ (experiment signal/control signal). Values in bold face indicate that they meet both M and p criteria; [c] Genes validated by RT-qPCR (see Fig. 1.5B). SS, growth in semisolid MM (0.6% agar); S, growth in solid MM (1.3% agar); L, growth in liquid MM.

13 out of the 15 surface-responsive genes related to iron uptake and metabolism were also significantly induced in solid MM versus broth after 14 hours of growth (see additional data file 1.1). Although the induction of these genes could be explained by the increased difficulty for iron acquisition during growth on agar containing media, it is surprising that up to 8 of these iron-related genes show higher expression in 0.6% swarm agar than in the harder 1.3% agar. This suggests that lower diffusion of iron is not the only factor controlling the expression of genes involved in iron uptake and metabolism, and furthermore that a specific connection may exist between swarming and iron-related genes. In *S. typhimurium* and *P. aeruginosa* induction of genes related to iron uptake and metabolism has also been detected in the transcriptomic analysis of swarmer cells [6,9]. Moreover, mutants of *E. coli* and *P. putida* affected in different systems of iron acquisition show defects in swarming [7,44]. These and our results suggest that different bacteria have acquired similar adaptation processes for swarming with iron acquisition systems playing an important role in this process.

Validation of the results from the microarray experiments by RT-qPCR.

To validate our microarray data we performed reverse transcription-quantitative PCR on several selected surface responsive genes as well as on genes showing response to swarming-specific conditions. Among suface responsive genes, we analyzed the expression of several motility genes belonging to different classes of the *S. meliloti* flagellar regulon [28,29]: the *visN* and *rem* genes coding for master regulators of class IA and class IB, respectively, which showed late (14h) upregulation in solid media vs. broth; the *flgB* gene as representative of class II genes, encoding a flagellar basal-body rod protein and showing late upregulation in solid and semisolid media vs. broth; and the class III genes *flaA* and *flaC*, encoding the principal and secondary flagellins, respectively, of the complex flagellar filament of *S. meliloti*. In our transcriptomic study, *flaC* showed late upregulation in solid and semisolid media vs. broth. *flaA* was not present in the list of differentially expressed genes. Since many motility genes were

upregulated in response to surface growth and FlaA is the main component of the flagellum, we hypothesized that the fact that this gene does not show differential expression in our study, like some other motility genes, could be due to the limitations inherent to microarray experiments. Therefore, we decided to test this hypothesis by analyzing the expression of *flaA* by RT-qPCR. The expression of the five motility genes was determined in solid, semisolid and liquid MM after 14 h of growth (Fig. 1.5A). Confirming the microarray data, all the motility genes analyzed showed surface specific induction. Furthermore, the RT-qPCR analyses revealed that, except for *rem*, the upregulation of these genes occurred in the two types of surfaces used (solid and semisolid) with a higher induction value in semisolid than in solid media, which is in agreement with the existence of a higher motility activity in swarming-inducing conditions. Only in the case of *flgB* and *flaC* which in our transcriptomic experiment showed higher induction in the comparison solid vs. broth or similar induction in solid and semisolid media vs. broth, the RT-qPCR data did not fit exactly with the transcriptomic data. This probably is due to the limitations of the microarray experiments. Also noticeable was that many of the induction values for the up-regulated genes were higher with the RT-qPCR analysis than those obtained with microarrays, a phenomenon which has also been observed in other transcriptomic analyses with the Sm6koligo arrays [21,42,45, 46].

To confirm the differential expression of genes showing response to swarming-specific conditions, the following genes were selected: four genes related to iron uptake and metabolism (*rhbB, rhtA, hmuS* and *exbB*) which showed early induction (7 h) in semisolid vs. solid; *nex18*, a symbiotically induced gene showing late (14 h) up-regulation in semisolid vs. solid; and *exsF*, a gene coding for a putative two-component response regulator with sequence similarity to CheY, and found as an early down-regulated gene in swarm cells compared to cells grown in solid MM. The expression of these six genes was determined in solid and semisolid MM after 7 and 14 hours of growth. As shown in figure 1.5B, the RT-qPCR results confirmed the microarrays data.

As we have explained earlier, genes showing differential expression in swarming-inducing conditions were identified from a transcriptomic analysis performed with bacteria that were spread plated and grown in semisolid MM, and not from a typical swarming assay. Although we have macroscopic evidence that under our experimental conditions cells of 1021FDC5 show surface motility that is absent in a bacteria that cannot swarm (Fig. 1.3), we decided to test whether the genes differentially expressed in semisolid MM in our study could be considered swarming-specific genes by analyzing the expression of *rhbB*, *rhtA* and *hmuS* by RT-qPCR on actively swarming colonies. Our results indicate that these three genes show higher expression in cells from the border of an active swarming colony of 1021FDC5 than in cells from a colony of the same strain grown in solid MM. The relative expression found for each gene in swarming cells vs non-swarming cells was 5.72 ± 0.54 for *rhbB*, 4.61 ± 0.38 for *rhtA* and 4.41 ± 0.69 for *hmuS*. The differences in the induction values found for these genes between cells spread plated on semisolid MM (Fig. 1.5B) and cells from the border of a typical swarming colony, could be explained by differences in the growth phase of the two samples. In our transcriptomic study, the genes analyzed showed early induction (early exponential phase, 7 hours of growth), whereas we do not know which is the growth phase in cells from the border of a swarming colony. Nevertheless, these data indicate that our experimental approach allows the identification of swarming-specific genes.

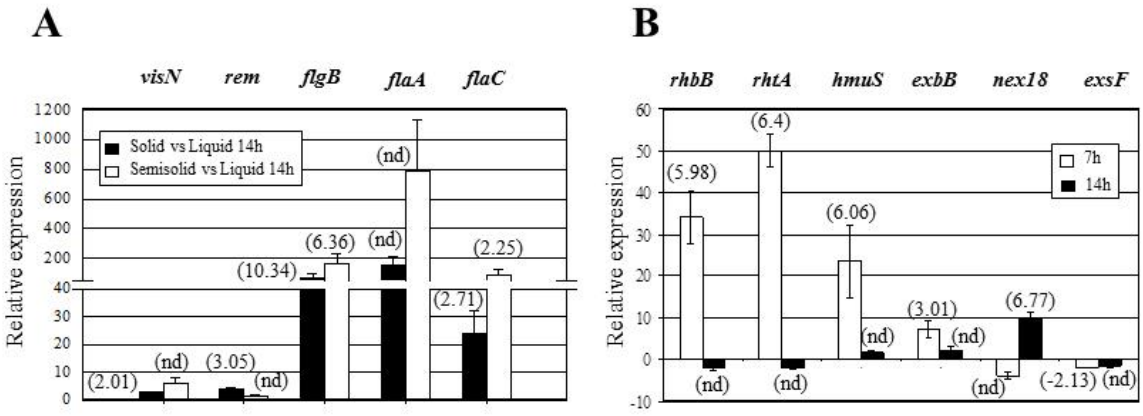

Figure 1.5. Confirmation of the differential expression of selected genes in a *fadD* mutant of *S. meliloti* in response to different growth conditions determined by quantitative real-time PCR. A) Relative expression of surface responsive genes is calculated as the fold change between cells grown on solid MM (black bars) or semisolid MM (white bars) compared to those grown in liquid MM after 14 hours of incubation. B) Relative expression of genes responding specifically to swarming-inducing conditions is calculated as the fold change between cells grown on semisolid MM compared to those grown on hard agar MM at 7 hours (white bars) or at 14 hours (black bars). The positive number indicates upregulation of gene expression in semisolid MM, and the negative number indicates downregulation compared to growth in solid MM. For comparisons, fold changes in gene expression obtained in the microarray experiments (calculated as 2^M) are shown in parenthesis. Results are averages from at least two independent biological experiments with three technical replicates. Error bars indicate standard error at 95% confidence. nd, not detected in the microarray experiments.

Role of pSymA, rhizobactin-related genes and iron in *S. meliloti* swarming

Since the proportion of genes belonging to pSymA present in the subset S36 of swarming-responsive genes was higher than expected, we investigated whether this megaplasmid played any role in surface translocation. The swarming ability of SmA818, a *S. meliloti* strain cured of pSymA, was tested. In contrast to the parental strain Rm2011, SmA818 did not show swarming in any of the numerous assays performed (Fig. 1.6A). Mutagenesis-based approaches performed in different bacteria have revealed that a wide variety of genes are involved in swarming [7,8,19]. Since pSymA harbous more than one-fifth of the genes present in the *S. meliloti* genome, the finding that loss of this megaplasmid results in loss of swarming, might be seen as not surprising. However, this result

prompt us to investigate what genes of pSymA could play a role in triggering conditional swarming in *S. meliloti*.

Among the pSymA swarming-specific induced genes there were genes involved in the biosynthesis and transport of the siderophore rhizobactin 1021 [30]. In *E. coli,* mutations in most of the genes involved in the utilization of the siderophore enterobactin strongly inhibit swarming [7]. Likewise, in *P. putida*, mutants either in the siderophore pyoverdine or in the FpvA siderophore receptor have been shown to be defective in surface motility [44]. Hence, the swarming-defective phenotype observed in SmA818 could be due to the lack of rhizobactin-related genes. To test this, swarming assays were performed with mutants affected in either of two different rhizobactin 1021 biosynthesis genes (*rhbA* and *rhbE*), a mutant lacking the RhtA outer membrane receptor for the siderophore, and with a *rhrA* mutant strain lacking the AraC-like regulator which positively regulates the production and transport of rhizobactin 1021. Additionally, we also looked at the swarming phenotype of a *rirA* mutant. RirA has been demonstrated to be the general regulator of the iron response in *S. meliloti*, regulating among others the genes involved in biosynthesis and transport of rhizobactin 1021 [42,43]. In our microarrays, *rirA* appeared to be induced 2-fold in growth in semisolid vs. solid media after 14 hours of incubation (see additional data file 1.2). As shown in Fig. 1.6B, neither the mutants in the rhizobactin biosynthesis genes (*rhb*) nor the *rhrA* mutant were able to swarm, while the absence of either the RhtA siderophore receptor or the RirA regulator did not prevent swarming. The motility defect shown by the *rhb* and *rhrA* mutants was specific for swarming since assays performed in Bromfield and MM (0.3% agar) showed that these strains were able to swim (Fig. 1.6C). Thus, the motility phenotypes shown by the *rhb* and *rhrA* mutants suggest that either rhizobactin-mediated iron uptake or rhizobactin *per se* play a role during swarming in *S. meliloti* Rm2011.

In *P. putida*, the defect on swarming shown by mutants unable to synthesize the siderophore pyoverdine could be restored by adding different sources of iron, suggesting that the intracellular iron level rather than the siderophore is the functional signal for swarming in this bacterium [44]. To test

whether the lack of surface motility in the *rhb* and *rhrA* mutants could be due to iron deficiency, increasing concentrations (22, 220, and 2200 μM) of either $FeCl_3$ or the iron chelate ferric citrate, whose uptake is independent on siderophore, were added to the media. None of these conditions could restore surface translocation in the mutants (data not shown), with the highest concentration used being toxic for cell growth. This result indicated that the presence of a low intracellular iron level was not responsible for the swarming deficiency of the *rhb* and *rhrA* mutants, and that the presence of rhizobactin 1021 is important for triggering swarming in *S. meliloti*. Furthermore, the fact that the *rhtA* mutant which is defective in rhizobactin 1021 utilization [30], still swarms (Fig. 1.6B) suggests that the function played by rhizobactin 1021 in swarming is exerted outside the cell. Rhizobactin 1021 is a citrate-based dihydoxamate siderophore structurally similar to schizokinen with the only but important difference that rhizobactin 1021 contains a long-chain fatty acid ((E)-2-decenoic acid) that gives the siderophore an asymmetric structure and amphiphilic properties [47]. The role of the decenoic acid residue in rhizobactin 1021 function has not been studied, although it has been proposed to play a role in the membrane translocation of the ferric complex by making the molecule more mobile. Considering our results, it is tempting to speculate that the surfactant properties of rhizobactin 1021 may promote surface translocation in *S. meliloti*. Similarly, the biosurfactant activity associated to long-chain AHLs produced by *R. etli* has been proved to play a direct role in surface movement of swarmer cells, adding a new function to these well known signalling molecules [18]. Curiously and in support of our hypothesis, *S. meliloti* GR4 which is not able to swarm in semisolid MM, does not produce siderophores in liquid MM as determined by the CAS assay (data not shown).

The restoration of surface motility of the rhizobactin-defective mutants was attempted by adding concentrated supernatants containing rhizobactin 1021. Although the addition of these supernatants functioned in iron nutrition bioassays restoring the growth of *rhb* mutants, they failed to promote swarming of the mutants and even hampered the surface motility of the wild type and *fadD* mutant strains (data not shown). This result might be due to the negative effect of

supraoptimal concentrations of nutrients or compounds excreted by Rm2011 on swarming.

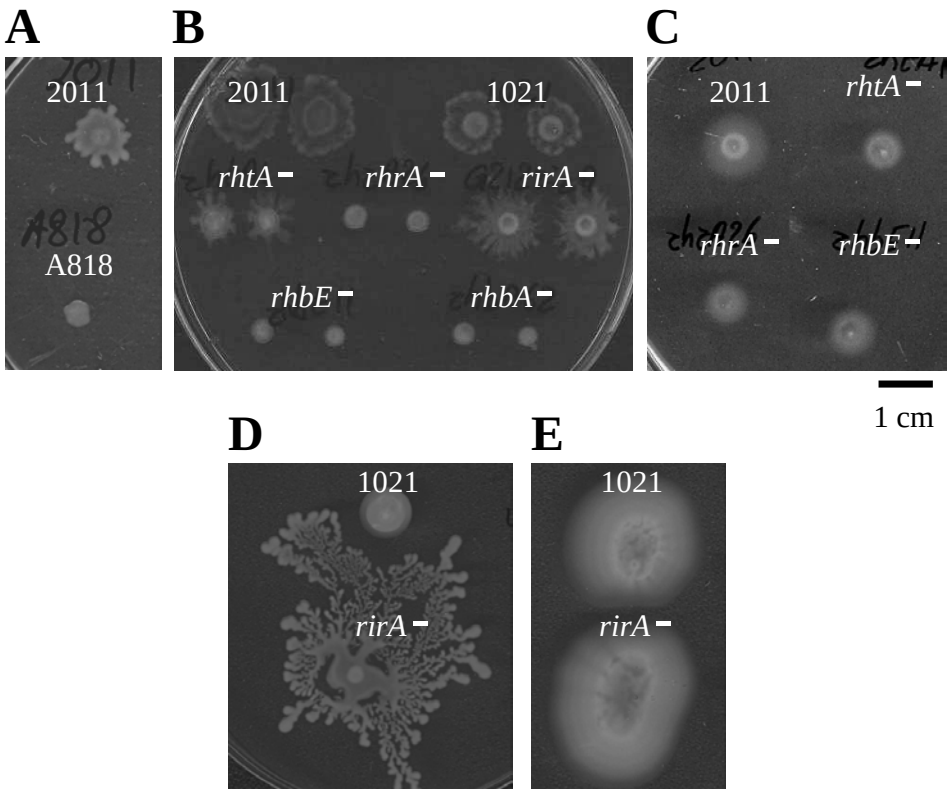

Figure 1.6. Effect of pSymA, rhizobactin-related genes, and iron concentration on motility of *S. meliloti*. A) Swarming test of wild type Rm2011 and a pSymA-cured derivative strain (SmA818). B) Swarming assay of mutants in biosynthesis and transport of rhizobactin 1021 and in the rhizobial iron regulator *rirA*. C) Swimming test of Rm2011 and rhizobactin 1021-related mutants in Bromfield (0.3% agar). D) Swarming and E) swimming tests of Rm1021 and the *rirA* mutant in MM containing high iron concentration (220 μM). Pictures were taken either 48 hours (A, B, and C) or 5 days (D and E) after inoculation and are representative of three replicates in at least three different experiments.

To further confirm that the presence of rhizobactin 1021 is important for triggering swarming in *S. meliloti*, the motility phenotype of Rm1021 and the *rirA* mutant was tested under iron-replete conditions as it has been reported that these conditions inhibit rhizobactin 1021 production in the wild type but not in the mutant [43]. CAS assays were performed to determine siderophore concentration in supernatants of these two strains under different growth conditions. We found that when cells were cultivated in MM containing 22 μM of $FeCl_3$ the wild type and the *rirA* mutant produced a similar amount of siderophore

(data not shown). The presence of 220 μM of $FeCl_3$ abolished siderophore production in Rm1021 but not in the *rirA* mutant (data not shown). Hence, swimming and swarming assays were performed in MM containing 220 μM of $FeCl_3$. No differences in swimming were observed between the two strains (Fig. 1.6E). However, swarming of Rm1021 was inhibited in the presence of a high iron concentration but not that of the *rirA* mutant in which swarming seemed even to be enhanced than at lower iron concentrations (Fig. 1.6D). This result not only supports that the presence of rhizobactin 1021 plays a role in swarming but also suggests that iron controls this multicellular phenotype in *S. meliloti* 1021 and that *rirA* plays a role in this control. The concentration of iron in the medium has been shown to be decisive for swarming in several bacteria like *Vibrio parahaemolyticus* [48], *P. aeruginosa* [49] and *P. putida* [44]. In *S. meliloti* strain Rm1021, like in *Pseudomonas* spp., an excess of iron inhibits swarming, an effect that in *S. meliloti* could be due at least in part to the inhibition of rhizobactin 1021 production. On the other hand, the enhanced motility shown by the *rirA* mutant under high iron conditions suggests that additional genes controlled by the regulator in response to the levels of iron in the medium might be involved.

The lack of a functional *fadD* gene restores swarming in pSymA-cured and rhizobactin-defective strains, and allows swarming in high-iron conditions

As described above, pSymA and at least the rhizobactin 1021-related genes *rhb* and *rhrA* are required for swarming in *S. meliloti* 1021. To investigate if these genes are also important in the surface motility shown by the *fadD* mutant, swarming assays were performed with the pSymA-cured strain SmA818 in which the *fadD* was inactivated as well as with the double mutants *rhbfadD* and *rhrAfadD*. As shown in figure 1.7A and B, the lack of a functional *fadD* gene restored surface motility in all the swarming-deficient strains. Thus, although rhizobactin and regulation genes were found to be upregulated in the *fadD* mutant under swarming-inducing conditions, these genes are not required for surface motility in this genetic background. This result should not be surprising as it is known that transcriptomic analysis reveal genes that migh play a role in

the biological process studied but not necessarily are essential for it. A possible explanation for our results is that the signal transduction connecting the detection of the environmental/physiological signals that trigger swarming in *S. meliloti* to the induction of the rhizobactin genes, is not altered in the *fadD* mutant. However, the function played by iron/rhizobactin 1021 in the control of swarming in Rm1021 (as a surfactant or signal molecule) is exerted in the *fadD* mutant by a different and unknown compound which is not present in the wild-type strain.

We also tested if the presence of high iron concentrations prevents swarming in a *fadD* mutant as it does in Rm1021. Swarming assays were performed in semisolid MM containing 220 μM of $FeCl_3$ with 1021 and GR4 as wild type strains, and their corresponding *fadD*-derivative mutants. As shown in figure 1.7C, swarming was never observed in GR4 but always in the *fadD* mutant QS77. As already mentioned, in Rm1021 swarming was observed at a certain frequency in MM containing 22 μM of $FeCl_3$ and never observed in high iron conditions but its corresponding *fadD* mutant showed swarming at both iron concentrations. In contrast to the *rirA* mutant, the iron-independent swarming phenotype shown by the *fadD* mutant cannot be explained by differences in the production of rhizobactin 1021 since the *fadD* mutant, like the wild type, inhibits siderophore production under high iron conditions (data not shown). Therefore in *S. meliloti*, the lack of a functional *fadD* gene relieves the control that iron has over swarming as well as the dependence on rhizobactin 1021 for this surface motility. A possibility worth investigating is if fatty acid derivatives whose concentration is dependent on FadD activity but not iron-responsive could replace siderophore function during swarming. Likewise, future investigations should address a possible connection between the *rirA* and *fadD* regulatory networks that could explain the iron-insensitivity of swarming shown by the *fadD* and *rirA* mutants.

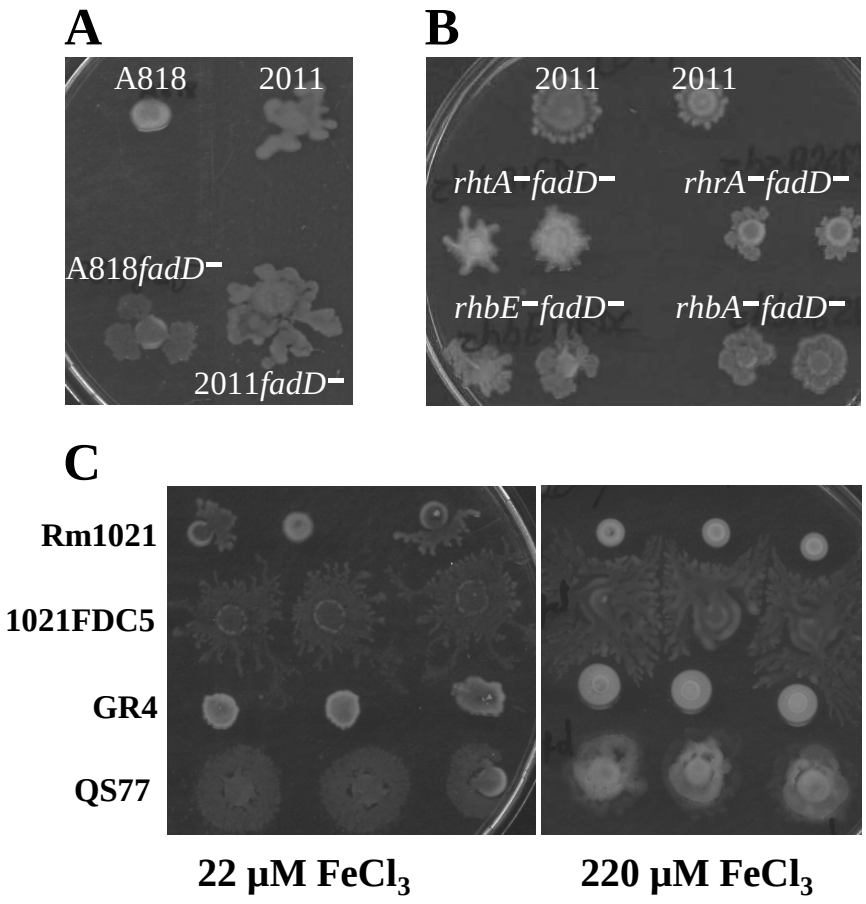

Figure 1.7. Role of pSymA, rhizobactin-related genes, and iron concentration on *fadD*-dependent swarming of *S. meliloti*. Swarming tests of fadD-derivative mutants of Rm2011 and the pSymA-cured strain A818 (A), of double mutants lacking fadD and rhizobactin 1021-related genes (B), and wild type and fadD-derivative mutants in standard (22 µM FeCl3) and high iron conditions (220 µM FeCl3) (C). Pictures were taken 48 hours after inoculation and are representative of three replicates in at least three different experiments.

1.5. Conclusions

To the best of our knowledge, the present work represents the first global gene expression analysis of *Rhizobium* growth on surfaces, including swarming-inducing conditions. The results reveal that the physiology of *S. meliloti* cells growing on the surface of agar media is significantly different from that of cells growing in broth, with the differential expression of more than a thousand genes. It is tempting to speculate that these major changes in gene expression could also take place in *Rhizobium* during colonization of root surfaces, an important

prerequisite for nodule formation. Thus, the approach used in this study may be helpful to identify genes and regulatory mechanisms that may be crucial during the early stages of the *Rhizobium*-legume symbiosis and it could serve as a model for studying gene expression in different plant-associated bacteria.

The surface motility shown by several *expR*-deficient strains in this work indicates that the role played by this LuxR-type regulator in swarming by *S. meliloti* needs to be re-examined. Moreover, the genomic analysis under swarming-inducing conditions allowed the identification of environmental signals (surface contact and iron concentration) and genes that play important roles in the control of this surface motility in a wild type strain of *S. meliloti*. Furthermore, the results suggest that rhizobactin 1021 plays a role in swarming although the requirement for rhizobactin-related genes and the inhibition of this surface motility by an excess of iron can be circumvented in a *fadD* mutant. Future work should focus on investigating the specific role of rhizobactin 1021 in swarming of *S. meliloti* as well as to identify why the lack of a functional *fadD* gene allows surface translocation of bacterial cells under conditions which negatively influence this type of multicellular migration.

Acknowledgements

We thank Dr M. Hynes and Dr. M. O'Connell for providing several strains used in this work. JN was supported by a postdoctoral contract (Consejería de Innovación, Ciencia y Empresa, Junta de Andalucía). This work was supported by a FPI fellowship from MICINN to CVA-G, and by grants BIO2007-62988 and CVI 03541 to MJS.

1.6. References

1. Fraser GM, Hughes C: Swarming motility. *Curr Opin Microbiol* 1999, 2:630-635.
2. Harshey RM: Bacterial motility on a surface: many ways to a common goal. *Annu Rev Microbiol* 2003, 57:249-273.
3. Rather PN: Swarmer cell differentiation in *Proteus mirabilis*. *Environ Microbiol* 2005, 7:1065-1073.
4. Verstraeten N, Braeken K, Debkumari B, Fauvart M, Fransaer J, Vermant J, Michiels J: Living on a surface: swarming and biofilm formation. *Trends Microbiol* 2008, 16:496-506.
5. Kim W, Surette MG: Metabolic differentiation in actively swarming *Salmonella*. *Mol Microbiol* 2004, 54:702-714.

6. Wang Q, Frye JG, McClelland M, Harshey RM: Gene expression patterns during swarming in *Salmonella typhimurium*: genes specific to surface growth and putative new motility and pathogenicity genes. *Mol Microbiol* 2004, 52:169-187.
7. Inoue T, Shingaki R, Hirose S, Waki K, Mori H, Fukui K: Genome-wide screening of genes required for swarming motility in *Escherichia coli* K-12. *J Bacteriol* 2007, 189:950-957.
8. Overhage J, Lewenza S, Marr AK, Hancock RE: Identification of genes involved in swarming motility using a *Pseudomonas aeruginosa* PAO1 mini-Tn*5-lux* mutant library. *J Bacteriol* 2007, 189:2164-2169.
9. Overhage J, Bains M, Brazas MD, Hancock REW: Swarming of *Pseudomonas aeruginosa* is a complex adaptation leading to increased production of virulence factors and antibiotic resistance. *J Bacteriol* 2008, 190:2671-2679.
10. Eberl L, Christiansen G, Molin S, Givskov M: Differentiation of *Serratia liquefaciens* into swarm cells is controlled by the expression of the *flhD* master operon. *J Bacteriol* 1996, 178:554-559.
11. Lai S, Tremblay J, Déziel E: Swarming motility: a multicellular behaviour conferring antimicrobial resistance. *Environ Microbiol* 2009, 11:126-136.
12. Gibson KE, Kobayashi H, Walker GC: Molecular determinants of a symbiotic chronic infection. *Annu Rev Genet* 2008, 42:413-441.
13. Oldroyd GED, Downie JA: Coordinating nodule morphogenesis with rhizobial infection in legumes. *Annu Rev Plant Biol.* 2008, 59:519-546.
14. Soto MJ, Sanjuán J, Olivares J: Rhizobia and plant-pathogenic bacteria: common infection weapons. *Microbiology* 2006, 152:3167-3174.
15. Soto MJ, Domínguez-Ferreras A, Pérez-Mendoza D, Sanjuán J, Olivares J: Mutualism *versus* pathogenesis: the give-and-take in plant-bacteria interactions. *Cell Microbiol* 2009, 11:381-388.
16. Soto MJ, Fernández-Pascual M, Sanjuán J, Olivares J: A *fadD* mutant of *Sinorhizobium meliloti* shows multicellular swarming migration and is impaired in nodulation efficiency on alfalfa roots. *Mol Microbiol* 2002, 43:371-382.
17. Daniels R, Vanderleyden J, Michiels J: Quorum sensing and swarming migration in bacteria. *FEMS Microbiol Rev* 2004, 28:261-289.
18. Daniels R, Reynaert S, Hoekstra H, Verreth C, Janssens J, Braeken K, Fauvart M, Beullens S, Heusdens C, Lambrichts I, De Vos DE, Vanderleyden J, Vermant J, Michiels J: Quorum signals molecules as biosurfactants affecting swarming in *Rhizobium etli*. *Proc Natl Acad Sci USA* 2006, 103:14965-14970.
19. Braeken K, Daniels R, Vos K, Fauvart M, Bachaspatimayum D, Vanderleyden J, Michiels J: Genetic determinants of swarming in *Rhizobium etli*. *Microbial Ecol* 2008, 55:54-64.
20. van Dillewijn P, Sanjuán J, Olivares J, Soto MJ: The *tep1* gene of *Sinorhizobium meliloti* coding for a putative transmembrane efflux protein and N-acetyl glucosamine affect *nod* gene expression and nodulation of alfalfa plants. *BMC Microbiol* 2009, 9:17.
21. Krol E, Becker A: Global transcriptional analysis of the phosphate starvation response in *Sinorhizobium meliloti* strains 1021 and 2011. *Mol Genet Genomics* 2004, 272:1-17.
22. Galibert F *et al*: The composite genome of the legume symbiont *Sinorhizobium meliloti*. *Science* 2001, 293:668-672.
23. Gao M, Chen H, Eberhard A, Gronquist MR, Robinson JB, Rolfe BG, Bauer WD: *sinI*- and *expR*-dependent quorum sensing in *Sinorhizobium meliloti*. *J Bacteriol* 2005, 187:7931-7944.

24. Bahlawane C, McIntosh M, Krol E, Becker A: *Sinorhizobium meliloti* regulator MucR couples exopolysaccharide synthesis and motility. *Mol Plant Microbe Interact* 2008, 21:1498-1509.
25. Pellock BJ, Teplitski M, Boinay RP, Bauer WD, Walker GC: A LuxR homolog controls production of symbiotically active extracellular polysaccharide II by *Sinorhizobium meliloti*. *J Bacteriol* 2002, 184:5067-5076.
26. Davalos M, Fourment J, Lucas A, Bergès H, Kahn D: Nitrogen regulation in *Sinorhizobium meliloti* probed with whole genome arrays. *FEMS Microbiol Lett* 2004, 241:33-40.
27. Becker A, Fraysse N, Sharypova L: Recent advances in studies on structure and symbiosis-related function of rhizobial K-antigens and lipopolysaccharides. *Mol Plant-Microbe Interact* 2005, 18:899-905.
28. Sourjik V, Muschler P, Scharf B, Schmitt R: VisN and VisR are global regulators of chemotaxis, flagellar, and motility genes in *Sinorhizobium* (*Rhizobium*) *meliloti*. *J Bacteriol* 2000, 182:782-788.
29. Rotter C, Mühlbacher S, Salamon D, Schmitt R, Scharf B: Rem, a new transcriptional activator of motility and chemotaxis in *Sinorhizobium meliloti*. *J Bacteriol* 2006, 188:6932-6942.
30. Lynch D, O'Brien J, Welch T, Clarke P, Cuiv PO, Crosa JH, O'Connell M: Genetic organization of the region encoding regulation, biosynthesis, and transport of rhizobactin 1021, a siderophore produced by *Sinorhizobium meliloti*. *J Bacteriol* 2001, 183:2576-2585.
31. Ó Cuív P, Clarke P, Lynch D, O'Connell M: Identification of *rhtX* and *fptX*, novel genes encoding proteins that show homology and function in the utilization of the siderophores rhizobactin 1021 by *Sinorhizobium meliloti* and pyochelin by *Pseudomonas aeruginosa*, respectively. *J. Bacteriol* 2004, 186:2996-3005.
32. Challis GL: A widely distributed bacterial pathway for siderophore biosynthesis independent of nonribosomal peptide synthetases. *ChemBioChem*. 2005, 6:601-611.
33. Wexler M, Yeoman KH, Stevens JB, de Luca NG, Sawers G, Johnston AWB: The *Rhizobium leguminosarum tonB* gene is required for the uptake of siderophore and haem as sources of iron. *Mol Microbiol* 2001,41:801-816.
34. Battistoni F, Platero R, Duran R, Cerveñansky C, Battistoni J, Arias A, Fabiano E: Identification of an iron-regulated, hemin-binding outer membrane protein in *Sinorhizobium meliloti*. *Appl Environ Microbiol* 2002, 68:5877-5881.
35. Ó Cuív P, Keogh D, Clarke P, O'Connell M: The *hmuUV* genes of *Sinorhizobium meliloti* 2011 encode the permease and ATPase components of an ABC transport system for the utilization of both haem and the hydoxamate siderophores, ferrichrome and ferrioxamine B. *Mol Microbiol* 2008, 70:1261-1273.
36. Wandersman C, Delepelaire P: Bacterial iron sources: from siderophores to hemophores. *Annu Rev Microbiol* 2004, 58:611-647.
37. Domínguez-Ferreras A, Pérez-Arnedo R, Becker A, Olivares J, Soto MJ, Sanjuán J: Transcriptome profiling reveals the importante of plasmid pSymB for osmoadaptation of *Sinorhizobium meliloti*. *J Bacteriol* 2006, 188:7617-7625.
38. Hellweg C, Pühler A, Weidner S: The time course of the transcriptomic response of *Sinorhizobium meliloti* 1021 following a shift to acidic pH. *BMC Microbiol* 2009, 9:37.
39. Yao SY, Luo L, Har KJ, Becker A, Rüberg S, Yu, G.Q, Zhu JB, Cheng HP: *Sinorhizobium meliloti* ExoR and ExoS proteins regulate both succinoglycan and flagellum production. *J Bacteriol* 2004, 186:6042-6049.

40. Gibson KE, Barnett MJ, Toman CJ, Long SR, Walker GC: The symbiosis regulator CbrA modulates a complex regulatory network affecting the flagellar apparatus and cell envelope proteins. *J Bacteriol* 2007, 189:3591-3602.
41. Hoang HH, Gurich N, González JE: Regulation of motility by the ExpR/Sin quorum sensing system in *Sinorhizobium meliloti*. *J Bacteriol* 2008, 190:861-871.
42. Chao TC, Buhrmester J, Hansmeier N, Pühler A, Weidner S: Role of the regulatory gene *rirA* in the transcriptional response of *Sinorhizobium meliloti* to iron limitation. *Appl Environ Microbiol* 2005, 71:5969-5982.
43. Viguier C, Ó Cuív P, Clarke P, O'Connell M: RirA is the iron response regulator of the rhizobactin 1021 biosynthesis and transport genes in *Sinorhizobium meliloti* 2011. *FEMS Microbiol Lett* 2005, 246:235-242.
44. Matilla MA, Ramos JL, Duque E, Alché JD, Espinosa-Urgel M, Ramos-González MI: Temperature and pyoverdine-mediated iron acquisition control surface motility of *Pseudomonas putida*. *Environ Microbiol* 2007, 9:1842-1850.
45. Sauviac L, Philippe H, Phok K, Bruand C: An extracytoplasmic function sigma factor acts as a general stress response regulator in *Sinorhizobium meliloti*. *J Bacteriol* 2007, 189:4204-4216.
46. Rossbach S, Mai DJ, Carter EL, Sauviac L, Capela D, Bruand C, de Bruijn F: Response of *Sinorhizobium meliloti* to elevated concentrations of cadmium and zinc. *Appl Environ Microbiol* 2008, 74:4218-4221.
47. Persmark M, Pittman P, Buyer JS, Schwyn B, Gill Jr. PR, Neilands JB: Isolation and structure of rhizobactin 1021, a siderophore from the alfalfa symbiont *Rhizobium meliloti* 1021. *J Am Chem Soc* 1993, 115:3950-3956.
48. McCarter L, Silverman M: Iron regulation of swarmer cell differentiation of *Vibrio parahaemolyticus*. *J Bacteriol* 1989, 171:731-736.
49. Déziel E, Lépine F, Milot S, Villemur R: *rhlA* is required for the production of a novel biosurfactant promoting swarming motility in *Pseudomonas aeruginosa*:3-(3-hydroxyalkanoylosy) alkanoic acids (HAAs), the precursors of rhamnolipids. *Microbiology* 2003, 149:2005-2013.
50. Sambrook J, Fritsch EF, Maniatis T: Molecular cloning: A laboratory manual. 2nd ed. Cold Spring Harbor Laboratory Press, Cold Spring Harbor N. Y; 1989.
51. Beringer JE: R factor transfer in *Rhizobium leguminosarum*. *J Gen Microbiol* 1974, 84:188-198.
52. Robertsen BK, Aiman P, Darwill AG, Mcneil M, Albersheim P: The structure of acidic extracellular polysaccharides secreted by *Rhizobium leguminosarum* and *Rhizobium trifolii*. *Plant Physiol* 1981, 67:389-400.
53. Miller J: *Experiments in Molecular Genetics*. Cold Spring Harbor, New York: Cold Spring Harbor Laboratory Press; 1972.
54. Schäfer A, Tauch A, Jäger W, Kalinowski J, Thierbach G, Pühler A: Small mobilizable multi-purpose cloning vectors derived from the *Escherichia coli* plasmids pK18 and pK19: selection of defined deletions in the chromosome of *Corynebacterium glutamicum*. *Gene* 1994, 145:69-73.
55. Finan TM, Hartwieg E, LeMieux K, Bergman K, Walker GC, Signer ER: General transduction in *Rhizobium meliloti*. *J Bacteriol* 1984, 159:120-124.
56. DeRisi JL, Iyer VR, Brown PO: Exploring the metabolic and genetic control of gene expression on a genomic scale. *Science* 1997, 278:680-686.
57. Dondrup M, Goesmann A, Bartels D, Kalinowski J, Krause L, Linke B, Rupp O, Sczyrba A, Pühler A, Meyer F: EMMA: a platform for consistent storage and efficient analysis of microarray data. *J Biotechnol* 2003, 106:135-146.

58. Pfaffl MW: A new mathematical model for relative quantification in real-time RT-PCR. *Nucleic Acids Res* 2001, 29:e45.
59. Schwyn B, Neilands JB: Universal chemical assay for the detection and determination of siderophores. *Anal Biochem* 1987, 160:47-56.
60. Simon R, Priefer U, Pühler A: A broad host range mobilization system for invivo genetic-engineering-transposon mutagenesis in Gram-negative bacteria. *Bio-Technology* 1983, 1:784-791.
61. Casadesús J, Olivares J: (Casadesus and Olivares 1979). *Mol Gen Genet* 1979, 174:203–209.
62. Meade HM, Signer ER: Genetic mapping of *Rhizobium meliloti*. *Proc Natl Acad Sci USA* 1977, 74:2076-2078.
63. Casse F, Boucher C, Julliot JS, Michel M, Denarié J: Identification and characterization of large plasmids in *Rhizobium meliloti* using agarose-gel electrophoresis. *J Gen Microbiol* 1979, 113:229-242.
64. Oresnik IJ, Liu SL, Yost CK, Hynes MF: Megaplasmid pRme2011a of *Sinorhizobium meliloti* is not required for viability. *J Bacteriol* 2000, 182:3582-3586.
65. Prentki P, Krisch HM: *In vitro* insertional mutagenesis with a selectable DNA fragment. *Gene* 1984, 29:303-312.
66. Fellay R, Frey J, Krisch H: Interposon mutagenesis of soil and water bacteria: A family of DNA fragments designed for in vitro insertional mutagenesis of Gram negative bacteria. *Gene* 1987, 52:147-154.
67. Nogales, J., Bernabéu-Roda, L., Cuéllar, V., and Soto, M.J. (2012) ExpR is not required for swarming but promotes sliding in *Sinorhizobium meliloti*. *J Bacteriol* 194: 2027–2035.

1.7. Suplementary material

Adittional file 1.1.

Genes differentially expressed in response to surface growth and/or swarming-specific conditions in *S. meliloti* 1021FDCS5

This tabular data list the 1166 genes showing differential expression in any of the six comparisons performed in this study.
Only M values above 1 or below -1 with $p \leq 0.05$ are shown.
The category in the Venn diagram (A-G) to which each gene belongs is also indicated.
L, growth in **l**iquid MM; **S**, growth on **s**olid MM (1.3% agar); **SS**, growth on **s**emi**s**olid MM (0.6% agar). Time of incubation is shown in parenthesis.

Gene ID	Category	M values						Description
		SS vs. L (7h)	S vs. L (7h)	SS vs L (14h)	S vs L (14h)	SS vs. S (7h)	SS vs.S (14)	
SMa0002	A				-1.38			*fodG* formate dehydrogenase, major subunit (formate dehydrogenase alpha subunit)
SMa0011	D			2.69	2.99			*selA* L-seryl-tRNA selenium transferase
SMa0018	A				1.67			Insertion sequence ISRm2011-2/ISRm11
SMa0034	D			1.08	1.24			Serralysin-like metalloprotease
SMa0036	A				1.42			ABC transporter, ATP-binding protein

SMa0044	B					1.26		conserved hypothetical protein
SMa0045	B					-1.47		*cah* Carbonic anhydrase
SMa0104	A				-1.09			ABC transporter, periplasmic solute-binding protein, likely involved in transport of lysine, ectoine, and asparagine
SMa0116	A				-1.30			DnaJ/CbpA-type protein
SMa0185	A				1.22			conserved hypothetical protein
SMa0189	D	3.37		3.07	3.14			hypothetical protein
SMa0190	D	4.47		2.98	4.20			putative transcriptional regulator, tetR family
SMa0203	D			-2.10	-1.75			ABC transporter, periplasmic solute-binding protein, likely transports galactose and, to a lesser extent, L-arabinose, glucose, D-arabinose, L-fucose and D- fucose
SMa0232	A				-1.47			conserved hypothetical protein
SMa0247	C			1.32				Conserved hypothetical protein
SMa0249	C			1.30				*gntA* TRAP-type small permease component, required for growth on gluconate
SMa0312	D			-2.29	-1.99			hypothetical protein
SMa0314	D			-2.34	-2.35			Conserved hypothetical protein
SMa0316	D			-2.21	-1.75			Hypothetical protein
SMa0355	A				1.23			Transcriptional regulator, LysR family
SMa0387	A				-1.69			*hisC3* Histidinol-phosphate aminotransferase
SMa0391	D			-2.13	-2.49			ABC transporter, ATP-binding protein
SMa0392	D			-4.00	-4.17			ABC transporter, periplasmic solute-binding protein
SMa0394	D			-2.81	-2.85			ABC transporter, permease
SMa0396	A				-1.58			ABC transporter, permease
SMa0398	D			-1.78	-2.31			*hisD2* HisD2 histidinol dehydrogenase
SMa0400	A				-1.48			Dehydrogenase, Zn-dependent
SMa0402	A				-1.26			Transcriptional regulator, GntR family
SMa0436	B					-1.12		hypothetical protein
SMa0512	B						1.53	*idnD* IdnD L-idonate 5-dehydrogenase

SMa0520	G	1.45	2.66	1.90	2.73	1.73	1.55	Transcriptional regulator, RpiR family
SMa0564	F			-1.12			2.78	Putative dehydrogenase
SMa0581	D			-2.52	-2.69			*ntrC* Nitrate transporter, ATP binding protein
SMa0583	D			-3.84	-3.79			*ntrB* Nitrate transporter, permease
SMa0585	D			-4.28	-4.15			*ntrA* Nitrate transporter, periplasmic nitrate binding protein
SMa0590	D			-2.38	-2.70			hypothetical protein
SMa0592	D			-1.10	-1.03			conserved hypothetical protein
SMa0616	A				-1.29			*fixQ3* FixQ3 nitrogen fixation protein
SMa0617	A				-1.14			*fixP3* FixP3 Diheme c-type cytochrome
SMa0621	A				-1.14			*fixI2* FixI2 E1-E2 type cation ATPase
SMa0629	C			1.15				hypothetical protein
SMa0636	A				-1.28			conserved hypothetical protein
SMa0647	A				-1.46			hypothetical protein
SMa0687	A				-2.06			hypothetical protein
SMa0699	A				-1.39			hypothetical protein
SMa0715	A				1.05			Nucleoside-diphosphate-sugar epimerase
SMa0734	A				-1.62			hypothetical protein
SMa0738	C			1.34				*cspA6* CspA6 cold shock protein
SMa0744	D			3.26	3.08			*groEL2* GroEL2 chaperonin
SMa0745	D			3.34	3.39			*groES2* GroES2 chaperonin
SMa0763	B					-1.86		hypothetical protein
SMa0799	C			-1.05				ABC transporter, periplasmic solute-binding protein
SMa0800	A				-1.16			ABC transporter, permease
SMa0814	C			-1.01				*nifB* NifB FeMo cofactor biosynthesis protein
SMa0815	D			-1.44	-1.36			*nifA* NifA transcriptional activator
SMa0819	C			-1.10				*fixB* FixB electron transfer flavoprotein alpha chain
SMa0831	A				-1.04			*nifX* NifX iron-molybdenum cluster-binding protein

SMa0848	D			2.05	1.91			hypothetical protein
SMa0853	C			-1.09				*nodE* NodE beta ketoacyl ACP synthase
SMa0869	B					-1.16		*nodA* NodA N-acyltransferase
SMa0878	C			1.03				*nodM* NodM Glucosamine--fructose-6-phosphate aminotransferase
SMa0890	C			-1.20				conserved hypothetical protein
SMa0903	A				-1.20			conserved hypothetical protein
SMa0952	A				-1.10			ABC transporter, permease
SMa0953	B						-1.2	ABC transporter, ATP-binding protei
SMa1029	D			1.18	1.35			TRm1b transposase
SMa1038	B					-1.08		Multicopper oxidase
SMa1050	B						1.03	hypothetical protein
SMa1052	F	1.01		1.24			1.56	Conserved hypothetical protein
SMa1077	G	1.16	1.05		-1.07		2.76	*next18* Nex18 Symbiotically induced conserved protein
SMa1078	F	1.89		1.74			1.93	Conserved hypothetical protein
SMa1079	F	1.36					1.91	*tspO* TspO Tryptophan rich sensory protein
SMa1100	F	1.31		1.61			1.57	Conserved hypothetical protein
SMa1104	C			-1.00				hypothetical protein fragment
SMa1122	E				-1.22	1.27		Putative permease
SMa1174	C			-1.11				hypothetical protein
SMa1214	C			1.03				*fixQ1* FixQ1 nitrogen fixation protein
SMa1220	C			1.04				*fixN1* FixN1 cytochrome c oxidase subunit 1
SMa1279	A		1.26					norE NorE accessory protein for nitric oxide reductase
SMa1339	C			-1.07				ABC transporter, permease, involved in amino acid or peptide transport
SMa1344	B					-1.08		ABC transporter, ATP-binding protein, involved in amino acid or peptide transport
SMa1347	C			1.08				dehydrogenase
SMa1371	A				-1.59			ABC transporter, ATP-binding protein

SMa1375	D			-1.54	-2.25			ABC transporter, periplasmic solute-binding protein
SMa1381	A				-1.00			Possible oxidase
SMa1389	D			1.48	1.04			*etfA2* EtfA2 electron-transport flavoprotein, alpha-subunit
SMa1391	C			1.25				etfB2 EtfB2 electron transport flavoprotein, beta subunit
SMa1400	A				-1.18			Acyl-CoA dehydrogenase
SMa1410	D			-1.69	-1.47			Oxidoreductase
SMa1414	A				-1.87			Dehydrogenase, FAD-dependent
SMa1450	A				-1.41			Thiolase
SMa1452	A				-1.01			short chain alcohol dehydrogenase-related dehydrogenase
SMa1461	A				-1.28			Mandelate racemase/muconate lactonizing enzyme family protein
SMa1462	D			-1.21	-1.24			ABC transporter, periplasmic solute-binding protein
SMa1473	A				-1.64			proline dipeptidase
SMa1507	D			-1.51	-2.83			Conserved hypothetical protein
SMa1513	D			-1.06	-1.52			ABC transporter, permease
SMa1562	D			-1.07	-1.28			Putative pilus assembly protein
SMa1564	B					-1.28		Putative pilus assembly protein
SMa1573	A				1.45			*cpaE2* CpaE2 pilus assembly protein
SMa1595	A				-1.01			hypothetical protein
SMa1623	A				-1.24			transposase, fragment
SMa1629	A				-1.04			short chain alcohol dehydrogenase-related dehydrogenase
SMa1635	D			-1.13	-1.52			hypothetical protein
SMa1672	B						-1.6	conserved hypothetical protein
SMa1731	B					-1.14		*betB2* BetB2 betaine aldehyde dehydrogenase
SMa1736	C			1.08				Transcriptional regulator, LysR family
SMa1740	B					1.02		Siderophore-interacting protein
SMa1742	B					1.01		ABC transporter, permease, Fe3+-siderophore

								transport system
SMa1746	C			1.32				ABC transporter, periplasmic solute-binding protein, Fe3+-siderophore transport system
SMa1755	D			-1.75	-1.08			ABC transporter, periplasmic solute-binding protei
SMa1760	A				-1.30			phosphotransferase
SMa1765	D			-1.70	-1.49			conserved hypothetical protein
SMa1793	A				-1.08			conserved hypothetical protein
SMa1803	D			1.20	1.17			TRm2011-2a transposase
SMa1808	C	1.04						Hypothetical protein
SMa1817	A		1.07					conserved hypothetical protein
SMa1820	C	1.78						conserved hypothetical protein
SMa1821	D	1.66	1.48					hydrolase
SMa1838	B						-1.1	dehydrogenase
SMa1851	C			1.10				hydrolase
SMa1961	A				-1.26			polyhydroxybutyrate depolymerase
SMa2037	A				-1.14			Oxidoreductase
SMa2075	C			1.03				ABC transporter, periplasmic solute-binding protein
SMa2129	B						1.97	conserved hypothetical protein
SMa2171	A				-1.02			Transposase
SMa2191	A				-1.08			Transposase, fragment
SMa2211	A				-1.54			Thiamine pyrophosphate-requiring protein
SMa2223	A				-1.41			oxidoreductase
SMa2245	D			1.06	1.05			conserved hypothetical protein
SMa2253	A				-1.16			conserved hypothetical protein
SMa2294	E				-1.33		1.38	*mrcA2* MrcA2 penicillin-binding protein
SMa2311	A				-1.05			ABC transporter, ATP-binding protein, likely transports tagatose
SMa2337	D			2.36	1.66			*rhtX*, RhtX rhizobactin transporter
SMa2339	G			1.33	1.35	1.55		Siderophore biosynthesis protein

SMa2347	D			-1.60	-1.93			conserved hypothetical protein
SMa2357	C			1.06				*cyaO* adenylate/guanylate cyclase
SMa2359	A				-1.27			conserved hypothetical protein
SMa2361	D			-1.13	-1.61			conserved hypothetical protein
SMa2373	D			1.89	1.83			TRm2011-2a transposase
SMa2383	C			-1.07				Dehydrogenase, Zn-dependent
SMa2395	C			-1.05				*repA2*, RepA2 replication protein
SMa2400	B					3.65		*rhbA* RhbA Diaminobutyrate--2-oxoglutarate aminotransferase involved in rhizobactin biosynthesis
SMa2402	G	1.84			1.04	2.58		*rhbB* RhbBL-2,4-diaminobutyrate decarboxylase
SMa2404	G			1.19	1.34	2.65		*rhbC* RhbC rhizobactin biosynthesis protein
SMa2406	E				1.35	2.82		*rhbD* RhbD rhizobactin biosynthesis protein
SMa2408	G	2.38		2.23	1.98	3.83		*rhbE* RhbE rhizobactin biosynthesis protein
SMa2410	G	2.36		1.34	1.27	3.76		*rhbF* RhbF rhizobactin biosynthesis protein
SMa2412	A		-1.81					*rhrA* RhrA transcriptional activator
SMa2414	G	1.43		1.64	1.11	2.68		*rhtA* RhtA rhizobactin transporter
SMb20005	F	2.34					-1.4	Putative glutathione S-transferase
SMb20007	A				-1.36			*catC* Catalase
SMb20010	E				1.23	1.88		Hypothetical protein
SMb20011	C			-1.03				Putative heavy-metal transporter
SMb20023	D			1.22	1.95			Probable 5-oxoprolinase
SMb20025	C			1.07				Conserved hypothetical protein
SMb20026	C			1.19				Conserved hypothetical protein
SMb20056	B					-1.52		*btuF*, ABC transporter, periplasmic solute-binding protein
SMb20057	B					-1.47	-1.1	btuC, ABC transporter, permease
SMb20058	B					-1.37	-1.1	btuD, ABC transporter, ATP-binding protein
SMb20059	B					-1.24		SAM-dependent methyltransferase, may be involved in cobalamin metabolism

SMb20072	C			-1.25				ABC transporter, periplasmic solute-binding protein, induced by myo-inositol
SMb20099	D			-1.45	-1.19			Putative trehalose synthase
SMb20100	C			-1.12				Putative dehydrogenase
SMb20111	A				-2.59			Putative oligopeptide ABC transporter ATP-binding protein
SMb20118	C			-1.00				Conserved hypothetical protein
SMb20125	A				-1.31			Putative xanthine and xanthosine ABC transporter, permease component
SMb20166	B					-1.13		Conserved hypothetical protein
SMb20167	D			-1.02	-1.04			Conserved hypothetical protein, signal peptide
SMb20194	D			1.83	2.61			Conserved hypothetical protein
SMb20195	D			1.91	2.56			ppe Ribulose-phosphate 3-epimerase
SMb20196	D			1.52	1.44			*cbbX* ATPase of the AAA+ class
SMb20197	D			1.59	1.70			*cbbS* Putative ribulose-1,5-bisphosphate carboxylase small subunit
SMb20198	D			2.70	2.54			*cbbL* Putative ribulose-1,5-bisphosphate carboxylase large subunit
SMb20199	D			1.08	1.70			*cbbA* Putative fructose-1,6-bisphosphate aldolase
SMb20200	D			1.10	1.16			*cbbT* Putative transketolase
SMb20203	B					-1.58		*cbbR* Probable transcriptional regulator
SMb20204	A				-1.05			*pqqA* Putative pyrroloquinoline quinone synthesis protein A
SMb20207	A				-1.01			*pqqD* Putative pyrroloquinoline quinone synthesis protein D
SMb20227	B					-1.12		*ndiA* 1 Putative nutrient deprivation-induced protein
SMb20246	B					-1.10		Putative oxidoreductase
SMb20260	A				-1.05			Hypothetical protein
SMb20261	A				-1.05			Malate dehydrogenase
SMb20263	D			1.53	1.83			Putative ABC transporter periplasmic amino acid-binding protein
SMb20265	D			1.93	1.76			Putative amino acid ABC transporter permease
SMb20270	B					-1.40		Probable proline racemase

SMb20277	E				-1.31	-1.00		Class-III pyridoxal-phosphate-dependent aminotransferase
SMb20292	A				-1.01			Hypothetical immunogenic protein
SMb20293	A				-1.01			Hypothetical protein
SMb20305	C			1.02				Probable ISRm2011-2 transposase protein, N-terminal portion
SMb20313	A				-1.01			Glycerone kinase
SMb20325	A				-1.31			*thuE* ABC transporter, periplasmic trehalose/maltose-binding protein
SMb20374	A				-1.35			Putative TRAP-type transporter, periplasmic substrate-binding protein
SMb20421	C			1.47				Putative Transposase for insertion sequence ISRm21 protein
SMb20431	C			-1.10				*eutA*, Putative ectoine utilization protein
SMb20432	B					-1.35		*eutB*, Putative threonine dehydratase, involved in ectoine utilization
SMb20436	D			-3.86	-3.73			Probable nitrate transporter
SMb20460	B					-1.18		Cellulose synthase (UDP-forming)
SMb20464	A				-1.16			Hypothetical protein
SMb20473	D			-1.23	-1.41			Hypothetical protein
SMb20483	A				-1.07			Probable transcription regulator, LacI family
SMb20556	B					-1.34	-1	Conserved hypothetical protein
SMb20571	C	1.09						Putative amine ABC transporter, permease component
SMb20581	D			-1.63	-1.31			Putative 4-hydroxyphenylpyruvate dioxygenase
SMb20590	D			-2.02	-1.75			Putative acylphosphatase
SMb20591	D			-2.52	-2.21			Hypothetical protein
SMb20592	D			-1.04	-1.05			*rpoE8* RNA polymerase sigma factor, ECF subfamily protein
SMb20596	C			1.01				Hypothetical protein
SMb20597	A				-1.22			Putative membrane protein
SMb20602	D			-2.75	-3.25			ABC transporter, ATP-binding protein
SMb20603	D			-3.12	-4.38			ABC transporter, permease

SMb20604	G			-4.84	-5.72		1.14	ABC transporter, permease
SMb20605	G			-5.55	-6.55		1.34	ABC transporter, periplasmic solute-binding protein
SMb20614	A				1.04			Hypothetical protein
SMb20618	B					-1.16		*thiE* Putative thiamine-phosphate pyrophosphorylase
SMb20620	C			1.08				Putative sugar ABC transporter
SMb20652	A				-1.14			*asnB* Putative asparagine synthetase
SMb20684	D			-1.03	-1.38			Conserved hypothetical protein
SMb20690	D			-1.00	-1.07			Hypothetical protein
SMb20704	C			-1.61				*glgA2* Putative glycogen synthase
SMb20706	D			-1.47	-1.82			Putative amino acid uptake ABC transporter periplasmic solute-binding protein precursor
SMb20727	C			1.04				Hypothetical protein
SMb20745	A				-1.24			*glnII* Glutamate-ammonia ligase
SMb20753	B						1.07	Acyl-CoA dehydrogenase
SMb20757	A				-1.06			*bhbA* Methylmalonyl-CoA mutase
SMb20786	D	-1.85	-1.90	-2.41	-2.43			Putative organic acid ABC transporter, permease component
SMb20807	C			1.31				Putative membrane protein
SMb20813	C			1.32				ABC transporter, ATP-binding and permease components
SMb20824	D			2.31	1.60			Putative glycosyltransferase involved in capsule biosynthesis
SMb20825	D			1.13	1.30			Putative acetyltransferase, cysElacA/lpxA/nodL family protein
SMb20829	A				-1.32			Putative secreted calcium-binding protein
SMb20836	A				-1.27			Hypothetical protein
SMb20861	D			-2.15	-1.55			Putative dehydrogenase, oxidoreductase FAD flavoprotein
SMb20867	C			-1.05				Hypothetical protein
SMb20885	C			1.42				Conserved hypothetical membrane protein
SMb20886	D			-1.55	-1.57			Conserved hypothetical protein

SMb20887	D			-1.15	-1.68			Conserved hypothetical protein
SMb20906	D			-1.44	-1.35			Hypothetical protein
SMb20911	A				-1.03			Hypothetical protein
SMb20915	C			-1.13				*aslA1* Putative arylsulfatase
SMb20934	B					-1.11		*exsF* Putative two-component response regulator.
SMb20957	D			-1.00	-1.32			*exoA* Glycosyltransferase, succinoglycan biosynthesis protein
SMb20958	A				-1.32			*exoM* Probable succinoglycan biosynthesis protein
SMb20960	D			-2.04	-2.18			*exoN* UDPglucose pyrophosphorylase
SMb20961	A				-1.19			*exoP* Protein-tyrosine kinase
SMb20964	C			1.00				Peroxidase
SMb20980	D			-2.71	-3.26			Putative small C4-dicarboxylate uptake permease
SMb20984	D			-2.34	-2.51			*nirB* Nitrite reductase [NAD(P)H]
SMb20985	D	1.07		-2.07	-2.72			*nirD* Nitrite reductase [NAD(P)H]
SMb20986	D	2.23		-1.32	-2.16			*narB* Putative nitrate reductase, large subunit
SMb20987	A				-1.15			Putative uroporphiryn-III C-methyltransferase
SMb20989	D			2.52	2.62			Putative stomatin-like protein
SMb20993	D			-1.11	-1.45			Acyl-CoA dehydrogenase
SMb20995	C			1.08				*engA* Putative GTP-binding protein
SMb21000	D			1.20	1.04			Putative transport protein
SMb21004	D			-1.30	-1.76			Hypothetical protein
SMb21011	D			-1.13	-1.48			*xdhA2* Xanthine dehydrogenase
SMb21030	B					-1.03		Hypothetical protein
SMb21050	A				-1.23			*wzx1* Putative succinoglycan biosynthesis transport protein
SMb21057	C			-1.35				Conserved hypothetical protein
SMb21097	D			-2.03	-2.73			ABC transporter, periplasmic solute-binding protein
SMb21112	D			1.30	1.45			*hpaG* Putative bifunctional enzyme 2-hydroxyhepta-2,4-diene-1,7-dioatesomerase 5-carboxymethyl-2-oxo-hex-3-ene-1,7-

								dioatedecarboxylase
SMb21114	D			-1.31	-1.64			Putative nitrate transport protein
SMb21115	D	-1.02		-2.82	-3.08			Putative response regulator
SMb21117	C			-1.16				Putative transcriptional regulator
SMb21132	D			1.64	1.99			Putative sulfate uptake ABC transporter, permease component
SMb21133	D	1.00		1.94	1.56			Putative sulfate uptake ABC transporter, periplasmic solute-binding protein
SMb21134	B					-1.08		Amino acid aldolase or racemase
SMb21135	D			1.47	1.37			ABC transporter, periplasmic solute-binding protein, may be involved in transport of sugar amines (galactosamine and glucosamine)
SMb21136	D			1.34	1.43			ABC transporter, permease component, may be involved in transport of sugar amines
SMb21151	D			-2.00	-2.06			Putative sugar amine ABC transporter, periplasmic solute-binding protein
SMb21163	D			-1.56	-1.65			*hutU* Putative urocanate hydratase (urocanase)
SMb21171	D			1.47	1.83			*phnM* Putative hydrolase
SMb21174	D			1.50	1.08			*phoT* Phosphate uptake ABC transporter permease
SMb21175	D			2.38	3.63			*phoE* Phosphate uptake ABC transporter permease
SMb21176	D			2.09	2.98			*phoD* Phosphate uptake ABC transporter periplasmic solute-binding protein precursor
SMb21177	D			2.25	2.90			*phoC* Phosphate uptake ABC transporter ATP-binding protein
SMb21184	D			-1.01	-1.36			*ackA2* Putative acetate kinase (acetokinase)
SMb21186	D			1.28	1.11			*gabT* Putative 4-aminobutyrate aminotransferase
SMb21189	C			1.66				Putative glycosyltransferase
SMb21192	D			1.10	1.08			*cbbA2* Putative fructose-bisphosphate aldolase
SMb21197	B					1.64		Putative amino acid ABC transporter, permease component
SMb21203	A				-1.73			Putative esteraselipase/thioesterase
SMb21221	D			-1.63	-1.63			putative sugar amine ABC transporter, periplasmic solute-binding protein
SMb21229	A				-1.77			Putative calcium-binding exported protein

SMb21230	A				-1.39			Putative glycosyltransferase
SMb21240	A				-1.10			Putative MPA1 family auxiliary surface saccharide export protein
SMb21249	A				-1.53			Putative sulfotransferase
SMb21255	A				-1.66			Hypothetical protein
SMb21256	D			1.01	1.22			Probable UDP-glucose/GDP-mannose dehydrogenase
SMb21257	C			1.94				Hypothetical protein
SMb21265	A				1.01			Putative glycosyl transferase
SMb21272	D			1.56	1.21			Putative lacI family transcritional regulator
SMb21273	D			1.91	1.40			ABC transporter, periplasmic solute-binding protein
SMb21274	C			1.64				ABC transporter, permease component
SMb21284	G			-1.55	-1.63		-1.1	Putative polysaccharide deacetylase
SMb21285	D			-1.18	-1.10			Conserved hypothetical protein, transthyretin-like protein
SMb21286	D			-1.64	-1.71			*xdhA1* Probable xanthine dehydrogenase
SMb21290	A				-1.08			Putative NADPH quinone oxidoreductase
SMb21292	D			-1.61	-1.15			Conserved hypothetical membrane protein, paralogue of Y20848
SMb21295	D			1.85	2.15			Putative small heat shock protein, hsp20 family
SMb21345	A				1.06			Putative galactose ABC transporter, periplasmic solute-binding protein
SMb21367	B					-1.14		cycA Putative cytochrome c class I protein, probably cytochrome c4
SMb21377	A				-1.10			Putative polyols and C6 monosaccharide ABC transporter, periplasmic solute-binding protein
SMb21397	D			1.58	1.16			Hypothetical calcium-binding protein
SMb21431	G		-1.32	1.75	2.25	1.44		Hypothetical protein, possibly C terminus of iron ABC transporter periplasmatic solute-binding protein
SMb21432	G	-1.07	-1.61	1.63	2.09	2.15		Putative iron uptake ABC transporter periplasmic solute-binding protein precursor
SMb21437	D			-2.04	-2.58			TRAP-type transporter, small permease component
SMb21438	D			-2.00	-2.36			TRAP-type transporter, periplasmic solute-

								binding protein
SMb21446	D			-1.25	-1.45			*glgX2* Isoamylase
SMb21449	C			-1.38				*gst12* Probable glutathione S-transferase
SMb21450	D			-2.82	-3.08			Conserved hypothetical protein
SMb21468	A				-1.11			Conserved hypothetical membrane protein
SMb21488	C			1.19				*cyoB* Putative cytochrome o ubiquinol oxidase chain I
SMb21489	C			1.38				*cyoC* Putative cytochrome o ubiquinol oxidase chain III
SMb21492	A				-1.19			Hypothetical protein
SMb21494	A				-1.58			*ocd* Putative ornithine cyclodeaminase
SMb21520	B					-1.03		Putative two-component response regulator
SMb21549	D	1.80		2.29	2.53			*thtR* Putative exported sulfurtransferase, Rhodanese protein
SMb21550	C			1.35				Conserved hypothetical protein
SMb21555	C			1.18				*kefB2* Probable glutathione-regulated potassium-efflux system
SMb21569	C			-1.06				Hypothetical protein
SMb21572	D			-1.30	-2.02			Putative amino acid uptake ABC transporter periplasmic solute-binding protein precursor
SMb21587	A				-1.06			Putative pentose monosaccharide ABC transporter, periplasmic solute-binding protein
SMb21600	A				-1.38			*ampC* Putative exported beta-lactamase
SMb21601	B					-1.02		Putative transcriptional regulator
SMb21630	D			1.32	1.55			Conserved hypothetical protein
SMb21664	A				-1.10			Hypothetical exported or membrane-anchored protein
SMb21676	F			1.92			1.96	Hypothetical protein
SMb21678	D			-1.25	-1.40			Hypothetical protein
SMb21697	C			1.12				Conserved hypothetical protein
SMb21702	D			1.16	1.48			Putative transposase of insertion sequence ISRm2011-2, orfB N-terminus protein
SMb21707	D			-3.28	-3.38			ABC transporter, ATP-binding protein

SMc00005	A				1.07			*fabI1* Putative enoyl-acyl-carrier-protein reductase NADH.
SMc00007	D			1.43	1.95			*aroC* Probable chorismate synthase
SMc00009	C			1.01				*ctaC* Putative cytochrome C oxidase subunit II
SMc00010	D			1.26	1.13			*ctaD* Putative cytochrome C oxidase polypeptide I transmembrane protein
SMc00013	D			1.40	1.39			*ctaE* Putative cytochrome C oxidase subunit III transmembrane protein
SMc00017	C			1.54				*thrB* Putative homoserine kinase
SMc00031	C			1.12				Hypothetical/unknown transmembrane protein
SMc00033	A				1.46			Diguanylate cyclase/phosphodiesterase
SMc00038	A				-1.36			Diguanylate cyclase/phosphodiesterase
SMc00043	D			1.56	1.18			*sodB* Probable superoxide dismutase FE protein
SMc00078	C			1.02				Putative methionine ABC transporter, periplasmic solute-binding protein
SMc00088	D			1.27	1.32			Hypothetical/unknown transmembrane protein
SMc00090	D	1.79		3.83	3.04			*cysN* Putative sulfate adenylate transferase cysteine biosynthesis protein
SMc00091	D	1.56		1.31	2.26			*cysD* Putative sulfate adenylate transferase subunit 2 cysteine biosynthesis protein
SMc00092	D	1.75		3.86	4.25			*cysH* Phosphoadenosine phosphosulfate reductase
SMc00101	A				-1.08			*dkgB* Putative 2,5-diketo-D-gluconic acid reductase B
SMc00114	D			1.30	1.09			*ptrB* Probable protease II oligopeptidase B hydrolase serine protease
SMc00130	A				-1.12			Hypothetical transmembrane protein
SMc00137	D			-1.44	-1.87			*usg1* Conserved hypothetical protein
SMc00153	D			1.83	1.94			Conserved hypothetical protein
SMc00155	D			1.09	1.18			*aroF* Probable phospho-2-dehydro-3-deoxyheptonate aldolase
SMc00158	D			-1.52	-2.23			Conserved hypothetical protein, signal peptide
SMc00159	D			-1.35	-2.15			Conserved hypothetical protein, signal peptide
SMc00170	A				-1.13			*sinR* Quorum sensing system, AHL autoinducer-binding, luxR family, regulator of sinI

SMc00171	A				1.44			Conserved hypothetical protein
SMc00198	C			1.34				Hypothetical/unknown protein
SMc00227	A				1.04			Conserved hypothetical protein
SMc00231	C			1.01				*glmS* Glucosamine--fructose-6-phosphate aminotransferase (nodm paralogue) protein
SMc00242	B					1.16		Hypothetical signal peptide protein
SMc00277	D			-1.87	-1.98			Hypothetical protein
SMc00278	A				-1.12			Transcription regulator AsnC family
SMc00282	B					-1.03		Conserved hypothetical protein
SMc00287	D			2.17	2.22			Probable NADH-ubiquinone oxidoreductase
SMc00293	D			2.16	2.25			*thrA* Probable homoserine dehydrogenase
SMc00302	D			1.06	1.49			Conserved hypothetical protein
SMc00320	D			2.13	2.51			*rbfA* Probable ribosome-binding factor A, rRNA processing protein
SMc00321	C			1.20				*truB* Probable tRNA pseudouridine synthase B
SMc00323	D			1.72	2.21			*rpsO* Probable 30S ribosomal protein S15
SMc00324	D			3.64	3.35			*pnp* Probable polyribonucleotide nucleotidyltransferase
SMc00326	D			1.52	1.89			*fabI2* Putative enoyl-acyl-carrier-protein reductase NADH
SMc00327	D			1.27	1.40			*fabB* Probable 3-oxoacyl-acyl-carrier-protein synthase I
SMc00328	A				1.08			*fabA* Probable 3-hydroxydecanoyl-acyl-carrier-protein dehydratase
SMc00329	C			1.17				*irr* Putative iron response regulator
SMc00332	D			2.76	2.77			Hypothetical protein
SMc00333	A				2.55			*aroA* Putative 3-phosphoshikimate 1-carboxyvinyltransferase
SMc00334	D			1.46	1.64			*cmk* Putative cytidylate kinase (CMP kinase)
SMc00335	D			3.03	3.55			*rpsA* 30S ribosomal protein S1
SMc00342	C			1.57				*rnd2* Putative ribonuclease D
SMc00346	C			1.31				Hypothetical transmembrane protein
SMc00347	D			-1.32	-1.26			*rnk1* Putative regulator of nucleoside

								diphosphate kinase
SMc00349	D			1.01	2.70			*lepA* Probable GTP-binding protein membrane
SMc00363	D			3.57	3.41			*rpmI* Probable 50S ribosomal protein L35
SMc00364	D			3.74	3.75			*rplT* Probable 50S ribosomal protein L20
SMc00365	D			1.37	2.64			*pheS* Probable phenylalanyl-tRNA synthetase alpha chain
SMc00366	A				1.01			*pheT* Probable phenylalanyl-tRNA synthetase beta chain
SMc00375	D			2.04	1.36			Probable oxidoreductase
SMc00389	A				1.14			Hypothetical/unknown protein
SMc00394	D			1.70	1.40			*guaA* Probable GMP synthase glutamine-hydrolyzing protein
SMc00401	C			1.21				Conserved hypothetical protein
SMc00402	G		-1.14	1.91	1.70	1.42		Hypothetical signal peptide protein
SMc00407	A				1.10			*gst4* Putative glutathione S-transferase
SMc00408	C			1.18				*uppP* Putative undecaprenyl-diphosphatase
SMc00409	D			2.60	2.23			Hypothetical signal peptide protein
SMc00410	D			1.11	1.35			Probable NADH-ubiquinone oxidoreductase
SMc00411	D			1.10	1.15			Conserved hypothetical protein
SMc00412	A				1.25			*pyrF* Probable orotidine 5'-phosphate decarboxylase
SMc00415	C			1.08				*dnaN* Probable DNA polymerase III, beta chain
SMc00421	C	1.01		1.91				*cysK1* Probable cysteine synthase A (O-acetylserine sulfhydrylase A) protein
SMc00422	C			1.16				Putative amino acid exporter
SMc00423	D			2.49	2.03			Putative amino acid exporter
SMc00430	B					-1.04		Putative sugar epimerase family protein
SMc00450	C			1.03				*ctaB* Putative protoheme IX farnesyltransferase
SMc00451	A				-1.02			Probable processing protease
SMc00456	D			-1.09	-1.71			Conserved hypothetical protein, signal peptide
SMc00469	C			1.56				*dksA* RNA polymerase-binding, DksA

SMc00470	A				-1.40			Hypothetical transmembrane protein
SMc00475	D			1.74	1.51			*alaS* Alanyl-tRNA ligase
SMc00480	D			1.73	2.32			*icd* Probable isocitrate dehydrogenase [NADP] protein
SMc00485	D			3.83	4.46			*rpsD* Probable 30S ribosomal subunit protein S4
SMc00489	C			1.48				Hypothetical/unknown signal peptide protein
SMc00491	C			1.10				Hypothetical protein
SMc00493	A				1.12			*purQ* Probable phosphoribosylformyl glycinamidine synthase I
SMc00507	A				-1.30			Hypothetical protein
SMc00517	A				-1.22			Conserved hypothetical protein
SMc00521	D			1.89	1.99			Conserved hypothetical protein
SMc00522	D			1.20	1.29			*rhlE1* Putative ATP-dependent RNA helicase
SMc00523	C			1.13				Hypothetical protein
SMc00526	D			1.47	1.20			*tyrS* Probable tyrosyl-tRNA synthetase
SMc00528	D			1.53	1.38			Conserved hypothetical protein
SMc00530	D			1.22	1.50			*sufB* UPF0051 family protein
SMc00533	C			1.51				*sufS* Probable cysteine desulfurase
SMc00535	A				1.07			Inositol monophosphatase family protein
SMc00551	D			1.36	1.01			*psd* Probable phosphatidylserine decarboxylase
SMc00555	D			1.60	1.74			*cvpA* Putative colicin V production homolog transmembrane protein
SMc00556	C			1.57				*radA* Putative DNA repair protein
SMc00562	A		-1.05					Transcription regulator, MarR family
SMc00565	D			2.17	1.99			*rplI* Probable 50S ribosomal protein L9
SMc00566	D			1.39	1.15			Hypothetical transmembrane protein
SMc00567	D			4.67	4.81			*rpsR* Putative 30S ribosomal protein S18
SMc00568	D			1.93	1.96			*rpsF* Putative 30S ribosomal protein S6
SMc00570	D			1.96	1.81			Probable oxidoreductase
SMc00572	A				1.30			*fabG* Probable 3-oxoacyl-acyl-carrier protein reductase

SMc00573	D			2.02	1.76			*acpP* Acyl carrier protein
SMc00574	D			1.89	1.58			*fabF* Probable 3-oxoacyl-acyl-carrier-protein synthase II
SMc00578	A				1.86			Hypothetical protein
SMc00583	C			1.08				Hypothetical, transmembrane protein
SMc00591	D			1.82	1.33			Hypothetical/unknown signal peptide protein
SMc00592	G		-1.49	1.47	1.52	1.30		Hypothetical, transmembrane protein
SMc00595	D			3.42	3.68			*ndk* Probable nucleoside diphosphate kinase
SMc00612	C			-1.12				Hypothetical protein signal peptide
SMc00615	D			2.05	1.83			*purM* 5'-phosphoribosyl-5-aminoimidazole synthetase
SMc00616	A				1.05			*perM* Putative permease
SMc00617	C			1.32				Conserved hypothetical protein
SMc00618	D			1.16	1.08			*ppk* Putative polyphosphate kinase
SMc00620	D			1.05	1.79			Hypothetical signal peptide protein
SMc00640	D	-1.00		2.50	2.52			*serC* Putative phosphoserine aminotransferase
SMc00641	D	-1.41		3.22	3.77			*serA* Putative D-3-phosphoglycerate dehydrogenase
SMc00643	D			1.14	1.48			*purA* Probable adenylosuccinate synthetase IMP--aspartate ligase
SMc00646	D			1.90	2.04			*rpoH1* RNA polymerase sigma factor (Sigma-32)
SMc00651	A				-1.14			Conserved hypothetical protein, signal peptide
SMc00654	A				-1.21			*ctrA* Cell cycle transcriptional regulator CtrA, autoregulated, response regulator
SMc00655	A				-1.11			Hypothetical protein
SMc00672	C			-1.16				*hisX* hutX Histidine ABC transporter, periplasmic solute-binding protein
SMc00677	A				-1.21			Putative aminotransferase
SMc00681	D			1.27	1.02			*lrp1* Probable leucine-responsive regulatory protein
SMc00687	D			1.24	1.27			Hypothetical protein
SMc00690	D			1.75	1.94			*accA* Probable acetyl-coenzyme A carboxylase carboxyl transferase subunit alpha protein

SMc00699	C			1.48				Hypothetical protein
SMc00701	A				1.03			*cobT* Probable Aerobic cobaltochelatase CobT subunit
SMc00704	D			2.01	1.96			*rpmB* Probable 50S ribosomal protein L28
SMc00720	A				-1.43			Putative 2-component receiver domain protein
SMc00725	A				1.69			*argH1* Probable argininosuccinate lyase asal protein
SMc00728	D			1.46	1.38			*etfA1* Putative electron transfer flavoprotein alpha-subunit alpha-ETF flavoprotein
SMc00738	C			1.01				Hypothetical transmembrane protein
SMc00770	D			-1.22	-1.13			*potF* Probable putrescine-binding periplasmic protein
SMc00777	D			-1.11	-1.88			Conserved hypothetical protein
SMc00784	E		-1.31			1.44		*fbpA* Fe3+ ABC transporter
SMc00785	B						1.01	*rirA* Transcriptional regulator of the iron limitation response
SMc00791	D			1.44	1.15			Conserved hypothetical protein
SMc00815	D			2.42	1.91			*guaB* Probable inosine-5'-monophosphate dehydrogenase
SMc00819	D	3.69		3.17	3.39			*katA* Catalase
SMc00821	B					-1.08		Hypothetical protein
SMc00825	D			1.47	1.81			*gsh1 gshA* Glutamate-cysteine ligase, GshA
SMc00833	B					-1.10		*glcE* Probable glycolate oxidase subunit
SMc00849	A				-1.30			Hypothetical protein
SMc00854	D			-1.27	-1.85			Hypothetical/unknown signal peptide protein
SMc00855	A				1.55			*glyQ* Probable glycyl-tRNA synthetase alpha chain
SMc00866	B					-1.06		Hypothetical protein
SMc00868	D			2.60	2.65			*atpF* Probable ATP synthase B chain transmembrane protein
SMc00869	D			3.59	3.38			*atpF2* Probable ATP synthase subunit B' transmembrane protein
SMc00870	D			3.33	3.16			*atpE* Probable ATP synthase subunit C transmembrane protein
SMc00871	D			3.80	3.02			*atpB* Probable ATP synthase A chain

								transmembrane protein
SMc00872	D			2.03	1.54			*atpI* Putative F0F1 ATP synthase, subunit I transmembrane protein
SMc00874	A				1.04			*corA2* Probable magnesium and cobalt transport transmembrane protein
SMc00878	A				-1.19			Putative transcriptional regulator
SMc00881	A				-1.03			*dgoK1* Putative 2-dehydro-3-deoxygalactonokinase
SMc00885	D			-1.30	-1.43			Hypothetical transmembrane signal peptide protein
SMc00887	A				1.20			Diguanylate cyclase/phosphodiesterase
SMc00894	C			1.27				*kdtA* Putative 3-deoxy-D-manno-octulosonic-acid transferase
SMc00895	D			1.59	1.31			Conserved hypothetical protein
SMc00897	C			1.00				*pmbA* Hypothetical PmbA protein
SMc00904	D			1.29	1.37			Hypothetical protein
SMc00912	D			3.40	3.64			*groES1* 10 KD chaperonin A
SMc00913	D			2.91	3.01			*groEL1* 60 KD chaperonin A
SMc00918	C			1.10				*hisZ* ATP phosphoribosyltransferase regulatory subunit
SMc00919	D			1.24	1.89			*hisS* Probable histidyl-tRNA synthetase
SMc00922	D			-1.63	-1.74			Probable cytosine/uracil/thiamine/allantoin permease
SMc00933	A				1.00			Conserved hypothetical protein
SMc00936	A				1.09			*ilvA* Probable threonine dehydratase biosynthetic protein
SMc00938	D			1.33	1.27			Hypothetical protein
SMc00950	D			2.09	1.45			Hypothetical protein signal peptide
SMc00951	D			1.77	1.79			Putative periplasmic solute-binding protein
SMc00964	D			1.94	1.55			*bioB* Putative biotin transporter
SMc00965	D			1.97	1.45			Putative acyl-CoA synthase
SMc00971	D			-1.26	-1.36			Probable pirin-related protein
SMc00975	D			2.06	1.37			*mcpU* Probable chemoreceptor (methyl-accepting chemotaxis) transmembrane protein

SMc00979	A				-1.01			Hypothetical transmembrane protein
SMc00980	A				-1.45			Glycosyl hydrolase family protein
SMc00985	A				1.07			*pdxR* 4-phospho-D-erythronate dehydrogenase
SMc00990	D	1.76			1.17			*fsr* Putative fosmidomycin resistance antibiotic resistance transmembrane protein
SMc00998	D			-1.45	-2.05			Conserved hypothetical signal peptide protein
SMc01002	D			-1.02	-1.03			Conserved hypothetical protein
SMc01004	A				1.02			*hisI* Putative phosphoribosyl-AMP cyclohydrolase
SMc01010	A				1.65			*thrS* Probable threonyl-tRNA synthetase
SMc01012	C			1.14				Conserved hypothetical protein
SMc01016	D			-1.19	-1.66			Hypothetical protein
SMc01017	D			-1.92	-1.83			Putative acetyltransferase
SMc01027	D			1.06	1.41			*kdsA* Probable 2-dehydro-3-deoxyphosphooctonate aldolase
SMc01028	D			1.09	1.68			*eno* Probable enolase
SMc01030	A				1.42			*pdhA* Pyruvate dehydrogenase E1 component alpha subunit
SMc01036	C			1.12				Hypothetical transmembrane protein
SMc01041	D			-1.96	-1.83			*dusB* tRNA-dihydrouridine synthase B
SMc01042	D			-1.48	-1.71			*ntrB* Nitrogen assimilation regulatory protein
SMc01043	D			-1.85	-1.91			*ntrc* Nitrogen assimilation regulatory protein
SMc01048	D			1.62	1.32			*hfq nrfA* Probable RNA binding protein
SMc01052	A				1.03			Conserved hypothetical protein
SMc01053	D			2.63	2.34			cysG Probable siroheme synthase
SMc01054	D			2.39	2.57			Conserved hypothetical protein
SMc01093	A				-1.13			Putative esterase/lipase
SMc01104	C			1.11				*mcpX* Probable chemoreceptor (methyl-accepting chemotaxis) transmembrane protein
SMc01106	D			1.80	1.49			Probable small heat shock protein
SMc01107	D			-1.40	-1.37			Conserved hypothetical protein

SMc01109	D			1.82	2.43			*metK* Probable S-adenosylmethionine synthetase
SMc01121	D			1.28	1.54			*trpS* Probable tryptophanyl-tRNA synthetase
SMc01122	D			-1.22	-1.04			Conserved hypothetical protein
SMc01126	C			1.22				*tme* NADP-dependent malic enzyme protein
SMc01127	A				1.33			*olsB* Protein required for first step of ornithine-containing lipid biosynthesis (N-acylation of ornithine forming lyso-ornithine lipid)
SMc01140	C			-1.13				Ribosomal protein S30Ae/sigma 54 modulation protein
SMc01142	C			1.10				*grpE* Probable heat shock protein
SMc01152	D			3.13	3.18			*rpsT* 30S ribosomal protein S20
SMc01159	A				-1.24			Putative FAD-dependent pyridine nucleotide-disulphide oxidoreductase
SMc01160	D			-1.36	-1.73			Conserved hypothetical protein
SMc01167	D			1.08	1.25			*dnaA* Chromosomal replication initiator
SMc01169	C			1.19				ald Probable alanine dehydrogenase oxidoreductase
SMc01174	C			1.27				*cysK2* Probable cysteine synthase A (O-acetylserine sulfhydrylase A) protein
SMc01204	C			1.07				Probable short-chain dehydrogenase
SMc01226	D			1.20	1.26			Transcriptional regulator, ArsR family
SMc01231	D			1.01	1.25			*gyrA* Probable DNA gyrase subunit A
SMc01236	D			1.28	1.32			Conserved hypothetical protein
SMc01237	B					-1.06	-1.3	*nrdJ* Vitamin B12-dependent ribonucleotide reductase
SMc01242	G			-1.35	-1.85		1.04	Conserved hypothetical signal peptide protein
SMc01263	A				1.02			Hypothetical transmembrane protein
SMc01266	D			-1.79	-2.08			Conserved hypothetical protein
SMc01267	D			-1.13	-1.19			Conserved hypothetical protein
SMc01272	C			1.06				Hypothetical transmembrane protein
SMc01283	D			3.56	3.41			*rplQ* Probable 50S ribosomal protein L17
SMc01285	D			3.88	4.00			*rpoA* DNA-directed RNA polymerase, alpha subunit

SMc01286	D			2.60	4.42			*rpsK* Probable 30S ribosomal protein S11
SMc01287	D			3.05	2.99			*rpsM* Probable 30S ribosomal protein S13
SMc01289	D			2.26	1.46			*secY* Preprotein translocase subunit SecY
SMc01290	D			4.30	3.99			*rplO* Probable 50S ribosomal protein L15
SMc01291	D			3.83	3.98			*rpmD* Probable 50S ribosomal protein L30
SMc01292	D			4.73	5.41			*rpsE* Probable 30S ribosomal protein S5
SMc01293	D			2.17	2.67			*rplR* Probable 50S ribosomal protein L18
SMc01294	D			2.80	4.43			*rplF* Probable 50S ribosomal protein L6
SMc01295	D			4.97	5.58			*rpsH* Probable 30S ribosomal protein S8
SMc01296	D			3.88	4.31			*rpsN* Probable 30S ribosomal protein S14
SMc01297	D			5.63	5.34			*rplE* Probable 50S ribosomal protein L5
SMc01298	D			3.71	4.92			*rplX* Probable 50S ribosomal protein L24
SMc01299	D			4.51	4.76			*rplN* Probable 50S ribosomal protein L14
SMc01300	D			1.98	3.20			*rpsQ* Probable 30S ribosomal protein S17
SMc01301	D			4.51	4.69			*rpmC* Probable 50S ribosomal protein L29
SMc01302	D			2.99	3.15			*rplP* Probable 50S ribosomal protein L16
SMc01303	D			3.62	3.83			*rpsC* Probable 30S ribosomal protein S3
SMc01304	D			4.08	4.47			*rplV* Probable 50S ribosomal protein L22
SMc01305	D			4.75	4.38			*rpsS* Probable 30S ribosomal protein S19
SMc01306	D			2.46	4.07			*rplB* Probable 50S ribosomal protein L2
SMc01307	D			4.05	4.82			*rplW* Probable 50S ribosomal protein L23
SMc01308	D			4.97	4.00			*rplD* Probable 50S ribosomal protein L4
SMc01309	D			2.85	3.76			*rplC* Probable 50S ribosomal protein L3
SMc01310	D			3.16	3.96			*rpsJ* Probable 30S ribosomal protein S10
SMc01311	D			4.39	4.82			*tufA* Probable elongation factor TU protein
SMc01312	D			2.72	3.80			*fusA1* Probable elongation factor G
SMc01313	D			4.83	4.41			*rpsG* Probable 30S ribosomal protein S7
SMc01314	D			3.86	5.12			*rpsL* Probable 30S ribosomal protein S12

SMc01315	C			1.35				Conserved hypothetical protein
SMc01316	D			1.69	2.40			*rpoC* Probable DNA-directed RNA polymerase beta' chain
SMc01317	D			2.11	2.51			*rpoB* Probable DNA-directed RNA polymerase beta chain
SMc01318	D			1.60	2.26			*rplL* Probable 50S ribosomal protein L7/L12 (L8)
SMc01319	D			4.12	3.94			*rplJ* Probable 50S ribosomal protein L10 (L8)
SMc01320	D			3.13	2.68			*rplA* Probable 50S ribosomal protein L1
SMc01321	D			3.52	4.06			*rplK* Probable 50S ribosomal protein L11
SMc01323	D			1.89	1.55			*secE* Putative preprotein translocase SecE subunit transmembrane
SMc01326	D			4.49	4.06			*tufB* Probable elongation factor TU protein
SMc01329	D	-1.00		1.37	1.12			*azoR* Probable FMN-dependent NADH-azoreductase
SMc01333	D			1.17	1.62			*prfB* Probable peptide chain release factor 2 (RF-2) protein
SMc01334	D			2.68	3.06			*mrcA1* Probable penicillin-binding 1A transmembrane protein
SMc01336	D			1.08	1.42			*rne* Probable ribonuclease E
SMc01339	D			1.58	1.06			Insertion sequence ISRm2011-2
SMc01343	D			1.74	1.56			*aroQ* Putative 3-dehydroquinate dehydratase
SMc01344	D			1.34	1.66			*accB* Probable biotin carboxyl carrier protein of acetyl-CoA carboxylase (bccp)
SMc01345	D			1.92	2.06			*accC* Probable biotin carboxylase
SMc01348	C			1.14				Hypothetical protein
SMc01350	A				1.03			*gatB* Putative glutamyl-tRNA amidotransferase subunit B
SMc01352	A				1.03			*gatA* Putative glutamyl-tRNA amidotransferase subunit A
SMc01353	A				1.03			*gatC* Putative glutamyl-tRNA(GLN) amidotransferase subunit C
SMc01360	C			1.69				*pyrB* Probable aspartate carbamoyltransferase catalytic chain
SMc01361	D			1.37	2.24			Dihydroorotase
SMc01364	A				1.39			*tpoA* Putative DNA topoisomerase I

SMc01365	D			1.52	1.37			*rnr* Putative exoribonuclease II
SMc01369	D			1.86	2.19			*rpmG* Probable 50S ribosomal protein L33
SMc01410	A				-1.38			Putative lipoprotein transmembrane
SMc01412	A				-1.03			Conserved hypothetical protein
SMc01417	F	1.26				1.12		Hypothetical protein
SMc01427	D			1.67	1.49			Hypothetical protein
SMc01428	D			3.40	3.12			*cspA2* Probable cold shock transcription regulator
SMc01430	A				1.01			*ilvH* Probable acetolactate synthase isozyme III small subunit
SMc01438	B					-1.24		*degP2* Probable serine protease
SMc01440	C			1.34				*hflC* Putative hydrolase serine protease transmembrane protein
SMc01441	A				1.01			*hflK* Putative membrane bound protease
SMc01453	C			-1.43				Insertion sequence ISRm22
SMc01459	A				-1.12			Hypothetical transmembrane protein
SMc01460	A				-1.35			Conserved hypothetical protein
SMc01463	A				-1.22			Conserved hypothetical protein
SMc01465	D			1.33	1.49			*creA* Putative CreA protein
SMc01488	D			-1.44	-2.25			Hypothetical transmembrane protein
SMc01489	D			-1.30	-1.92			Conserved hypothetical signal peptide protein containing calcium-binding EF-hand regions
SMc01490	D			-1.74	-1.61			Hypothetical protein
SMc01494	A				1.58			*serB* Putative phosphoserine phosphatase
SMc01496	D			1.27	1.21			*smoE* Putative C6 polyol ABC transporter, periplasmic solute-binding component
SMc01497	D			2.40	1.93			*smoF* Putative C6 polyol ABC transporter, permease component
SMc01498	D			2.19	2.11			*smoG* Putative C6 polyol ABC transporter, permease component
SMc01499	A				1.18			*smoK* Putative C6 polyol ABC transporter, ATP-binding component
SMc01500	D			1.69	1.30			smoS Probable sorbitol dehydrogenase (L-iditol 2-dehydrogenase)

SMc01501	D			1.45	1.47			*mtlK* Probable mannitol 2-dehydrogenase
SMc01502	D			1.33	1.20			Hydrolase phosphatase
SMc01510	G		-1.82	1.48		1.53		*hmuV* Putative hemin transport system ATP-binding ABC transporter
SMc01512	F			1.49		1.39		*hmuT* Putative hemin binding periplasmic transmembrane protein
SMc01513	G			1.34	1.12	2.60		*hmuS* Putative hemin transport protein
SMc01514	G	-1.14		1.50	1.62	2.37		Conserved hypothetical protein
SMc01517	C			1.32				Conserved hypothetical protein
SMc01518	E				1.37	1.08		Conserved hypothetical protein
SMc01524	A				1.23			Putative dipeptidase
SMc01527	D			1.08	1.38			*dppC2* Putative dipeptide transport system permease ABC transporter
SMc01561	C			1.08				Hypothetical protein
SMc01562	A		1.01					Conserved hypothetical protein
SMc01563	D			2.35	1.26			*rpoD* sigA RNA polymerase sigma factor transcription regulation protein
SMc01568	A				-1.05			Conserved hypothetical protein
SMc01569	D			1.48	1.59			*carA* Probable carbamoyl-phosphate synthetase, glutamine-hydrolyzing protein
SMc01578	D			2.42	2.82			*aatA* Aspartate aminotransferase A (transaminase)
SMc01579	A				1.12			Conserved hypothetical protein
SMc01582	D			-1.56	-1.93			Putative alcohol dehydrogenase
SMc01585	A				-1.09			*cspA* Putative cold shock transcription regulator
SMc01588	D			-2.70	-2.50			Putative aldehyde dehydrogenase
SMc01591	A				-1.15			Hypothetical transmembrane protein
SMc01594	D			-4.66	-4.27			Putative glutamine synthetase
SMc01597	D			-4.96	-5.12			Putative amino-acid permease
SMc01600	D			-1.92	-2.36			Conserved hypothetical protein
SMc01602	D			-1.64	-1.94			Conserved hypothetical protein
SMc01605	D			-2.77	-1.85			Putative periplasmic binding ABC transporte

SMc01606	D			-1.98	-1.91			Transport system permease
SMc01607	D			-1.25	-1.35			Transport system permease
SMc01609	D			1.71	1.90			*ribH2* Putative 6,7-dimethyl-8-ribityllumazine synthase
SMc01611	D			1.55	1.68			*fhuA1* Putative ferrichrome-iron receptor precursor protein
SMc01613	D			-3.09	-2.85			*rpiB* Putative ribose 5-phosphate isomerase B
SMc01614	D			-1.15	-1.01			*tpiA2* Triosephosphate isomerase
SMc01619	C			-1.01				Putative class II aldolase/adducin family protein
SMc01625	D			-1.51	-1.56			Putative polyol ABC transporter, ATP-binding component
SMc01632	D			-1.82	-1.36			Substrate-binding periplasmic protein precursor
SMc01642	D			-1.17	-1.71			*prbA* ABC transporter, periplasmic solute-binding protein, mediates the uptake of proline betaine at both high and low osmolarities
SMc01649	A				-1.20			Hypothetical protein
SMc01652	A				-1.15			Putative putrescine and agmatine ABC transporter, periplasmic solute-binding component
SMc01653	A				-1.23			Putative putrescine and agmatine ABC transporter, ATP-binding component
SMc01656	D			-1.23	-1.14			Putative aldehyde dehydrogenase
SMc01657	C			1.07				*fhuA2* Putative ferrichrome-iron receptor precursor protein
SMc01658	G			1.28	1.46	2.03		Putative ferric iron reductase
SMc01659	G			1.85	1.79	2.60		Putative ABC transporter, periplasmic component
SMc01671	A				1.01			*puuC* Putative gamma-glutamyl-gamma-aminobutyraldehyde dehydrogenase
SMc01700	D			1.93	2.23			*ppiA* Putative peptidyl-prolyl cis-trans isomerase A signal peptide protein
SMc01709	C			1.04				Hypothetical signal peptide protein
SMc01710	D			1.32	1.04			Hypothetical protein
SMc01712	C			1.05				*lldD2* Putative L-lactate dehydrogenase (cytochrome) protein
SMc01719	A				-1.30			*mcpT* Probable chemoreceptor (methyl-accepting chemotaxis) transmembrane protein

SMc01720	A				1.38			*rnpA* Probable ribonuclease P protein component (protein C5)
SMc01721	D			2.30	2.82			*oxaA* Putative inner-membrane transmembrane protein
SMc01726	A				1.23			*argB* Probable acetylglutamate kinase (NAG kinase)
SMc01747	G			1.29	1.22	2.23		Hypothetical protein
SMc01763	D			1.86	1.70			Hypothetical transmembrane protein
SMc01764	D			-1.06	-1.15			ate Putative arginyl-tRNA--protein transferase
SMc01770	D			2.07	2.05			*glyA1* Probable serine hydroxymethyltransferase
SMc01771	D			2.01	1.63			nrdR Putative transcriptional repressor
SMc01772	D			2.26	2.04			*ribD* Probable riboflavin biosynthesis protein (deaminase/reductase)
SMc01781	D			1.83	1.88			Hypothetical transmembrane protein
SMc01782	A				1.78			Hypothetical protein
SMc01784	A				1.13			*plsX* Putative fatty acid/phospholipid synthesis protein
SMc01785	D			1.19	1.37			*fabH* Probable 3-oxoacyl-acyl-carrier-protein synthase III
SMc01788	C			-1.35				Hypothetical protein
SMc01798	C			1.33				Conserved hypothetical protein
SMc01799	C			1.16				Conserved hypothetical signal peptide protein
SMc01803	D			4.65	3.50			*rpsI* Probable 30S ribosomal protein S9
SMc01804	D			4.71	4.48			*rplM* Probable 50S ribosomal protein L13
SMc01806	A				1.09			Putative enoyl CoA hydratase
SMc01814	D			-3.63	-3.99			Probable glutamate synthase small chain
SMc01815	D			-3.91	-4.48			Dihydropyrimidine dehydrogenase family protein
SMc01818	C			1.20				*cyaC* Putative adenylate cyclase transmembrane protein
SMc01819	A				-1.08			Transcription regulator TetR family
SMc01820	D			-1.67	-3.26			Putative N-carbamyl-L-amino acid amidohydrolase
SMc01823	D			-1.66	-1.56			Putative uracil and uridine ABC transporter, ATP-binding component

SMc01827	D			-2.09	-2.21			Putative uracil and uridine ABC transporter, periplasmic solute-binding protein
SMc01828	A				-1.04			Multidrug resistance protein
SMc01834	D			1.62	1.15			Conserved hypothetical protein
SMc01842	C	-1.00		1.20				Probable transcriptional regulator
SMc01847	D			1.28	1.79			*btaB* S-adenosylmethionine : diacylgycerolhomoserine-N-methyltransferase
SMc01848	D			1.90	2.49			*btaA* Protein required for diacylglyceryl-N,N,N-trimethylhomoserine biosynthesis
SMc01862	A				-1.31			murF ProbableUDP-N-acetylmuramoylalanyl-D-glutamyl-2, 6-diaminopimelate--D-alanyl-D-alanyl ligase
SMc01869	D			1.70	1.22			Probable MFS permease
SMc01877	C			1.30				*recN* Probable DNA repair protein
SMc01878	A				1.08			*ligA* Probable DNA ligase
SMc01880	C			1.08				*panC* Probable pantoate--beta-alanine ligase
SMc01882	D			1.42	1.75			Conserved hypothetical protein, inner membrane protein
SMc01905	D			1.34	1.09			*lon* Probable ATP-dependent protease LA protein
SMc01906	D			1.68	1.37			*hupB* DNA-binding protein HU
SMc01907	A				1.05			Hypothetical transmembrane protein
SMc01911	D			1.44	1.71			Conserved hypothetical protein
SMc01912	D			3.58	2.98			*nuoA1* NADH dehydrogenase I chain A
SMc01913	D			1.70	1.28			*nuoB1* NADH-ubiqionone oxidoreductase subunit K transmembrane protein
SMc01914	D			2.00	2.20			*nuoC1* NADH dehydrogenase I chain C
SMc01915	D			1.39	1.31			*nuoD1* Probable NADH-quinone oxidoreductase subunit D 1
SMc01916	C			1.34				Hypothetical signal peptide protein
SMc01917	F			1.21		-1.13		*nuoE1* NADH dehydrogenase I chain E
SMc01919	D			1.79	1.23			Hypothetical transmembrane protein
SMc01920	D			1.73	1.98			*nuoG1* Probable NADH dehydrogenase I chain G
SMc01922	D			2.40	2.12			*nuoI* Probable NADH-ubiquinone

								oxidoreductase chain I
SMc01923	D			1.91	1.34			*nuoJ* Probable NADH dehydrogenase I chain J transmembrane protein
SMc01924	D			2.05	2.21			*nuoK1* Probable NADH dehydrogenase I chain K transmembrane protein
SMc01925	D			2.77	2.94			*nuoL* Probable NADH dehydrogenase I chain L transmembrane protein
SMc01926	D			1.93	2.65			*nuoM* Probable NADH dehydrogenase I chain M transmembrane protein
SMc01927	C			1.09				*nuoN* Probable NADH dehydrogenase I chain N transmembrane protein
SMc01934	D			1.04	1.34			*proS* Probable prolyl-tRNA synthetase
SMc01942	D			1.21	1.25			*ureD* Probable urease accessory protein
SMc01943	D			1.34	1.57			D-isomer specific 2-hydroxyacid dehydrogenase family protein
SMc01944	A				1.11			*cpo* Non-heme chloroperoxidase F (Chloride peroxidase, CPO-F)
SMc01953	D			-2.76	-2.64			Putative 2-component receiver domain protein
SMc01964	A				-1.40			Putative spermidine/putrescine transport system permease ABC transporter
SMc01965	A				-1.04			Spermidine/putrescine ABC transporter ATP-binding subunit
SMc01966	D			-3.58	-3.68			Putative spermidine/putrescine-binding periplasmic ABC transporter
SMc01967	D			-4.38	-4.33			*speB2* Putative agmatinase
SMc01968	D			-1.34	-1.82			Transcription regulator LysR family
SMc01976	D			-1.08	-1.10			Putative cystathionine gamma-synthase, trans-sulfuration enzyme family protein
SMc01977	D			-1.69	-1.90			Sugar-binding periplasmic protein precursor
SMc01978	D			-3.17	-3.46			Putative sugar transport system permease ABC transporter
SMc01979	D			-1.89	-2.07			Sugar transport system permease
SMc02025	A				1.38			Periplasmic dipeptide transport protein precursor
SMc02047	A				-1.17			*gcvT* Probable aminomethyltransferase (glycine cleavage system T protein)
SMc02048	D			-1.58	-1.43			*gcvH* Probable glycine cleavage system H
SMc02049	D			-1.28	-1.29			*gcvP* Probable glycine dehydrogenase

								decarboxylating protein
SMc02050	D			4.06	4.25			tig Probable trigger factor
SMc02052	D			2.05	1.55			Conserved hypothetical protein
SMc02053	C			1.20				*trmFO* Methylenetetrahydrofolate--tRNA-(uracil-5-)-methyltransferase
SMc02057	C			1.35				*secD1* Putative protein-export membrane protein
SMc02058	C			1.03				Probable YajC protein
SMc02060	A				-1.16			*lppB* Lipoprotein precursor
SMc02061	A				1.55			*bioS* Biotin-regulated protein
SMc02072	A				-1.56			Hypothetical transmembrane protein
SMc02073	D			1.12	1.30			*argS* Probable arginyl-tRNA synthetase (arginine--tRNA ligase)
SMc02084	G			1.48	1.60	1.16		*exbD* Probable biopolymer transport transmembrane protein
SMc02085	G			1.82	1.59	1.55		*exbB* Probable biopolymer transport transmembrane protein
SMc02092	A				1.09			*fabZ* Probable 3R-hydroxymyristoyl-acyl carrier protein dehydratase
SMc02093	D			1.47	1.79			*lpxD* Probable UDP-3-O-3-hydroxymyristoyl glucosamine N-acyltransferase
SMc02094	A				1.42			omp Putative outer membrane transmembrane protein
SMc02100	D			1.91	2.45			*tsf* Probable elongation factor TS (EF-TS) protein
SMc02101	D			4.60	2.73			*rpsB* Probable 30S ribosomal protein S2
SMc02111	D			-1.72	-2.12			Conserved hypothetical protein
SMc02114	C			1.04				Putative hydrolase
SMc02118	D			-1.52	-1.65			*aapJ* Probable general L-amino acid-binding periplasmic ABC transporter
SMc02119	D			-1.10	-1.67			*aapQ* Probable general L-amino acid transport permease ABC transporter
SMc02120	D			-1.50	-1.77			*aapM* Probable general L-amino acid transport permease ABC transporter
SMc02121	D			-1.61	-1.35			*aapP* Probable general L-amino acid transport ATP-binding ABC transporter
SMc02122	C			1.07				*fpr* Probable ferredoxin--NADP reductase

SMc02123	D			1.98	2.07			Sulfate or sulfite assimilation protein
SMc02124	D	1.35		4.26	4.22			*cysI* Putative sulfite reductase
SMc02136	C			1.01				*hslO* 33 kDa chaperonin, Hsp33 protein
SMc02137	D			2.29	1.75			*argF1* Probable ornithine carbamoyltransferase
SMc02141	C			1.62				*phoU* Probable phosphate transport system transcriptional regulator
SMc02142	A				1.47			*pstB* Probable phosphate import ATP-binding ABC transporter
SMc02143	D			1.50	1.93			*pstA* Putative phosphate transport system permease ABC transporter
SMc02144	A				1.27			Truncated 'pstC
SMc02146	D			3.34	2.99			*pstS* Phosphate binding periplasmic protein
SMc02153	D			1.06	1.01			Conserved hypothetical protein
SMc02154	D			1.57	1.20			Hypothetical protein
SMc02156	D			-1.03	-1.88			Conserved hypothetical protein
SMc02157	A				-1.21			*cdsA2* Putative phosphatidate cytidylyltransferase transmembrane protein
SMc02163	D			1.35	1.46			*pgi* Probable glucose-6-phosphate isomerase
SMc02164	C			1.19				*frk* Probable fructokinase
SMc02165	C			1.07				*pyrE* Probable orotate phosphoribosyltransferase
SMc02166	C			1.34				*pyrC* Probable dihydroorotase
SMc02169	A				1.15			*frcA* Putative fructose ABC-type transport system, ATPase component
SMc02177	A				-1.03			Hypothetical protein
SMc02178	D			-1.44	-1.69			Hypothetical protein
SMc02217	D			2.06	1.15			*metZ* Probable O-succinylhomoserine sulfhydrylase
SMc02218	C			1.10				Putative deoxycytidine triphosphate deaminase
SMc02221	A				1.29			Conserved hypothetical protein
SMc02223	B					-1.07		Transcriptional regulator
SMc02227	D			-1.37	-1.58			*fadB* Putative fatty oxidation complex alpha subunit includes: enoyl-CoA hydratase, 3-hydroxyacyl-CoA dehydrogenase, 3-

								hydroxybutyryl-CoA epimerase transmembrane protein
SMc02229	B					-1.60		Putative acyl-CoA dehydrogenase
SMc02235	C			1.23				Conserved hypothetical protein
SMc02236	C			1.14				Conserved hypothetical protein
SMc02240	D			-3.34	-3.91			Hypothetical transmembrane protein
SMc02244	C			1.18				*dinF* Putative transmembrane protein
SMc02251	D			1.96	1.47			Aspartate aminotransferase
SMc02254	A				-1.60			*qxtB* Putative quinol oxidase subunit II transmembrane protein
SMc02255	A				-1.20			*qxtA* Putative quinol oxidase subunit I transmembrane protein
SMc02259	D			-1.57	-2.80			Putative periplasmic binding ABC transporter
SMc02264	D			1.29	1.09			Hypothetical transmembrane protein
SMc02265	D			1.86	1.12			*secD2* Putative protein-export membrane protein
SMc02266	D			2.23	1.27			Conserved hypothetical protein
SMc02273	C			1.05				*rkpA* wcbR Putative fatty acid synthase
SMc02291	D			1.35	1.05			Insertion sequence ISRm2011-2
SMc02305	D			1.51	2.04			*murA* Probable UDP-N-acetylglucosamine 1-carboxyvinyltransferase
SMc02312	A				1.05			Conserved hypothetical protein
SMc02325	A				-1.76			*rhaT* ATP-binding component of rhamnose transport system
SMc02337	A				-1.08			*rnhA2* Probable ribonuclease HI protein
SMc02339	A				-1.56			Putative oxidoreductase
SMc02340	D			-1.14	-1.32			Transcription regulator GntR family
SMc02345	D			1.35	1.61			Putative glycine-betaine and choline ABC transporter, permease component
SMc02347	C	1.19						*asfB* Putative ferredoxin AsfB iron-sulfur protein
SMc02349	C	1.64		2.48				*asfA* Oxidoreductase
SMc02350	D			1.16	1.47			Conserved hypothetical protein
SMc02351	A				1.07			Conserved hypothetical protein

SMc02352	C			-1.04				Putative glutamine synthetase
SMc02353	A				-1.34			Conserved hypothetical protein
SMc02356	D			-2.02	-1.91			Putative branched chain amino acid binding periplasmic ABC transporter
SMc02357	D			-1.34	-1.71			Putative high-affinity branched-chain amino acid transport ATP-binding ABC transporter
SMc02359	A				-1.59			Putative high-affinity branched-chain amino acid transport permease ABC transporter
SMc02361	C			1.34				*cycH* Cytochrome C-type biogenesis transmembrane protein
SMc02366	C			1.22				*ragA* Probable response regulator
SMc02378	D			-1.42	-2.27			Putative glycine betaine ABC transporter, periplasmic substrate-binding component
SMc02392	A				-1.08			Hypothetical protein
SMc02398	C			1.06				Insertion sequence ISRm2011-2
SMc02404	D			2.75	1.93			*dapA1* Putative dihydrodipicolinate synthase
SMc02408	D			2.00	1.87			*rpoZ* DNA-directed RNA polymerase omega subunit
SMc02412	C			-2.02				Conserved hypothetical protein
SMc02417	C			-1.28				Putative allantoin and other purine derivative ABC transporter, periplasmic solute-binding component
SMc02434	D			1.58	1.62			Hypothetical protein
SMc02435	D			1.38	1.43			*hemK1* Putative methyltransferase
SMc02438	D			2.68	2.77			*lysC* Probable aspartokinase
SMc02440	C			1.11				*ubiG* Putative 3-demethylubiquinone-9 3-methyltransferase
SMc02443	D			1.62	1.33			*grxC* Probable glutaredoxin 3 protein
SMc02451	D			1.12	1.57			Conserved hypothetical protein, contains a peptidyl-prolyl cis-trans isomerase signature
SMc02463	D			1.07	1.57			*sdhC* Probable succinate dehydrogenase cytochrome B-556 subunit transmembrane protein
SMc02464	C			1.04				*sdhD* Probable succinate dehydrogenase membrane anchor subunit
SMc02466	D			1.28	1.07			*sdhB* Probable succinate dehydrogenase iron-sulfur protein

SMc02479	D			2.87	3.50			*mdh* Probable malate dehydrogenase
SMc02480	D			3.24	4.11			*sucC* Probable succinyl-CoA synthetase beta chain
SMc02481	D			2.37	3.10			*sucD* Probable succinyl-CoA synthetase alpha chain
SMc02482	D			2.48	2.60			*sucA* Probable 2-oxoglutarate dehydrogenase E1 component protein
SMc02483	D			1.74	2.14			*sucB* Probable dihydrolipoamide succinyl transferase component of 2-oxoglutarate dehydrogenase complex (E2) protein
SMc02484	D			1.01	1.08			Amino acid efflux protein
SMc02486	A				1.13			Putative oxidoreductase
SMc02487	A				1.23			*lpdA2* Probable dihydrolipoamide dehydrogenase (E3 component of 2-oxoglutarate dehydrogenase complex) transmembrane protein
SMc02498	D			3.84	3.84			*atpH* Putative ATP synthase delta chain
SMc02499	D			4.31	4.24			*atpA* Probable ATP synthase subunit alpha
SMc02500	D			3.79	3.49			*atpG* Probable ATP synthase gamma chain
SMc02501	D			3.66	4.24			*atpD* Probable ATP synthase beta chain
SMc02502	D			2.10	2.67			*atpC* Probable ATP synthase epsilon chain
SMc02503	A				-1.33			Conserved hypothetical protein
SMc02514	A				-1.16			Putative glycerol-3-phosphate and glycerol ABC transporter, periplasmic solute-binding component
SMc02521	C			-1.08				*glpR* Glycerol-3-phosphate regulon repressor
SMc02522	A				-1.24			Short-chain type dehydrogenase/reductase
SMc02545	D			1.08	1.07			Hypothetical transmembrane protein
SMc02546	A				-1.18			*leuA2* Putative 2-isopropylmalate synthase
SMc02551	A				1.02			*cysS* Probable cysteinyl-tRNA synthetase
SMc02552	B					-1.61		Hypothetical unknown protein
SMc02557	C			1.03				Hypothetical protein
SMc02562	D			2.32	2.62			*pckA* Phosphoenolpyruvate carboxykinase
SMc02567	A				1.22			*coaA* Probable pantothenate kinase

SMc02574	D			1.36	1.45			*hisB* Probable imidazoleglycerol-phosphate dehydratase
SMc02575	A				1.08			*hslV* Probable heat shock protein
SMc02577	C			1.28				*hslU* Probable heat shock protein
SMc02580	D			2.15	2.39			Putative hydantoinase/oxoprolinase family protein
SMc02582	C			1.39				Conserved hypothetical protein
SMc02588	A				-1.43			Putative permease ABC transporter
SMc02598	D			1.02	1.29			*nadC* Probable nicotinate-nucleotide pyrophosphorylase carboxylating protein
SMc02605	D			-2.21	-2.32			*soxG* Putative sarcosine oxidase gamma subunit
SMc02606	C			-2.42				*soxA1* Putative sarcosine oxidase alpha subunit transmembrane protein
SMc02607	D			-2.94	-3.23			*soxD* Sarcosine oxidase delta subunit
SMc02608	A				-1.14			*soxB* Sarcosine oxidase beta subunit
SMc02610	D			-1.76	-2.12			*glxB* Putative glutamine amidotransferase
SMc02611	D			-1.13	-1.69			*glxC* Putative glutamate synthase alpha subunit, C-termial domain
SMc02612	C			-1.65				*glxD* Putative glutamate synthase, central-C domain
SMc02613	D			-1.65	-1.35			*glnT* Glutamine synthetase III
SMc02618	A				-1.06			Conserved hypothetical transmembrane protein
SMc02634	D			2.46	2.99			Monomeric alkaline phosphatase
SMc02636	D			1.56	1.50			Conserved hypothetical protein
SMc02637	D			1.12	1.29			Hypothetical protein
SMc02645	A				-1.46			*cfa2* Cyclopropane-fatty-acyl synthase
SMc02648	C			1.01				aqpS aquaglyceroporin
SMc02649	C			1.06				*arsC* Arsenate reductase
SMc02652	A				1.01			*rnc* Probable ribonuclease III
SMc02655	C			1.14				Hypothetical transmembrane protein
SMc02678	D			1.02	1.22			Hypothetical protein
SMc02681	D			1.11	1.85			*lgt* Probable prolipoprotein diacylglyceryl transferase

SMc02682	A				1.01			Conserved hypothetical protein
SMc02683	A				1.01			Conserved hypothetical protein
SMc02684	D			1.08	1.21			Hydrolase/peptidase
SMc02686	D			2.35	1.91			*prs* Probable ribose-phosphate pyrophosphokinase
SMc02692	D			4.10	4.16			*rplY* Putative 50S ribosomal protein L25
SMc02693	D			1.43	1.52			*pth* Probable peptidyl-tRNA hydrolase
SMc02695	A				1.98			*engD* Putative GTP-dependent nucleic acid-binding protein EngD
SMc02696	C			1.21				Conserved hypothetical protein
SMc02705	D			4.12	4.44			Hypothetical transmembrane protein
SMc02707	C			1.05				Putative acetyltransferase
SMc02717	D			1.34	1.40			*leuA*1 2-isopropylmalate synthase
SMc02718	D			1.16	1.57			Hypothetical/unknown protein
SMc02723	C			1.34				*queF* probable NADPH-dependent 7-cyano-7-deazaguanine reductase
SMc02726	G			2.02	1.34	2.84		*shmR* Hemin-binding outer membrane receptor
SMc02730	D			1.30	1.26			Conserved hypothetical protein
SMc02732	D			1.31	1.46			Conserved hypothetical protein
SMc02753	A				1.01			Putative IIA component of PTS system
SMc02754	D			1.51	1.77			Putative phosphocarrier HPR transmembrane protein
SMc02755	D			2.80	2.88			*ahcY* Probable adenosylhomocysteinase
SMc02758	D			1.50	1.25			Putative nucleotidyl transferase
SMc02761	D			1.34	1.27			*trxA* Probable thioredoxin protein
SMc02763	A				1.10			*folC* Probable FolC bifunctional protein includes: folylpolyglutamate synthase and dihydrofolate synthase
SMc02764	D			1.77	1.97			*accD* Probable acetyl-coenzyme A carboxylase carboxyl transferase subunit beta protein
SMc02765	A				1.06			*trpA* Probable tryptophan synthase alpha chain
SMc02767	D			1.36	1.96			*trpF* Probable N-5'-phosphoribosylanthranilate isomerase

SMc02769	A				1.29			Conserved hypothetical transmembrane protein
SMc02770	D			-1.05	-1.24			Putative intracellular PHB depolymerase
SMc02773	A				-1.11			Putative D-fucose, pyruvic acid or L-fucose ABC transporter, ATP-binding component
SMc02788	D			2.02	2.11			*secB* Probable protein-export
SMc02796	D			1.67	1.89			*rho* Probable transcription termination factor Rho protein
SMc02804	D			1.76	1.11			*leuS* Probable leucyl-tRNA synthetase
SMc02820	C			1.01				*cpaF1* Putative pilus assembly protein
SMc02822	C			1.03				Hypothetical transmembrane protein
SMc02830	D			1.02	1.63			Putative taurine, valine, isoleucine and leucine ABC transporter, permease component
SMc02835	A				1.24			*glk* Probable glucokinase transmembrane protein
SMc02836	A				1.25			ABC transporter, ATP-binding and permease components
SMc02846	D			2.18	1.57			Putative sugar kinase
SMc02847	D			2.13	1.80			Hypothetical protein
SMc02857	D			2.16	1.99			*dnaK* Heat shock protein 70 (HSP70) chaperone
SMc02858	B					1.77		*dnaJ* Probable chaperone protein
SMc02862	A				1.07			Putative pit accessory protein
SMc02863	A				1.26			*recF* DNA repair protein
SMc02864	C			1.19				*moeB* Probable Molybdopterin biosynthesis protein
SMc02867	A				1.61			Putative multidrug-efflux system transmembrane protein
SMc02868	D			1.48	1.56			Putative multidrug efflux system
SMc02871	A				-1.68			Putative ABC transporter
SMc02873	D			-1.44	-1.89			Probable ABC transporter
SMc02878	C			1.02				*nagA* Probable N-acetylglucosamine-6-phosphate deacetylase
SMc02887	B					1.01		Hypothetical protein
SMc02888	D			1.42	1.47			Putative transcription regulator
SMc02890	A				2.59			Probable outer membrane receptor

SMc02893	A				1.24			Probable transcriptional regulator
SMc02894	D			1.34	1.14			Hypothetical protein
SMc02895	D			1.14	2.02			Conserved hypothetical transmembrane protein
SMc02897	D			2.28	2.43			Putative cytochrome C transmembrane protein
SMc02898	D			1.97	2.39			*kdsB* Probable 3-deoxy-manno-octulosonate cytidylyltransferase (CMP-KDO synthetase)
SMc02899	D			1.31	1.42			*pheA* Putative prephenate dehydratase
SMc02900	D			4.42	3.67			Conserved hypothetical protein
SMc02901	C			1.02				Hypothetical protein
SMc02904	D			1.34	1.19			Hypothetical protein
SMc02905	D			1.19	1.15			*dnaX* Putative DNA polymerase III subunit TAU protein
SMc02909	D			2.66	2.72			*mltB1* Membrane-bound lytic murein transglycosylase B
SMc02910	D			1.70	1.83			Probable MFS permease
SMc02911	D			2.13	3.20			Conserved hypothetical protein
SMc02912	D			1.51	2.09			*nusA* Probable N utilization substance protein A
SMc02913	A				1.06			Hypothetical protein
SMc02914	D			2.00	1.97			*infB* Probable translation initiation factor IF-2 protein
SMc02941	A				1.01			Conserved hypothetical transmembrane protein, signal peptide
SMc02978	D			1.26	1.64			Conserved hypothetical protein
SMc02983	C			1.32				Putative ornithine, DAP, or arginine decarboxylase
SMc03004	C			1.43				*icpA* mcpE IcpA/McpE internal chemotaxis protein
SMc03007	D			1.58	1.02			*cheA* Chemotaxis protein (sensory transduction histidine kinase)
SMc03009	C			1.23				*cheR* Chemotaxis protein methyltransferase
SMc03010	C			1.02				*cheB1*Chemotaxis response regulator protein-glutamate methylesterase
SMc03013	C			1.04				Conserved hypothetical protein
SMc03014	D			2.20	3.18			*fliF* Flagellar M-ring transmembrane protein

SMc03015	A				1.01			*visN* Transcriptional regulator of motility genes, LuxR family
SMc03017	D			1.91	2.04			Conserved hypothetical protein
SMc03019	A				1.06			*fliG* Flagellar motor switch protein
SMc03021	D			1.23	2.09			*fliM* Flagellar motor switch transmembrane protein
SMc03022	A				1.14			*motA* Chemotaxis (motility protein A) transmembrane
SMc03023	D			1.56	1.98			Conserved hypothetical protein
SMc03024	D			2.05	1.99			*flgF* Flagellar basal-body rod protein
SMc03027	D			2.67	3.37			*flgB* Flagellar basal-body rod protein
SMc03028	D			1.05	2.33			*flgC* Flagellar basal-body rod protein
SMc03029	D			1.66	2.16			*fliE* Flagellar hook-basal body complex protein
SMc03030	D			1.14	2.99			*flgG* Flagellar basal-body rod protein
SMc03031	A				1.32			*flgA* Flagellar precursor transmembrane protein
SMc03032	A				1.71			*flgI* Flagellar P-ring precursor transmembrane protein
SMc03033	D			1.26	1.66			*motE* MotE chaperone specific for MotC folding and stability
SMc03034	A				1.63			*flgH* Flagellar L-ring protein precursor (basal body L-ring protein)
SMc03035	D			1.26	1.75			*fliL* Flagellar transmembrane protein
SMc03039	A				1.13			*flaD* Flagellin D
SMc03040	D			1.17	1.43			*flaC* Flagellin C
SMc03042	A				1.01			*motB* Chemotaxis (motility protein B) transmembrane
SMc03043	A				1.10			*motC* Chemotaxis precursor (motility protein C) transmembrane
SMc03044	C			1.31				*fliK* FliK hook length control protein
SMc03045	D			1.47	1.49			Conserved hypothetical protein, signal peptide
SMc03046	A				1.61			rem Response regulator of exponential growth motility
SMc03047	C			1.62				*flgE* Flagellar hook protein
SMc03048	D			1.34	1.32			*flgK* Putative flagellar hook-associated protein

SMc03049	D			1.59	2.25			*flgL* Putative flagellar hook-associated protein
SMc03050	D			1.82	2.04			*flaF* Putative flagellin synthesis regulator
SMc03051	A				2.19			*flbT* Putative flagellin synthesis repressor protein
SMc03052	D			1.64	2.12			*flgD* Putative basal-body rod modification protein
SMc03057	D			2.06	2.96			Conserved hypothetical transmembrane protein
SMc03063	C	1.04						*aglG* Alpha-glucosides ABC transporter, permease component
SMc03068	A				-1.11			*edd* Phosphogluconate dehydratase
SMc03071	D			1.22	2.10			Hypothetical protein
SMc03072	C			1.47				Conserved hypothetical protein
SMc03088	C			1.13				Transposase for insertion sequence element ISRm11/ISRm2011-2
SMc03090	A				-1.18			*cheW3* Putative chemotaxis protein
SMc03091	A				-1.47			*argI1* Probable arginase
SMc03107	A				-1.09			Conserved hypothetical protein
SMc03110	D			1.15	1.33			Conserved hypothetical protein
SMc03124	D			1.24	1.72			Putative arginine ABC transporter, periplasmic solute-binding component
SMc03130	D			1.29	1.69			Conserved hypothetical protein
SMc03131	B						1.59	Putative DL-2-aminoadipic acid ABC transporter, periplasmic solute-binding component
SMc03132	E				1.61	1.63		Oxidoreductase
SMc03138	A				-1.26			Sugar kinase
SMc03151	C			1.71				Conserved hypothetical protein
SMc03152	C			1.37				Hypothetical transmembrane protein
SMc03157	D			2.56	2.86			*metQ* Probable D-methionine-binding lipoprotein MetQ
SMc03158	D	1.05		1.97	2.31			*metI* Probable D-methionine transport system permease protein MetI
SMc03163	A				1.08			*xylA* Probable xylose isomerase
SMc03167	F	1.09				1.27		MFS-type transport protein

SMc03168	C			-1.45				Multidrug resistance efflux system
SMc03172	A				1.75			*gltX* Glutamyl-tRNA synthetase
SMc03175	C			1.34				Inosine-uridine preferring nucleoside hydrolase family protein
SMc03207	D			-1.28	-1.33			Conserved hypothetical protein
SMc03208	D			-3.08	-2.26			*hmgA* Homogentisate 1,2-dioxygenase
SMc03209	D			-1.46	-1.76			Putative transcription regulator
SMc03211	D			-1.56	-2.02			Putative 4-hydroxyphenylpyruvate dioxygenase
SMc03227	A				1.49			Conserved hypothetical protein
SMc03238	D			1.91	1.83			Hypothetical transmembrane protein
SMc03239	D			2.85	3.15			ppa Probable inorganic pyrophosphatase
SMc03242	D			1.43	2.41			*typA* Predicted membrane GTPase
SMc03253	C	1.16						L-proline cis-4-hydroxylase
SMc03267	C			1.29				Putative dipeptidase
SMc03286	A				-1.07			Serine protease
SMc03313	C			1.48				Insertion sequence ISRm2011-2
SMc03770	D			2.36	1.95			*rplU* Probable 50S ribosomal protein L21
SMc03772	D			2.74	2.71			*rpmA* Probable 50S ribosomal protein L27
SMc03773	D			2.83	1.99			Putative acetyltransferase
SMc03787	E		-1.16			1.17		Conserved hypothetical protein
SMc03790	A				-1.20			Conserved hypothetical protein
SMc03795	A				1.40			*leuD* Probable 3-isopropylmalate dehydratase small subunit
SMc03797	C			1.02				*metA* Probable homoserine O-succinyltransferase
SMc03799	D			-1.38	-2.87			Conserved hypothetical protein
SMc03800	A				-1.13			Hypothetical protein
SMc03802	A				1.09			Putative peptidase
SMc03806	D			-1.86	-1.48			*glnK* Probable nitrogen regulatory protein PII 2
SMc03807	D			-1.11	-1.30			*amtB* Probable ammonium transporter

SMc03815	A				-1.01			Putative ATP binding ABC transporter
SMc03823	C			1.11				*leuC* Probable 3-isopropylmalate dehydratase large subunit
SMc03826	D			2.60	2.76			*argG* Probable argininosuccinate synthase
SMc03828	D			1.44	1.15			Putative ATP-binding ABC transporter
SMc03829	D			1.74	1.60			Putative transport system permease ABC transporter
SMc03830	D			2.27	1.85			Conserved hypothetical protein
SMc03846	C			1.92				*acnA* Probable aconitate hydratase
SMc03850	C			1.02				*ccmD* Putative heme exporter D (cytochrome C-type biogenesis protein) transmembrane
SMc03854	A				1.06			*ftsY* Putative cell division protein
SMc03858	D			3.17	3.76			*pheA* a Putative chorismate mutase
SMc03859	D			2.50	2.98			*rpsP* Probable 30S ribosomal protein S16
SMc03861	D			1.18	2.08			*trmD* Probable tRNA guanine-N1-methyltransferase
SMc03863	D			3.04	2.58			*rplS* Probable 50S ribosomal protein L19
SMc03864	D			1.33	1.36			Putative amino acid-binding periplasmic (signal peptide) ABC transporter
SMc03866	D			1.11	1.34			Putative ATP-binding ABC transporter
SMc03867	A				1.08			Conserved hypothetical protein
SMc03875	A				1.50			Putative ferredoxin protein
SMc03877	D			2.01	2.39			Putative ATP-dependent RNA helicase
SMc03878	A				-1.08			*phbB* Acetoacetyl-CoA reductase
SMc03879	A				-1.17			*phbA* Acetyl-CoA acetyltransferase
SMc03881	D			2.39	2.11			*rpmF* Probable 50S ribosomal protein L32
SMc03882	D			1.07	1.04			*gst8* Putative glutathione S-transferase
SMc03887	C			1.07				Amino acid efflux protein
SMc03891	D			1.56	1.29			Putative amino acid-binding periplasmic ABC transporter
SMc03892	C			1.66				Putative transposase
SMc03900	D			1.90	1.25			*ndvA* Beta-1-->2glucan export ATP-binding protein

SMc03933	D			1.40	2.29			*soxB2* Putative sarcosine oxidase subunit B
SMc03934	D			1.86	1.47			*rpsU2* Probable 30S ribosomal protein
SMc03936	C			-1.05				Conserved hypothetical signal peptide protein
SMc03937	A				-1.11			*cyaG1* Putative adenylate/guanylate cyclase
SMc03969	D			1.11	1.31			Conserved hypothetical protein
SMc03978	D			2.41	2.04			*tkt2* Probable transketolase
SMc03979	D			1.51	1.28			*gap* Probable glyceraldehyde 3-phosphate dehydrogenase
SMc03981	A				1.08			*pgk* Probable phosphoglycerate kinase
SMc03999	A				-1.01			Hypothetical protein
SMc04003	D			1.13	1.27			*rpmJ* Probable 50S ribosomal protein L36
SMc04009	D			1.93	2.19			Conserved hypothetical protein
SMc04011	D			-1.13	-1.32			*tacA* Putative sigma-54-dependent transcription regulator
SMc04012	D			1.21	1.25			*pepF* Putative oligoendopeptidase F
SMc04023	A				-1.12			e*xoN2* Probable UTP--glucose-1-phosphate uridylyltransferase
SMc04024	A				-1.06			Membrane-bound lytic murein transglycosylase precursor
SMc04026	D			-1.73	-2.21			*gltD* Probable glutamate synthase small chain
SMc04029	A				1.30			Putative low specificity L-threonine aldolase
SMc04037	D			-1.05	-1.14			Putative amino acid or peptide ABC transporter, periplasmic solute-binding component
SMc04040	D			1.13	1.33			*ibpA* Probable heat shock protein
SMc04042	D			1.34	1.66			Inositol-1-monophosphatase family protein
SMc04047	D			-1.22	-1.47			*azu2* Probable pseudoazurin (blue copper protein)
SMc04048	D			-1.69	-2.67			Putative cytochrome C
SMc04049	D			-2.48	-3.46			Putative sulfite oxidase
SMc04051	C			1.02				*rpoE4* Putative RNA polymerase sigma-E factor (sigma-24) protein
SMc04059	D			1.55	1.05			Conserved hypothetical protein, signal peptide
SMc04083	A				1.15			*cynT* Putative carbonic anhydrase

SMc04113	A				-1.07			*cpaA1* Putative pilus assembly transmembrane protein
SMc04114	A				-1.04			*pilA1* Putative pilin subunit
SMc04118	A				-1.45			Conserved hypothetical transmembrane protein
SMc04147	D			-1.64	-1.60			Putative amino-acid permease
SMc04149	D			-1.14	-1.57			Flavin-containing monooxygenase family protein / FMO family protei
SMc04150	A				-1.01			Conserved hypothetical protein
SMc04153	D			-1.33	-2.47			Putative aminomethyltransferase
SMc04164	A				-1.39			Conserved hypothetical protein
SMc04165	A				-1.07			Oxidoreductase
SMc04172	D			-1.16	-1.00			*cyaH* Adenylate/guanylate cyclase
SMc04190	A				-1.10			Hypothetical protein signal peptide
SMc04194	A				-1.23			Putative transmembrane protein
SMc04207	A		1.28					*rspD* Rhizobiocin secretion protein
SMc04214	D			1.40	1.20			*cobU* Probablenicotinate-nucleotide--dimethylbenzimidazolephosphoribosyltransferase
SMc04217	C			1.11				Hypothetical transmembrane signal peptide protein
SMc04218	C			1.07				Probable ABC transporte
SMc04225	D			-1.39	-1.89			Hypothetical protein
SMc04234	D			2.05	2.04			*cspA4* Cold shock protein
SMc04237	A				-1.00			Hypothetical protein
SMc04243	D			-1.25	-1.42			*znuB* Probable high-affinity zinc uptake system membrane ABC transporter
SMc04244	D			-1.07	-2.55			*znuC* Probable high-affinity zinc uptake system ATP-binding ABC transporter
SMc04245	D			-1.05	-2.41			*znuA* Probable high-affinity zinc uptake system ABC transporter
SMc04246	D			-1.02	-2.53			Hypothetical transmembrane signal peptide protein
SMc04247	A				-2.06			Putative beta-xylosidase
SMc04255	D			-1.07	-1.06			*manB* Putative beta-mannosidase

SMc04256	D			-1.23	-2.09			Putative gentiobiose, salicin, and cellobiose ABC transporter, ATP-binding component
SMc04257	D			-1.01	-2.80			Putative gentiobiose, salicin, and cellobiose ABC transporter, permease component
SMc04258	D			-1.16	-2.90			Binding-protein-dependent transport systems inner membrane component
SMc04259	A				-2.66			Putative gentiobiose, salicin, and cellobiose ABC transporter, periplasmic solute-binding component
SMc04260	A				-1.46			Probable transcriptional regulator
SMc04262	C			1.39				*gnd* Probable 6-phosphogluconate dehydrogenase (decarboxylating) protein
SMc04273	A				1.16			Putative 3-oxoacyl-acyl-carrier-protein synthase
SMc04274	C			1.13				Conserved hypothetical protein
SMc04278	D			1.45	2.34			*acpXL* Acyl carrier protein, involved in the transfer of long hydroxylated fatty acids to lipid A
SMc04280	C			1.15				Hypothetical signal peptide protein
SMc04285	A				1.04			*cobE* Probable cobalamin biosynthesis protein
SMc04292	A				-1.56			*cyaF3* Probable adenylate/guanylate cyclase
SMc04317	D			1.67	1.95			ABC transporter, periplasmic solute-binding componen
SMc04318	C			1.27				*cspA1* Cold shock transcriptional regulator
SMc04320	D			1.66	1.31			*rpsU1* 30S ribosomal protein S21
SMc04325	C			1.60				*bmt* Betaine-homocysteine methyltransferase
SMc04341	D			-1.17	-1.27			Periplasmic substrate-binding protein
SMc04345	D			1.17	1.69			Hypothetical protein
SMc04346	C			1.54				*ilvC* Ketol-acid reductoisomerase
SMc04381	D			1.83	1.92			*opgC* Putative glucan succinyltransferase, may be involved in succinylation of cyclic-beta-1,2-glucans
SMc04405	D			1.14	1.63			*leuB* Probable 3-isopropylmalate dehydrogenase
SMc04409	D			1.00	1.67			Hypothetical protein
SMc04410	A				1.25			*asd* Putative aspartate-semialdehyde dehydrogenase

SMc04411	D			1.38	1.82			Membrane-bound lytic murein transglycosylase
SMc04429	A				1.73			Conserved hypothetical protein
SMc04434	D			3.10	3.86			*rpmH* Probable 50S ribosomal protein L34
SMc04437	A				1.00			Hypothetical protein
SMc04444	D			-1.18	-1.32			*fdsA* Probable NAD-dependent formate dehydrogenase alpha subunit
SMc04452	D			2.68	2.49			*ndh* Putative NADH dehydrogenase transmembrane protein
SMc04454	D			1.23	1.32			Putative ATP-binding ABC transporter
SMc04458	D			1.78	2.35			Probable preprotein translocase SecA subunit

Adittional file 1.2.

Swarming-responsive genes identified in *S. meliloti* 1021FDCS5

This tabular data list the 294 genes showing differential expression in response to swarming-specific conditions.

Only M values above 1 or below -1 with $p \leq 0.05$ are shown.

The category in the Venn diagram (A-G in Fig. 1.4) to which each gene belongs is also indicated.

L, growth in **l**iquid MM; **S**, growth on **s**olid MM (1.3% agar); **SS**, growth on **s**emi**s**olid MM (0.6% agar). Time of incubation is shown in parenthesis.

Gene ID	Category	M value				Description
		SS vs. L (7h)	SS vs. L (14h)	SS vs S (7h)	SS vs S (14h)	
SMa0044	B			1.26		Conserved hypothetical protein
SMa0045 (*cah*)	B			-1.47		Carbonic anhydrase
SMa0247	C		1.32			Conserved hypothetical protein
SMa0249 (*gntA*)	C		1.30			TRAP-type small permease component, required for growth on gluconate
SMa0436	B			-1.12		Hypothetical protein
SMa0512 (*idnD*)	B				1.53	IdnD L-idonate 5-dehydrogenase
SMa0520	G	1.45	1.90	1.73	1.55	Transcriptional regulator, RpiR family
SMa0564	F		-1.12		2.78	Putative dehydrogenase
SMa0629	C		1.15			Hypothetical protein
SMa0738 (*cspA6*)	C		1.34			CspA6 cold shock protein
SMa0763	B			-1.86		Hypothetical protein
SMa0799	C		-1.05			ABC transporter, periplasmic solute-binding protein
SMa0814 (*nifB*)	C		-1.01			NifB FeMo cofactor biosynthesis protein
SMa0819 (*fixB*)	C		-1.10			FixB electron transfer flavoprotein alpha chain
SMa0853 (*nodE*)	C		-1.09			NodE beta ketoacyl ACP synthase
SMa0869 (*nodA*)	B			-1.16		NodA N-acyltransferase
SMa0878 (*nodM*)	C		1.03			NodM Glucosamine--fructose-6-phosphate aminotransferase
SMa0890	C		-1.20			Conserved hypothetical protein
SMa0953	B				-1.22	ABC transporter, ATP-binding protein
SMa1038	B			-1.08		Multicopper oxidase
SMa1050	B				1.03	Hypothetical protein
SMa1052	F	1.01	1.24		1.56	Conserved hypothetical protein

SMa1077 (*next8*)	G	1.16			2.76	Nex18 Symbiotically induced conserved protein
SMa1078	F	1.89	1.74		1.93	Conserved hypothetical protein
SMa1079 (*tspO*)	F	1.36			1.91	TspO Tryptophan rich sensory protein
SMa1100	F	1.31	1.61		1.57	Conserved hypothetical protein
SMa1104	C		-1.00			Hypothetical protein fragment
SMa1122	E			1.27		Putative permease
SMa1174	C		-1.11			Hypothetical protein
SMa1214 (*fixQ1*)	C		1.03			FixQ1 nitrogen fixation protein
SMa1220 (*fixN1*)	C		1.04			FixN1 cytochrome c oxidase subunit 1
SMa1339	C		-1.07			ABC transporter, permease, involved in amino acid or peptide transport
SMa1344	B			-1.08		ABC transporter, ATP-binding protein, involved in amino acid or peptide transport
SMa1347	C		1.08			Dehydrogenase
SMa1391 (*etfB2*)	C		1.25			EtfB2 electron transport flavoprotein, beta subunit
SMa1564	B			-1.28		Putative pilus assembly protein
SMa1672	B				-1.56	Conserved hypothetical protein
SMa1731 (*betB2*)	B			-1.14		BetB2 betaine aldehyde dehydrogenase
SMa1736	C		1.08			Transcriptional regulator, LysR family
SMa1740	B			1.02		Siderophore-interacting protein
SMa1742	B			1.01		ABC transporter, permease, Fe3+-siderophore transport system
SMa1746	C		1.32			ABC transporter, periplasmic solute-binding protein, Fe3+-siderophore transport system
SMa1808	C	1.04				Hypothetical protein
SMa1820	C	1.78				Conserved hypothetical protein
SMa1838	B				-1.09	Dehydrogenase
SMa1851	C		1.10			Hydrolase
SMa2075	C		1.03			ABC transporter, periplasmic solute-binding protein
SMa2129	B				1.97	Conserved hypothetical protein
SMa2294 (*mrcA2*)	E				1.38	MrcA2 penicillin-binding protein
SMa2339	G		1.33	1.55		Siderophore biosynthesis protein
SMa2357 (*cyaO*)	C		1.06			Adenylate/guanylate cyclase
SMa2383	C		-1.07			Dehydrogenase, Zn-dependent
SMa2395 (repA2)	C		-1.05			RepA2 replication protein
SMa2400	B			3.65		Diaminobutyrate--2-

(*rhbA*)						oxoglutarate aminotransferase involved in rhizobactin biosynthesis
SMa2402 (*rhbB*)	G	1.84		2.58		L-2,4-diaminobutyrate decarboxylase
SMa2404 (*rhbC*)	G		1.19	2.65		RhbC rhizobactin biosynthesis protein
SMa2406 (*rhbD*)	E			2.82		RhbD rhizobactin biosynthesis protein
SMa2408 (*rhbE*)	G	2.38	2.23	3.83		RhbE rhizobactin biosynthesis protein
SMa2410 (*rhbF*)	G	2.36	1.34	3.76		RhbF rhizobactin biosynthesis protein
SMa2414 (*rhtA*)	G	1.43	1.64	2.68		RhtA rhizobactin transporter
SMb20005	F	2.34			-1.38	Putative glutathione S-transferase
SMb20010	E			1.88		Hypothetical protein
SMb20011	C		-1.03			Putative heavy-metal transporter
SMb20025	C		1.07			Conserved hypothetical protein
SMb20026	C		1.19			Conserved hypothetical protein
SMb20056 (*btuF*)	B			-1.52		ABC transporter, periplasmic solute-binding protein
SMb20057 (*btuC*)	B			-1.47	-1.07	ABC transporter, permease
SMb20058 (*btuD*)	B			-1.37	-1.06	ABC transporter, ATP-binding protein
SMb20059	B			-1.24		SAM-dependent methyltransferase, may be involved in cobalamin metabolism
SMb20072	C		-1.25			ABC transporter, periplasmic solute-binding protein, induced by myo-inositol
SMb20100	C		-1.12			Putative dehydrogenase
SMb20118	C		-1.00			Conserved hypothetical protein
SMb20166	B			-1.13		Conserved hypothetical protein
SMb20203 (*cbbR*)	B			-1.58		Probable transcriptional regulator
SMb20227 (*ndiA1*)	B			-1.12		Putative nutrient deprivation-induced protein
SMb20246	B			-1.10		Putative oxidoreductase
SMb20270	B			-1.40		Probable proline racemase
SMb20277	E			-1.00		Class-III pyridoxal-phosphate-dependent aminotransferase
SMb20305	C		1.02			Probable ISRm2011-2 transposase protein, N-terminal portion
SMb20421	C		1.47			Putative Transposase for insertion sequence ISRm21 protein
SMb20431 (*eutA*)	C		-1.10			Putative ectoine utilization protein
SMb20432 (*eutB*)	B			-1.35		Putative threonine dehydratase, involved in ectoine utilization
SMb20460	B			-1.18		Cellulose synthase (UDP-forming)

SMb20556	B			-1.34	-1.05	Conserved hypothetical protein
SMb20571	C	1.09				Putative amine ABC transporter, permease component
SMb20596	C		1.01			Hypothetical protein
SMb20604	G		-4.84		1.14	ABC transporter, permease
SMb20605	G		-5.55		1.34	ABC transporter, periplasmic solute-binding protein
SMb20618 (*thiE*)	B			-1.16		Putative thiamine-phosphate pyrophosphorylase
SMb20620	C		1.08			Putative sugar ABC transporter
SMb20704 (*glgA2*)	C		-1.61			Putative glycogen synthase
SMb20727	C		1.04			Hypothetical protein
SMb20753	B				1.07	Acyl-CoA dehydrogenase
SMb20807	C		1.31			Putative membrane protein
SMb20813	C		1.32			ABC transporter, ATP-binding and permease components
SMb20867	C		-1.05			Hypothetical protein
SMb20885	C		1.42			Conserved hypothetical membrane protein
SMb20915 (*aslA1*)	C		-1.13			Putative arylsulfatase
SMb20934 (*exsF*)	B			-1.11		Putative two-component response regulator.
SMb20964	C		1.00			Peroxidase
SMb20995 (*engA*)	C		1.08			Putative GTP-binding protein
SMb21030	B			-1.03		Hypothetical protein
SMb21057	C		-1.35			Conserved hypothetical protein
SMb21117	C		-1.16			Putative transcriptional regulator
SMb21134	B			-1.08		Amino acid aldolase or racemase
SMb21189	C		1.66			Putative glycosyltransferase
SMb21197	B			1.64		Putative amino acid ABC transporter, permease component
SMb21257	C		1.94			Hypothetical protein
SMb21274	C		1.64			ABC transporter, permease component
SMb21284	G		-1.55		-1.15	Putative polysaccharide deacetylase
SMb21367 (*cycA*)	B			-1.14		Putative cytochrome c class I protein, probably cytochrome c4
SMb21431	G		1.75	1.44		Hypothetical protein, possibly C terminus of iron ABC transporter periplasmatic solute-binding protein
SMb21432	G	-1.07	1.63	2.15		Putative iron uptake ABC transporter periplasmic solute-binding protein precursor
SMb21449 (*qst12*)	C		-1.38			Probable glutathione S-transferase
SMb21488	C		1.19			Putative cytochrome o

(*cyoB*)						ubiquinol oxidase chain I
SMb21489 (*cyoC*)	C		1.38			Putative cytochrome o ubiquinol oxidase chain III
SMb21520	B			-1.03		Putative two-component response regulator
SMb21550	C		1.35			Conserved hypothetical protein
SMb21555 (*kefB2*)	C		1.18			Probable glutathione-regulated potassium-efflux system
SMb21569	C		-1.06			Hypothetical protein
SMb21601	B			-1.02		Putative transcriptional regulator
SMb21676	F		1.92		1.96	Hypothetical protein
SMb21697	C		1.12			Conserved hypothetical protein
SMc00009 (*ctaC*)	C		1.01			Putative cytochrome C oxidase subunit II
SMc00017 (*thrB*)	C		1.54			Putative homoserine kinase
SMc00031	C		1.12			Hypothetical/unknown transmembrane protein
SMc00078	C		1.02			Putative methionine ABC transporter, periplasmic solute-binding protein
SMc00198	C		1.34			Hypothetical/unknown protein
SMc00231 (*glmS*)	C		1.01			Glucosamine--fructose-6-phosphate aminotransferase (nodm paralogue) protein
SMc00242	B			1.16		Hypothetical signal peptide protein
SMc00282	B			-1.03		Conserved hypothetical protein
SMc00321 (*truB*)	C		1.20			Probable tRNA pseudouridine synthase B
SMc00329 (*irr*)	C		1.17			Putative iron response regulator
SMc00342 (*rnd2*)	C		1.57			Putative ribonuclease D
SMc00346	C		1.31			Hypothetical transmembrane protein
SMc00401	C		1.21			Conserved hypothetical protein
SMc00402	G		1.91	1.42		Hypothetical signal peptide protein
SMc00408 (*uppP*)	C		1.18			Putative undecaprenyl-diphosphatase
SMc00415 (*dnaN*)	C		1.08			Probable DNA polymerase III, beta chain
SMc00421 (*cysK1*)	C	1.01	1.91			Probable cysteine synthase A (O-acetylserine sulfhydrylase A) protein
SMc00422	C		1.16			Putative amino acid exporter
SMc00430	B			-1.04		Putative sugar epimerase family protein
SMc00450 (*ctaB*)	C		1.03			Putative protoheme IX farnesyltransferase
SMc00469 (*dksA*)	C		1.56			RNA polymerase-binding, DksA
SMc00489	C		1.48			Hypothetical/unknown signal peptide protein
SMc00491	C		1.10			Hypothetical protein
SMc00523	C		1.13			Hypothetical protein

SMc00533 (*sufS*)	C		1.51			Probable cysteine desulfurase
SMc00556 (*radA*)	C		1.57			Putative DNA repair protein
SMc00583	C		1.08			Hypothetical, transmembrane protein
SMc00592	G		1.47	1.30		Hypothetical, transmembrane protein
SMc00612	C		-1.12			Hypothetical protein signal peptide
SMc00617	C		1.32			Conserved hypothetical protein
SMc00672 (*hisX hutX*)	C		-1.16			Histidine ABC transporter, periplasmic solute-binding protein
SMc00699	C		1.48			Hypothetical protein
SMc00738	C		1.01			Hypothetical transmembrane protein
SMc00784 (*fbpA*)	E			1.44		Fe3+ ABC transporter
SMc00785 (*rirA*)	B				1.01	Transcriptional regulator of the iron limitation response
SMc00821	B			-1.08		Hypothetical protein
SMc00833 (*glcE*)	B			-1.10		Probable glycolate oxidase subunit
SMc00866	B			-1.06		Hypothetical protein
SMc00894 (*kdtA*)	C		1.27			Putative 3-deoxy-D-manno-octulosonic-acid transferase
SMc00897 (*pmbA*)	C		1.00			Hypothetical PmbA protein
SMc00918 (*hisZ*)	C		1.10			ATP phosphoribosyltransferase regulatory subunit
SMc01012	C		1.14			Conserved hypothetical protein
SMc01036	C		1.12			Hypothetical transmembrane protein
SMc01104 (*mcpX*)	C		1.11			Probable chemoreceptor (methyl-accepting chemotaxis) transmembrane protein
SMc01126 (*tme*)	C		1.22			NADP-dependent malic enzyme protein
SMc01140	C		-1.13			Ribosomal protein S30Ae/sigma 54 modulation protein
SMc01142 (*grpE*)	C		1.10			Probable heat shock protein
SMc01169 (*ald*)	C		1.19			Probable alanine dehydrogenase oxidoreductase
SMc01174 (*cysK2*)	C		1.27			Probable cysteine synthase A (O-acetylserine sulfhydrylase A) protein
SMc01204	C		1.07			Probable short-chain dehydrogenase
SMc01237 (*nrdJ*)	B			-1.06	-1.31	Vitamin B12-dependent ribonucleotide reductase
SMc01242	G		-1.35		1.04	Conserved hypothetical signal peptide protein
SMc01272	C		1.06			Hypothetical transmembrane protein
SMc01315	C		1.35			Conserved hypothetical protein

SMc01348	C		1.14			Hypothetical protein
SMc01360 (*pyrB*)	C		1.69			Probable aspartate carbamoyltransferase catalytic chain
SMc01417	F	1.26		1.12		Hypothetical protein
SMc01438 (*degP2*)	B			-1.24		Probable serine protease
SMc01440 (*hflC*)	C		1.34			Putative hydrolase serine protease transmembrane protein
SMc01453	C		-1.43			Insertion sequence ISRm22
SMc01510 (*hmuV*)	G		1.48	1.53		Putative hemin transport system ATP-binding ABC transporter
SMc01512 (*hmuT*)	F		1.49	1.39		Putative hemin binding periplasmic transmembrane protein
SMc01513 (*hmuS*)	G		1.34	2.60		Putative hemin transport protein
SMc01514	G	-1.14	1.50	2.37		Conserved hypothetical protein
SMc01517	C		1.32			Conserved hypothetical protein
SMc01518	E			1.08		Conserved hypothetical protein
SMc01561	C		1.08			Hypothetical protein
SMc01619	C		-1.01			Putative class II aldolase/adducin family protein
SMc01657 (*fhuA2*)	C		1.07			Putative ferrichrome-iron receptor precursor protein
SMc01658	G		1.28	2.03		Putative ferric iron reductase
SMc01659	G		1.85	2.60		Putative ABC transporter, periplasmic component
SMc01709	C		1.04			Hypothetical signal peptide protein
SMc01712 (*lldD2*)	C		1.05			Putative L-lactate dehydrogenase (cytochrome) protein
SMc01747	G		1.29	2.23		Hypothetical protein
SMc01788	C		-1.35			Hypothetical protein
SMc01798	C		1.33			Conserved hypothetical protein
SMc01799	C		1.16			Conserved hypothetical signal peptide protein
SMc01818 (*cyaC*)	C		1.20			Putative adenylate cyclase transmembrane protein
SMc01842	C	-1.00	1.20			Probable transcriptional regulator
SMc01877 (*recN*)	C		1.30			Probable DNA repair protein
SMc01880 (*panC*)	C		1.08			Probable pantoate--beta-alanine ligase
SMc01916	C		1.34			Hypothetical signal peptide protein
SMc01917 (*nuoE1*)	F		1.21	-1.13		NADH dehydrogenase I chain E
SMc01927 (*nuoN*)	C		1.09			Probable NADH dehydrogenase I chain N transmembrane protein
SMc02053 (*trmFO*)	C		1.20			Methylenetetrahydrofolate--tRNA-(uracil-5-)-methyltransferase
SMc02057	C		1.35			Putative protein-export

(*secD1*)						membrane protein
SMc02058	C		1.03			Probable YajC protein
SMc02084 (*exbD*)	G		1.48	1.16		Probable biopolymer transport transmembrane protein
SMc02085 (*exbB*)	G		1.82	1.55		Probable biopolymer transport transmembrane protein
SMc02114	C		1.04			Putative hydrolase
SMc02122 (*fpr)*	C		1.07			Probable ferredoxin--NADP reductase
SMc02136 (*hslO*)	C		1.01			33 kDa chaperonin, Hsp33 protein
SMc02141 (*phoU*)	C		1.62			Probable phosphate transport system transcriptional regulator
SMc02164 (*frk*)	C		1.19			Probable fructokinase
SMc02165 (*pyrE*)	C		1.07			Probable orotate phosphoribosyltransferase
SMc02166 (*pyrC*)	C		1.34			Probable dihydroorotase
SMc02218	C		1.10			Putative deoxycytidine triphosphate deaminase
SMc02223	B			-1.07		Transcriptional regulator
SMc02229	B			-1.60		Putative acyl-CoA dehydrogenase
SMc02235	C		1.23			Conserved hypothetical protein
SMc02236	C		1.14			Conserved hypothetical protein
SMc02244 (*dinF*)	C		1.18			Putative transmembrane protein
SMc02273 (*rkpA wcbR*)	C		1.05			Putative fatty acid synthase
SMc02347 (*asfB*)	C	1.19				Putative ferredoxin AsfB iron-sulfur protein
SMc02349 (*asfA*)	C	1.64	2.48			Oxidoreductase
SMc02352	C		-1.04			Putative glutamine synthetase
SMc02361 (*cycH*)	C		1.34			Cytochrome C-type biogenesis transmembrane protein
SMc02366 (*ragA*)	C		1.22			Probable response regulator
SMc02398	C		1.06			Insertion sequence ISRm2011-2
SMc02412	C		-2.02			Conserved hypothetical protein
SMc02417	C		-1.28			Putative allantoin and other purine derivative ABC transporter, periplasmic solute-binding component
SMc02440 (*ubiG*)	C		1.11			Putative 3-demethylubiquinone-9 3-methyltransferase
SMc02464 (*sdhD*)	C		1.04			Probable succinate dehydrogenase membrane anchor subunit
SMc02521 (*glpR*)	C		-1.08			Glycerol-3-phosphate regulon repressor
SMc02552	B			-1.61		Hypothetical unknown protein
SMc02557	C		1.03			Hypothetical protein

SMc02577 (*hslU*)	C		1.28			Probable heat shock protein
SMc02582	C		1.39			Conserved hypothetical protein
SMc02606 (*soxA1*)	C		-2.42			Putative sarcosine oxidase alpha subunit transmembrane protein
SMc02612 (*glxD*)	C		-1.65			Putative glutamate synthase, central-C domain
SMc02648 (*aqpS*)	C		1.01			Aquaglyceroporin
SMc02649 (*arsC*)	C		1.06			Arsenate reductase
SMc02655	C		1.14			Hypothetical transmembrane protein
SMc02696	C		1.21			Conserved hypothetical protein
SMc02707	C		1.05			Putative acetyltransferase
SMc02723 (*queF*)	C		1.34			Probable NADPH-dependent 7-cyano-7-deazaguanine reductase
SMc02726 (*shmR*)	G		2.02	2.84		Hemin-binding outer membrane receptor
SMc02820 (*cpaF1*)	C		1.01			Putative pilus assembly protein
SMc02822	C		1.03			Hypothetical transmembrane protein
SMc02858 (*dnaJ*)	B			1.77		Probable chaperone protein
SMc02864 (*moeB*)	C		1.19			Probable Molybdopterin biosynthesis protein
SMc02878 (*nagA*)	C		1.02			Probable N-acetylglucosamine-6-phosphate deacetylase
SMc02887	B			1.01		Hypothetical protein
SMc02901	C		1.02			Hypothetical protein
SMc02983	C		1.32			Putative ornithine, DAP, or arginine decarboxylase
SMc03004 (*icpA mcpE*)	C		1.43			IcpA/McpE internal chemotaxis protein
SMc03009 (*cheR*)	C		1.23			Chemotaxis protein methyltransferase
SMc03010 (*cheB1*)	C		1.02			Chemotaxis response regulator protein-glutamate methylesterase
SMc03013	C		1.04			Conserved hypothetical protein
SMc03044 (*fliK*)	C		1.31			FliK hook length control protein
SMc03047 (*flgE*)	C		1.62			Flagellar hook protein
SMc03063 (*aglG*)	C	1.04				Alpha-glucosides ABC transporter, permease component
SMc03072	C		1.47			Conserved hypothetical protein
SMc03088	C		1.13			Transposase for insertion sequence element ISRm11/ISRm2011-2
SMc03131	B				1.59	Putative DL-2-aminoadipic acid ABC transporter, periplasmic solute-binding component
SMc03132	E			1.63		Oxidoreductase
SMc03151	C		1.71			Conserved hypothetical protein

SMc03152	C		1.37			Hypothetical transmembrane protein
SMc03167	F	1.09		1.27		MFS-type transport protein
SMc03168	C		-1.45			Multidrug resistance efflux system
SMc03175	C		1.34			Inosine-uridine preferring nucleoside hydrolase family protein
SMc03253	C	1.16				L-proline cis-4-hydroxylase
SMc03267	C		1.29			Putative dipeptidase
SMc03313	C		1.48			Insertion sequence ISRm2011-2
SMc03787	E			1.17		Conserved hypothetical protein
SMc03797 (*metA*)	C		1.02			Probable homoserine O-succinyltransferase
SMc03823 (*leuC*)	C		1.11			Probable 3-isopropylmalate dehydratase large subunit
SMc03846 (*acnA*)	C		1.92			Probable aconitate hydratase
SMc03850 (*ccmD*)	C		1.02			Putative heme exporter D (cytochrome C-type biogenesis protein) transmembrane
SMc03887	C		1.07			Amino acid efflux protein
SMc03892	C		1.66			Putative transposase
SMc03936	C		-1.05			Conserved hypothetical signal peptide protein
SMc04051 (*rpoE4*)	C		1.02			Putative RNA polymerase sigma-E factor (sigma-24) protein
SMc04217	C		1.11			Hypothetical transmembrane signal peptide protein
SMc04218	C		1.07			Probable ABC transporte
SMc04262 (*gnd*)	C		1.39			Probable 6-phosphogluconate dehydrogenase (decarboxylating) protein
SMc04274	C		1.13			Conserved hypothetical protein
SMc04280	C		1.15			Hypothetical signal peptide protein
SMc04318 (*cspA1*)	C		1.27			Cold shock transcriptional regulator
SMc04325 (*bmt*)	C		1.60			Betaine-homocysteine methyltransferase
SMc04346 (*ilvC*)	C		1.54			Ketol-acid reductoisomerase

Chapter 2: First evidence for interlinked control of surface motility and biofilm formation in *Sinorhizobium meliloti*

First evidence for interlinked control of surface motility and biofilm formation in *Sinorhizobium meliloti*.

Carol V Amaya-Gómez [1,2], Ann M. Hirsh[2], and María J. Soto [1].

[1]Dpto. Microbiología del Suelo y Sistemas Simbióticos. Estación Experimental del Zaidín, Consejo Superior de Investigaciones Científicas (CSIC), Profesor Albareda 1, 18008 Granada, Spain; [2]Department of Molecular, Cell and Developmental Biology, University of California-Los Angeles, Los Angeles, CA 90095-1606, USA.

Submitted to Environmental Microbiology

2.1. Abstract

Swarming motility and biofilm formation are surface-associated social behaviors representing two opposite lifestyles that in some bacteria are subjected to inverse co-regulation. In the alfalfa symbiont *Sinorhizobium meliloti*, swarming and biofilm formation are largely unexplored. Our previous work demonstrated different swarming abilities among two *S. meliloti* strains (Rm1021 and GR4) and unveiled bacterial genes (*fadD*, *rhb* and *rirA*) and environmental conditions (iron concentration) that play crucial roles in the control of surface motility in this *Rhizobium*. In the current study, we investigated whether factors known to influence swarming motility in *S. meliloti* have an impact on its capability to form biofilms. We found that strain GR4 which behaves as non-motile over surfaces is more efficient in developing biofilms than Rm1021. Moreover, the phenotype exhibited by an *rhb* mutant indicates that siderophore rhizobactin 1021 which is essential for Rm1021 surface motility is also crucial for biofilm formation. In addition, this study demonstrates that iron serves as a signal for *S. meliloti* biofilm development. High iron conditions induce the formation of highly structured biofilms that develop faster than the flat biofilms formed under low iron concentrations. Similar to *rhb*, mutations in *fadD* and *rirA* prevent normal biofilm development regardless of iron levels. Moreover, these mutations negatively affect alfalfa root colonization. Altogether, our results support the existence of regulatory mechanisms that inversely co-regulate swarming motility and biofilm formation in *S. meliloti* in order to allow for optimal plant root colonization.

2.2. Introduction

It is well accepted that the majority of bacteria spend most of their lifecycle associated to surfaces. Swarming motility and biofilms are two different and opposite behaviors displayed by bacteria living on surfaces. Biofilms are sessile assemblages of microorganisms embedded in a self-produced polymeric matrix which adhere to a surface or are associated with interfaces (Davey and O'Toole, 2000). By contrast, swarming is a mode of surface translocation dependent on

rotating flagella and is characterized by the rapid and coordinated movement of multicellular groups of bacteria (Kearns, 2010). Several studies have revealed the existence of a link between swarming and biofilm formation: i) both are surface-associated multicellular processes in which cell-cell communication and quorum sensing play important roles; ii) in both processes, the participation of the same cell surface-associated structures such as flagella, polysaccharidic matrix and biosurfactants has been reported; and iii) swarming bacteria, like bacteria in biofilms, show increased resistance to several antimicrobial agents (Daniels *et al.*, 2004; Verstraeten *et al.*, 2008; Overhage *et al.*, 2008; Lai *et al.*, 2009; Kearns, 2010; Tambalo *et al.*, 2010; McDougald *et al.*, 2012). Studies performed in bacteria like *Pseudomonas aeruginosa*, *Vibrio cholerae* or *V. parahaemolyticus* have revealed that the two lifestyles are inversely regulated by a common pathway that is modulated by the intracellular second messenger cyclic di-GMP (Caiazza *et al.*, 2007; Kuchma *et al.*, 2007; Merritt *et al.*, 2007; Pratt *et al.*, 2009; Trimble and McCarter, 2011; Kuchma *et al.*, 2012).

For obvious reasons, swarming motility and biofilm formation have been extensively studied in pathogenic bacteria. In contrast, scarce information is available about these multicellular surface-associated behaviors in rhizobia, soil-dwelling bacteria which are able to induce nitrogen-fixing nodules in legume plants upon a complex and continuous molecular dialogue that allows to co-ordinate bacterial infection with nodule organogenesis (Oldroyd and Downie, 2008).

Sinorhizobium meliloti, the alfalfa symbiont, forms biofilms on both abiotic surfaces and roots (Fujishige *et al.*, 2006a, b). On abiotic surfaces, the capability of *S. meliloti* to form biofilms is affected by environmental stresses and nutrient status (Rinaudi *et al.*, 2006). Like in many other bacteria, rhizobial exopolysaccharides (EPS) and flagella play a role in biofilm formation. *S. meliloti* mutants defective in EPS I or succinoglycan, an EPS involved in successful bacterial invasion of plant roots, do not develop mature biofilms (Fujishige *et al.*, 2006b). It is also known that the low molecular weight fraction of EPS II or galactoglucan, another symbiotically important EPS whose synthesis requires a

functional ExpR/Sin quorum sensing system, is crucial for *in vitro* and *in vivo* biofilm formation, and for root colonization (Rinaudi and González, 2009). On the other hand, mutants that overproduce EPS I exhibit more adherence and develop thicker although less stable biofilms than the wild type strain (Fujishige *et al.*, 2006b, Wells *et al.*, 2007). Like defects in EPS production and as described for other bacteria, the lack of flagella in *S. meliloti* also leads to a significant reduction in biofilm capability in microtiter plates compared to the wild type, probably because of an impairment in bacterial adherence to surfaces (Fujishige *et al.*, 2006b). Besides EPS and flagella, core Nod Factor, an essential molecule for the nodulation process, has been shown to be critical for biofilm formation in *S. meliloti* (Fujishige *et al.*, 2008).

Swarming motility in *S. meliloti* was first described for a *fadD* derivative mutant of the GR4 strain (Soto *et al.*, 2002). GR4 is unable to translocate over semisolid surfaces. However, inactivation of the *fadD* gene coding for a long-chain fatty acyl-coenzyme A ligase is sufficient to promote swarming motility on semisolid minimal medium, suggesting that FadD plays a role in the control of this multicellular surface-associated behavior. Recently, we showed that, in contrast to GR4, the commonly used *S. meliloti* laboratory strain Rm1021 was able to move over semisolid surfaces using at least two different types of motility: flagellum-independent surface spreading promoted by the production of high levels of EPS (EPS I or EPS II), and swarming motility (Nogales *et al.*, 2012). This work unveiled the existence in GR4 and Rm1021 of different control mechanisms for surface motility in general, and swarming motility in particular, although in both strains, a mutation in the *fadD* gene promotes surface translocation by yet unidentified mechanisms (Nogales *et al.*, 2010).

A transcriptomic analysis of *S. meliloti* under swarming-inducing conditions led to the discovery that biosynthesis of the siderophore rhizobactin 1021 (Rhb1021) was essential for surface translocation of the wild-type strain Rm1021 (Nogales *et al.*, 2010, 2012). It was demonstrated that the defect in surface motility shown by mutants unable to produce Rhb1021 was not due to iron deficiency. Most likely the amphiphilic structure of this siderophore confers

surfactant properties to the molecule that facilitate translocation of *S. meliloti* cells over surfaces. Like in *Pseudomonas* spp., high iron conditions inhibit swarming motility in the wild-type strain Rm1021, most probably by preventing Rhb1021 production. This inhibitory effect however is not observed in mutants lacking either the iron limitation response regulator RirA in which Rhb1021 synthesis is not abolished or FadD (Nogales *et al.*, 2010).

The connection between swarming motility and biofilm formation in *S. meliloti* has not yet been explored. In this work, we examined whether the different surface motility phenotypes shown by strains GR4 and Rm1021 could be correlated with different biofilming abilities. Furthermore, the impact on biofilm formation of bacterial genes (*fadD*, *rhb* and *rirA*) and environmental conditions (iron concentration) known to play a role in *S. meliloti* surface motility was analyzed. Our data demonstrate that iron serves as a signal for biofilm development of this bacterium and uncover Rhb101 as an additional component that, together with flagella, is crucial for both swarming and biofilm formation. In addition, the results shown here support the existence of an inverse co-regulation of these two different lifestyles in *S. meliloti* in which at least *fadD* and *rirA* seem to participate.

2.3. Material and Methods

Bacterial strains, plasmids and growth conditions

Bacterial strains and plasmids used in this study are listed in Table 2.1. *E. coli* strains were grown in Luria-Bertani medium (LB) (Sambrook and Fritsch, 1989) at 37 °C. *S. meliloti* strains were routinely cultured in Tryptone-Yeast extract complex medium (TY) (Beringer, 1974), or in Minimal Medium (MM) containing glutamate (6.5 mM), mannitol (55 mM), mineral salts (K_2HPO_4, 1.3 mM; KH_2PO_4 $3H_2O$, 2.2 mM; $MgSO_4$ $7H_2O$, 0.6 mM; $CaCl_2$ $2H_2O$, 0.34 mM; $FeCl_3$ $6H_2O$, 0.022 mM; NaCl, 0.86 mM) and vitamins (biotin (0.2 mg/L); calcium pantothenate (0.1 mg/L)) (Robertsen *et al.*, 1981) at 30 °C. Iron replete MM containing 220 μM of $FeCl_3$ was prepared by adding the appropriate volume of a

100 fold concentrated stock solution of $FeCl_3$ to MM without iron. Plasmid pHC60 was introduced into *S. meliloti* strains by biparental mating using the *E. coli* mobilizing strain S17-1. Antibiotics were added, as appropriate, at the following final concentrations: for *E. coli*, tetracycline (Tc) 10 µg/ml; for *S. meliloti*, streptomycin (Sm) 200 µg/ml, spectinomycin (Sp) 100 µg/ml, kanamycin (Km) 100 µg/ml, neomycin sulphate (Nm) 100 µg/ml, and Tc 10 µg/ml. The *fadD* mutant strain GR4FDCSS was obtained following the same procedure as for 1021FDCSS (Nogales *et al.*, 2010).

Table 2.1. Bacterial strains and plasmids used in this study

Strain or plasmid	Relevant characteristics[a]	Source or reference
Escherichia coli		
S17.1	*thi*, *pro*, *recA*, *hsdR*, *hsdM*, Rp4Tc::Mu, Km::Tn*7*; Tp^r, Sm^r, Sp^r	(Simon *et al.*, 1983)
Sinorhizobium meliloti		
GR4	Wild-type	(Casadesus and Olivares, 1979)
GR4FDCSS	GR4 (Δ*fadD*:: SmSp), Sm^r Sp^r	This study
Rm1021	SU47 *expR102*::IS*Rm*2011-1, Sm^r	(Meade and Signer, 1977)
1021FDCSS	Rm1021 (Δ*fadD*::SmSp), Sm^r Sp^r	(Nogales *et al.*, 2010)
1021rhbA	Rm1021 *rhbA*::Tn*5lac*; Sm^r Nm^r	(Nogales *et al.*, 2012)
G212rirA	Rm1021 (*lac*, *rirA*::Km), Sm^r Km^r	O'Connell, M.
GR4-*gfp*	GR4 (pHC60), Tc^r	This study
GR4FDCSS-*gfp*	GR4FDCSS (pHC60), Sm^r Sp^r Tc^r	This study
Rm1021-*gfp*	Rm1021 (pHC60), Sm^r Tc^r	This study
1021FDCSS-*gfp*	1021FDCSS (pHC60),), Sm^r Sp^r Tc^r	This study
1021rhbA-*gfp*	1021rhbA (pHC60),), Sm^r Nm^r Tc^r	This study
G212rirA-*gfp*	G212rirA (pHC60),), Sm^r Km^r Tc^r	This study
Plasmids		
pHC60	IncP plasmid constitutively expressing GFP, Tc^r	(Cheng and Walker, 1998)

[a] Tp^r Sm^r Sp^r Nm^r Km^r Tc^r: trimethoprim, streptomycin, spectinomycin, neomycin, kanamycin and tetracycline resistance, respectively.

Microtiter plate method for biofilm formation assay

This assay was performed essentially as described by Fujishige *et al.* (2006b) with some modifications and with the main variation that bacterial cells were grown in different media. Briefly, the rhizobial cells were grown to OD_{590} = 1.5-2 in MM. They were then washed twice with MM without iron and resuspended in MM containing the appropriate $FeCl_3$ concentration (22 µM for low

iron or 220 μM for iron-replete conditions) to OD_{590} = 0.2. One hundred and fifty microliters of the diluted washed cells or MM alone were added to individual wells of a 96-well polyvinylchloride (PVC) plate (Falcon 3911, Becton Dickinson, Franklin Lakes, NY). The plates were covered with a lid for flexible plate (Falcon 3913, Becton Dickinson, Franklin Lakes, NY) and incubated at 30 ºC for 48 h without agitation and under humidified conditions to prevent evaporation. At the end of the incubation time, the OD_{590} was read in a Sunrise™ microtiter plate reader (Tecan Group Ltd, Männedorf, Switzerland), to verify that there were no major differences in growth among the wells. Then, the content of each well was gently removed and the biofilms were stained with 180 μl of 0.01% crystal violet (CV, Sigma-Aldrich) for 20 min. After removing the excess of dye with water, the plates were air dried and biofilm formation was quantified by adding 180 μl of ethanol:acetone (80:20) to each well and the absorbance at 550 nm of the solubilised CV was determined using the Sunrise™ microtiter plate reader. Bacterial growth and adherence measurements were performed in triplicate, repeated at least three times and averaged.

Confocal laser scanning microscopy (CLSM)

To visualize the structure and the different stages of biofilm formation, rhizobial cells carrying the pHC60 plasmid which constitutively expresses the green fluorescent protein (GFP) and a confocal laser scanning inverted microscope Nikon Eclipse TE2000-U (Nikon Instruments, Melville, NY) were employed. Biofilms were established on chambered cover glass slides containing a 1-μm-thick borosilicate glass base (Lab-Tek no. 155411; Nunc) as described by Russo *et al.* (2006). GFP-labeled rhizobial cells were grown and diluted as described above for the microtiter plate biofilm formation assay except for the 1021rhbA-*gfp* strain which was unable to reach a high OD in MM broth. For this reason, the inoculum of this strain was prepared by diluting in MM broth, the cell mass freshly grown in MM plates. Five hundred microliters of the diluted cultures (OD_{600} = 0.2) were inoculated into each chamber and grown under static conditions at 30 ºC, for up to 10 days. To prevent desiccation, the chambers were incubated in a sterile Petri dish under humidified conditions. At defined times,

the medium was removed, and unbound bacteria were eliminated by washing each chamber with 500 µl of sterile water. Images of the biofilm were acquired by scanning with settings optimal for GFP (488-nm excitation with argon laser line and 500-nm long-pass emission) and were processed using the digital image processing Nikon software, EZ-C1 Freeviewer.

Plant assays

Alfalfa (*Medicago sativa* L.) seeds were sterilized and germinated as described by Olivares *et al.* (1980). Seedlings 1 day old (1 cm long) were transferred to square Petri dishes containing nitrogen free medium (Olivares *et al.*, 1980) solidified with 0.8% agarose (Pronadisa) and overlaid with sterile filter paper moisten with 2 ml sterile water. To observe biofilm formation over the root surface, seedlings were straight away inoculated with 30 µl of a GFP-labelled *S. meliloti* suspension containing approximately 1×10^6 bacterial cells/ml. To prepare the rhizobial suspension cells were previously grown on TY plates at 30 ºC. Then, cell mass was resuspended in TY broth up to an OD_{600} = 0.1 and diluted 100-fold in sterile water to inoculate approximately with 3×10^4 bacterial cells/plant. At determined times, from one to four days, at least 10 roots inoculated with each rhizobial strain were extensively washed in sterile water, and placed on a microscope slide. Using a Leica DMI600B epifluorescence inverted microscope, the distribution of bacteria along the root was observed. Digital images of biofilms on roots were taken using a Nikon Eclipse TE2000-U inverted microscope (488-nm argon laser excitation and 500-nm long-pass emission) and analyzed using digital image processing EZ-C1 Freeviewer Nikon software.

The colonization of the bacteria to the root and the root hairs was also evaluated by determining colony forming units (CFUs). For this, two days old seedlings were inoculated with 30 µl of a suspension containing approximately 3×10^5 bacterial cells, prepared as described above. At defined times, 15 seedlings were extensively washed with sterile water to remove the not firmly attached bacteria. The excess of water was removed on sterile filter paper and the roots

were weighed. Three roots were placed into a 1.5 ml Eppendorf tube containing 1 ml of sterile TE buffer and attached cells were released by 2 sonication pulses of 1 min each with pause time of 1 min between the pulses, in an Ultrasons-H (J.P. Selecta) sonication bath and quantified by counting CFUs (normalized to grams of root). The experiment was repeated three times.

Statistical analysis

Values presented are the means of repeated experiments. Data were subject to Student's *t* test or one-way ANOVA followed by comparison of multiple treatment levels with the control using *pots hoc* Games-Howell test. All statistical analyses were performed with SPSS software version 15.0 for windows.

2.4. Results

GR4 is more efficient in developing biofilms on glass and on root surfaces than Rm1021

S. meliloti Rm1021 and GR4 strains show different swarming motility phenotypes. Whereas Rm1021 can spread over semisolid surfaces using flagella-dependent and independent mechanisms, GR4 behaves as non-motile under the same conditions (Nogales *et al.*, 2010, 2012). To investigate if this different behavior on semisolid surfaces could be associated to different biofilm formation abilities, we compared the biofilms formed by these two strains on both abiotic surfaces (PVC and glass) and alfalfa roots.

To ensure that the environmental conditions used for these assays were similar to those employed for detecting swarming motility, biofilm formation on abiotic surfaces was assessed by growing cells in MM as described in Experimental procedures. It should be mentioned that under these conditions, Rm1021 exhibits reduced biofilm formation on PVC than when *Rhizobium* defined medium (RDM) is used (Rinaudi *et al.*, 2006), an effect that could be due to the different nutrient compositions of the two media. In the microtiter plate assay, no

differences in either planktonic growth or biofilm mass could be detected between Rm1021 and GR4 over a 48 h period (Fig. S2.1A and data not shown). To analyze the structural characteristics of biofilms developed by these two strains, confocal imaging of green fluorescent protein (GFP)-labelled GR4 and Rm1021 was performed during a 10 day-long experiment. Biofilms formed by the two strains during the first two days of incubation were unstable and detached easily from the glass surface during the washing step, making it impossible to determine biofilm morphology. After three days post inoculation (dpi), it was observed that Rm1021 and GR4 developed unorganized flat biofilms whose thickness increased with time reaching a maximum at the end of the experiment (Fig. 2.1A). The biofilm formed by GR4 exhibited higher resistance to the washing step and CLSM images showed that this strain developed thicker and more robust biofilms than Rm1021 throughout the experiment (Fig.2.1A). It should be mentioned that the classical morphology of structured biofilms consisting of towers and ridges could not be observed for any of the two strains under the assayed experimental conditions.

To extend the findings from abiotic surfaces, biofilm formation on alfalfa roots was examined. Three days after inoculation, plants inoculated with either Rm1021 or GR4 showed the development of microcolonies along the root surface which remained attached after an extensive washing of the roots (Fig. 2.1B). In both cases, the majority of cells were located in the oldest part of the root and only few cells could be observed adhered to the root apex. However, in the case of plants inoculated with GR4, more cell clusters could be observed colonizing the root surface and specially the root hair zone, compared to plants inoculated with Rm1021 (Fig. 2.1B). The number of colony-forming units (CFU) per gram of root tissue revealed no differences in the attachment ability of Rm1021 and GR4, 2 h and 24 h post inoculation. However, the number of GR4 cells attached to root surfaces 2 and 3 dpi was approximately 3 fold higher than those for Rm1021 (Fig. 2.1C). These results indicate that GR4 is more efficient than Rm1021 forming biofilms on both glass and root surfaces.

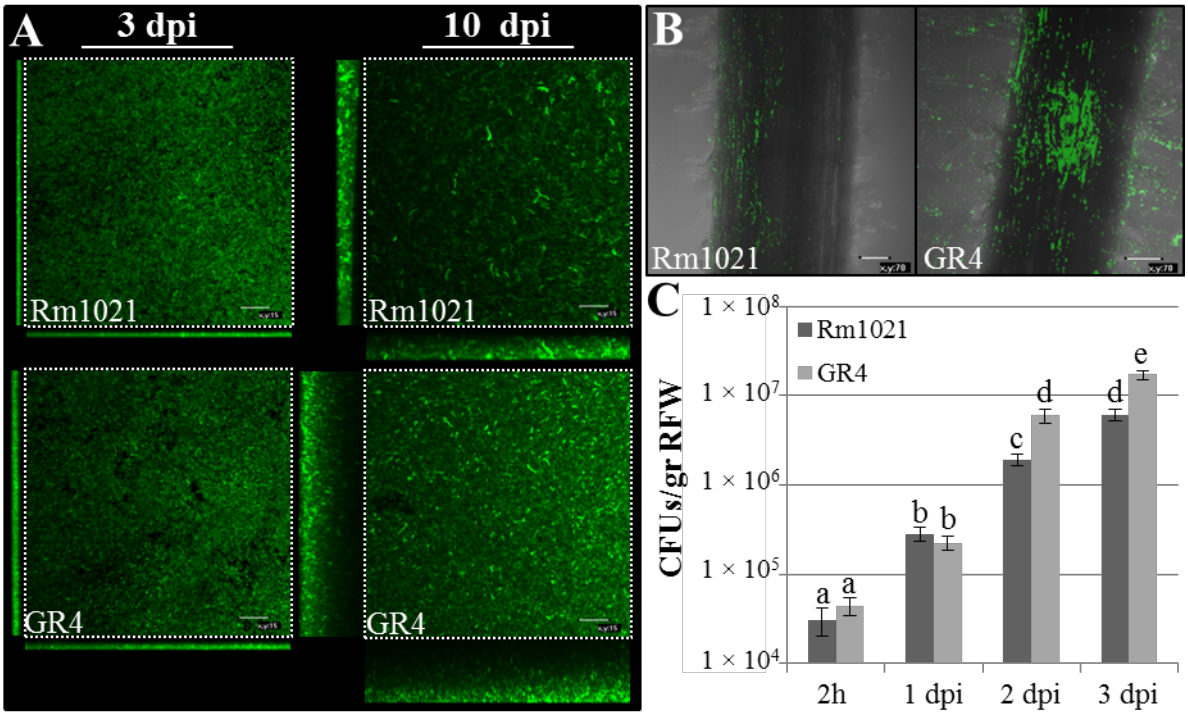

Figure 2.1.- Biofilm formation of *S. meliloti* wild type strains Rm1021 and GR4. A) Confocal images showing the *xz* and *yz* planes of biofilm development on chambered cover glass slides at 3 and 10 dpi. Bars, 15 µm. B) Confocal images of alfalfa roots inoculated with GFP-labelled Rm1021 and GR4 strains at 3 dpi. Bars 70 µm. C) Colony forming unit (CFU) counts recovered from alfalfa roots. Data are expressed per gram of fresh root weight (FRW). Error bars indicate the standard deviation from the mean. According to the Games-Howell test ($P \leq 0.05$) values followed by the same letter do not differ significantly. Each experiment was repeated by triplicate.

A *fadD* mutation interferes with normal biofilm development in *S. meliloti*

Our previous studies revealed that besides its function in lipid metabolism *fadD* plays a role in the control of surface motility in *S. meliloti* (Soto *et al.*, 2002; Nogales *et al.*, 2010; Pech-Canul *et al.*, 2011). A *fadD* mutation promotes surface migration in Rm1021 and GR4 strains as well as in siderophore Rhb1021 defective mutants. We investigated if *fadD* could also contribute to biofilm formation in *S. meliloti*.

In PVC microtiter plates, *fadD* derivative mutants of GR4 and Rm1021 (GR4FDCSS and 1021FDCSS, respectively) showed a significant increase in

biofilm formation compared with their parental strains (Fig. 2.2A and 2.3A). In contrast, confocal images of biofilms established on glass surfaces revealed that the *fadD* mutation negatively affected biofilm development in the two strains (Fig. 2.2B and 2.3B), with the most notable effects being observed for GR4FDCCS (Fig. 2.2B). This mutant strain exhibited thinner biofilms than those formed by its parental strain GR4 throughout the experiment although the biggest differences were noticed 10 dpi. Biofilms developed by 1021FDCSS were significantly thinner than those formed by Rm1021 10 dpi, but in contrast to the *fadD* mutant of GR4, no differences could be detected at earlier stages of biofilm development (3 dpi) (Fig. 2.3B).

Similar behaviour was noticed for biofilms formed on the surface of alfalfa roots. Confocal images and CFU counting revealed that GR4FDCSS showed a significantly decreased ability to attach to and colonize root surfaces compared to GR4 (Fig. 2.2C, 2.2D), although this difference diminished in time (see 3 dpi in Fig. 2.2D). In the case of 1021FDCSS, reduced biofilm formation on alfalfa roots was also detected (Fig. 2.4), although the effect was transitory and less noticeable than for GR4FDCSS. We could only appreciate differences when counting CFU 1 dpi in which the number of attached 1021FDCSS cells was found to be approximately 3 fold lower than that of Rm1021 (Fig. 2.4B). Therefore, a *fadD* mutation in *S. meliloti* interferes with normal development of biofilms on both abiotic and root surfaces, although the effects are more prominent in the GR4 strain background than in Rm1021.

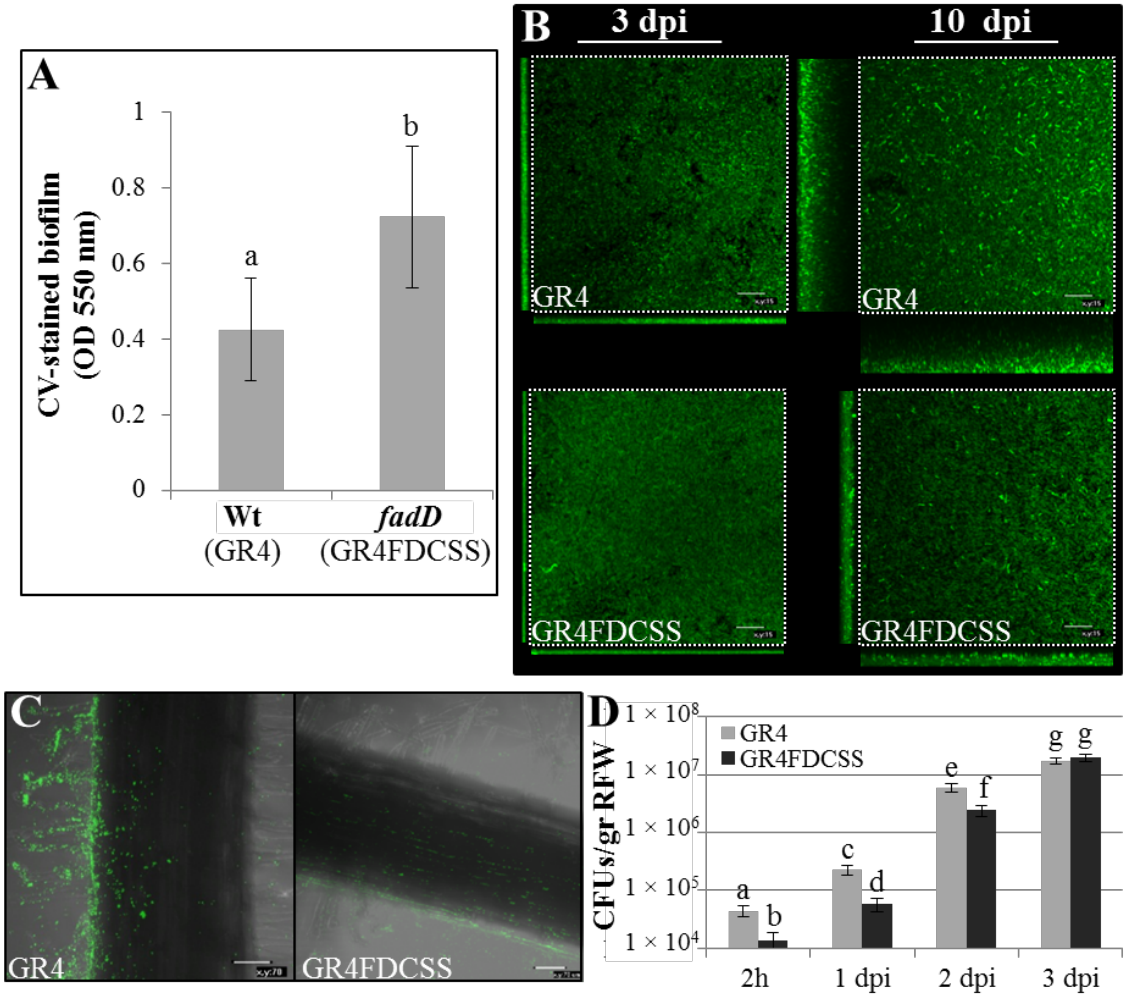

Figure 2.2.- Effect of *fadD* mutation on biofilm formation in *S. meliloti* GR4. A) Quantification of biofilm formation on PVC microtiter plate dishes, 48 h after inoculation. Each data point is the average of at least 20 wells from a representative experiment. Error bars indicate the standard deviation of the mean. According to the Student's *t* test ($P \leq 0.01$) biofilm values followed by the same letter do not differ significantly. B) Confocal images showing the *xz* and *yz* planes of biofilm development on chambered cover glass slides at 3 and 10 dpi. Bars, 15 µm. C) Confocal images showing wild type (GR4) and *fadD* mutant (GR4FDCSS) cells attached to alfalfa root surfaces 3 dpi. Bars 70 µm. D) Colony forming unit (CFU) counts recovered from alfalfa roots. Data are expressed per gram of root fresh weight (RFW). Error bars indicate the standard deviation from the mean. According to the Games-Howell test ($P \leq 0.05$) values followed by the same letter do not differ significantly. Each experiment was repeated by triplicate.

Rhizobactin 1021 biosynthesis genes (*rhb*) and *rirA* play important roles in *S. meliloti* biofilm formation

rhb derivative mutants of Rm1021 unable to synthesize the siderophore Rhb1021 cannot translocate on semisolid surfaces (Nogales *et al.*, 2010, 2012).

On the other hand, loss of function of the iron response regulator RirA in Rm1021, apparently does not have consequences for surface motility under low iron conditions but leads to a hypermotile phenotype in the presence of high levels of iron which suggests a role for this regulator in the control of swarming-related genes in response to iron concentration (Nogales *et al.*, 2010). Here, we have analyzed the effects of *rhb* and *rirA* mutations on the biofilm formation ability of Rm1021 under low iron conditions.

In MM containing 22 μM $FeCl_3$, Rm1021 derivative mutants in *rhbA* and *rirA* exhibited a reduced growth rate compared with the wild type Rm1021 (Fig. S2.1C). Whereas the reduction of growth of the *rhbA* mutant might be due to iron nutrition deficiency, in the *rirA* mutant it could be the result of oxidative stress caused by derepressed iron uptake (Chao *et al.*, 2005). Despite exhibiting growth defects in MM, mutants in *rhbA* and *rirA* showed statistically significantly increased biofilm formation on PVC microtiter plates compared with the wt a strain (Fig. 2.3A). However, like *fadD* mutants, a different behavior was observed when analyzing GFP-labelled biofilms established on glass surfaces. Although at early stages (3 dpi) the *rhbA* mutant developed a biofilm indistinguishable from that formed by the wild type, a significant reduction in biofilm thickness was observed at 10 dpi for the *rhbA* mutant strain compared to Rm1021 (Fig. 2.3B). The reduction in biofilm thickness shown by the *rhbA* mutant could be the result of its impaired growth resulting from the inability to acquire iron through Rhb1021, its failure to translocate over surfaces or both. Under the same conditions, the *rirA* mutant could form thicker biofilms than the parent at early stages (3 dpi; Fig. 2.3B) suggesting that a planktonic growth defect does not necessarily imply decreased biofilm formation. After 10 days of incubation and before the washing step, biofilms established by wt and *rirA* on glass were indistinguishable. However, the *rirA* mutant biofilms did not firmly adhere to the glass surface and were easily removed during the washings. Consequently, confocal images showed that after 10 days *rirA* developed thinner biofilms than those formed by the wild type strain.

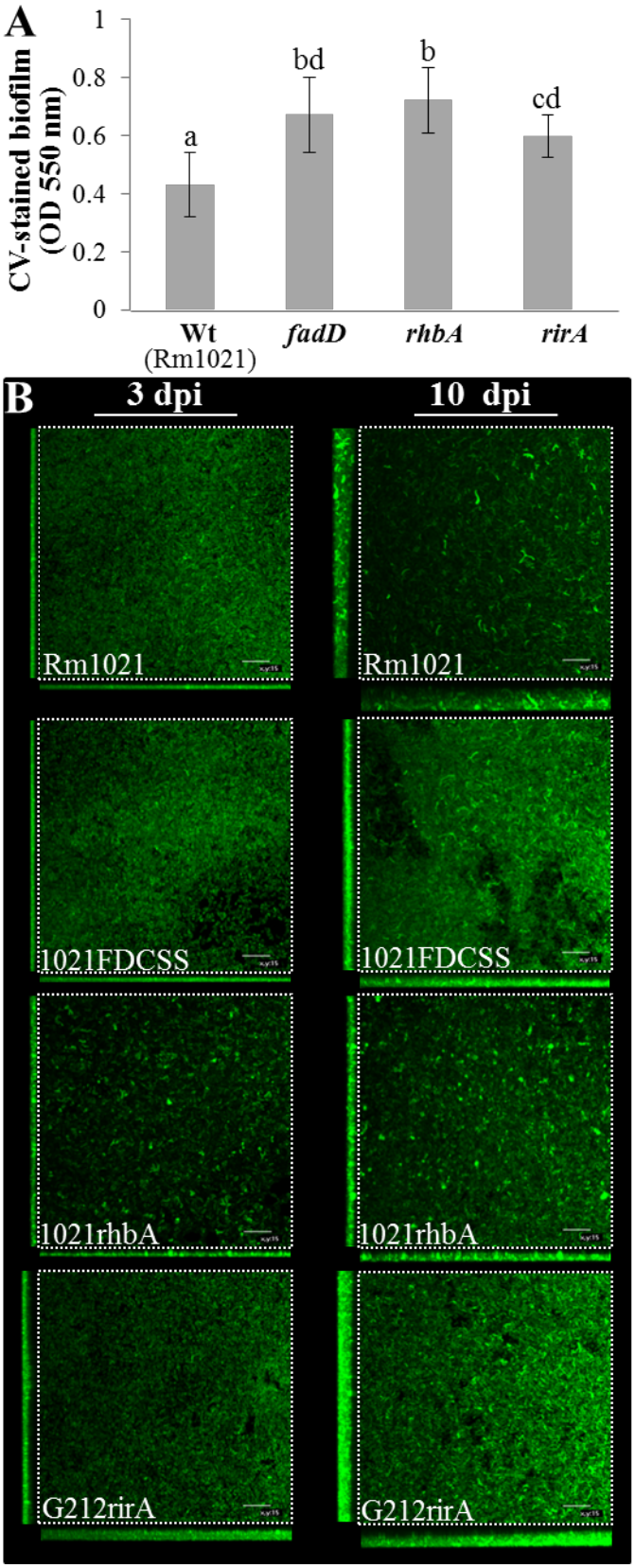

Figure 2.3. Effect of *fadD*, *rhbA* and *rirA* mutations on biofilm formation on abiotic surfaces in *S. meliloti* Rm1021. A) Quantification of biofilm formation on PVC microtiter plate dishes, 48 h after inoculation. Each data point is the average of at least 20 wells from a representative experiment. Error bars indicate the standard deviation of the mean. According to the Games-Howell test ($P \leq 0.05$) biofilm values followed by the same letter do not differ significantly. B) Confocal images showing the *xz* and *yz* planes of biofilm development on chambered cover glass slides at 3 and 10 dpi. Bars, 15 µm. Each experiment was repeated by triplicate

Examining biofilm formation *in planta* by CLSM revealed that the *rhbA* mutant and especially the *rirA* mutant were impaired in establishing bacterial communities on the surface of alfalfa roots (Fig. 2.4A). In contrast to the significant root colonization observed for Rm1021 3 dpi, plants inoculated with the *rhbA* mutant only exhibited scarce groups of a few bacteria attached to the central part of the root and root hairs. In the case of the *rirA* mutant, the effect was even more drastic. Three dpi, plants inoculated with this mutant showed only a few cells attached to the main root and single cells dispersed along the root hairs. These results were confirmed by CFU counting (Fig. 2.4B). The number of *rhbA* mutant cells colonizing alfalfa roots was 5, 2 and 2.6 fold lower that those observed for Rm1021 at 1, 2 and 3 dpi, respectively. For the same period, the number of *rirA* mutant cells recovered from alfalfa roots was 22, 68 and 25 fold lower than for the parent. Altogether our results demonstrate an important role of *rhb* and *rirA* in the development of biofilms on both abiotic and plant roots.

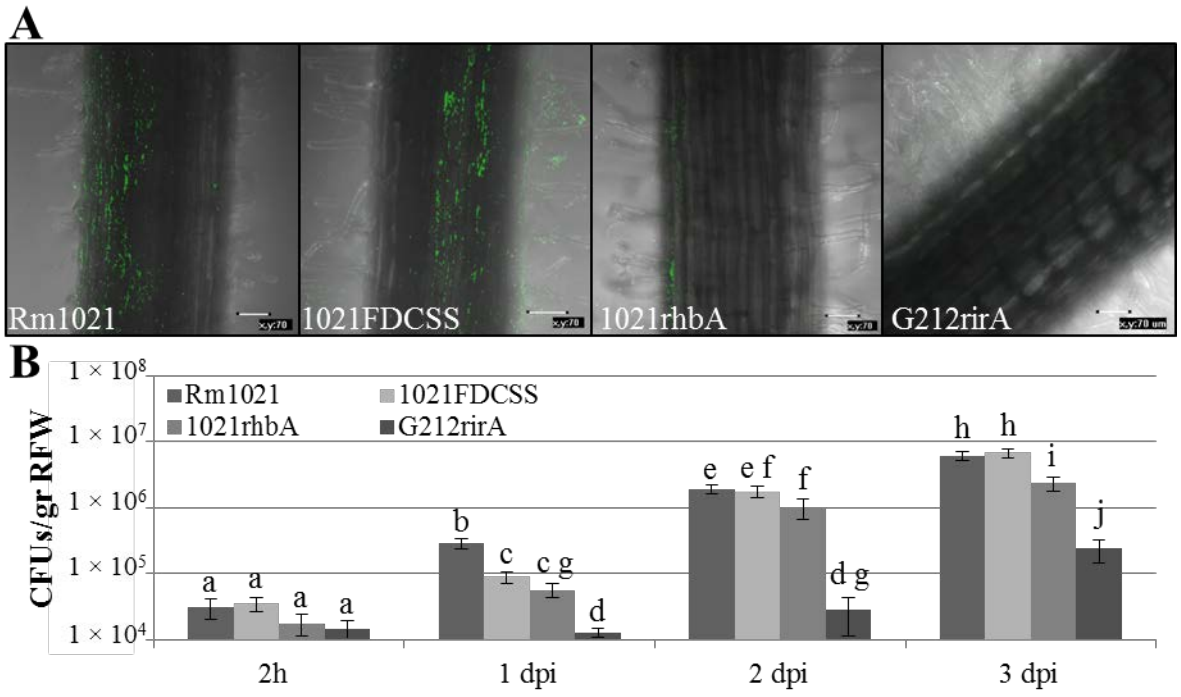

Figure 2.4. *In planta* biofilm formation by Rm1021 and *fadD*, *rhbA* and *rirA* derivative mutants. A) Confocal images of biofilms established on alfalfa root surfaces 3 dpi. Bars 70 µm. B) Colony forming unit (CFU) counts recovered from alfalfa roots. Data are expressed per gram of root fresh weight (RFW). Error bars indicate the standard deviation from the mean of three independent experiments. According to the Games-Howell test ($P \leq 0.05$) values followed by the same letter do not differ significantly.

Iron is a signal for biofilm development in *S. meliloti*

Iron can regulate biofilm formation in multiple bacterial species. In some species, iron limitation induces biofilm development whereas in others, inhibition of biofilms occurs in response to low iron availability (Banin *et al.*, 2005; Ojha and Hatfull, 2007; Hindré *et al.*, 2008; Wu and Outten, 2009; Trapetti *et al.*, 2011). Previous studies from our group showed that high concentrations of iron inhibit swarming motility in *S. meliloti* wild type Rm1021 (Nogales *et al.*, 2010). To investigate if iron could be a signal in the co-regulation of swarming motility and biofilm formation in *S. meliloti*, we compared the biofilms formed by the wild type strains GR4 and Rm1021 on abiotic surfaces (PVC and glass) under high iron conditions (MM containing 220 μM $FeCl_3$) with those formed under low iron levels (22 μM $FeCl_3$).

Growth of both strains was improved under iron replete conditions compared to low iron media (Fig. S2.1A). Concurrent with this observation, high iron levels resulted in increased biofilm formation on PVC in GR4 and Rm1021 (Fig. 2.5A and 2.5B). Analysis of biofilms developed on glass revealed that iron-supplemented MM induced a significant change in the structure of biofilms developed by the two wild type strains of *S. meliloti* (Fig. 2.5C). For both, Rm1021 and GR4, growth in the presence of 220 μM of $FeCl_3$ resulted in the formation of highly structured biofilms characterized by the presence of clearly distinguishable microcolonies in which cells were embedded in a thick extracellular matrix (ECM). Moreover, iron replete medium significantly increased the thickness of biofilms developed by the two wt strains at early stages, 3 dpi (Fig. 2.5D and 2.5E). This effect was especially notorious for GR4 (Fig. 2.5E) which under high iron conditions was able to develop a biofilm with a robustness and thickness very similar to that developed under low iron levels after 10 days. Ten days after inoculation, no differences in thickness could be observed between biofilms developed by Rm1021 under low and high iron conditions (Fig. 2.5D), although they exhibited distinct structures. Strain GR4 developed the thickest and most structured biofilms observed in this study, after six dpi in iron replete medium. Later, 10 dpi, the biofilm developed by GR4 under these conditions lost the

organization in microcolonies and became thinner, suggesting the initiation of biofilm dispersal. These results indicate that high iron availability induces biofilm formation in *S. meliloti*, triggering the formation of highly structured biofilms that develop faster than under low iron conditions. These effects are more pronounced in GR4 than in Rm1021, suggesting differences in some iron-regulated mechanisms governing biofilm development between these two strains.

***fadD*, *rhb* and *rirA* mutations also interfere with normal biofilm development under high iron conditions**

In a previous report we demonstrated that the addition of high concentrations of iron did not restore surface translocation of Rhb1021 deficient strains (*rhb* and *rhrA* mutants) (Nogales *et al.*, 2010). Moreover, it was shown that in contrast to the behavior displayed by Rm1021, high iron conditions did not prevent swarming motility of *fadD* and *rirA* mutants (Nogales *et al.*, 2010). We decided to investigate if Rhb1021, as well as the *fadD* and *rirA* genes were also required for biofilm formation under iron replete conditions.

As occurred for the wt strains Rm1021 and GR4, growth of most of the mutant strains was improved under high iron conditions compared to growth in media containing low iron levels except in the case of the *rirA* mutant in which no significant differences were detected (Fig. S2.1B and S2.1C). In iron-replete medium, GR4FDCSS (*fadD*) exhibited a slight but significant increase in growth compared with the wild type strain GR4 (Fig. S2.1B). In contrast, the *fadD* derivative mutant of Rm1021 showed a slight decrease in growth rate compared to the wild type under these conditions. On the other hand, whereas the presence of high iron concentrations restored the growth deficiencies shown by the *rhbA* mutant to wild type levels, no significant response was detected for the *rirA* mutant.

When biofilm formation under iron-replete conditions was quantified on PVC plates, an increase in biofilm mass was observed for all the mutants compared to the biofilm developed by their corresponding parent strains, except

for 1021FDCSS whose biofilm formation ability was similar to that shown by Rm1021 (Fig. 2.5A and 2.5B).

CLMS images of biofilms established on glass revealed that a *fadD* mutation interfered with *S. meliloti* biofilm formation under high iron conditions although the extent of this interference depended on the strain. At early stages, iron-replete medium induced in 1021FDCSS the formation of a biofilm with a similar structure and thickness as that developed by the wt strain Rm1021 under the same conditions (Fig. 2.5D). Nevertheless ten days after inoculation, the structured biofilm developed by 1021FCDCSS was thinner than the biofilm formed by Rm1021. The defect on biofilm development under iron sufficient conditions caused by *fadD* disruption was more severe in the GR4 genetic background. In this strain, the loss-of-function of *fadD* prevented the formation of structured biofilms in response to high iron levels and in addition, it caused a significant reduction of thickness in biofilms developed 6 and 10 dpi compared to those developed by the wt strain GR4 under the same conditions (Fig. 2.5E). These results indicate that in *S. meliloti* a functional *fadD* gene is required for complete biofilm development under iron replete conditions.

Increased iron availability could not restore biofilm development in either *rhbA* or *rirA* mutant strains (Fig. 2.5D). High iron conditions induced changes in the structure of biofilms developed by the 1021rhbA mutant in which formation of microcolonies similar to those detected in structured wt biofilms could be observed. However, iron replete conditions did not increase the thickness of *rhbA* biofilms that remained as thin as those formed under low iron levels, at both early and late stages of biofilm development (Fig. 2.5D). This result suggests that Rhb1021 synthesis is essential for normal biofilm development in *S. meliloti*. On the other hand, no changes in either structure or thickness were detected in *rirA* mutant biofilms developed in iron replete media compared to those formed under low iron levels, indicating that this regulator plays a pivotal role in controlling functions required for biofilm development in response to iron availability.

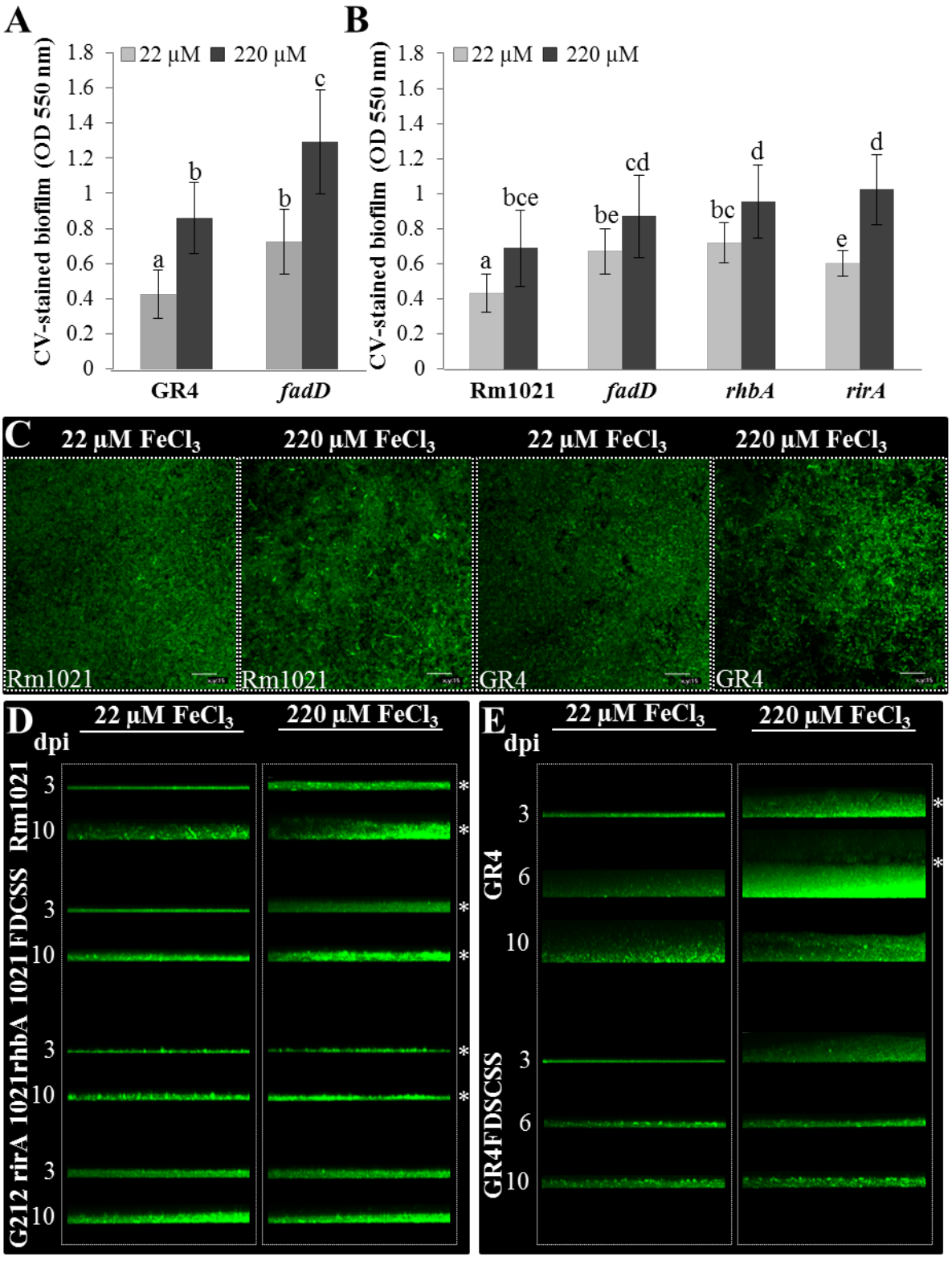
A
B
CV-stained biofilm (OD 550 nm)
22 µM
220 µM
GR4
fadD
Rm1021
rhbA
rirA
C
22 µM FeCl3
220 µM FeCl3
Rm1021
GR4
D
E
dpi
G212 rirA 1021rhbA 1021 FDCSS Rm1021
GR4FDSCSS GR4

Figure 2.5. Biofilm formation of *S. meliloti* strains on abiotic surfaces in response to iron availability. Biofilm formation on PVC plates of GR4 derivative strains (A) and Rm1021 derivative strains (B) at 48 h post inoculation. Light bars represent biofilm mass formed in MM containing low iron levels (22 μM $FeCl_3$) and darked bars represent biofilm mass formed in MM containing high iron levels (220 μM $FeCl_3$). Each data point is the average of at least 20 wells from a representative experiment. Error bars indicate the standard deviation of the mean. According to the Games-Howell test ($P \leq 0.05$) biofilm values followed by the same letter do not differ significantly. C) CLSM images showing the architecture of 3-day-old biofilms developed by GFP-labelled Rm1021 and GR4 cells on chambered cover glass slides after growth in MM containining different concentrations of $FeCl_3$. Bars, 15 μm. D) CLMS images showing the thickness of 3- and 10-day-old biofilms developed by Rm1021 and its derivative mutant strains on chambered cover glass slides in response to low (22 μM $FeCl_3$) and high (220 μM $FeCl_3$) iron availability. E) CLMS images showing the thickness of 3- 6-and 10-day-old biofilms developed by GR4 and GR4FDCSS. The biofilm thickness is represented by the *xz* planes. Highly structured biofilms developed in MM containing 220 μM of FeCl3 are indicated with a star (*). Each experiment was repeated by triplicate.

2.5. Discussion

Extensive investigations on swarming motility and biofilm formation in pathogenic bacteria have demonstrated the intimate link between these two multicellular surface-associated behaviors as well as their impact in host colonization and infection. By contrast, very little is known about genes and regulatory mechanisms governing these two opposite lifestyles in *Rhizobium*. The aim of this work was to investigate the existence of a possible connection between swarming motility and biofilm formation in *Sinorhizobium meliloti* by analyzing the effect on biofilm development in different genetic backgrounds and environmental conditions known to influence surface motility in this bacterium. Our data support the existence of a link between the two surface-associated behaviors by uncovering siderophore Rhizobactin 1021 (Rhb1021) as an essential component for both swarming motility and biofilm formation and by providing evidence of an inverse co-regulation of the two phenotypes in which iron acts as a signal and the *fadD* and *rirA* genes seem to be involved.

Biofilm formation was analyzed on two different abiotic surfaces (PVC and glass) and on alfalfa roots. Despite using the same growth conditions, contradictory results were found comparing bacterial biofilms formed on PVC with those established on glass. Although these two systems are commonly used in investigations on bacterial biofilms, it is obvious that they represent “non-

natural" surfaces for *S. meliloti*. However, we found that biofilm development on glass surfaces reflected accurately the behaviour shown by the different strains on alfalfa roots. In other words, strains showing some defects in biofilm formation on glass exhibited worse performance in colonizing alfalfa roots than those strains with increased abilities in biofilm development on the abiotic surface. Therefore, and at least under our experimental conditions, biofilm assessment on PVC plates is not the best approach to reach conclusions about factors influencing biofilm development in *S. meliloti* under more natural conditions.

The results presented in this work reveal Rhb1021 to be an additional component that, together with flagella is essential for both swarming motility and biofilm development in *S. meliloti*. Rhb1021 is a citrate-based dihydroxamate siderophore with an asymmetric structure conferred by the presence of a long-chain fatty acid ((E)-2-decenoic acid) that gives this siderophore amphiphilic properties (Persmark *et al.*, 1993). Mutations and environmental conditions (high iron levels) that abolish Rhb1021 production, prevent surface translocation in *S. meliloti* (Nogales *et al.*, 2010; Nogales *et al.*, 2012). It was speculated that surfactant properties inherent to Rhb1021 might be responsible for its role in promoting bacterial motility over surfaces. Defects in biofilm development shown by the *rhbA* mutant suggest that Rhb1021 synthesis is also essential for biofilm formation. Several siderophores have been implicated in bacterial biofilm development. The role of most of these siderophores in establishing surface-associated bacterial communities is related with the important regulatory function that intracellular iron plays in biofilm formation in different bacteria. In *Pseudomonas aeruginosa*, the pyoverdine system is required for normal biofilm development under iron depleted conditions while high iron concentrations suppress the mutant defect (Banin *et al.*, 2005). Likewise, in *Mycobacterium smegmatis*, the exochelin biosynthesis and uptake systems are essential for biofilm development under iron-limiting conditions, though not for planktonic growth (Ojha and Hatfull, 2007). More recently, enterobactin was shown to be required for biofilm development in reduced-genome *Escherichia coli* (May and Okabe, 2011). Mutants of *P. syringae* pv. tabaci unable to produce the siderophore pyoverdine are hyperswarmers and impaired in the development of

mature biofilms, but the effects were correlated with an increased production of biosurfactant in the absence of siderophore (Taguchi *et al.*, 2010).

In contrast to *P. aeruginosa*, biofilm development by a *S. meliloti* Rhb1021-defective mutant is not restored under iron replete conditions (Fig. 2.5D). This result indicates that the role played by Rhb1021 in biofilm development is not only related to iron acquisition. It is tempting to speculate that the function exerted by this siderophore in biofilm formation might be linked to its surfactant activity. Different molecules with surfactant activities that play a role in swarming motility have been shown to influence bacterial biofilms (Mireles *et al.*, 2001). In some bacteria, an inverse relationship between the presence of a surfactant or wettability factor and biofilm formation has been found, for instance the effect observed for the lipopeptides surfactin, serrawettin or putisolvins (Mireles *et al.*, 2001; Kuiper *et al.*, 2004). Among the best studied are the biosurfactants produced by *P. aeruginosa* via RhlA (rhamnolipids and its precursors) which are surface active amphipathic molecules known to be responsible for the complex swarming pattern of this bacterium (Tremblay *et al.*, 2007). Overproduction of rhamnolipids can also impede biofilm formation (Davey *et al.*, 2003). However, different and elegant studies have demonstrated that rhamnolipids play multiple roles at different stages of biofilm development: i) by facilitating surface-associated motility, they are necessary for initial microcolony formation and contribute to formation of the cap portion of mushroom-shaped structures in the biofilm in later stages (Pamp and Tolker-Nielsen, 2007); ii) they affect biofilm architecture by preserving cell-free regions between mushroom-shaped macrocolonies (Davey *et al.*, 2003), and iii) they have also been involved in biofilm dispersion (Boles *et al.*, 2005). The timing of induction of rhamnolipid gene expression is also crucial for the development of structured biofilms (Glick *et al.*, 2010). Thus, early induction of rhamnolipid biosynthetic gene expression caused for example by iron limitation, results in increased surface motility and a flat biofilm phenotype.

It is tempting to speculate that the essential role of Rhb1021 in biofilm formation by *S. meliloti* is the result of it displaying two important functions that

in the case of other bacteria (e.g. *P. aeruginosa*) are exerted by two different molecules: as a siderophore participating in controlling intracellular iron levels, and as biosurfactant facilitating the formation of microcolonies and influencing biofilm architecture. Like for rhamnolipids, the production of Rhb1021 must be tightly regulated within the *S. meliloti* biofilm in order to reach levels sufficient for maintaining the structure of the biofilm but below the levels which would impede or destroy biofilm structure. In favour of this hypothesis, we found that a *rirA* mutant that produces high levels of Rhb1021 regardless of iron levels in the medium is also affected in biofilm development (Fig. 2.5D). Under low- iron conditions, the *rirA* mutant develops thicker biofilms than the wt at early stages, but in contrast to wt biofilms, the thickness of *rirA* biofilms does not increase with time. The mutant is especially impaired in biofilm formation under high-iron conditions, where it is unable to develop the thick structured biofilms observed for the wt. These results could be explained by the increased and deregulated production of Rhb1021 in the *rirA* mutant, which would favour the initiation of biofilm formation under low iron conditions but interfere with the later stages of biofilm development as well as with biofilm formation under iron-replete conditions. Nevertheless, the involvement of additional functions regulated by RirA cannot be discarded. The analysis of the temporal and spatial expression of Rhb1021 genes in wt and *rirA* biofilms would help increase our understanding of the role played by the siderophore in biofilm formation.

In addition, several results obtained during this study provide the first evidence in *Rhizobium* of an inverse co-regulation of swarming motility and biofilm formation:

i) *S. meliloti* wt strain GR4 which exhibits stricter control over surface motility under laboratory conditions, is more efficient in biofilm development on abiotic and root surfaces than strain Rm1021 which is prone to exhibit surface motility (Fig. 2.1). The difference is especially noticeable under high-iron conditions where GR4 develops the thickest and most structured biofilm 6 dpi (Fig. 2.5D and 2.5E). These results suggest that like for control of swarming motility, different regulatory mechanisms seems to govern biofilm development in these two strains. The increased biofilm formation efficiency shown by GR4 could

be at least one of the reasons for the higher nodule formation efficiency of this strain compared to Rm1021 (Toro and Olivares, 1986)

ii) *fadD* and *rirA* mutations known to promote *S. meliloti* surface translocation, interfere with normal biofilm development on glass surfaces. *fadD* and *rirA* mutants are affected mainly at late stages of biofilm formation. Moreover, as has been observed for swarming motility, disruption of these genes interferes with the effects caused by high-iron levels on biofilm development. The biggest defects in biofilm formation were displayed by the *fadD* derivative mutant of GR4 and *rirA*. Both were unable to develop the thick structured biofilms formed by their respective parent strains under high iron conditions. Interestingly, these mutants, like *rhb*, were affected in alfalfa root colonization. This suggests that the biofilm phenotype shown on glass by *S. meliloti* strains might reflect their efficiency in host colonization.

iii) High-iron conditions that inhibit swarming motility in *S. meliloti* induce biofilm formation. This demonstrates that iron serves as a signal that inversely co-regulates the two surface-associated phenotypes. Iron has been shown to be a nutrient that regulates biofilm formation in multiple bacterial species. In some such as *Legionella pneumophila*, *Acinetobacter baumannii* and *Staphylococcus aureus*, iron limitation induces biofilm formation (Johnson *et al.*, 2005; Hindré *et al.*, 2008; Gaddy *et al.*, 2009). In contrast, iron limitation inhibits biofilm formation in other species such as *E. coli, P. aeruginosa*, *Vibrio cholerae* and *Xylella fastidiosa* (Singh *et al.*, 2002; Banin *et al.*, 2005, 2006; Koh and Toney, 2005; Mey *et al.*, 2005; Wu and Outten, 2009). These different responses to iron availability might be the result of differences in iron acquisition systems, characteristics of the cell surface or different properties of the extracellular matrix. The role of iron in *S. meliloti* biofilm formation shares some similarities with the role of iron in biofilm development by *P. aeruginosa*. Both bacteria form flat unstructured biofilms under low iron conditions. In *P. aeruginosa* this phenotype was explained by iron regulated production of rhamnolipids (Glick et al. 2010). Likewise, and as explained above, control of Rhb1021 expression in response to iron levels could impact biofilm formation.

In bacteria such as *P. aeruginosa*, *V. cholerae* or *V. parahaemolyticus* swarming motility and biofilm formation are inversely regulated by a common pathway that is modulated by the intracellular second messenger cyclic di-GMP (Caiazza *et al.*, 2007; Kuchma *et al.*, 2007; Merritt *et al.*, 2007; Pratt *et al.*, 2009; Trimble and McCarter, 2011; Kuchma *et al.*, 2012). Our study provides evidence for an interlinked control of these two surface-associated phenotypes as well for *S. meliloti*, in which iron as an environmental cue and *fadD* and *rirA* as regulatory genes seem to play pivotal roles. The fact that *fadD* and *rirA* mutants are affected in plant root colonization might indicate that inverse co-regulation of surface motility and biofilm formation is a requisite for efficient interaction with the host plant. Further investigations of iron acquisition systems and iron-dependent regulation in *S. meliloti* as well as of the effects caused by the disruption of *fadD* will undoubtedly facilitate the identification of new components which govern biofilm formation in this bacterium that might also impact the establishment of the *Rhizobium*-legume symbiosis.

Acknowledgements

This work was supported by grants BIO2007-62988 and BIO2010-18005 from the Ministerio de Ciencia e Innovación (MICINN, Spain), CVI 03541 from the Junta de Andalucía (Spain), and FEDER funds. CAVG was supported by a FPI fellowship from MICINN. We also thank the help of the Microscopy Service of the Estación Experimental del Zaidín (CSIC).

2.6. References

Banin, E., Vasil, M.L., and Greenberg, E.P. (2005) Iron and *Pseudomonas aeruginosa* biofilm formation. *Proc Natl Acad Sci USA* 102: 11076–11081.

Banin, E., Brady, K.M., and Greenberg, E.P. (2006) Chelator-induced dispersal and killing of *Pseudomonas aeruginosa* cells in a biofilm. *Appl Environ Microb* 72: 2064–2069.

Beringer, J.E. (1974) R factor transfer in *Rhizobium leguminosarum*. *J Gen Microbiol* 84: 188–198.

Boles, B.R., Thoendel, M., and Singh, P.K. (2005) Rhamnolipids mediate detachment of *Pseudomonas aeruginosa* from biofilms. *Mol Microbiol* 57: 1210–1223.

Caiazza, N.C., Merritt, J.H., Brothers, K.M., and O'Toole, G.A. (2007) Inverse regulation of biofilm formation and swarming motility by *Pseudomonas aeruginosa* PA14. *J Bacteriol* 189: 3603–3612.

Casadesus, J., and Olivares, J. (1979) Rough and fine linkage mapping of the *Rhizobium meliloti* chromosome. *Mol Gen Genet* 174: 203–209.

Chao, T.-C., Buhrmester, J., Hansmeier, N., Pühler, A., and Weidner, S. (2005) Role of theregulatory gene *rirA* in the transcriptional response of *Sinorhizobium meliloti* to iron limitation. *Appl Environ Microbiol* 71: 5969–5982.

Cheng, H.-P., and Walker, G.C. (1998) Succinoglycan is required for initiation and elongation of infection threads during nodulation of alfalfa by *Rhizobium meliloti*. *J Bacteriol* 180: 5183–5191.

Daniels, R., Vanderleyden, J., and Michiels, J. (2004) Quorum sensing and swarming migration in bacteria. *Fems Microbiol Rev* 28: 261–289.

Davey, M.E., and O'toole, G.A. (2000) Microbial Biofilms: from ecology to molecular genetics. *Microbiol Mol Biol Rev* 64: 847–867.

Davey, M.E., Caiazza, N.C., and O'Toole, G.A. (2003) Rhamnolipid surfactant production affects biofilm architecture in *Pseudomonas aeruginosa* PAO1. *J Bacteriol* 185: 1027–1036.

Fujishige, N.A., Kapadia, N.N., and Hirsch, A.M. (2006a) A feeling for the micro-organism: structure on a small scale. Biofilms on plant roots. *Bot J Linn Soc* 150: 79–88.

Fujishige, N.A., Kapadia, N.N., De Hoff, P.L., and Hirsch, A.M. (2006b) Investigations of *Rhizobium* biofilm formation. *FEMS Microbiol Ecol* 56: 195–206.

Fujishige, N.A., Lum, M.R., De Hoff, P.L., Whitelegge, J.P., Faull, K.F., and Hirsch, A.M. (2008) *Rhizobium* common nod genes are required for biofilm formation. *Mol Microbiol* 67: 504–515.

Gaddy, J.A., and Actis, L.A. (2009) Regulation of *Acinetobacter baumannii* biofilm formation. *Future Microbiol* 4: 273.

Glick, R., Gilmour, C., Tremblay, J., Satanower, S., Avidan, O., Déziel, E. et al. (2010) Increase in rhamnolipid synthesis under iron-limiting conditions influences surface motility and biofilm formation in *Pseudomonas aeruginosa*. *J Bacteriol* 192: 2973–2980.

Hindré, T., Brüggemann, H., Buchrieser, C., and Héchard, Y. (2008) Transcriptional profiling of *Legionella pneumophila* biofilm cells and the influence of iron on biofilm formation. *Microbiology* 154: 30–41.

Johnson, M., Cockayne, A., Williams, P.H., and Morrissey, J.A. (2005) Iron-responsive regulation of biofilm formation in *Staphylococcus aureus* involves Fur-dependent and Fur-independent mechanisms. *J Bacteriol* 187: 8211–8215.

Kearns, D.B. (2010) A field guide to bacterial swarming motility. *Nat Rev Microbiol* 8: 634–644.

Koh, M.L., and Toney, J. (2005) Sensitivity of *Xylella fastidiosa* biofilm to tetracycline, vancomycin, EDTA, and lactoferrin. FASEB J. 19:A276–A276.

Kuchma, S.L., Griffin, E.F., and O'Toole, G.A. (2012) Minor pilins of the type IV pilus system participate in the negative regulation of swarming motility. *J. Bacteriol* 194: 5388–5403.

Kuchma, S.L., Brothers, K.M., Merritt, J.H., Liberati, N.T., Ausubel, F.M., and O'Toole, G.A. (2007) BifA, a cyclic-di-GMP phosphodiesterase, inversely regulates biofilm formation and swarming motility by *Pseudomonas aeruginosa* PA14. *J. Bacteriol* 189: 8165–8178.

Kuiper, I., Lagendijk, E.L., Pickford, R., Derrick, J.P., Lamers, G.E.M., Thomas-Oates, J.E. et al. (2004) Characterization of two *Pseudomonas putida* lipopeptide biosurfactants, putisolvin I and II, which inhibit biofilm formation and break down existing biofilms. *Mol Microbiol* 51: 97–13.

Lai, S., Tremblay, J., and Déziel, E. (2009) Swarming motility: a multicellular behaviour conferring antimicrobial resistance. *Environ Microbiol* 11: 126–136

May, T., and Okabe, S. (2011) Enterobactin is required for biofilm development in reduced-genome *Escherichia coli*. *Environ Microbiol* 13: 3149–3162.

McDougald, D., Rice, S.A., Barraud, N., Steinberg, P.D., and Kjelleberg, S. (2012) Should we stay or should we go: mechanisms and ecological consequences for biofilm dispersal. *Nat Rev Microbiol* 10: 39–50.

Meade, H.M., and Signer, E.R. (1977) Genetic mapping of *Rhizobium meliloti*. *Proc Natl Acad Sci USA* 74: 2076–2078.

Merritt, J.H., Brothers, K.M., Kuchma, S.L., and O'Toole, G.A. (2007) SadC reciprocally influences biofilm formation and swarming motility via modulation of exopolysaccharide production and fagellar function. *J Bacteriol* 189: 8154–8164.

Mey, A.R., Craig, S.A., and Payne, S.M. (2005) Characterization of *Vibrio cholerae* RyhB: the RyhB regulon and role of *ryhB* in biofilm formation. *Infect Immun* 73: 5706–5719.

Mireles, J.R., Toguchi, A., and Harshey, R.M. (2001) *Salmonella enterica* Serovar Typhimurium swarming mutants with altered biofilm-forming abilities: surfactin inhibits biofilm formation. *J Bacteriol* 183: 5848–5854.

Nogales, J., Bernabéu-Roda, L., Cuéllar, V., and Soto, M.J. (2012) ExpR is not required for swarming but promotes sliding in *Sinorhizobium meliloti*. *J Bacteriol* 194: 2027–2035.

Nogales, J., Domínguez-Ferreras, A., Amaya-Gómez, C., van Dillewijn, P., Cuéllar, V., Sanjuán, J. et al. (2010) Transcriptome profiling of a *Sinorhizobium meliloti fadD* mutant reveals the role of rhizobactin 1021 biosynthesis and regulation genes in the control of swarming. *BMC Genomics* 11: 157.

Ojha, A., and Hatfull, G.F. (2007) The role of iron in *Mycobacterium smegmatis* biofilm formation: the exochelin siderophore is essential in limiting iron conditions for biofilm formation but not for planktonic growth. *Mol Microbiol* 66: 468–483.

Oldroyd, G.E.D., and Downie, J.A. (2008) Coordinating nodule morphogenesis with rhizobial infection in legumes. *Ann Rev Plant Biol* 59: 519–546.

Olivares, J., Casadesús, J., and Bedmar, E.J. (1980) Method for testing degree of infectivity of *Rhizobium melioti* strains. *App Environ Microb* 39: 967–970.

Overhage, J., Bains, M., Brazas, M.D., and Hancock, R.E.W. (2008) Swarming of *Pseudomonas aeruginosa* is a complex adaptation leading to increased production of virulence factors and antibiotic resistance. *J Bacteriol* 190: 2671–2679.

Pamp, S.J., and Tolker-Nielsen, T. (2007) Multiple roles of biosurfactants in structural biofilm development by *Pseudomonas aeruginosa*. *J Bacteriol* 189: 2531–2539.

Pech-Canul, Á., Nogales, J., Miranda-Molina, A., Álvarez, L., Geiger, O., Soto, M.J., and López-Lara, I.M. (2011) FadD is required for utilization of endogenous fatty acids released from membrane lipids. *J Bacteriol* 193: 6295–6304.

Persmark, M., Pittman, P., Buyer, J.S., Schwyn, B., Gill, P.R., and Neilands, J.B. (1993) Isolation and structure of rhizobactin 1021, a siderophore from the alfalfa symbiont *Rhizobium meliloti* 1021. *J Am Chem Soc* 115: 3950–3956.

Pratt, J.T., McDonough, E., and Camilli, A. (2009) PhoB regulates motility, biofilms, and cyclic di-GMP in *Vibrio cholerae*. *J Bacteriol* 191: 6632–6642.

Rinaudi, L., Fujishige, N.A., Hirsch, A.M., Banchio, E., Zorreguieta, A., and Giordano, W. (2006) Effects of nutritional and environmental conditions on *Sinorhizobium meliloti* biofilm formation. *Res Microbiol* 157: 867–875.

Rinaudi, L.V., and González, J.E. (2009) The low-molecular-weight fraction of exopolysaccharide II from *Sinorhizobium meliloti* is a crucial determinant of biofilm formation. *J Bacteriol* 191: 7216–7224.

Robertsen, B.K., Åman, P., Darvill, A.G., McNeil, M., and Albersheim, P. (1981) The structure of acidic extracellular polysaccharides secreted by *Rhizobium leguminosarum* and *Rhizobium trifolii*. *Plant Physiol* 67: 389–400.

Russo, D.M., Williams, A., Edwards, A., Posadas, D.M., Finnie, C., Dankert, M. et al. (2006) Proteins exported via the PrsD-PrsE type I secretion system and the acidic exopolysaccharide are involved in biofilm formation by *Rhizobium leguminosarum*. *J Bacteriol* 188: 4474–4486.

Sambrook, J., and Fritsch, E. (1989) Maniatis: T Molecular clonning: A laboratory manual. *Cold Spring Harbor Laboratory Press* 2: Cold Spring Harbor N.Y.

Simon, R., Priefer, U., and Pühler, A. (1983) A broad host range mobilization system for in vivo genetic engineering: Transposon mutagenesis in gram negative bacteria. *Nat Biotechnol* 1: 784–791.

Singh, P.K., Parsek, M.R., Greenberg, E.P., and Welsh, M.J. (2002) A component of innate immunity prevents bacterial biofilm development. *Nature* 417: 552–555.

Soto, M.J., Fernández-Pascual, M., Sanjuán, J., and Olivares, J. (2002) A *fadD* mutant of *Sinorhizobium meliloti* shows multicellular swarming migration and is impaired in nodulation efficiency on alfalfa roots. *Mol Microbiol* 43: 371–382.

Taguchi, F., Suzuki, T., Inagaki, Y., Toyoda, K., Shiraishi, T., and Ichinose, Y. (2010) The siderophore pyoverdine of *Pseudomonas syringae* pv. tabaci 6605 is an intrinsic virulence factor in host tobacco infection. *J Bacteriol* 192: 117–126.

Tambalo, D.D., Yost, C.K., and Hynes, M.F. (2010) Characterization of swarming motility in *Rhizobium leguminosarum* bv. *viciae*. *FEMS Microbiol lett* 307: 165–174.

Toro, N., and Olivares, J. (1986) Characterization of a large plasmid of *Rhizobium meliloti* involved in enhancing nodulation. *Mol Gen Genet MGG* 202: 331–335.

Trappetti, C., Gualdi, L., Di Meola, L., Jain, P., Korir, C., Edmonds, P. et al. (2011) The impact of the competence quorum sensing system on *Streptococcus pneumoniae* biofilms varies depending on the experimental model. *BMC Microbiology* 11: 75.

Tremblay, J., Richardson, A.-P., Lépine, F., and Déziel, E. (2007) Self-produced extracellular stimuli modulate the *Pseudomonas aeruginosa* swarming motility behaviour. *Environ Microbiol* 9: 2622–2630.

Trimble, M.J., and McCarter, L.L. (2011) Bis-(3′-5′)-cyclic dimeric GMP-linked quorum sensing controls swarming in *Vibrio parahaemolyticus*. *Proc Natl Acad Sci USA* 108: 18079–18084.

Verstraeten, N., Braeken, K., Debkumari, B., Fauvart, M., Fransaer, J., Vermant, J., and Michiels, J. (2008) Living on a surface: swarming and biofilm formation. *Trends Microbiol* 16: 496–506.

Wells, D.H., Chen, E.J., Fisher, R.F., and Long, S.R. (2007) ExoR is genetically coupled to the ExoS–ChvI two-component system and located in the periplasm of *Sinorhizobium meliloti*. *Mol Microbiol* 64: 647–664.

Wu, Y., and Outten, F.W. (2009) IscR controls iron-dependent biofilm formation in *Escherichia coli* by regulating type I fimbria expression. *J Bacteriol* 191: 1248–1257.

2.7. Suplementary material

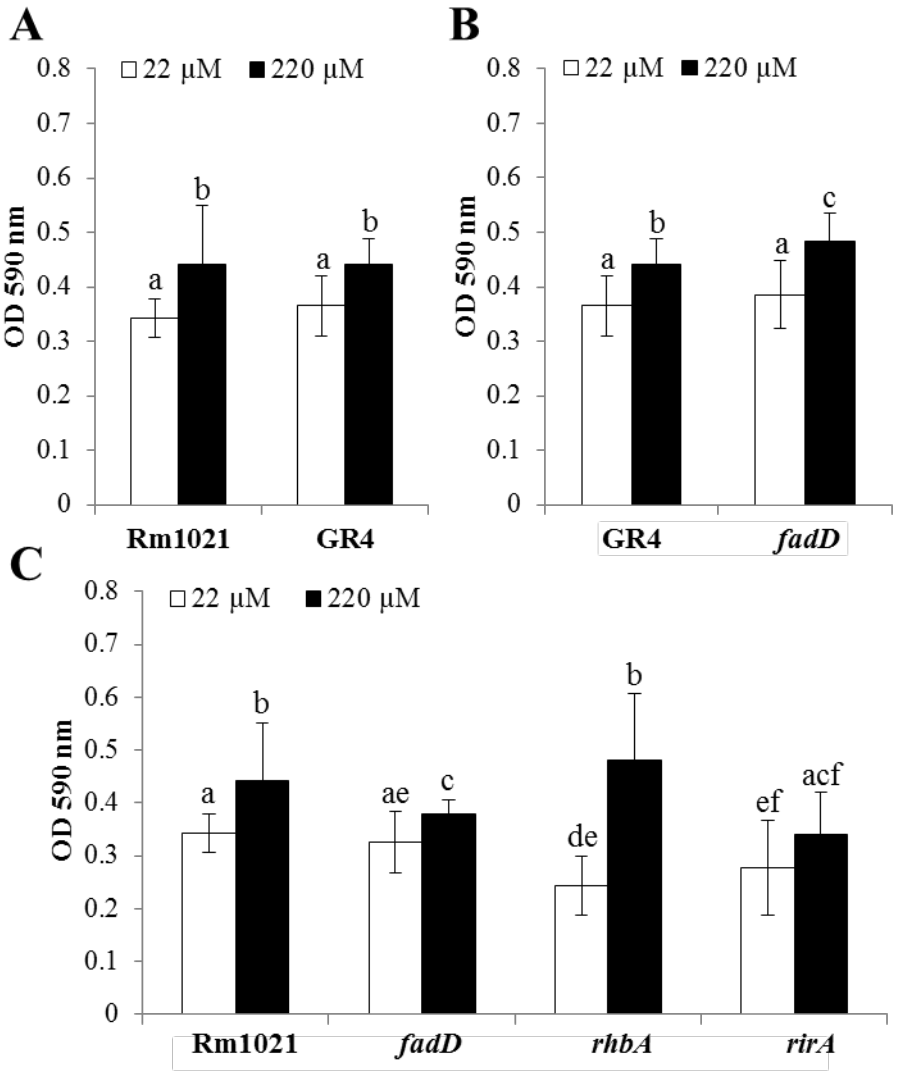

Figure S2.1. Baterial growth in MM containing different concentrations of iron on PVC microtiter plates. Bacterial growth of the A) wt strains, Rm1021 and GR4, B) GR4 and its *fadD* derivative mutant and C) Rm1021 and ist dreivative mutant starains. Each data point is the average of at least 20 wells from the representative experiment in which biofilm formation on PVC was determined. Error bars indicate the standard deviation of the mean. According to the Games-Howell test ($P \leq 0.05$) growth values followed by the same letter do not differ significantly. Each experiment was repeated by triplicate.

CHAPTER 3: Role of siderophore Rhizobactin 1021 (Rhb1021) in *Sinorhizobium meliloti* surface-associated behaviors

Role of siderophore Rhizobactin 1021 (Rhb1021) in *Sinorhizobium meliloti* surface-associated behaviors.

Carol V Amaya-Gómez[1,2], Lijiang Song [2], Joaquina Nogales[1], Gregory Challis[2] and Soto, María J[1].

[1]Departamento de Microbiología del Suelo y Sistemas Simbióticos, Estación Experimental del Zaidín, CSIC, 18008 Granada, Spain. [2]Department of Chemistry, University of Warwick, CV4 7AL Coventry, United Kingdom

In preparation.

3.1. Abstract

Under iron-limiting conditions, *Sinorhizobium meliloti* Rm1021 produces rhizobactin 1021 (Rhb1021), an unusual citrate-based dihydroxamate siderophore with an enoyl-lipid moiety. Our recent investigations have shown that besides its function in iron uptake, Rhb1021 also plays a crucial role in the surface motility and biofilm development of *S. meliloti* Rm1021 by a mechanism which cannot exclusively be attributed to iron nutrition. In this work, we attempted to gain further insights into the additional role/s played by Rhb1021 in the two surface-associated phenotypes. Drop collapse assays performed with purified Rhb1021 revealed that this siderophore shows surfactant activity that could impact both surface motility and biofilm formation. Furthermore, *S. meliloti* deletion mutants in either of the two genes (*rhbD* and *rhbG*) potentially involved in incorporating the acyl moiety into Rhb1021 were obtained and characterized. Our results clearly demonstrate that contrary to what was previously proposed, *SMa2339* (*rhbG*) is not responsible for incorporating the lipid moiety into Rhb1021 and at present its function remains unknown. Moreover, in contrast to genes belonging to the *rhbA-F* operon, *rhbG* is not essential for either siderophore synthesis or surface motility in *S. meliloti* although it influences bacterial surface-associated phenotypes. Loss-of function of *rhbG* promotes flagella-independent surface translocation and interferes with normal biofilm development with similar effects as those observed with *rhbA* and *rhbD* mutants. In addition, the *rhbG* mutation led to an accumulation of (2E)-N-[3-(acetylamino)propyl]-N-hydroxydec-2-enamide) in culture supernatants and to a decreased production of Rhb1021. Comparison of the transcriptome profiles of Rm1021 and an *rhbD* derivative mutant after growth on semisolid surfaces revealed that either Rhb1021 or some of its biosynthetic intermediates, are required to enable maximal expression of the siderophore synthesis and uptake genes.

3.2. Introduction

Soil bacteria known collectively as the rhizobia are able to establish nitrogen-fixing symbiosis with leguminous plants. During the symbiotic interaction, the bacteria induce the formation of the root nodules, within which they differentiate into bacteroids that are able to convert atmospheric nitrogen to ammonia which can be assimilated by the host plant. There is a high demand of iron in the *Rhizobium*-legume interaction. Different proteins with crucial roles in the symbiosis contain iron, like the nitrogenase enzyme complex responsible for the nitrogen fixation reaction, or the high abundant nodule protein leghemoglobin that buffers the oxygen level to avoid inactivation of the nitrogenase complex. In addition, as soil-dwelling bacteria, rhizobia must compete to acquire iron. Despite its abundance on earth, iron is biologically unavailable in most environments. Under aerobic and neutral conditions, iron is present essentially in the oxidized ferric form Fe(III) which forms insoluble polymers. One of the strategies that microorganisms have evolved to obtain iron under limiting conditions is the production and excretion of low-molecular high-affinity iron chelators, termed siderophores which are able to scavenge iron from many different sources (Wandersman and Delepelaire, 2004). Many species of rhizobia have been reported to produce siderophores (Johnston et al., 2004). *Sinorhizobium meliloti* Rm1021, the endosymbiont of alfalfa (*Medicago sativa*), produces the siderophore rhizobactin 1021 (Rhb1021) (Persmark et al., 1993). Rhb1021 is a citrate-based dihydroxamate siderophore structurally similar to schizokinen, a siderophore produced by *Bacillus megaterium* (Mullis et al., 1971) and *Rhizobium leguminosarum* IARI 917 (Storey et al., 2006), and aerobactin, a well-known siderophore produced by *Escherichia coli* (Challis, 2005a) (Fig. 3.1). The most remarkable feature of Rhb1021 structure is the lipid moiety ((E)-2-decenoic acid) that gives the siderophore an asymmetric structure and is responsible for its amphiphilic properties. Very few siderophores have been reported to have a lipid moiety. Some examples of this type of siderophores are mycobactin (Gobin and Horwitz, 1996), siderophores produced by different marine bacteria (Martin et al., 2006; Gauglitz et al., 2012), and synechobactins produced by the marine

cyanobacteria *Synechococcus* sp. PCC7002 (Ito and Butler, 2005). The latter are very similar to Rhb1021 differing only in the nature of the acyl moiety (octanoic, decanoic or dodecanoic acids) (Fig. 3.1).

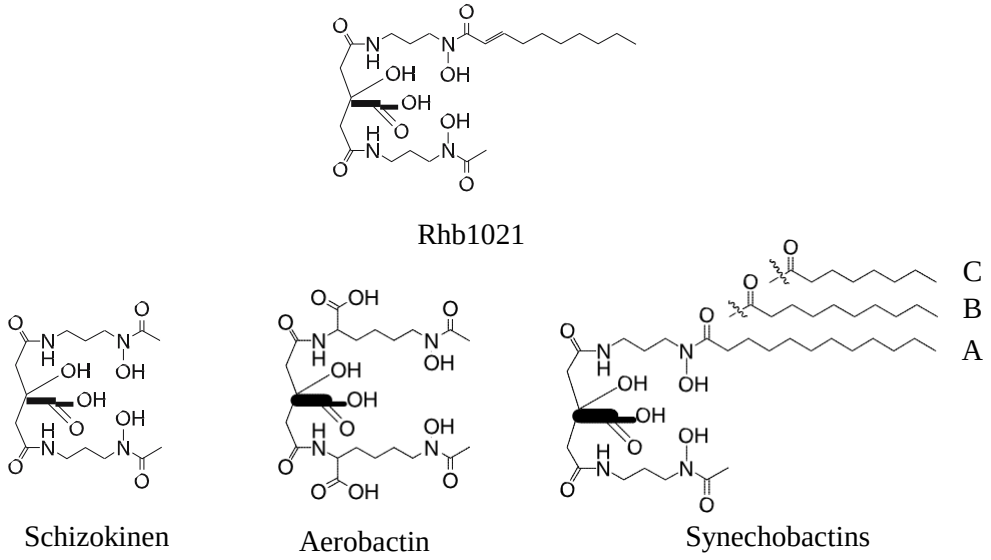

Figure 3.1. Structure of citrate-based dihydroxamate siderophores. Rhb1021, rhizobactin 1021.

Rhb1021 biosynthesis and transport requires participation of at least nine genes located on the pSymA megaplasmid of *S. meliloti* Rm1021 (Lynch et al., 2001; Ó Cuív et al., 2004) (Fig. 3.2). Six of the genes, *rhbABCDEF*, form an operon and code for different enzymes involved in the biosynthesis of the siderophore. The products of the *rhtA* and *rhtX* genes participate in the uptake of Rhb1021, coding for the outer membrane receptor and inner membrane permease, repectively, of the siderophore. The *rhrA* gene located between the *rhb* and *rhtA* genes, codes for an AraC-type transcriptional activator that positively regulates the expression of genes involved in the synthesis (*rhb*) and uptake (*rht*) of the siderophore (Lynch et al., 2001). Rhb1021 production is regulated in response to environmental iron availability through the global iron response regulator, RirA (Chao et al., 2005; Viguier et al., 2005). Under iron sufficient conditions, this regulator prevents expression of the *rhb* and *rht* genes, an indirect regulation that takes place by repressing transcription of *rhrA*. The chrome azurol S (CAS) assay exhibited that disruption of either the *rhbABCDEF* operon or the *rhrA* gene

prevents siderophore production. However, disruption of *rhtA* or *SMa2339* (*rhbG*), both located in another cluster downstream of *rhrA*, did not abolish the siderophore synthesis (Lynch et al., 2001).

Figure 3.2. Genetic organization of Rhb1021-related genes. Rhb1021 biosynthesis genes are highlighted in grey, the transporter genes in white and the gen that codes for the regulator of the synthesis and uptake genes in black.

Lynch et al. (2001) and Challis (2005a) have proposed two different biosynthetic pathways to Rhb1021 (Fig. 3.3). Their proposals were based on: 1) the sequence homology between RhbA and RhbB with the *dat* and *dcc* gene products, enzymes of *Acinetobacter baumannii* involved in the production of 1,3-diaminopropane and 2) the structural similarities between Rhb1021 and aerobactin together with the homology shown by RhbC, RhbD, RhbF and RhbE with the aerobactin synthesis proteins IucA, IucB, IucC and IucD, respectively. According to Lynch et al. (2001) RhbD catalyses the acetylation of **1** (N^4-hydroxy-1-aminopropane) leading to the formation of **2** (N^4-acetyl-N^4-hydroxy-1-aminopropane). Subsequently, RhbC and RhbF add two molecules of **2** to each of the extremes of citric acid resulting in the synthesis of a molecule structurally identical to schizokinen. Finally, the enoyl lipid tail is bound to this molecule in a reaction that could be catalyzed by RhbG, leading to Rhb1021. On the other hand, Challis (2005b) suggested that **1** might be the substrate of two enzymes: RhbD which catalyzes the acetylation reaction leading to **2**, and RhbG which catalyses the acylation of **1** with 2-decenoyl CoA to form **3** (N^4-decenoyl-N^4-hydroxy-1-aminopropane). In the subsequent step, either **2** or **3** are bound to citric acid to form **4** by RhbC, and then, RhbF would catalyse the last reaction that leads to the formation of Rhb1021.

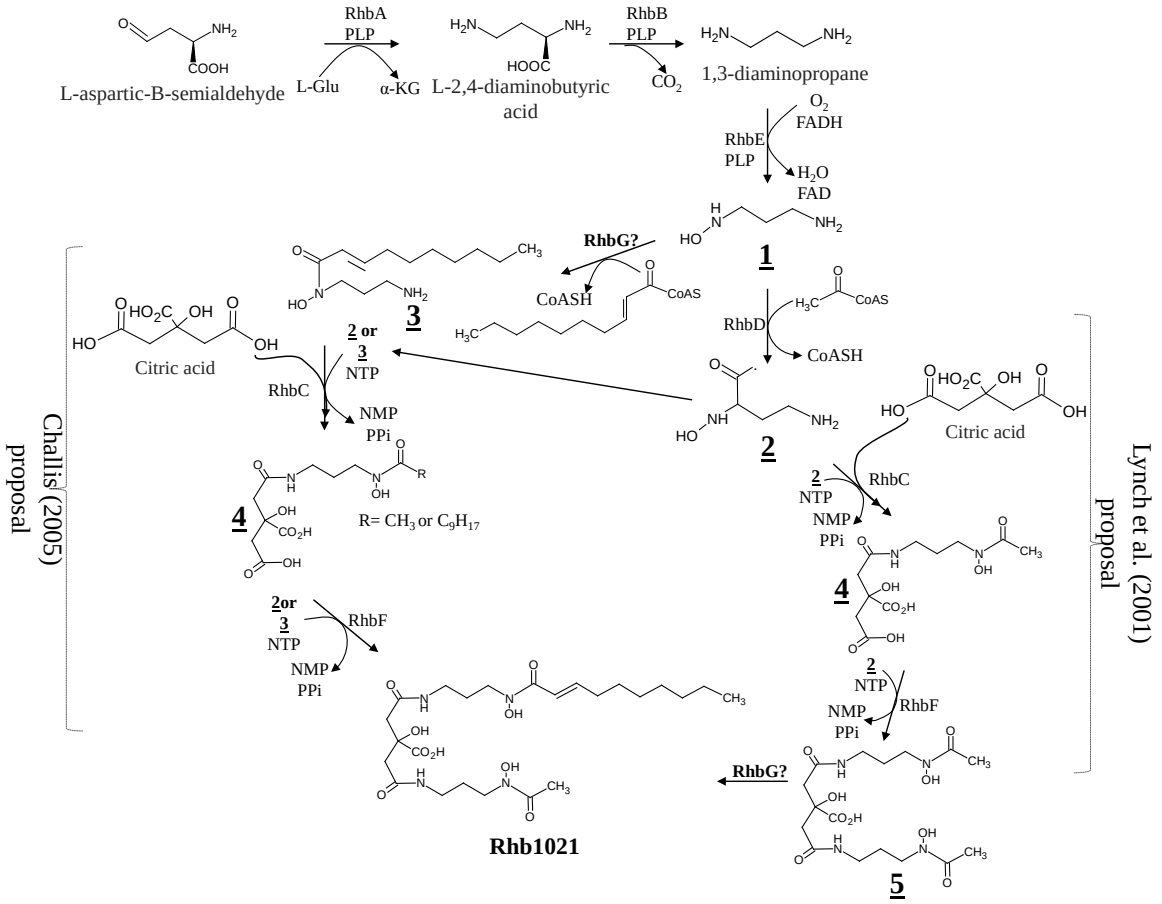

Figure 3.3. Rhb1021 biosynthesis pathway proposals made by Challis (2005) and Lynch et al. (2001). Challis (2005) proposal is shown on the left and Lynch et al. (2001) proposal is shown on the right. N^4-hydroxy-1-aminopropane (**1**), N^4-acetyl-N^4-hydroxy-1-aminopropane (**2**), N^4-decenoyl-N^4-hydroxy-1-aminopropane (**3**), e or 2-[2-({3-[(2*E*)-decenoyl(hydroxy)amino]propyl}amino)-2-oxoethyl]-2-hydroxybutanedioic acid (**4**).

Besides its function as siderophore, Rhb1021 has also been shown to be a key factor during surface motility and biofilm development of *S. meliloti* Rm1021 (Nogales et al., 2010; Amaya-Gómez et al., submitted). This strain can move over surfaces using at least two different types of motility (Nogales et al., 2012). One is a flagella-driven movement known as swarming that enables groups of bacteria to move coordinately atop semisolid surfaces. The other type of surface spreading is known as sliding. Sliding is defined as passive translocation of bacteria over a surface promoted by expansive forces of bacterial growth. The production of surfactant agents which reduce the friction between cells and surfaces, is required for both swarming and sliding to take place. We demonstrated that

mutations and environmental conditions (high iron levels) that abolish Rhb1021 production prevent surface translocation in *S. meliloti* (Nogales et al., 2010; Nogales et al., 2012). On the contrary, an *rhtA* mutant (defective in Rhb1021 utilization) can translocate over semisolid surfaces. This indicated that low intracellular iron levels are not responsible for the inability to swarm shown by Rhb1021-defective mutants and suggested that the function carried out by Rhb1021 in swarming is exerted outside the cell (Nogales et al., 2010). We hypothesize that surfactant properties inherent to Rhb1021 might be responsible for its role in promoting bacterial motility over surfaces.

Investigations performed in our group have demonstrated that Rhb1021 is also an important factor for biofilm formation in *S. meliloti*. Biofilms consist of groups of bacteria attached to surfaces and encased in a hydrated polymeric matrix. Disruption of the *rhbA* gene in *S. meliloti* Rm1021, interferes with the formation of thick and robust biofilms on glass surfaces and *in planta* (Amaya-Gómez et al., submitted). As observed for swarming, the biofilm phenotype of the *rhbA* mutant strain was not restored in the presence of high concentrations of iron indicating that the function of this siderophore in biofilm establishment cannot attributed only to iron acquisition. It has been speculated that the essential role of Rhb1021 in biofilm formation by *S. meliloti* is the result of it displaying two important functions that in the case of other bacteria (e.g. *Pseudomonas aeruginosa*) are exerted by two different molecules: as a siderophore participating in controlling intracellular iron levels, and as biosurfactant facilitating the formation of microcolonies and influencing biofilm architecture.

Another non-excluding possibility could be that Rhb1021 exerts its function in surface motility and biofilm formation as a signal molecule. There are examples in the literature of siderophores and surfactants that also play a role as signal molecules. The siderophore pyoverdine produced by *P. aeruginosa* works also as a signal molecule inducing the production of virulence factors: pyoverdine itself, PrpL and AprA proteases, and exotoxin A (Lamont et al., 2002).

Furthermore, the siderophore mediates the production of the ferric-pyoverdine receptor FpvA (Visca et al., 2002). On the other hand, the *N*-acylhomoserine lactones (NHLs) produced by *Rhizobium etli* have a dual role in swarming in this *Rhizobium*: as quorum sensing signals and as biosurfactants which promote surface translocation (Daniels et al., 2006).

In this work, we sought to get further insights about the role played by Rhb1021 in bacterial surface spreading and biofilm formation in *S. meliloti* Rm1021. To achieve this goal, Rhb1021 was purified, analyzed for surfactant properties, and used to complement the surface motility and biofilm formation phenotypes of *rhb* mutants. In addition, to test if the role played by Rhb1021 in surface motility and biofilm formation was associated to its surfactant properties, we obtained and characterized in-frame deletion mutants in two genes, *rhbD* and *rhbG,* that could be involved in incorporating the acyl moiety into the siderophore. Finally, we also investigated the possible function of Rhb1021 as a signal molecule by comparing the transcriptome profile of *S. meliloti* wild type with that of an Rhb1021-defective mutant.

3.3. Material and Methods

Bacterial strains, plasmids and culture conditions

The bacterial strains and plasmids used in this study are listed in Table 3.1. *E. coli* strains were grown in Luria-Bertani medium (LB) (Sambrook and Fritsch, 1989) at 37° C. *S. meliloti* strains were grown at 30° C either in Triptone-Yeast extract complex medium (TY) (Beringer, 1974), in Bromfield medium (BM) (0.04% tryptone, 0.01% yeast extract, and 0.01% $CaCl_2.2H_2O$) or in Minimal Medium (MM) containing glutamate (6.5 mM), mannitol (55 mM), mineral salts (K_2HPO_4, 1.3 mM; KH_2PO_4 $3H_2O$, 2.2 mM; $MgSO_4$ $7H_2O$, 0.6 mM; $CaCl_2$ $2H_2O$, 0.34 mM; $FeCl_3$ $6H_2O$, 0.022 mM; NaCl, 0.86 mM) and vitamins (biotin (0.2 mg/L); calcium pantothenate (0.1 mg/L)) (Robertsen et al., 1981). Standard MM contains 22μM $FeCl_3$. In order to prepare MM containing 220 μM $FeCl_3$, MM

without iron was supplemented with a 100 fold concentrated stock solution of $FeCl_3$. Iron-deficient liquid medium (IDM) (Müller and Raymond, 1984), was used to enhance Rhb1021 production. IDM contained K_2SO_4 (11.5 mM), K_2HPO_4 (17.2 mM), NaCl (17.1 mM) and NH_4Cl (93.5 mM). These salts were made iron deficient by stirring over night the solution with 100 g/l of Chelex (Na^+ form). Thiamine (2 mg) and trace elements were added: 7.98 mM $CuSO_4$, 5.92 mM $MnSO_4$ H_2O, 0.57 M $ZnSO_4$ $7H_2O$, 19.71 M $MgSO_4$ $7H_2O$. $CaCl_2$ (0.9 mM), sucrose (13 mM) and yeast extract (5 %) were sterilized by filtration as a 1 % stock solution and added to the IDM just before being used. To determine the optimal conditions of Rhb1021 production IDM was supplemented with different concentrations of ferric chloride (1 µM, 5 µM, 10 µM), fumarate (12.5 mM), cysteine (12.5 mM), a mix of fumarate and cysteine (12.5 mM), or citric acid (500 µM, 8 mM, 12.5 mM). Ferric chloride was added to the IDM from the beginning and cultures were allowed to grow during 4 days (O.D. 600nnm 1). The rest of the compounds tested to enhance siderophore yields, were added to the IDM when cultures reached the mid log phase (48 h). Subsequently, the cultures were allowed to grow during 4 days more until they reached an OD_{600nm} of 1-1.2. When required, antibiotics were added at the following final concentrations: for *E. coli*, Ampicillin (Ap) 200 µg/ml, kanamycin (Km) 50 µg/ml and tetracycline (Tc) 10 µg/ml; for *S. meliloti*, streptomycin (Sm) 200 µg/ml, Km 100 µg/ml, neomycin sulphate (Nm) 100 µg/ml, and Tc 10 µg/ml. The ability of the different strains to grow in liquid TY, BM and MM was monitored by measuring the optical density (OD) at 600nm using spectrophotometer (Pharmacia LBK, Novaspec II), until they reached the stationary phase.

Table 3.1. Strains and plasmids used in this study

Strain or plasmid	Relevant characteristics	Source or reference
Escherichia coli		
DH5α	*supE*44, Δ*lacU*169, *f*80, *lacZ*ΔM, *recA*1, *endA*1, *gyrA*96, *thi*1, *relA*1, *5hsdR*171	Bethesda Research Lab®
S17.1	*thi*, *pro*, *recA*, *hsdR*, *hsdM*, Rp4Tc::Mu, Km::Tn*7*; Tp^r, Sm^r, Sp^r	(Simon et al., 1983)
Sinorhizobium meliloti		
Rm1021	SU47 *expR102*::IS*Rm*2011-1, Sm^r	(Meade and Signer, 1977)
1021rhbA	Rm1021 *rhbA*::Tn*5lac*; Sm^r Nm^r	(Nogales et al., 2012)
1021rhbD	Rm1021 Δ*rhbD*; Sm^r	This study
1021rhbG	Rm1021 Δ*SMa2339*; Sm^r	This study
G212rirA	Rm1021 (lac^-, *rirA*::Km), Sm^r Km^r	(Osterås et al., 1995)
Rm2011	Wild type, Sm^r	(Casse et al., 1979)
2011rhtA1	Rm2011 (*rhtA::*Tn*5*), Sm^r Rif^r Nm^r	(Lynch et al., 2001)
Rm1021-*gfp*	Rm1021 harboring the pHC60 plasmid;Sm^r Tc^r	(Carol V. Amaya-Gómez. et al., unpublished)
1021rhbD-*gfp*	1021rhbD harboring the pHC60 plasmid; Sm^r Tc^r	This study
1021rhbG-*gfp*	1021rhbG harboring the pHC60 plasmid; Sm^r Tc^r	This study
Plasmids		
pGem-T Easy	Cloning vector; Ap^r	Promega
pK18mobsacB	Suicide plasmid; Km^r	(Schäfer et al., 1994)
pG-ΔrhbD	pGem-T Easy carrying the deleted version of *rhbD*; Ap^r	This study
pG-ΔrhbG	pGem-T Easy carrying the deleted version of *rhbG*; Ap^r	This study
pK-ΔrhbD	pK18*mobsacB* carrying the deleted version of *rhbD*; Km^r	This study
pK-ΔrhbG	pK18*mobsacB* carrying the deleted version of *rhbG*; Km^r	This study
pHC60	Stable *Rhizobium* plasmid constitutively expressing GFP, Tc^r	(Cheng and Walker, 1998)

Construction of plasmids and *S. meliloti* mutants

Unless otherwise indicated, standard protocols of DNA manipulation and related techniques were used as described previously (Maniatis et al., 1989). Restriction endonucleases and ligase (Roche) were used according to the manufacturer's instructions. The SMa2339 (*rhbG*) deletion was generated in vitro by overlap extension PCR (Ho et al., 1989) using primers rhbGA1 and rhbGD4 (Table 3.2). The resulting fusion product, in which a deletion of 1640 bp was

created, was cloned into pGem-T Easy and sequenced. Using the *Hind*III restriction sites included in the outside primers, the insert was cloned into pK18*mobsacB* yielding plasmid pK-ΔrhbG. This construction was introduced into Rm1021 via conjugation with S17-1 and allele replacement events were selected as described previously (Schäfer et al., 1994). Likewise, the deletion of *rhbD* was generated by *in vitro* overlap extension PCR using the primers rhbD1 and rhbD4 listed in table 3.2. The resulting PCR product, in which deletion of 435 bp was created was cloned into pGem-T Easy, sequenced, and by using the restriction sites included in the outside primers, subcloned into vector pk18*mobsacB*. The pK-ΔrhbD was introduced into Rm1021, and after allelic replacement 1021rhbD was obtained. Mutants 1021rhbG and 1021rhbD were confirmed by PCR and Southern hybridization with specific probes.

Table 3.2. Primers used in *rhbG* and *rhbD* deletions

Primer	Sequence (5´ to 3´)*	Aplication
rhbGA1	AAAAAGCTTAGGTCTACGCCAATTTCAGC (*Hind*III)	*rhbG* deletion
rhbGB2	GGAGATCGACATGAGAAAGGAGCGAAAG	*rhbG* deletion
rhbGC3	CTTTCGCTCCTTTCTCATGTCGATCTCC	*rhbG* deletion
rhbGD4	AAAAAGCTTCGATAGACGTTACCGTCACG (*Hind*III)	*rhbG* deletion
rhbD1	ATAAAGCTTAGAACATCGTGGTCGAGATC (*Hind*III)	*rhbD* deletion
rhbD2	TTGTCGGGAAGGTCGAAGCTGATCGTCC	*rhbD* deletion
rhbD3	GGACGATCAGCTTCGACCTTCCCGACAA	*rhbD* deletion
rhbD4	TAAGGATCCGGTGCCAACGTCTTGATCTG (*Bam*HI)	*rhbD* deletion

* Restriction sites used for cloning (underlined) are given in parenthesis.

Motility assays

Swarming assays were performed as previously described by Soto et al. (2002), with the only modification of using Noble agar (Difco™) instead of purified agar (Pronadisa). Plates were incubated overnight (14–20 h) at 30 ºC. To test sliding motility, plates with semisolid MM were prepared following the procedure used for swarming motility assays. The migration zone of swarming and sliding colonies was measured as the average length of the two sides of a rectangle exactly able to frame each colony 20 h post inoculation. Swimming tests were carried out in Bromfield media (BM) as described previously (Nogales et al., 2012).

Biofilm formation assay

S. meliloti strains, constitutively expressing the green fluorescent protein (GFP) were used to observed the different stages of biofilm development. Biofilms were established on chamber covered glass slides containing a 1-µm-thick borosilicate glass base (Lab-Tek no. 155411; Nunc) as described Russo et al. (2006). Rhizobial cells grown to OD_{590nm} = 2 in MM were washed twice, and diluted (OD_{600nm} = 0.2) in MM. 500 µl of the diluted cultures were placed on the wells of the chamber and bacteria were allowed to grow without agitation at 30 ºC for up to 10 days. To prevent desiccation, the chambers were incubated in a sterile Petri dish under humidified conditions. At defined times, the growth media was removed, and unbound bacteria were eliminated by washing each chamber with 500 µl of sterile water. A confocal laser scanning inverted microscope Nikon Eclipse TE2000-U (Nikon Instruments, Melville, NY) motorized using 488-nm argon laser excitation and 500-nm long-pass emission filter was used to visualize the different events of biofilm formation. Confocal images were processed by using the digital image processing Nikon software, EZ-C1 Freeviewer (Nikon).

Drop collapse assay

The drop collapse test was performed as reported previously Caiazza et al. (2005). First, the swarming assay of *S. meliloti* strains was performed as specified above. The cell mass of the different strains grown on semisolid MM plates was scraped and resuspended in phosphate-buffered saline (PBS). The OD of the cell suspension was measured at 600 nm using a spectrophotometer (Pharmacia LBK, Novaspec II) and adjusted to OD_{600nm} of 8 using PBS. Cells were removed by centrifugation and the supernatants were kept. 20 µl-drops of the supernatant were spotted on the underside of the lid of a 96-well polystyrene microtiter plate. When the samples contained surfactants, the diameter of the bead was larger than that of PBS or no bead formation was observed. A drop of SDS (0.02%) was used as positive control.

Siderophore detection by CAS assay

The determination of siderophores in MM broth was performed using the Chrome azurol S (CAS) assay solution described by Schwyn and Neilands (1987). Supernatants of *S. meliloti* cultures grown in MM containing 22 µM of $FeCl_3$ were mixed 1:1 with the CAS assay solution. After 20 min of incubation in darkness, the absorbance was measured at 630 nm.

High resolution Liquid Chromatography- Mass Spectrometry (LC-MS)

The organic compounds present in the culture supernatants (including Rhb1021) of the wild-type and mutant strains of *S. meliloti* grown in IDM supplemented with different compounds were visualized by using LC-MS. Cells were removed by centrifugation and 20 µl of the spent supernatant were injected to perform the analysis. LC-MS analysis was carried with Dionex 3000RS UHPLC coupled with Bruker MaXis Q-TOF mass spectrometer. Sigma Ascentis Express columns (C18, 150x2.1mm) with different particles size were used to analyse the supernatant of rhizobial cultures. For the analysis of Rm1021 vs G212rirA or Rm1021 vs 1021rhbG a column with 2.7µm particle size was used, while for the analysis of Rm1021 vs 1021rhbD a column with a 1.8µm particle size was employed. Mobile phases consisted of A (water with 0.1% formic acid) and B (methanol with 0.1% formic acid). A gradient of 0% B to 100% B in 20 minutes and then isocratic at 100% B for 5 minutes was employed with flow rate at 0.2 ml/min, UV was set at 240 nm. Mass spectrometer was operated in electrospray positive mode with a scan range 50-2,000 m/z. Source conditions are, end plate offset at -500 V; capillary at -4500 V; nebulizer gas (N_2) at 1.6 bar; dry gas (N_2) at 8 l/min; dry temperature at 180° C. Ion transfer conditions as, ion funnel RF at 200 Vpp; multiple RF at 200 Vpp; quadruple low mass set at 55 m/z; collision energy at 5.0 ev; collision RF at 600 Vpp; ion cooler RF at 50-350 Vpp; transfer time set at 121 µs; pre-Pulse storage time set at 1 µs. Calibration was done with sodium formate (10 mM) through a loop injection of 20 µl of standard solution at beginning of each run.

Purification of Rhb1021 and the molecule overproduced by 1021rhbG (RhbGdec)

The 250 ml of culture used to purify Rhb1021 were obtained growing G212rirA in 50 ml plastic flasks containing 5 ml of IDM supplemented with 10 μM of $FeCl_3$ incubated in rotary shaker at 30 ºC during 4 days (OD_{600nm} of 1.5). In order to purify 1021rhbG overproduced molecule (RhbGdec), 50 ml of 1021rhbG culture were obtained growing this strain in plastic flasks of 50 ml containing 5 ml of IDM supplemented with 500 μM of citric acid. Citric acid was added to the media when 1021rhbG cultures grown in IDM alone reached an OD_{600nm} of 0.5 (48 h after inoculation). Then, 1021rhbG cultures were allowed to grow during 4 days more until they reached an $OD_{600\ nm}$ of 1.2. The 250 ml of G212rirA culture were distributed in aliquots of 50 ml. The aliquots of 50 ml of G212rirA culture, and the 50 ml of culture of 1021rhbG, were pelleted by centrifugation and the supernatant of cells was kept and lyophilized. Each 50 ml of dried material were dissolved in 4 ml of methanol: water (80:20). Rhb1021 (*m/z* 531, [m+H]) or rhbGdec (*m/z* 372.02, [M+Na]+) were purified by High-Performance Liquid Chromatography (HPLC). An Agilent 1100 Semi-preparative HPLC was used to purify the target compounds with a reverse phase column (21 × 100 mm, C18, 5 μm particle size), equipped with guard cartridge 21 × 10 mm. Aliquots of 500 μl were injected into the column (20 injections for Rhb1021 and eight for RhbGdec in total) and eluted using a gradient of solvent A consisting of H_2O containing 0.1% formic acid (HCOOH) and solvent B consisting of methanol containing 0.1% HCOOH at a constant flow-rate of 5 ml/min. The elution profile was as follows: 65:35 solvent A/solvent B for 5 min, then 0:100 solvent A/solvent B over 30 min. Fractions containing target compounds were pooled together based on High Resolution Mass Spectrometry (HRMS) analysis and freeze-dried after the organic solvent was removed under reduced pressure at room temperature. The retention time for *m/z* 531 was 27.3-28.3 min, and for *m/z* 372.2 was 27.3-29 min. The initial purified material was resuspended in 2 ml of 60:40 MetOH/H_2O and further purified by a second HPLC using the same column with a different elution profile (70:30 solvent A: solvent B for 5 min, then 0:100 solvent A: solvent B over

30 min). The fractions collected containing *m/z* 531 (retention time 14.8-17.8) and *m/z* 372.2 (retention time 17.8-18.5 min) were pooled together and then freeze-dried after the solvent had been removed under reduced pressure. The residues were dried under vacuum and dissolve in 0.1 % trifluoroacetic acid in 50% methanol:water overnight. The main peak of a last HPLC using the same column and elution profile of the second HPLC was collected. The solvent from the collected fraction containing m/z 531 or m/z 372.2 was removed under rotary evaporator. The structure of the compounds was determined by Nuclear Magnetic Resonance (NMR). All NMR experiments (^{1}H, correlation spectroscopy (COSY), heteronuclear single quantum coherence spectroscopy (HSQC) and heteronuclear multiple bond correlation (HMBC)) were carried out with a Bruker Avance 700 MHz equipped with a TCI Cryoprobe at 25° C. Free-dried crude sample and purified samples were dissolved in 200 µl of DMSO and 180 µl of this solution was transferred into a 3 mm NMR tube.

Complementation assays

In order to test the ability of Rm1021 and the siderophore mutant 1021rhbA to grow in presence of DMSO and Rhb1021, bacteria were grown in MM supplemented with purified Rhb1021 to a final concentration of 10 µM, 20 µM and 50 µM. The OD at 600 nm of the cultures was monitored until they reached the stationary phase. For complementation of the surface motility assays, purified Rhb1021 was added to either TY cultures or to washed concentrated cell suspension at final concentrations of either 20 µM or 100 µM. The surface motility assays were performed as described above. The biofilm complementation assay was carried out by adding Rhb1021 to a final concentration of 100 µM into the 500 µl of the cell suspension (OD_{600nm}=0.2) which was placed into the chambered cover glass slide. The biofilm formation was visualized as described above.

Sample preparation, RNA isolation and synthesis of labelled cDNA for transcriptomic analyses

S. meliloti Rm1021 and 1021rhbD cells were grown in 20 ml of TY broth to late logarithmic phase ($OD_{600\ nm}$ = 1-1.2). Cells were washed twice in MM and resuspended in 0.1 volume of the latter medium (2 ml). Aliquots of 100 µl of the rhizobial suspension were evenly spread over the surface of semisolid MM (10^9 cells/plate), allowed to dry for 10 min and then inverted and incubated at 30 ºC. Samples from plates were collected at different time points for cell count determination. Cells were harvested by scraping the surface with 2 ml of MM. For RNA isolation, cells grown on the surface of 3 plates during fourteen hours were harvested, washed with sarkosyl 0.1% and cell pellets were immediately frozen in liquid nitrogen and conserved at -80°C until RNA isolation. RNA was isolated using the Qiagen RNeasy RNA purification kit (Qiagen). Residual DNA was removed with RNase-free Dnase I Set (ROCHE). All manipulations were performed according to the manufacturer's instructions. Samples purity and concentration were assessed by spectrophotometry (NanoDrop ND-1000) and on 1.4% agarose gel electrophoresis. Only samples showing ratios of A260/A280 and 260/230 superior to 2 were used.

Cy3- and Cy5-labelled cDNAs were prepared according to (DeRisi et al., 1997) from 15 µg of total RNA. Three slide hybridizations were performed using the labeled cDNA synthesized from each of the RNA preparations from three independent bacterial cultures.

Sm14KOLI microarray hybridization and data analysis

Sm14KOLI microarrays were purchased from A. Becker (University of Bielefeld, Bielefeld, Germany). Hybridizations were performed as described previously Nogales et al. (2010). Image acquisition was performed using a GenePix 4100A scanner (Axon Instruments, Inc., Foster ciry, CA, USA). Lowest normalization and significance test (Holm) were performed with the EMMA 2.6

microarray data analysis software (http://www.genetik.uni-bielefeld.de/EMMA/) (Dondrup et al., 2003). Only genes showing a *p*-value < 0.05, A ≥ 6.95 and either M ≥ 0.9 or M ≤ -0.9 (A, average signal to noise; M value is $\log_2$ experiment/control ratio) were considered for data analysis. Detailed protocols and raw data resulting from the microarray experiments have been deposited in the ArrayExpress database with the accession number E-MEXP-3769.

Reverse transcription quantitative real-time PCR (RT-qPCR)

Total ARN (1 μg) isolated as previously described, treated with RNase-free Dnase I Set (ROCHE), was reversely transcribed using Superscript II reverse transcriptase (INVITROGEN) and random hexamers (ROCHE) as primers. Quantitative real-time PCR was performed on an iCycler IQ5 (Bio-Rad, Hercules, CA, USA). The 16S rRNA gene was used as housekeeping control. Cycling parameters were 3 min at 95 ºC followed by 35 cycles of 30 s at 95 ºC, 45 s at 55 ºC and 45 s at 72 ºC. Each 25 μl reaction contained either 1 μl of the cDNA or a dilution (1:10.00, for amplification of the 16S rRNA gene), 200 nM of each primer IQ SyBrGreen Supermix (Biorad). Control PCR reactions of the RNA samples not treated with reverse transcriptase were also performed to confirm the absence of contaminating genomic DNA. A melting curve was conducted to ensure amplification of a single product. Sequences of primers used for RT-qPCR analysis are listed in table 3.3. The relative expression of each gene was normalized to that of 16 S rRNA and the fold-change was calculated using the comparative critical threshold $\Delta\Delta C_T$ method (Pfaffl, 2001).

Table 3.3. Sequences of the primers used for quantitative real-time PCR.

Gene	Forward Primer (5' to 3')	Reverse Primer (5' to 3')
SMc03224 (16S)	TCTACGGAATAACGCAGG	GTGTCTCAGTCCCAATGT
SMc01513 (*hmuS*)	ACATCAAGCAAGGACACG	CACTTGTCGAAGAACTGC
SMc02726 (*shmR*)	CGACAATGATCTCAGAGC	CGAAATCATAGTCCAGCG
SMa2412 (*rhrA*)	CTCCTGACGAATTATGCG	TATCTTGAGCAAGCACCG
SMa2402 (*rhbB*)	TGAACATCAACGTCGCTG	GGAGTAGAGACTGCTTGC
SMa2414 (*rhtA*)	CATCATCACGAAGAAGGG	TCGCTGTTATAGGTGACC
SMa2339 (*rhbG*)	TCGGACCTTTCTCAGGTG	ACATCAGATGCAGAAGGG

3.4. Results

In silico analyses of RhbD and SMa2339 (RhbG)

Although two proposals for the biosynthetic pathway to Rhb1021 have been raised (see Fig 3.3. based on Lynch et al. (2001) and Challis (2005a)), the role of each of the RhbABCDEF enzymes has not been established yet. Remarkably, the gene or genes responsible for the addition of the lipid moiety that gives the siderophore amphiphilic properties has/have not been identified. The significant similarity shown by *SMa2339* (*rhbG*) to IucB (N^6-hydroxylysine acetyltransferase involved in aerobactin biosynthesis) and other acyl-CoA-dependent acyl transferases, led to propose that RhbG could catalyse the acylation reaction. Lynch and coworkers (2001) reported that the disruption of the *rhbG* gene did not abolish the siderophore production as determined by CAS assays. However, this result does not discard the possibility that *rhbG* is involved in Rhb1021 biosynthesis as the production of Rhb1021, or a related siderophore (like schizokinen which lacks the enoyl lipid moiety), was not investigated.

The *rhbD* gene codes for a 196 amino acid (aa) long protein. Analysis of the amino acid sequence of RhbD with SMART identifies the AlcB domain in the N-end of the protein (aa 27-74). AlcB is the conserved 45 residue region of one of the proteins of a complex which mediates alcaligin biosynthesis in *Bordetella* and aerobactin biosynthesis in *E. coli* and other bacteria. The protein appears to catalyse N-acylation of the hydroxylamine group in N-hydroxyputrescine with succinyl CoA - an activated mono-thioester derivative of succinic acid that is an intermediate in the Krebs cycle. On the other hand, Pfam identifies the acetyltransferase_8 GNAT domain which covers most of the protein (aa 26-183). *SMa2339* (*rhbG*) codes for a protein of 370 aas. SMART and Pfam programs predict AlcB and GNAT domains comprising aas 190-237 and 190-346, respectively. It shows 37% identity with RhbD, although the latter lacks the 130 amino acid present in the N-end of RhbG. The sequence profile search of RhbD and RhbG with the PSI-BLAST program (http://blast.ncbi.nlm.nih.gov) revealed a

large number of acyl-CoA-dependent acyl transferases homologs. An hypothetical IucB family biosynthesis protein of 199 aas from *Synechococcus* sp. (YP_001733131.1) seems to be the most similar protein to RhbD with a 49% of identity. An acetyltransferase from *S. meliloti* GR4 (YP_007192375.1) of 370 aas and a siderophore biosynthesis protein from *S. meliloti* BL225C of 371 aas (YP_005717370.1) are predicted to be the most similar proteins to RhbG with a 99 % and 98% of identity respectively. Apart from the homologs of these *S. meliloti* strains, the third predicted protein similar to RhbG is a putative acetylase of 362 aas from *Bradyrhizobium* sp. ORS 285 (ZP_09473131.1) which shows a 46% of identity. Furthermore, RhbD and RhbG present a 38% identity to the well characterized IucB protein of 315 aas from *E. coli* (YP_002400669.1) (de Lorenzo et al., 1986). Notwithstanding, RhbD and RhbG show a different percentage of coverage this protein (94% and 72% respectively). Figure 3.4 shows the sequence alignment of these similar proteins.

In summary, the *in silico* analysis predicts that both RhbD and RhbG could potentially catalyze the N-acylation required for the incorporation of the lipid moiety to Rhb1021. Therefore, in order to test our hypothesis we decided to obtain mutants in *rhbD* and *rhbG*.

Figure 3.4. Multiple sequence alignment of RhbD from *Sinorhizobium meliloti* Rm1021 (NP_436507.1) SmRhbD, SMa2339 (RhbG) from *S. meliloti* Rm1021 (NP_436512.1) SmRhbG, an hypothetical IucB family biosynthesis protein from *Synechococcus* sp. Pcc7002 (YP_001733131.1) Synec, a putative acetylase from *Bradyrhizobium* sp. ORS 285 (ZP_09473131.1) BradR, and IucB from *Escherichia coli* ED1a (YP_002400669.1) EcIucB. Conserved amino acids in the all four proteins are highlighted in red whereas conserved amino acids in at least three of the sequences are highlighted in blue. The AlcB (in yellow) and GNAT (underlined sequence) domains were identified by using the SMART (http://smart.embl-heidelberg.de) and Pfam (http://pfam.sanger.ac.uk) programs, respectively.

Phenotypic characterization of *S. meliloti rhbD* and *rhbG* mutants

Siderophore production measured by CAS assay

Lynch et al. (2001) reported that siderophore production, as measured by the CAS assay, was abolished in an *rhbA* mutant strain but not in a mutant in which the *rhbG* gene was disrupted. In agreement with this, the CAS assays performed with supernatants of 1021rhbD and 1021rhbG cultures grown in standard MM revealed the absence of siderophore activity in the former but not in the latter, although a significant reduction in siderophore production of approximately 20% could be detected in 1021rhbG culture supernatants compared to that of the parental strain (data not shown). These results suggested that *rhbG* is not essential for siderophore biosynthesis but it affects the total amount of iron chelator activity produced and/or released by *S. meliloti* through some yet unknown mechanism.

Growth curves

As the next step in the phenotypic characterization of *S. meliloti rhbD* and *rhbG* mutant strains, we studied their growth curves in liquid MM containing different concentrations of $FeCl_3$ (2.2 μM, 22 μM and 220 μM) and compared their behavior with that of the Wt strain and of the 1021rhbA (*rhbA*) mutant (Fig. 3.5). 1021rhbA exhibited slower growth rates than the Wt in all three different conditions. However, in MM containing 220 μM $FeCl_3$ the growth deficiencies shown by 1021rhbA diminished along the time and at the end of the experiment the culture reached the same OD than the Wt (Fig. 3.5C). In standard MM (22 μM $FeCl_3$), some variability in the growth curves of 1021rhbA was noticed. Sometimes, a behavior similar as that exhibited in MM containing 220 μM $FeCl_3$ was detected as shown in figure 3.5B. However in different experiments like the one shown in figure 3.12, the growth deficiencies shown by 1021rhbA compared to the Wt were more noticeable in late logarithmic and stationary phases. We interpret this variability in growth as the result of differences in the real

concentration of available iron which might be in the limit of iron sufficiency for this mutant.

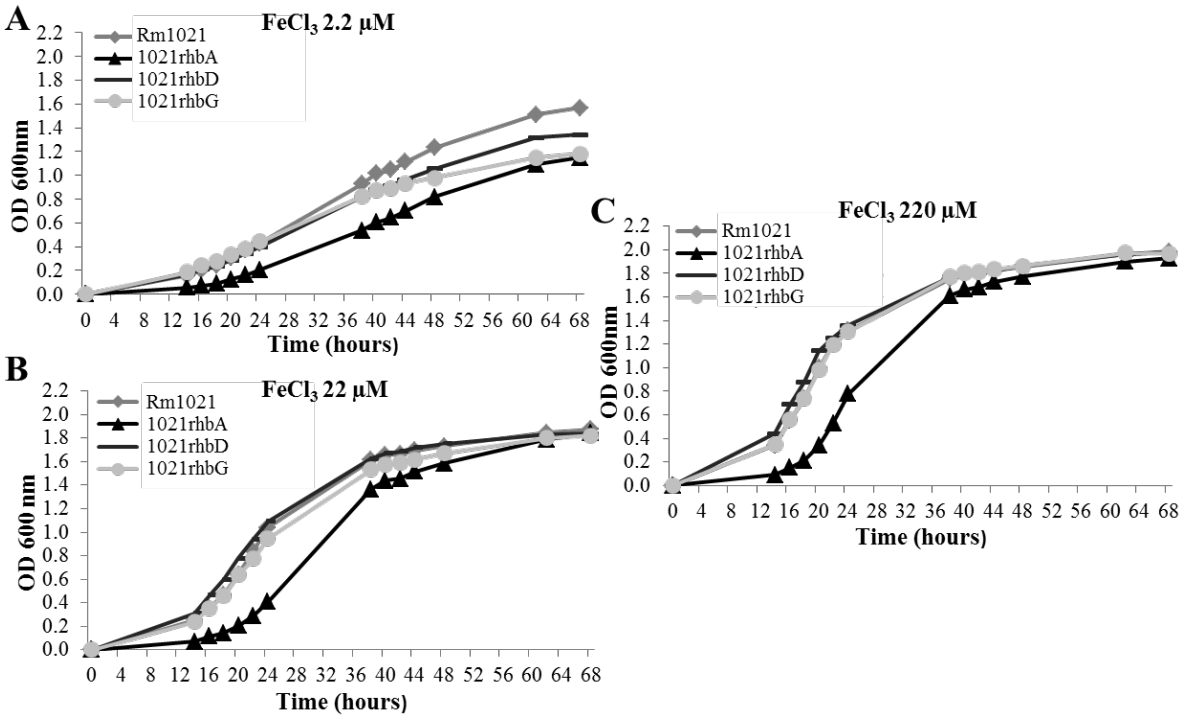

Figure 3.5. Growth curves of Rm1021, 1021rhbA, 1021rhbD and 1021rhbG in MM broth containing different concentrations of $FeCl_3$.

In contrast to the *rhbA* mutant strain, no differences in growth rates could be detected between 1021rhbD or 1021rhbG and the Wt strain in liquid MM containing 22 µM or 220 µM $FeCl_3$. In MM containing the lowest iron concentration (2.2 µM $FeCl_3$), cultures of the *rhbD* and *rhbG* mutants exhibited a slight decrease in the final OD compared to that of the Wt. The fact that 1021rhbD grows as the Wt strain in MM containing 22 µM $FeCl_3$, indicates that although these conditions induce Rhb1021 production (Nogales et al. 2010), Rhb1021 itself is not necessary for satisfying the iron demands for growth. The different growth behavior shown by the two siderophore defective mutants (*rhbA* and *rhbD*) is intriguing but it has not been investigated in this work. One might speculate that the different ways these two mutants were created are leading to different effects besides the lack of siderophore activity. 1021rhbD was obtained by an in-frame marker-free deletion, potentially allowing transcription of the *rhb*

genes of the same operon. However, the *rhbA* mutant was created by a transposon insertion which renders the strain neomycin resistant (Nm^R). Most likely, the presence of the transposon in this mutant is causing polar effects which prevent transcription of the remaining genes belonging to the *rhbABCDEF* operon and somehow this causes a major growth defect than in the *rhbD* mutant in which all the *rhb* genes are being transcribed.

Motility phenotypes

The motility phenotypes of 1021rhbD and 1021rhbG were also tested (Fig. 3.6). No differences in swimming motility were observed for these two mutant strains compared with the wild type strain (Fig. 3.6A). Surface motility assays performed on semisolid MM revealed that, as expected for an Rhb1021 defective mutant, 1021rhbD was severely impaired in surface spreading (Fig. 3.6B and 3.6C). However, the *rhbG* mutant exhibited an increased ability in surface translocation, colonizing almost the entire surface of the Petri dish, 20 hours after inoculation (Fig. 3.6B). Although slightly reduced compared with the parent strain, a non-flagellated derivative mutant of 1021rhbG (1021rhbGF) still exhibited significant surface spreading (Fig. 3.6B and 3.6C). Moreover, 1021rhbGF spread over the surface more than a non-flagellated derivative mutant of Rm1021 (1021F). Altogether, these results indicate that the *rhbG* mutation promotes flagella-independent surface translocation and in contrast to *rhbA* and *rhbD* mutants, it does not prevent swarming motility. In addition to an increased surface spreading, the two *rhbG* derivative mutants of Rm1021 exhibited a different surface translocation pattern compared to their corresponding $rhbG^+$ strains. Surface migrating colonies of *rhbG* mutants were characterized by the presence of long isolated and irregularly shaped tendrils radiating from a core of cells that were more evident in 1021rhbGF than in 1021rhbG (Fig. 3.6C). This effect on surface motility patterns caused by the *rhbG* mutation resembled the effects reported for rhamnolipids and its biosynthetic precursors on *Pseudomonas aeruginosa* swarming motility (Caiazza et al. 2005; Tremblay et al. 2007). In this bacterium, rhamnolipids are surface-wetting agents

required for swarming. However, a gradient of rhamnolipids/precursors ratio is also responsible for maintaining tendril organization and preventing the colonization of the area between tendrils. Likewise, it is tempting to hypothesize that in *S. meliloti* the ratio Rhb1021 versus some of its biosynthetic precursors might impact the pattern of surface motility.

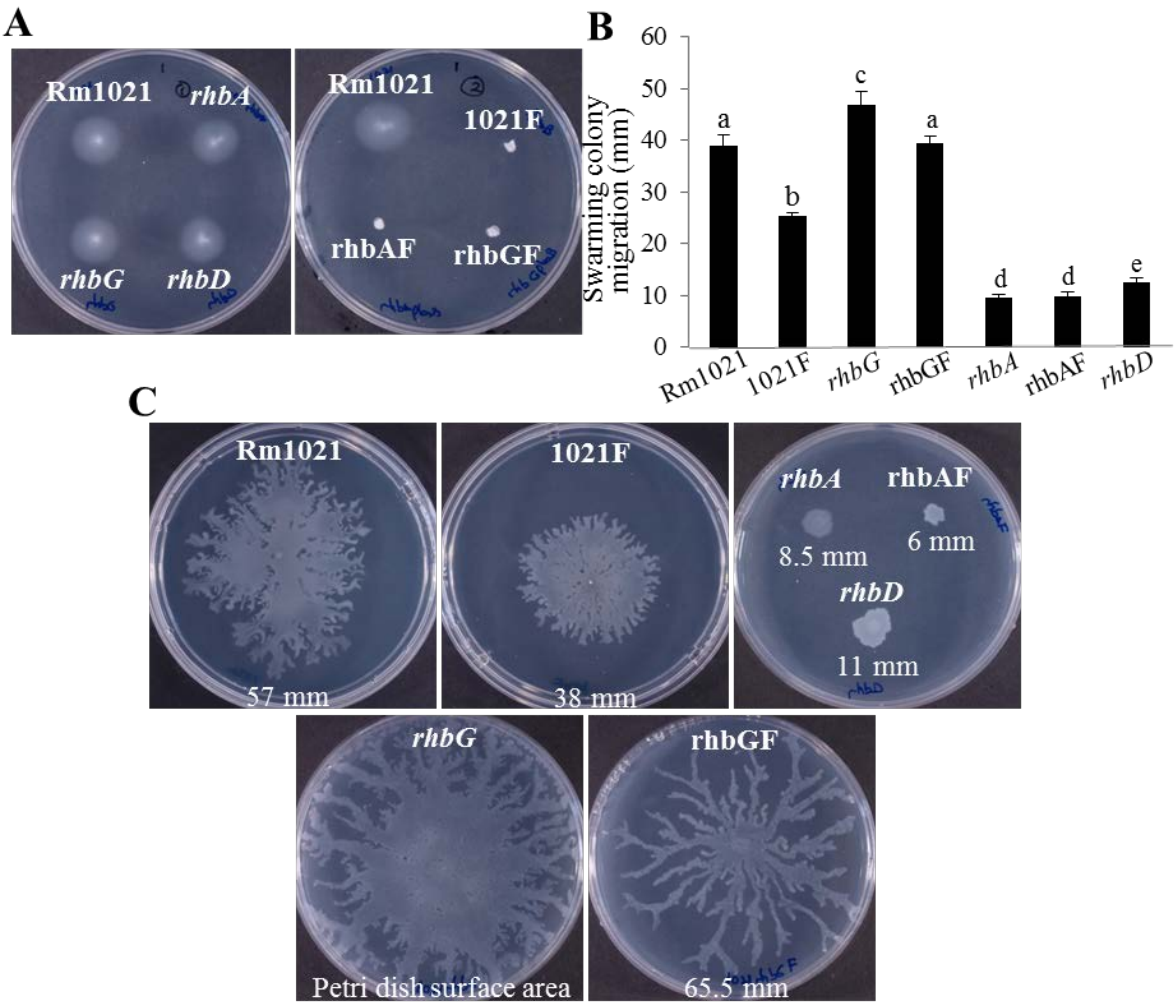

Figure 3.6. Motility phenotypes of the wild type strain and Rhb1021-derivative mutants. A) Swimming in BM (0.3% agar).) B) Measurement of swarming colony migration 20 h post inoculation. Values are the mean and standard error of migration zones (given in millimeters and measured as described in Materials and Methods) obtained from at least nine measurements. Values followed by the same letter do not differ significantly (Tukey test, $P \leq 0.05$). C) Representative images showing the surface spreading pattern of the different strains. Pictures were taken once the mucous aspect of the swarm colony has increased (48 h post-inoculation). Values under each image are the migration zone of the representative picture.

Surfactant production

Swarming motility is highly dependent on surfactants production. As it has been speculated that Rhb1021 can act as a surfactant molecule, we performed the drop collapse assay to determine surfactant production in Rm1021, 1021rhbD and 1021rhbG cells grown on semisolid MM. As shown in figure 3.7, drop expansion was not observed for Rm1021 or 1021rhbD. The fact that Rm1021 bead did not collapse suggests that high concentrations of Rhb1021 are possibly required in order to observe drop expansion. In the case of the *rhbG* mutant, drop collapse activity was observed, indicating the presence of surfactant molecules.

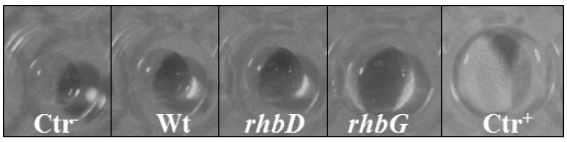

Figure 3.7. Drop collapse assay. *Sinorhizobium meliloti* Rm1021 (Wt), 1021rhbD, and 1021rhbG cells grown on semisolid minimal medium were scraped and suspended in PBS to obtain an OD_{600nm} of 8. Drops of 20 µl were spotted on the circles located on the underside of the lid of the 96-well polystyrene microtiter plate. PBS and SDS 0.02% were used as negative control (Ctr^-) and positive control (Ctr^+) for drop expansion respectively.

Biofilm formation

The different stages of biofilm formation by GFP-labelled 1021rhbD and 1021rhbG strains was analyzed as previously described by Amaya-Gómez et al. (submitted) in a 10-day time course experiment using chambered cover glass slides and CLSM (Fig. 3.8). Before the third day, the biofilms formed by the wild-type Rm1021 and mutant strains detached easily from the glass surface during the washing step. As previously reported, under our experimental conditions, 3 days post inoculation (dpi) Rm1021 developed an unstructured biofilm composed by a uniform flat layer of cells covering the entire surface of the slide. Biofilms of similar structure and thickness were also developed by 1021rhbD and 1021rhbG (data not shown). However, at 10 dpi, both mutants were highly impaired in the development of a mature biofilm as determined by comparing the thickness of

mutant biofilms with that formed by the wild type strain (Fig. 3.8A). The defect in biofilm formation seemed to be more severe for 1021rhbD than for 1021rhbG. The phenotype shown by 1021rhbD confirms previous results indicating that essential genes for Rhb1021 biosynthesis and most likely, siderophore itself, plays an important role in biofilm development. Furthermore, results presented here also evidence the role played by *rhbG* in this multicellular surface-associated behavior.

Our previous work showed that iron is an important signal for biofilm development in *S. meliloti* (Amaya-Gómez et al. submitted). Iron-replete conditions that abolish Rhb1021 synthesis (among other effects), induce the formation of structured biofilms in the Wt and an *rhbA* derivative mutant. Nonetheless, these conditions cannot overcome the defect of the *rhbA* mutant to develop a biofilm as thick as the one developed by the Wt. To test if the biofilm deficiencies shown by *rhbD* and *rhbG* mutants were the result of a nutritional iron deficiency, we followed the biofilm development of these two mutants under high iron conditions (220 μM of $FeCl_3$). As reported for the *rhbA* mutant (Amaya-Gómez et al. submitted), these conditions induced the development of structured biofilms in 1021rhbD and 1021rhbG, but they remained incapable of developing biofilms as thick as those formed by Rm1021 (Fig. 3.8B). Therefore, disruption of *rhbG* negatively impacts biofilm development in a similar way to that described for *rhb* mutants (*rhbA* and *rhbD*) in which Rhb1021 synthesis is fully abolished.

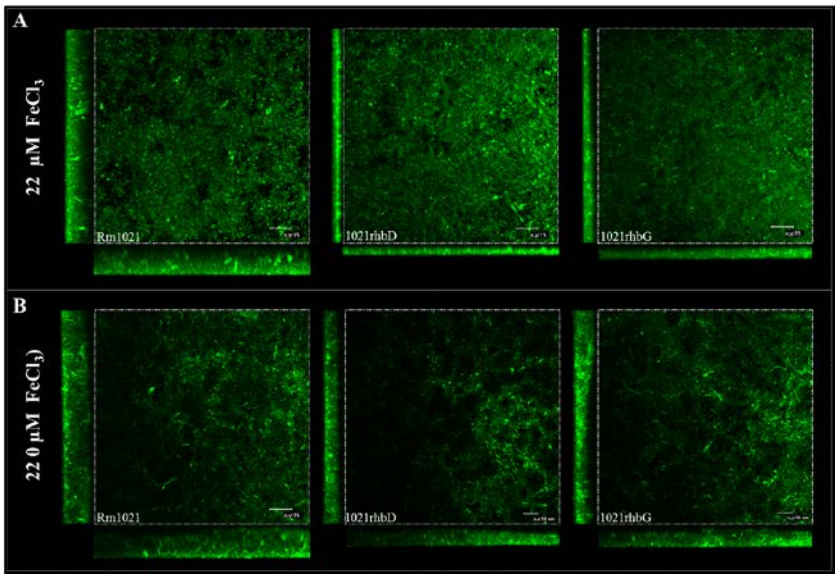

Figure 3.8. CLSM images of biofilm formation in MM containing either low (A) or high (B) concentrations of $FeCl_3$, at 10 dpi. Biofilms were grown in chambered cover glass slides during 10 days. The CLSM images show the *xy*, *xz* and *yz* planes. The experiments were performed in triplicate as described in Materials and Methods. Bars, 15 µm.

Purified Rhb1021 shows surfactant activity

To gain further insights about the role/s played by Rhb1021 in swarming motility and biofilm formation, we pursued purification of the siderophore. It has been reported that a mutation in the global iron response regulator gene *rirA* results in derepression of the Rhb1021 biosynthesis and transport genes. Therefore, a *rirA* mutant produces the siderophore regardless of the iron concentration present in the media (Chao et al., 2005; Viguier et al., 2005). By using the semiquantitative liquid CAS assay, Chao et al. (2005) observed that when cultivated under low-iron conditions (no $FeCl_3$), Rm1021 and the *rirA* mutant exhibited siderophore production, but the amount in the *rirA* mutant was ~125-fold higher. Under our experimental conditions, the liquid CAS assay revealed that when grown in MM containing 220 µM $FeCl_3$, the production of the siderophore was abolished in Rm1021 but not in the *rirA* mutant (Nogales et al. 2010). Under low iron conditions (MM containing 22 µM $FeCl_3$), and similar to the results described by Chao et al., we detected siderophore production by both

strains, but the levels of siderophore produced by the G212rirA mutant were approximately 15 fold higher than those produced by Rm1021. Thereby, we decided to use the G212rirA mutant to obtain purified Rhb1021. We firstly attempted production and purification of Rhb1021 by growing G212rirA in Iron Deficient Medium (IDM) which has been used for the purification of different siderophores (Müller and Raymond, 1984; Chen et al., 2012) and which is similar to the medium used by Persmark et al. (1993) for the first isolation and chemical characterization of Rhb1021. The levels of Rhb1021 identified as *m/z* 531 for $[M+H]^+$ or 584 for $[M-2H+Fe]^+$ in Rm1021 and G212rirA were detected by LC-MS. Although under these conditions G212rirA still produced more Rhb1021 than Rm1021 (data not shown), yields were too low to perform the purification process. In order to increase G212rirA's growth and siderophore production we supplemented the IDM with different concentrations of $FeCl_3$ (1 µM, 5 µM, 10 µM). Addition of 10 µM $FeCl_3$ resulted in the highest Rhb1021 yield by *rirA* mutant cells. Figure 3.9. shows the extracted ion chromatogram (EIC) of *m/z* 584 peak in Rm1021 and G212rirA.

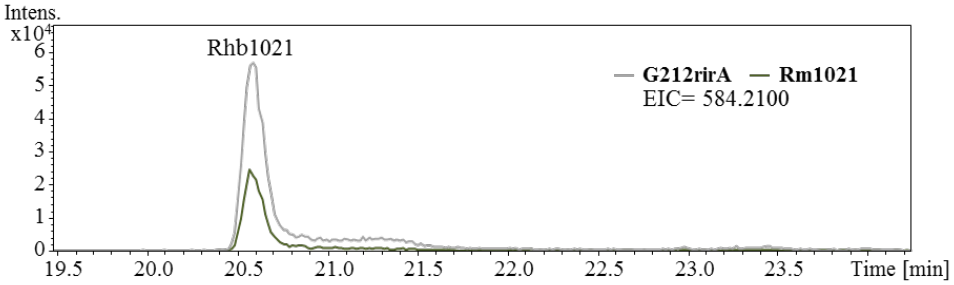

Figure 3.9. Rhb1021 production in G212rirA and Rm1021. Extracted Ion Chromatogram (EIC) showing Rhb1021 peak *m/z* = 584 $[M-2H+Fe]^+$. LC-MS analysis was carried out using a Sigma Ascentis Express (C18, 150x2.1mm, 2.7µm) column.

Rhb1021 was purified from 250 ml of G212rirA culture supernatant as described in the Materials and Methods section, obtaining a total amount of 11 mg of siderophore. The structure of the purified Rhb1021 was confirmed by NMR as (E)-4-[[3-(acetylhydroxyamino)propyl]-amino]-2-hydroxy-2-[2-[3-[hydroxy(1-oxo-2-decenyl)amino]propyl]amino]-2-oxoethyl]-4-oxobutanoic acid (Table. 3.4).

Table 3.4. ^{1}H and ^{13}C NMR spectral data of Rhb1021.

Atom	δH^{a}/ppm	δC^{a}/ppm
C-1	0.86	13.5
C-2	1.23	21.7
C-3	1.24	31.0
C-4	1.26	28.1
C-5	1.26	28.2
C-6	1.40	27.5
C-7	2.18	31.3
C-8	6.69	146.5
C-9	6.51	119.5
C-10		165.1
C-11(NO<u>H</u>)	9.80	
C-11	3.55	45.1
C-12	1.65	26.1
C-13	3.03	36.2
NH	7.94	
C-14		169.1
C-15	2.48, 2.56	42.9
C-16		73.4
C-16($\underline{C}O_2H$)		174.7
C-16(O<u>H</u>)	6.10	
C-17	2.48, 2.56	42.9
C-18		169.1
C-19(N<u>H</u>)	7.92	
C-19	3.03	36.2
C-20	1.65	26.1
C-21	3.48	44.7
C-21(NO<u>H</u>)	9.80	
C-22		169.7
C-23	1.97	19.8

Spectra were measured at 700 MHz using DMSO as solvent.
[a] assigments are made based on COSY and HMBC spectrum.

It has been reported that Rhb1021 shows high amphiphilic properties manifested by solubility in both water and a range of organic solvents (Persmark et al., 1993). To test whether these inherent amphiphilic properties conferred surfactant activity to Rhb1021, a drop collapse assay was performed using different concentrations of the siderophore. As shown in Fig. 3.10, drop collapse was clearly observed in all the samples except for the dilution 1:8 (111 μM)

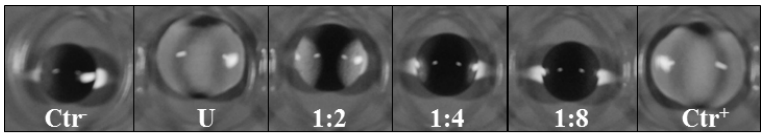

Figure 3.10. Drop collapse assay. Drops of 20 μl of purified Rhb1021 (1mM) (U), and diluted solutions were spotted on the circles located on the underside of the lid of the 96-well polystyrene microtiter plate. As DMSO formed a bead similar to that of PBS, PBS was used as negative (Ctr^{-}). A drop of SDS 0.02% was used as positive control (Ctr^{+}) of drop expansion.

Complementation of *S. meliloti rhb* mutants with Rhb1021

To confirm that the lack of Rhb1021 was responsible for the different phenotypes exhibited by *S. meliloti rhb* mutants, complementation experiments were performed by adding the purified siderophore. As already mentioned, in MM containing 22 µM $FeCl_3$ growth defects were observed for 1021rhbA but not for 1021rhbD. Thus, growth curves of 1021rhbA were performed in MM supplemented or not with the purified siderophore. Since Rhb1021 was dissolved in DMSO, the effect of DMSO on bacterial growth was also tested (Fig. 3.11).

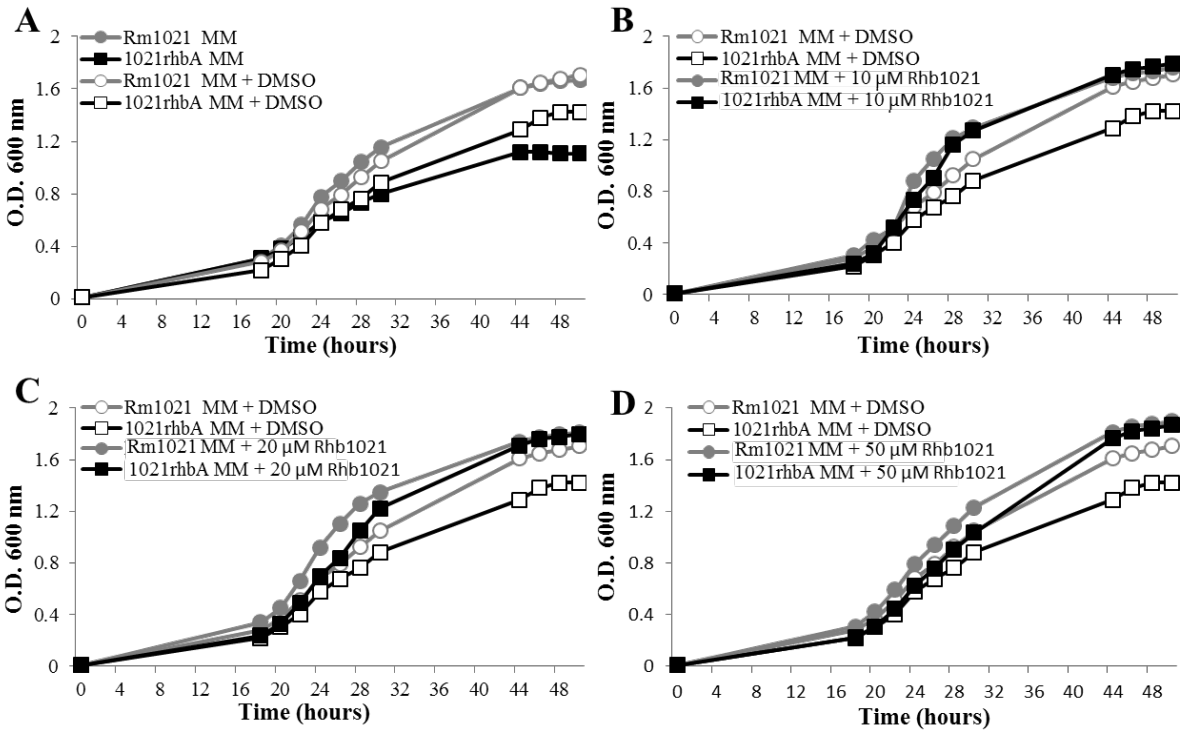

Figure 3.11. Effect of Rhb1021 addition on the growth curves of Rm1021 and 1021rhbA in MM. A) Bacterial growth in MM and MM supplemented with DMSO. Bacterial growth in MM supplemented with DMSO and MM supplemented with Rhb1021 to a final concentration of B) 10 µM, C) 20 µM, and D) 50 µM. As Rhb1021 was dissolved in DMSO, the bacterial growth was compared among the strains in presence of DMSO and Rhb1021.

Addition of DMSO to liquid MM resulted in a slight improvement of 1021rhbA growth although this treatment did not allow the mutant strain to reach Wt growth rates (Fig. 3.11A). Addition of different amounts of purified

Rhb1021 (final concentrations of 10, 20 and 50 μM) improved the growth rates shown by both the Wt and the *rhbA* mutant strain, and in the case of the latter, growth was restored to wild type levels as shown in figure 3.11B, C and D.

The surface spreading phenotype of the wild type, 1021rhbA, 1021rhbAF and 1021rhbD strains was also tested in the presence of DMSO and Rhb1021. We attempted complementation of the surface motility phenotype by adding different amounts of purified Rhb1021 (final concentrations of 20 μM and 100 μM) into either TY cultures, or into the concentrated and washed cell suspension. In either of these two conditions, the addition of DMSO showed no interference with bacterial surface translocation. Nevertheless, addition of purified Rhb1021 could not restore the surface motility phenotype of the mutants (data no shown).

We also attempted to complement the defect on biofilm development shown by 1021rhbD by adding purified Rhb1021 to a final concentration of 100 μM. The addition of DMSO did not alter significantly biofilm development in Rm1021 or 1021rhbD. By contrast, the addition of purified Rhb1021 negatively affected the biofilm development in both strains with drastic effects on Wt biofilms. In the presence of Rhb1021, the biofilm formed by 1021rhbD detached from the glass surface more easily than the biofilm formed in MM with DMSO. Moreover, we could observe that the addition of Rhb1021 prevented the development of a confluent biofilm in 1021rhbD (Fig. 3.12). Ten days after inoculation, just patches of a slime layer of 1021rhbD cells were attached to the glass slide surface. In the case of Rm1021, the addition of purified Rhb1021 significantly decreased biofilm formation as determined by the thickness of the surface-associated bacterial community (Fig. 3.12). These results indicate that exogenous addition of Rhb1021 is not sufficient to complement the defect in biofilm formation shown by a siderophore defective mutant and it impacts negatively the biofilm development in the Wt.

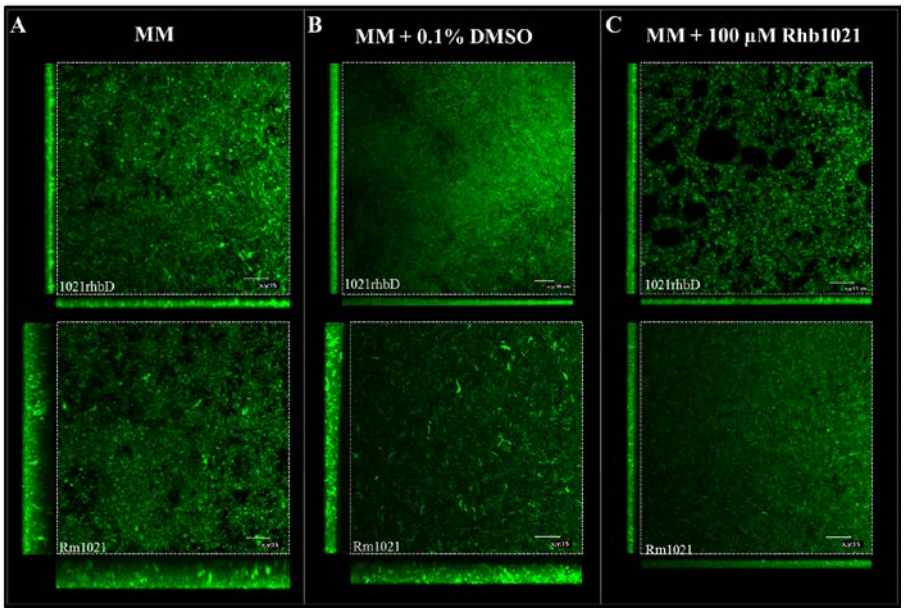

Figure 3.12 CLSM images of 1021rhbD and Rm1021 biofilms formed on chambered cover glass slides. Biofilm development of Rm1021 and 1021rhbD in (A) MM, (B) MM supplemented with DMSO and (C) MM supplemented with Rhb1021 100 µM after 3 (upper images) or 10 (lower images) days post-inoculation.

LC-MS analyses demonstrate that disruption of *rhbG* does not abolish Rhb1021 synthesis

As described above, CAS assays revealed the absence of siderophore activity in culture supernatants of the 1021rhbD mutant as well as a 20% reduction in the CAS activity associated to 1021rhbG culture supernatants compared with that shown by the Wt Rm1021. To corroborate the lack of siderophore production by 1021rhbD cells and to investigate whether the CAS activity associated to the *rhbG* mutant was due to Rhb1021 or to a different siderophore, we decided to analyze culture supernatants of the *rhbD* and *rhbG* mutant strains together with that of the Wt by LC-MS. It was noticed that conditions that resulted in the highest Rhb1021 yield from G212rirA cultures (IDM supplemented with 10 µM $FeCl_3$) were not the optimal for siderophore production in Rm1021. Persmark et al. (1993) obtained increased siderophore yields by adding fumarate and cysteine (12.5 mM) to mid log phase cultures grown in MOPS-buffered media. In order to enhance Rhb1021 production in

Rm1021, mid log phase cultures grown in IDM were supplemented with different compounds such as cysteine (12.5 mM), fumarate (12.5 mM), cysteine and fumarate (12.5 mM each) and citric acid (12.5 mM, 8 mM or 500 μM). Although addition of any of these compounds led to higher Rhb1021 yields by Rm1021 cultures, the most significant induction in siderophore production was obtained by adding citric acid to a final concentration of 500 μM (data no shown). Hence, Rm1021, 1021rhbD and 1021rhbG cultures were grown in IDM supplemented with citric acid and their supernatants analyzed by LC-MS. These analyses confirmed the CAS assays results. Thus, in 1021rhbD culture supernatants, only trace amounts of Rhb1021 could be detected (Fig. 3.13A). An additional remarking difference was the absence in 1021rhbD culture supernatants of two peaks which were present in the supernatant of Rm1021 cultures: one with *m/z* 175.1075 and retention time of 2.6-2.7 min (Fig. 3.13B), and a second one with *m/z* 307.1063 and retention time of 2.8-2.9 min (Fig. 3.13C). The putative chemical structure of the latter compound coincides with that of intermediate **4** of the Rhb1021 biosynthesis pathway proposed by Lynch and coworkers and represented in figure 3.3. Likewise, we presume that the compound with *m/z* 307.1063, an acetylated derivative of **2** (Fig. 3.3) is also probably an intermediate form produced during the Rhb1021 synthesis. The absence of Rhb1021 and compounds *m/z* 175.1075 and 307.1063 in supernatants of 1021rhbD cultures fits with the proposed role of RhbD as the enzyme that catalyzes acetylation of N^4-hydroxy-1-aminopropane to give N^4-acetyl-N^4-hydroxy-1-aminopropane, although this should be biochemically proved.

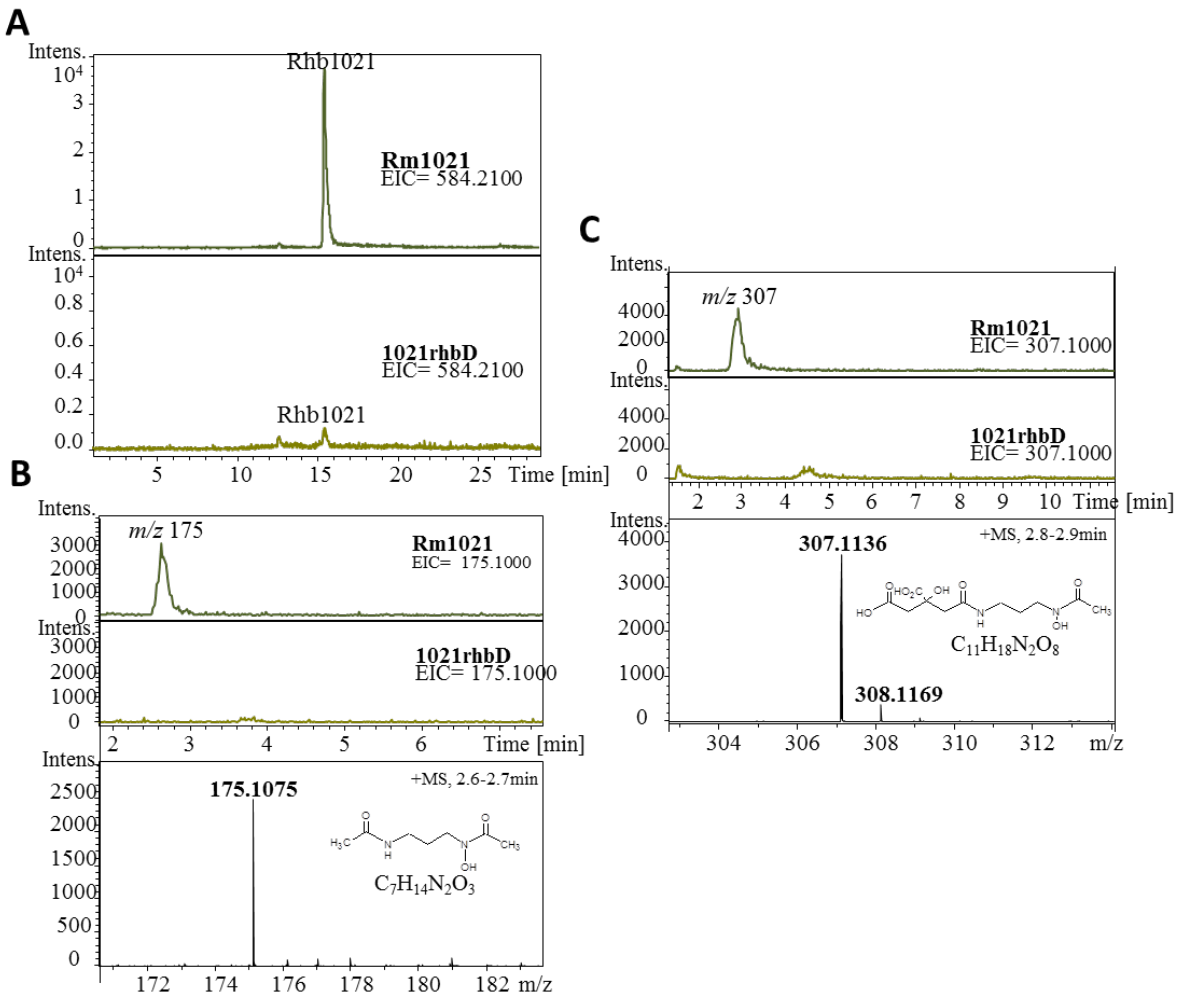

Figure 3.13. LC-MS analysis of *S. meliloti* Rm1021 and 1021rhbD culture supernatants. A) EIC showing the peak corresponding to Rhb1021 (*m/z* 584), B) EIC of *m/z* = 174.1004, C) EIC of *m/z* = 306.1063. Plausible chemical structures of the *m/z* in B and C and their chemical formula are also shown. EIC, Extracted Ion Chromatogram

When 1021rhbG culture supernatants were analyzed by LC-MS, Rhb1021 could be detected although at lower levels than those observed in Rm1021 cultures (Fig. 3.14A). It should be mentioned that the retention time exhibited by Rhb1021 (*m/z* 584) differs between the analysis Rm1021 vs. 1021rhbD (15.2-15.3 min, Fig. 3.14A) and the analysis Rm1021 vs. 1021rhbG (20.4-20.8, Fig. 3.14A), due to the different columns used for the LC-MS analysis (see Materials and Methods). Besides detecting Rhb1021 production, it was also remarkable in the analyses of 1021rhbG culture supernatants, the absence of a peak that could correspond to schizokinen *m/z* 421 [M+H]. These results demonstrate that *rhbG* is not essential for Rhb1021 production and they suggest that RhbG is not responsible for incorporating the acyl moiety into the Rhb1021 molecule. Interestingly, a peak with *m/z* 285 [M+H] and retention time of 21.6-21.9 min whose levels were significantly higher in 1021rhbG than in Rm1021 was detected (Fig. 3.14B).

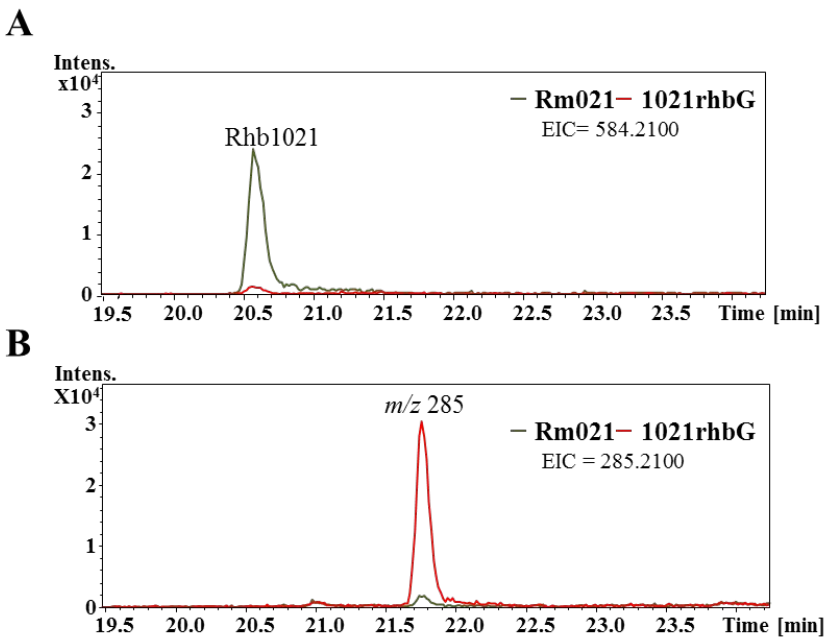

Figure 3.14. LC-MS analysis of *S. meliloti* Rm1021 and 1021rhbG culture supernatants. A) EIC showing the peak corresponding to Rhb1021 (*m/z* 584), B) EIC of *m/z* = 285.

To gain further insights about the role played by RhbG, the molecule overproduced by 1021rhbG was purified by HPLC and analyzed by NMR

spectroscopy. These analyses revealed that the product accumulated in 1021rhbG was (2E)-N-[3-(acetylamino)propyl]-N-hydroxydec-2-enamide) (Table 3.5.). From now on, we will refer to this molecule as RhbGdec (Fig. 3.16).

Table 3.5. ^{1}H and ^{13}C NMR spectral data of accumulated compound in 1021rhbG.

Atom	δ_H/ppm[a]	δ_C/ppm*	HMBC
C-1	0.86(t, 7.5)		C2, C3
C-2	1.24,1.27 (m)		C4
C-3	1.22,1.26 (m)		
C-4	1.24 (m)	28.7	
C-5	1.27 (m)	28.4	C3, C4, C7
C-6	1.40 (m)	27.8	C4, C8
C-7	2.18 (m)	31.4	C5, C6, C9
C-8	6.69 (dt, 7.0, 15.2)		C10
C-9	6.50 (d, 15.2)		
C-10		165.1	
C-11	3.54 (t, 7.6)	45.3	
C-12	1.65 (m)	26.5	C11, C13
C-13	3.01 (dt, 6.9, 6.7)	36.3	C11, C14
C-13(NH)	7.81 (s, br)		
C-14		168.9	
C-15	1.78 (s)	22.5	C14

Spectra were measured at 700 MHz using DMSO as solvent.
[a] assigments are made based on COSY and HMBC spectrum.
* assigments are made based on HMBC and HSQC data.

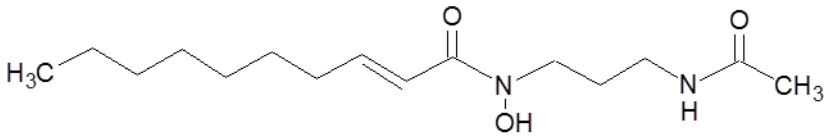

RhbGdec
$(C_{15}H_{28}N_2O_3)$

Figure 3.16 Chemical structure of the compound accumulated in 1021rhbG supernatants: RhbGdec is (2E)-N-[3-(acetylamino)propyl]-N-hydroxydec-2-enamide (confirmed by NMR). EIC, Extracted Ion Chromatogram

The presence of low amounts of Rhb1021 in supernatants of 1021rhbG cultures, together with the higher levels of RhbGdec detected in the mutant strain compared with those observed in the Wt, suggest that RhbG does not function as proposed by either Lynch and colleagues or Challis (see Fig. 3.3). In fact, our results suggest that RhbG is not responsible for the incorporation of (E)-2-

decenoic acid into the Rhb1021 molecule. Therefore, at this point, the function of RhbG is unknown and warrants further investigations. Another unresolved question arisen from the results of this study is what is the enzyme involved in incorporating the enoyl-lipid moiety into Rhb1021. The answer to these questions would help to elucidate if the hyperswarmer phenotype shown by 1021rhbG is the result of RhbGdec accumulation and if its defect in biofilm formation is the consequence of the diminished levels of Rhb1021, the overproduction of RhbGdec, or both.

Global transcriptional analysis of 1021rhbD cells grown on semisolid MM

As explained before, the surfactant properties inherent to Rhb1021 could be responsible for its effects on bacterial surface motility and biofilm development. However, another non-excluding possibility could be that Rhb1021 impacts these two surface-associated behaviors acting as a signal molecule that controls the expression of genes playing crucial roles in surface translocation and biofilm formation, a function that has been reported for other siderophores and surfactants (Lamont et al., 2002; Daniels et al., 2006). In order to test this hypothesis, we compared the transcriptome profile of Rm1021 cells grown over the surface of semi-solid MM with that of 1021rhbD cells (unable to produce Rhb1021) grown under the same conditions. As a first step, bacterial growth curves in semisolid MM was determined for both strains to ensure that the respective transcriptomes were obtained in the same growth phase. Figure 3.17 shows that the growth profiles of the two strains were quite similar. Samples for RNA extraction were collected at mid exponential phase, 14 hours after inoculation.

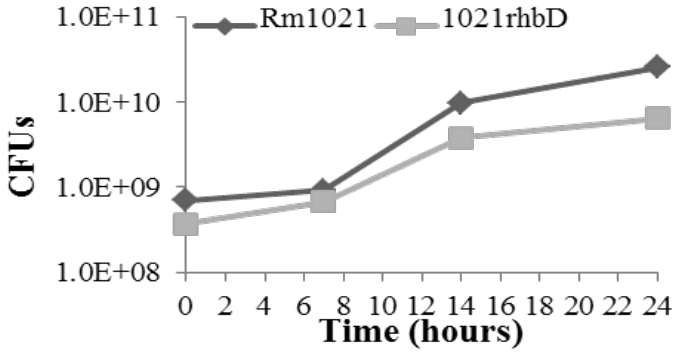

Figure 3.17. Growth curves of Rm1021 and 1021rhbD on semisolid MM plates. 100 µl of a suspension of cells containing approximately 10^9 cells of Rm1021 and 1021rhbD were evenly spread over the surface of MM containing 0.6% of agar. CFU refers to colony forming units per plate.

Duplicated samples of each strain were taken from three independent experiments yielding a total of six replicates per experimental microarray set. Under these experimental conditions, 29 genes showed differential expression in the *rhbD* mutant as compared to the Wt (Table 3.6.).

Twenty two genes out of the 29 were up-regulated and only 7 were found to be down-regulated in the 1021rhbD mutant strain compared to the Wt. 45% of the genes showing differential expression (13 genes) were related with iron uptake and metabolism: all of them showed up-regulation in 1021rhbD except 5 *rhb* genes involved in Rhb1021 biosynthesis which exhibited down-regulation. Considering that the lack of *rhbD* prevents Rhb1021 synthesis, it was not surprising to detect up-regulation of genes involved in alternative iron acquisition systems such as haem and xenosiderophores uptake genes (*shmR*, *hmuS, hmuT, hmuV*, *fhuF* and *fhuP*) (Cuív et al., 2008). *shmR*, encoding the outer membrane receptor for haem acquisition (Battistoni et al., 2002), was the most up-regulated gene found in our study. The up-regulation of alternative iron acquisition systems detected in 1021rhbD suggests that these cells face a higher nutritional iron deficiency than Rm1021 cells when grown on semisolid MM.

Table 3.6. *S. meliloti* genes differentially expressed in 1021rhbD versus Rm1021 after growth in semisolid MM.

Gene	Gene description	M value[a]
SMa1683	Arylsulfatase	1.1488019
SMa2294 (*mrcA2*)	Penicillin-binding protein	0.9177869
SMa2402 (*rhbB*)	L-2,4-diaminobutyrate decarboxylase	-0.90247
SMa2404 (*rhbC*)	Rhizobactin 1021 biosynthesis protein	-1.506987
SMa2406 (*rhbD*)	Rhizobactin 1021 biosynthesis protein	-2.047386
SMa2408 (*rhbE*)	Rhizobactin 1021 biosynthesis protein	-1.637362
SMa2410 (*rhbF*)	Rhizobactin 1021 biosynthesis protein	-1.616273
SMa2412 (*rhrA*)	RhrA transcription regulator	1.7746001
SMb20005 (*gst15*)	Putative glutathione S-transferase protein	-1.620982
SMb20006	Hypothetical protein, FMN-binding domain	-1.353862
SMb20032	Hypothetical protein	0.9997762
SMb20345	Probable acriflavine family protein	1.353544
SMb20346	Putative efflux transmembrane protein	2.1810485
SMb20600	Hypothetical protein	0.9810468
SMb21676	Hypothetical protein	0.9794667
SMc01510 (*hmuV*)	Putative hemin transport system ATP-binding ABC transporter	1.4149306
SMc01512 (*hmuT*)	Putative hemin binding periplasmic transmembrane protein	1.4274398
SMc01513 (*hmuS*)	Putative hemin transport protein	1.2690038
SMc01514	Conserved hypothetical protein	1.3043614
SMc01517	Conserved hypothetical protein	1.1488003
SMc01626	Putative polyol ABC transporter, permease component	0.9491022
SMc01627	Putative polyol ABC transporter, permease component	1.225947
SMc01658 (*fhuF*)	Siderophore reductase	1.0907803
SMc01659 (*fhuP*)	Hydroxamate siderophore specific (ferrichrome and ferrioxamine B) ABC transporter, periplasmic component	1.4875657
SMc01747 (*hmuP*)	Regulatory protein that modulates hemin acquisition by regulating *shmR* transcription	1.1505371
SMc02726 (*shmR*)	Hemin-binding outer membrane receptor	3.7182691
SMc03167	MFS-type transport protein	1.9135745
SMc03168	Multidrug resistance efflux system	1.9508288
SMc03799	Conserved hypothetical protein	0.9252545

In bold are shown those genes that were found by Nogales et al. (2010) to be differentially expressed under swarming specific conditions in *S. meliloti* (subset S36).[a] $\log_2$ (experiment signal/control signal).

Another remarkable feature of this transcriptomic study was that more than 50% of the genes showing differential expression between 1021rhbD and Rm1021 cells (15 genes; shown in bold in Table 3.6) were also present in the subset S36 of *S. meliloti* genes differentially expressed under swarming inducing conditions (Nogales et al., 2010) which reinforces the close link between Rhb1021 and swarming motility. It is also interesting that the r*hbD* mutation leads to the up-regulation of several genes predicted to be involved in the resistance to toxic compounds such as *mrcA2*, and several components of putative multidrug resistance efflux systems:*Smb20345*, *Smb20346*, *Smc03167* and *Smc03168*. Especially noticeable was the opposite behavior shown by Rhb1021 biosynthesis genes (*rhb*) and *rhrA*, the gene coding for the transcriptional activator of siderophore synthesis and uptake genes (*rhb* and *rht*, respectively). Whereas *rhrA* displayed up-regulation in 1021rhbD, reflecting higher iron deficiency in the mutant than in the Wt, surprisingly *rhb* genes exhibited down-regulation. This surprising result, prompted us to select *rhrA* and *rhbB* genes as candidates amongst other genes to corroborate our transcriptomic study by using an independent technique.

To validate the microarray data, reverse transcription-quantitative PCR (RT-qPCR) was performed for *hmuS, shmR, rhrA,* and *rhbB* using the RNA isolated from 1021rhbD and Rm1021 cells grown on semisolid MM for 14 h. Expression of *hmuS*, *shmR* and *rhrA* was found to be higher in siderophore-defective cells than in the Wt strain, whereas the opposite was observed for *rhbB* gene expression (Fig. 3.18), thereby confirming the microarray results. In our transcriptomic study neither *rhtA* nor *rhbG* were found amongst differentially expressed genes, which could be due to the intrinsic limitations of the technique. In fact, RT-qPCR performed on these genes revealed that like *rhbB, rhtA* and *rhbG* exhibited lower expression levels in the 1021rhbD mutant than in the Wt. Altogether, these results suggest that the presence of either Rhb1021 or some of its biosynthetic intermediates, activates transcription of the *rhb* and *rht* genes.

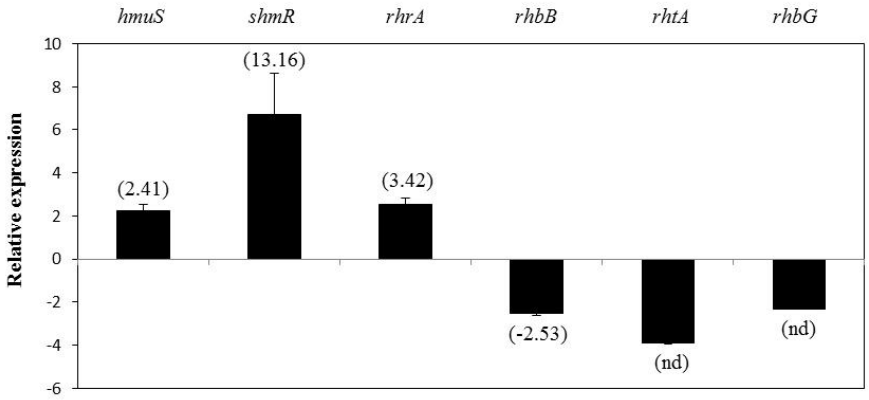

Figure 3.18. Relative expression of iron-related genes between 1021rhbD and Rm1021 cells as determined by RT-qPCR. The relative expression of the selected genes was calculated as the fold change between 1021rhbD compared to Rm1021 after 14 h. of growth on semisolid MM. For comparisons, fold changes in gene expression obtained in the microarray experiment (calculated as 2^M) are shown in parenthesis. Results are averages of two independent biological experiments with three technical replicates. Error bars indicate standard error of the mean. Nd, not detected in the microarray experiment.

3.5. Discussion

Bacterial siderophores have been profusely investigated for their crucial role in iron uptake. Rhizobactin 1021 (Rhb1021) produced by *S. meliloti* Rm1021 is an unusual siderophore in several aspects. On the one hand, Rhb1021 is a citrate-based dihydroxamate siderophore with the remarkable feature of having an enoyl-lipid moiety that gives the siderophore an asymmetric structure and is responsible for its highly amphiphilic properties (Persmark et al 1993). Amphiphilic and lipophilic siderophores are relatively uncommon amongst terrestrial bacteria with the exception of mycobactins. On the other hand, our recent investigations have shown that besides its function in iron uptake, Rhb1021 also plays a crucial role in the surface motility and biofilm development of *S. meliloti* Rm1021 by a mechanism which cannot exclusively be attributed to iron nutrition (Nogales et al., 2010; Amaya-Gómez et al., submitted). Surfactant properties inherent to Rhb1021 were suggested to be responsible for Rhb1021 effects on the two surface-associated behaviors. The assignment of additional functions to siderophores is scarce in the literature with the exception of

pyoverdine produced by *P. aeruginosa* which is recognized to act as a signaling molecule (Lamont et al., 2002). In this work we have investigated if the role of Rhb1021 in surface motility and in biofilm formation could be related to the special structure of this siderophore as well as the possible function of Rhb1021 as signaling molecule.

By using a drop collapse assay, we have confirmed that purified Rhb1021 shows surfactant activity. To the best of our knowledge, there are no reports in the literature about surfactant activity associated to other amphiphilic siderophores like mycobactins or more than half of the known marine siderophores like marinobactins, liohichelins, ochrobactins or synechobactins (Butler, 2005). For marine bacteria, the production of amphiphilic siderophores has been suggested to be advantageous because the presence of the lipid moiety confers the ability to partition into the bacterial membrane avoiding dilution in the liquid media, an effect observed for hydrophilic siderophores (Sandy and Butler, 2009). For a soil-dwelling bacterium like *S. meliloti*, the same advantage could be obtained under conditions of high water content. In addition, the surfactant activity of Rhb1021 might facilitate surface-associated behaviors as it has been reported for other surface active molecules like different lipopeptides (Mireles et al., 2001; Kuiper et al., 2004), or rhamnolipids and its precursors produced by *P. aeruginosa* (Tremblay et al., 2007).

We tried to confirm our hypothesis of the surfactant activity of Rhb1021 as being responsible for its role in surface motility and biofilm formation, by analyzing the phenotypes of mutants which potentially could produce a siderophore lacking the lipid moiety and therefore amphiphilic properties. *In silico* analyses predicted that both RhbD and RhbG could potentially catalyze the N-acylation required for the incorporation of the lipid moiety to Rhb1021, thereby mutants in *rhbD* and *rhbG* were obtained. As reported for other *rhb* mutants (Lynch et al., 2001), *rhbD* was unable to produce Rhb1021 or any other siderophore. The absence of Rhb1021, as well as two other compounds likely representing biosynthetic intermediates of Rhb1021, fit with the proposed role of

RhbD as the enzyme that catalyzes acetylation of N^4-hydroxy-1-aminopropane to give N^4-acetyl-N^4-hydroxy-1-aminopropane, although this should be biochemically proved. Our results also clearly demonstrated that contrary to what was previously proposed by Lynch et al (2001) and Challis (2005), *rhbG* is not responsible for incorporating the lipid moiety into Rhb1021 and at present its function remains unknown. Moreover, in contrast to genes belonging to the *rhbA-F* operon, *rhbG* is not essential for either siderophore synthesis or surface motility in *S. meliloti* although it influences bacterial surface-associated phenotypes. Loss-of function of *rhbG* promoted flagella-independent surface translocation and interfered with normal biofilm development with similar effects as those observed with *rhbA* and *rhbD* mutants. In addition to an increased surface spreading, *rhbG* mutants exhibited a different surface translocation pattern compared to their corresponding *rhbG*$^+$ strains. The effect on surface motility patterns caused by the *rhbG* mutation resembled the effects reported for rhamnolipids and its biosynthetic precursors on *P. aeruginosa* swarming motility (Caiazza et al., 2005; Tremblay et al., 2007). In this bacterium, rhamnolipids are surface-wetting agents required for swarming. However, a gradient of rhamnolipids/precursors ratio is also responsible for maintaining tendril organization and preventing the colonization of the area between tendrils. Likewise, it is tempting to hypothesize that in *S. meliloti* the ratio Rhb1021 versus some of its biosynthetic precursors might impact the pattern of surface motility. Chemical analyses of compounds present in culture supernatants of the 1021rhbG strain, revealed that the *rhbG* mutation led to an accumulation of (2E)-N-[3-(acetylamino)propyl]-N-hydroxydec-2-enamide) (RhbGdec) and to a decreased production of Rhb1021. We have not investigated if RhbGdec is responsible for the phenotypes associated to the *rhbG* mutant.

Exogenous addition of purified Rhb1021 could restore 1021rhbA growth to rates shown by the Wt. However, using the same approach we were unable to restore the surface spreading capacity of 1021rhbA and 1021rhbD as well as the biofilm formation capacity of 1021rhbD. The difficulties in complementing the surface-associated phenotypes of *rhb* mutants by adding the purified siderophore

could be due to the experimental setup. However, we can also speculate that a tight control of both timing and levels of Rhb1021 production might be crucial for its role in surface motility and biofilm formation. This might also explain why exogenous addition of Rhb1021 impacts negatively the biofilm development in the Wt. Like described for rhamnolipids of *P. aeruginosa*, the production of Rhb1021 must be tightly regulated within the *S. meliloti* biofilm in order to reach levels sufficient for maintaining the structure of the biofilm but below the levels which would impede or destroy biofilm structure. In favour of this hypothesis, we found that a *rirA* mutant that produces high levels of Rhb1021 regardless of iron levels in the medium is also affected in biofilm development (Amaya-Gómez et al., submitted). The analysis of the temporal and spatial expression of Rhb1021 genes in Wt and *rirA* biofilms would help increase our understanding of the role played by the siderophore in biofilm formation.

The transcriptomic analyses performed in this work unveiled 29 genes showing differential expression between 1021rhbD and Rm1021 after growth on semisolid MM. If this effect is directly caused by the lack of Rhb1021 which would function as a signaling molecule, or if it is an indirect effect caused by the lack of the ferric chelator has not been investigated in this study. Nevertheless, a significant proportion of the differentially expressed genes were related to alternative iron acquisition systems which showed up-regulation in 1021rhbD. This result might suggest that Rhb1021-defective cells deal with a higher nutritional iron deficiency than Rm1021 cells when grown on semisolid MM as a result of lacking the siderophore. The most remarkable feature of the transcriptomic study was the opposite behavior shown by Rhb1021 biosynthesis and uptake genes (*rhb* and *rhtA*) and *rhrA*, the gene coding for the AraC-like transcriptional activator of *rhb* and *rht* genes. Whereas *rhrA* displayed up-regulation in 1021rhbD, reflecting higher iron deficiency in the mutant than in the Wt, surprisingly *rhb* and *rhtA* genes exhibited down-regulation. These data suggest that the presence of either Rhb1021 or some of its biosynthetic intermediates, activates transcription of the *rhb* and *rht* genes. Regulation of siderophore synthesis and uptake genes by its cognate siderophore is not

unusual as allows bacteria to avoid the waste of energy caused by induction of all their acquisition systems in response to iron limitation irrespectively of the nature of the iron source available. This goal is achieved by a variety of regulatory mechanisms (Wandersman and Delepelaire, 2004). Interestingly, several siderophores have been found to bind to AraC-like proteins in the cytoplasm and positively regulate the genes for their own biosynthesis and uptake. This type of autoregulation has been demonstrated for production of pyochelin by *P. aeruginosa* (Reimmann et al., 1998) and alcaligin by *Bordetella* species (Brickman et al., 2001). To prove that this is also the case for Rhb1021 production in *S. meliloti*, additional experiments are required.

Altogether, our findings show that Rhb1021 function is far beyond being a simple siderophore. Its implication in bacterial processes such as surface motility, biofilm formation and autoregulation deserves further experimentation.

3.6. References

Battistoni, F., Platero, R., Duran, R., Cerveñansky, C., Battistoni, J., Arias, A., and Fabiano, E. (2002) Identification of an iron-regulated, hemin-binding outer membrane protein in *Sinorhizobium meliloti*. *Applied and Environmental Microbiology* 68: 5877–5881.

Beringer, J.E. (1974) R factor transfer in *Rhizobium Leguminosarum* *Journal of General Microbiology* 84: 188-198.

Brickman, T.J., Kang, H.Y., and Armstrong, S.K. (2001) Transcriptional activation of *Bordetella* alcaligin siderophore genes requires the AlcR regulator with alcaligin as inducer. *Journal of Bacteriology* 183: 483–489.

Butler, A. (2005) Marine siderophores and microbial iron mobilization. *BioMetals* 18: 369–374.

Caiazza, N.C., Shanks, R.M.Q., and O'Toole, G.A. (2005) Rhamnolipids modulate swarming motility patterns of *Pseudomonas aeruginosa*. *Journal of Bacteriology* 187: 7351–7361.

Casse, F., Boucher, C., Julliot, J.S., Michel, M., and Denarie, J. (1979) Identification and characterization of large plasmids in *Rhizobium meliloti* using agarose gel electrophoresis. *Journal of General Microbiology* 113: 229–242.

Cuív, P.Ó., Keogh, D., Clarke, P., and O'Connell, M. (2008) The *hmuUV* genes of *Sinorhizobium meliloti* 2011 encode the permease and ATPase components of an ABC transport system for the utilization of both haem and the hydroxamate siderophores, ferrichrome and ferrioxamine B. *Molecular Microbiology* 70: 1261–1273.

Challis, G.L. (2005) A widely distributed bacterial pathway for siderophore biosynthesis independent of nonribosomal peptide synthetases. *ChemBioChem* 6: 601–611.

Chao, T.-C., Buhrmester, J., Hansmeier, N., Pühler, A., and Weidner, S. (2005) Role of theregulatory gene *rirA* in the transcriptional response of *Sinorhizobium meliloti* to iron limitation. *Applied and Environmental Microbiology* 71: 5969-5982.

Chen, Y., Unger, M., Ntai, I., McClure, R.A., Albright, J., Thomson, R.J., and Kelleher, N.L. (2012) Gobichelin A and B: mixed-ligand siderophores discovered using proteomics. *MedChemComm*.

Cheng, H.P., and Walker, G.C. (1998) Succinoglycan is required for initiation and elongation of infection threads during nodulation of alfalfa by *Rhizobium meliloti*. *Journal of Bacteriology* 180: 5183-5191.

Daniels, R., Reynaert, S., Hoekstra, H., Verreth, C., Janssens, J., Braeken, K. et al. (2006) Quorum signal molecules as biosurfactants affecting swarming in *Rhizobium etli*. *Proceedings of the National Academy of Sciences* 103: 14965-14970.

de Lorenzo, V., Bindereif, A., Paw, B.H., and Neilands, J.B. (1986) Aerobactin biosynthesis and transport genes of plasmid ColV-K30 in *Escherichia coli* K-12. *Journal of Bacteriology* 165: 570–578.

DeRisi, J.L., Iyer, V.R., and Brown, P.O. (1997) Exploring the metabolic and genetic control of gene expression on a genomic scale. *Science* 278: 680–686.

Dondrup, M., Goesmann, A., Bartels, D., Kalinowski, J., Krause, L., Linke, B. et al. (2003) EMMA: a platform for consistent storage and efficient analysis of microarray data. *Journal of Biotechnology* 106: 135–146.

Gauglitz, J.M., Zhou, H., and Butler, A. (2012) A suite of citrate-derived siderophores from a marine *Vibrio species* isolated following the deepwater horizon oil spill. *J Inorg Biochem* 107: 90–95.

Gobin, J., and Horwitz, M.A. (1996) Exochelins of *Mycobacterium tuberculosis* remove iron from human iron-binding proteins and donate iron to mycobactins in the *M. tuberculosis* cell wall. *The Journal of experimental medicine* 183: 1527–1532.

Ho, S.N., Hunt, H.D., Horton, R.M., Pullen, J.K., and Pease, L.R. (1989) Site-directed mutagenesis by overlap extension using the polymerase chain reaction. *Gene* 77: 51–59.

Ito, Y., and Butler, A. (2005) Structure of synechobactins, new siderophores of the marine cyanobacterium *Synechococcus* sp. PCC 7002. *Limnology and oceanography*: 1918–1923.

Johnston, A., Crosa, J., Mey, A., and Payne, S. (2004) Mechanisms and regulation of iron uptake in the Rhizobia. *Iron transport in bacteria*: 469–488.

Kuiper, I., Lagendijk, E.L., Pickford, R., Derrick, J.P., Lamers, G.E.M., Thomas-Oates, J.E. et al. (2004) Characterization of two *Pseudomonas putida* lipopeptide biosurfactants, putisolvin I and II, which inhibit biofilm formation and break down existing biofilms. *Molecular Microbiology* 51: 97–13.

Lamont, I.L., Beare, P.A., Ochsner, U., Vasil, A.I., and Vasil, M.L. (2002) Siderophore-mediated signaling regulates virulence factor production in *Pseudomonas aeruginosa*. *Proceedings of the National Academy of Sciences* 99: 7072–7077.

Lynch, D., O'Brien, J., Welch, T., Clarke, P., ÓCuív, P., Crosa, J.H., and O'Connell, M. (2001) Genetic organization of the region encoding regulation, biosynthesis, and transport of rhizobactin 1021, a siderophore produced by *Sinorhizobium meliloti*. *Journal of Bacteriology* 183: 2576-2585.

Maniatis, T., Fritsch, E.F., and Sambrook, J. (1989) Molecular cloning : a laboratory manual / J. Sambrook, E.F. Fritsch, T. Maniatis. In: New York : Cold Spring Harbor Laboratory Press.

Martin, J., Ito, Y., Homann, V., Haygood, M., and Butler, A. (2006) Structure and membrane affinity of new amphiphilic siderophores produced by *Ochrobactrum* sp. SP18. *Journal of Biological Inorganic Chemistry* 11: 633–641.

Meade, H.M., and Signer, E.R. (1977) Genetic mapping of *Rhizobium meliloti*. *Proceedings of the National Academy of Sciences of the United States of America* 74: 2076-2078.

Mireles, J.R., Toguchi, A., and Harshey, R.M. (2001) *Salmonella enterica* Serovar Typhimurium swarming mutants with altered biofilm-forming abilities: surfactin inhibits biofilm formation. *Journal of Bacteriology* 183: 5848–5854.

Müller, G., and Raymond, K.N. (1984) Specificity and mechanism of ferrioxamine-mediated iron transport in *Streptomyces pilosus*. *Journal of Bacteriology* 160: 304–312.

Mullis, K.B., Pollack, J.R., and Neilands, J.B. (1971) Structure of schizokinen, an iron-transport compound from *Bacillus megaterium*. *Biochemistry* 10: 4894–4898.

Nogales, J., Bernabéu-Roda, L., Cuéllar, V., and Soto, M.J. (2012) ExpR is not required for swarming but promotes sliding in *Sinorhizobium meliloti*. *Journal of Bacteriology*.

Nogales, J., Domínguez-Ferreras, A., Amaya-Gómez, C., van Dillewijn, P., Cuéllar, V., Sanjuán, J. et al. (2010) Transcriptome profiling of a *Sinorhizobium meliloti fadD* mutant reveals the role of rhizobactin 1021 biosynthesis and regulation genes in the control of swarming. *BMC Genomics* 11: 157.

Ó Cuív, P., Clarke, P., Lynch, D., and O'Connell, M. (2004) Identification of *rhtX* and *fptX*, novel genes encoding proteins that show homology and function in the utilization of the siderophores rhizobactin 1021 by *Sinorhizobium meliloti* and pyochelin by *Pseudomonas aeruginosa*, Respectively. *Journal of Bacteriology* 186: 2996–3005.

Osterås, M., Driscoll, B.T., and Finan, T.M. (1995) Molecular and expression analysis of the *Rhizobium meliloti* phosphoenolpyruvate carboxykinase (pckA) gene. *Journal of Bacteriology* 177: 1452-1460.

Persmark, M., Pittman, P., Buyer, J.S., Schwyn, B., Gill, P.R., and Neilands, J.B. (1993) Isolation and structure of rhizobactin 1021, a siderophore from the alfalfa symbiont *Rhizobium meliloti* 1021. *Journal of the American Chemical Society* 115: 3950–3956.

Pfaffl, M.W. (2001) A new mathematical model for relative quantification in real-time RT–PCR. *Nucleic Acids Research* 29: e45.

Reimmann, C., Serino, L., Beyeler, M., and Haa, D. (1998) Dihydroaeruginoic acid synthetase and pyochelin synthetase, products of the *pchEF*, are induced by extracellular pyochelin in *Pseudornonas aeruginosa*. *Microbiology* 144: 3135–3148.

Robertsen, B.K., Aman, P., Darvill, A.G., McNeil, M., and Albersheim, P. (1981) The structure of acidic extracellular polysaccharides secreted by *Rhizobium leguminosarum* and *Rhizobium trifolii*. *Plant Physiology* 67: 389-400.

Russo, D.M., Williams, A., Edwards, A., Posadas, D.M., Finnie, C., Dankert, M. et al. (2006) Proteins exported via the PrsD-PrsE type I secretion system and the acidic exopolysaccharide are involved in biofilm formation by *Rhizobium leguminosarum*. *Journal of Bacteriology* 188: 4474-4486.

Sambrook, J., and Fritsch, E. (1989) Maniatis: T Molecular clonning: A laboratory manual. *Cold Spring Harbor Laboratory Press* 2: Cold Spring Harbor N.Y.

Sandy, M., and Butler, A. (2009) Microbial iron acquisition: marine and terrestrial siderophores. *Chemical Reviews* 109: 4580–4595.

Schäfer, A., Tauch, A., Jäger, W., Kalinowski, J., Thierbach, G., and Pühler, A. (1994) Small mobilizable multi-purpose cloning vectors derived from the *Escherichia coli* plasmids pK18 and pK19: selection of defined deletions in the chromosome of *Corynebacterium glutamicum*. *Gene* 145: 69-73.

Schwyn, B., and Neilands, J.B. (1987) Universal chemical assay for the detection and determination of siderophores. *Analytical Biochemistry* 160: 47–56.

Simon, R., Priefer, U., and Pühler, A. (1983) A broad host range mobilization system for In vivo genetic engineering: Transposon mutagenesis in Gram negative bacteria. *Nat Biotech* 1: 784-791.

Soto, M.J., Fernández-Pascual, M., Sanjuan, J., and Olivares, J. (2002) A *fadD* mutant of *Sinorhizobium meliloti* shows multicellular swarming migration and is impaired in nodulation efficiency on alfalfa roots. *Molecular Microbiology* 43: 371-382.

Storey, E.P., Boghozian, R., Little, J., Lowman, D., and Chakraborty, R. (2006) Characterization of 'Schizokinen'; a dihydroxamate-type siderophore produced by *Rhizobium leguminosarum* IARI 917. *BioMetals* 19: 637–649.

Tremblay, J., Richardson, A.-P., Lépine, F., and Déziel, E. (2007) Self-produced extracellular stimuli modulate the *Pseudomonas aeruginosa* swarming motility behaviour. *Environmental Microbiology* 9: 2622–2630.

Viguier, C., Ó Cuív, P., Clarke, P., and O'Connell, M. (2005) RirA is the iron response regulator of the rhizobactin 1021 biosynthesis and transport genes in *Sinorhizobium meliloti* 2011. *FEMS microbiology letters* 246: 235-242.

Visca, P., Leoni, L., Wilson, M.J., and Lamont, I.L. (2002) Iron transport and regulation, cell signalling and genomics: lessons from *Escherichia coli* and *Pseudomonas*. *Molecular Microbiology* 45: 1177–1190.

Wandersman, C., and Delepelaire, P. (2004) Bacterial iron sources: from siderophores to hemophores. *Annual Review of Microbiology* 58: 611–647.

Chapter 4: Symbiotic phenotype of mutants altered in multicellular surface-associated processes

Symbiotic phenotype of mutants altered in multicellular surface-associated processes

Carol V Amaya-Gómez, Virginia Cuellar and María J. Soto.

Dpto. Microbiología del Suelo y Sistemas Simbióticos. Estación Experimental del Zaidín, Consejo Superior de Investigaciones Científicas (CSIC), Profesor Albareda 1, 18008 Granada, Spain.

4.1. Abstract

Swarming motility and biofilm formation are two bacterial surface-associated behaviors known to impact bacteria-host pathogenic interactions. In soil-dwelling beneficial bacteria collectively known as *Rhizobium*, swarming and biofilm formation as well as their roles in the establishment of symbiosis with legume plants, remain largely unexplored. Previous studies in our group demonstrated that essential genes for the biosynthesis of the siderophore rhizobactin 1021 (Rhb1021) (*rhb* and *rhrA* genes) as well as *rirA*, the gene coding for the global iron response regulator in the alfalfa symbiont *Sinorhizobium meliloti* play important functions in surface motility and biofilm formation. Different studies have claimed that genes involved in the regulation, synthesis and uptake of Rhb1021 as well as the *rirA* gene, are not essential for nodulation or nitrogen fixation. In order to investigate the importance of surface motility and biofilm formation abilities on the establishment of *Rhizobium*-legume symbiosis, in this work we assessed in more detail the symbiotic properties of *S. meliloti* Rhb1021-defective and *rirA* mutants, analyzing their nodule formation efficiencies and competitive abilities. We also studied the symbiotic performance of an *rhtA* mutant displaying increased motility on surfaces. Our results indicated that the different mutants analyzed exhibited some kind of defect in one or several symbiotic properties. These defects were more pronounced for mutant strains displaying increased surface motility (*rhtA* and *rirA*) than for those impaired in surface translocation (Rhb1021-defective mutants). The most severe symbiotic phenotype was shown by the *rirA* mutant which was highly impaired in nodule formation on alfalfa roots and exhibited a Fix$^-$ phenotype.

4.2. Introduction

Swarming motility and biofilm formation are two multicellular surface-associated behaviors profusely investigated in pathogenic bacteria as they have been shown to influence the outcome of host interactions (Verstraeten et al., 2008). Swarming motility is a type of translocation dependent on rotating flagella characterized by the rapid and co-ordinated movement of multicellular groups of

bacteria (Kearns, 2010). Cell-cell communication by quorum sensing, cell surface components like exopolysaccharides (EPS), and production of surfactant agents, are required for swarming (Daniels et al., 2004; Kearns, 2010). Biofilms consist of groups of bacteria attached to surfaces and encased in a self-produced polymeric matrix (Davey and O'toole, 2000). Although they represent two different lifestyles (motile vs sessile), swarming motility and biofilms are two processes closely related.

The soil bacterium *Sinorhizobium meliloti* is able to establish nitrogen-fixing symbiosis with alfalfa plants. Recent investigations have shown that this *Rhizobium* is able to spread over semisolid surfaces (Nogales et al., 2010; Nogales et al., 2012) and it can also form biofilms on both abiotic surfaces and roots (Fujishige et al., 2006;). However, the roles played by these two surface associated phenomena in the establishment of the *Rhizobium*-legume symbiosis are not clear yet. Like in other bacteria, several components involved in swarming motility in *S. meliloti* are also important for biofilm formation. Interestingly, some of them have been shown to influence in different ways bacterial symbiotic properties. Thus, the lack of flagella, essential for swarming motility, leads to a significant reduction in biofilm capability in microtiter plates compared to the Wt, probably because of an impairment in bacterial adherence to surfaces (Fujishige et al., 2006; our unpublished results). *S. meliloti* mutants lacking flagella are able to establish symbiosis with its legume hosts but they show a delay in nodule development (Fujishige et al., 2006). Production of the symbiotically important exopolysaccharide II (EPS II) or galactoglucan promotes surface translocation and is crucial for biofilm formation and for root colonization (Rinaudi and González, 2009; Nogales et al., 2012). Another example of a *S. meliloti* gene required for swarming motility and biofilm formation is *fadD*. Initial investigations showed that inactivation of the *fadD* gene coding for a long-chain fatty acyl-coenzyme A ligase promoted swarming motility and impaired bacterial nodulation efficiency and competitiveness (Soto et al., 2002). More recently we found that *fadD* is also required for normal biofilm development in *S. meliloti* (Amaya-Gómez et al. submitted).

A transcriptomic analysis of *S. meliloti* under swarming-inducing conditions led to the discovery that biosynthesis of the siderophore rhizobactin 1021 (Rhb1021) was essential for surface translocation of the wild-type strain Rm1021 (Nogales et al., 2010; Nogales et al., 2012). Rhb1021 is a citrate-based dihydroxymate siderophore which is produced by *S. meliloti* Rm1021 under iron-limiting conditions (Persmark et al., 1993). Genes belonging to the *rhbABCDEF* operon code for different proteins involved in the synthesis of this siderophore (Lynch et al., 2001). Its transport into the cell is mediated by the outer membrane receptor protein RhtA and the inner receptor protein RhtX (Ó Cuív et al., 2004). Rhb1021 biosynthesis and transport genes are positively regulated by the AraC transcriptional activator RhrA whose expression is induced by iron limitation as well as by loss-of-function of the iron response regulator RirA (Chao et al., 2005). *S. meliloti rhb* and *rhrA* mutants which are defective in Rhb1021 synthesis do not exhibit swarming motility whereas an *rhtA* mutant impaired in Rhb1021 uptake is able to swarm (Nogales et al., 2010). More recently, using a different source of agar for surface motility experiments, it was observed that the *rhtA* mutant exhibited increased surface translocation compared with the corresponding parental strain (J. Nogales, unpublished). These results supported the hypothesis that low intracellular iron levels were not responsible for the swarming deficiency of the *rhb* and *rhrA* mutants, and that the presence of Rhb1021 outside the cell was important for facilitaing surface motility in *S. meliloti*. Moreover, high iron conditions were found to inhibit swarming motility in *S. meliloti* Wt but not in a *rirA* mutant in which surface motility seemed even to be enhanced compared to lower iron concentrations. This suggested a role for the iron regulator in the control of this multicellular type of translocation (Nogales et al., 2010). More recently, we found that the *rhb* and *rirA* genes are also important for normal biofilm development by *S. meliloti* Rm1021 on both abiotic and root surfaces (Amaya-Gómez et al. submitted). Mutations in *rhb* or in *rirA* prevented the formation of thick mature biofilms on glass surfaces and negatively affected alfalfa root colonization. Surfactant properties associated to Rhb1021 could be responsible for its effects on both swarming motility and biofilm formation.

Different studies analyzing the symbiotic properties of mutants in the synthesis, uptake and regulation of Rhb1021 concluded that Rhb1021 is not essential for nodulation or nitrogen fixation (Barton et al., 1992; Gill et al., 1991; Lynch et al., 2001; Ó Cuív et al., 2009). However, under certain experimental conditions (i.e. long term experiments or under low iron conditions) the synthesis of the siderophore seemed to contribute to the efficiency of nitrogen fixation. Likewise, no differences in nodulation efficiency or nitrogen fixation have been detected between plants inoculated with a *S. meliloti rirA* mutant and plants inoculated with the Wt strain, indicating that RirA is not essential for symbiosis (Chao et al., 2005; Viguier et al., 2005).

Given the role played by *rhb* and *rirA* genes in bacterial surface motility and biofilm formation, two surface-associated behaviors known to impact bacteria-host interactions, we decided to assess in more detail the symbiotic properties of *S. meliloti rhb* and *rirA* mutants, analyzing their nodule formation efficiencies and competitive abilities. Moreover, considering the hypermotile phenotype recently observed for an *rhtA* mutant, we also studied the symbiotic performance of this strain. Our results show that the different mutants analyzed exhibited some kind of defect in one or several symbiotic properties. These defects were more pronounced for mutant strains displaying increased surface motility (*rhtA* and *rirA*) than for those impaired in surface translocation (*rhb*).

4.3. Materials and Methods.

Bacterial strains and growth conditions

Bacterial strains used in this study are listed in Table 4.1. *S. meliloti* strains were routinely cultured in Tryptone-Yeast extract complex medium (TY) (Beringer, 1974) at 30 ºC. When required, antibiotics were added at the following final concentrations: *S. meliloti*, streptomycin (Sm) 200 µg/ml, kanamycin (Km) 200 µg/ml, rifampin (Rif) 100 µg/ml, and neomycin sulphate (Nm) 100 µg/ml.

Table 4.1. Strains used in this study.

Strain	Relevant characteristics	Reference or source
Sinorhizobium meliloti		
Rm1021	SU47 expR102::ISRm2011-1, Smr	(Meade and Signer, 1977)
1021rhbA	Rm1021 (*rhbA*::Tn5lac); Sm^r Nm^r	(Nogales et al., 2012)
Rm2011	SU47 expR102::ISRm2011-1, Smr	(Casse et al., 1979)
2011rhbE11	Rm2011 (*rhbE*::Tn5lac), Smr Rifr Nmr	(Lynch et al., 2001)
2011rhtA1	Rm2011 (*rhtA*::Tn5), Smr Rifr Nmr	(Lynch et al., 2001)
2011rhrA26	Rm2011 (*rhrA*::Tn5lac), Smr Rifr Nmr	(Lynch et al., 2001)
G212rirA	Rm1021 (*lac*-, rirA::Km), Smr Kmr	(Osterås et al., 1995)
Rm1021(pGus3)	Rm1021(pGus3); Sm^r Km^r	(Amaya-Gómez, 2009)
Rm2011(pGus3)	Rm2011(pGus3); Sm^r Km^r	This work

Nodule formation efficiency assays

Alfalfa seeds were sterilized and germinated as described by Olivares et al. (1980). Germinated seeds (1 cm long) were transferred to square Petri dishes containing nitrogen free medium (Olivares et al., 1980) solidified with agarose 0.8% (Pronadisa) and overlaid with a wet sterile Whatman filter paper. In order to test the infectivity of a rhizobial strain, at least 30 plants were inoculated with a bacterial suspension prepared as follows. Rhizobia were previously grown on plates of TY medium at 30 ºC. Then, cell mass was resuspended in TY broth up to an O.D. $_{600nm}$ = 0.1, washed and diluted in sterile water to obtain a cell suspension containing 1×10^4 bacterial cells/ml. Each plant was inoculated with 30 µl of this cell suspension. The number of nodulated plants and the number of nodules per plant were recorded daily.

Competition nodulation assays

Plants were grown in the glass assembly device described by Leonard (1943). The upper part of the jars was filled with vermiculite. The nutrient plant solution described by Rigaud and Puppo (1975) was used for fertilization. Alfalfa seeds (*Medicago sativa* L.) were germinated and sterilized as described Olivares et al. (1980). Before inoculation, germinated seeds were planted into the vermiculite and allowed to grow for one day in the plant growth chamber. Two days old seedlings were inoculated with 1 ml of a bacterial suspension containing 1×10^2 CFUs/ml. The bacterial suspension contained a mixture of the wild-type strain or

the strain to be tested with the wild-type strain harbouring the pGus3 plasmid at ratio of 1:1. The plasmid pGus3 contains the marker gene coding for β-glucuronidase (GUS) (Garcia-Rodriguez and Toro, 2000). After 15 days of incubation, roots were collected and washed with water. Then they were incubated overnight in the dark at 37 ºC in 1mM X-Gluc (5-bromo-4-chloreo-3-indolyl-β-D-glucuronide; Apollo Scientific) in 50 mM sodium phosphate buffer (pH 7.5) with 1% SDS. The nodules occupied by the wild-type strain containing the pGus3 plasmid stained blue, so nodule occupancy could be determined by counting blue and white nodules.

Root adsorption and colonization

In order to quantify the number of *Rhizobium* cells attached per gr of root fresh weight (RFW), alfalfa plants were grown and inoculated as follows. Alfalfa (*Medicago sativa* L.) seeds were sterilized, germinated and grown as specified above for the nodule efficiency assay. Transferred-germinated seeds were allowed to grow for one day more before to be inoculated. Two days old seedlings were inoculated with 30 µl of a suspension containing approximately 1×10^5 bacterial cells/ml, prepared as described above. At defined times, 15 seedlings were extensively washed with sterile water to remove the unattached bacteria. The excess of water over the roots was removed and they were weighed. Three roots were immerse in 1 ml of sterile TE buffer and exposed to sonication. 2 sonication pulses of 1 min each with a pause time of 1 min between the pulses in an Ultrasons-H (J.P. Selecta, S.A) sonication bath were made to release the attached cells which were quantified by colony counting (normalized to the root weight). The experiment was repeated three times.

4.4. Results and Discussion

Symbiotic properties of *S. meliloti* mutants affected in Rhb1021-related genes

Different laboratories have reported that genes involved in regulation, biosynthesis and uptake of the siderophore Rhb1021 are not essential for nodulation or nitrogen fixation in *S. meliloti* (Barton et al., 1992; Gill et al., 1991; Lynch et al., 2001; Ó Cuív et al., 2004). Our previous studies revealed that an Rhb1021-defective mutant (1021rhbA) unable to translocate over surfaces was highly impaired in alfalfa root colonization (Amaya-Gómez et al. submitted) but its symbiotic phenotype was not further analyzed. Recently, we detected that a *S. meliloti rhtA* mutant, unable to utilize Rhb1021, is hypermotile on semisolid surfaces. We wondered whether this surface-associated phenotype could also have an effect on alfalfa root colonization and infection. Hence, we investigated the ability of the siderophore uptake mutant 2011rhtA to attach and colonize alfalfa roots by colony forming units (CFUs) counting (Fig. 4.1).

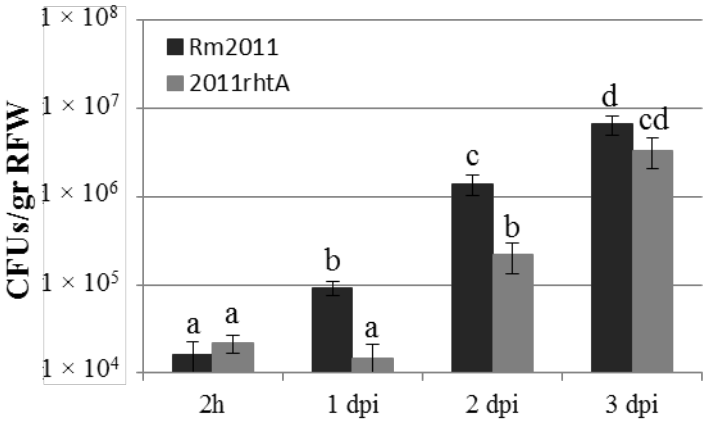

Fig. 4.1. Colony forming unit (CFUs) counts recovered from alfalfa roots. Data are expressed per gram of root fresh weight (RFW). Error bars indicate the standard deviation from the mean. According to the Games Howell test ($P \leq 0.05$) values followed by the same letter do not differ significantly. Dpi, days post inoculation.

As observed for 1021rhbA (Amaya-Gómez et al. submitted), 2011rhtA did not show differences in root adsorption compared to the Wt strain (CFUs recovered from alfalfa plants, 2 hours after inoculation). However, the number of 2011rhtA cells colonizing roots after 1 and 2 days post inoculation (dpi) was 6

and 5.6 fold lower, respectively, than those observed for Rm2011 whereas no differences were detected 3 dpi. These results indicate that like 1021rhbA, the *rhtA* mutant is impaired in root colonization during the first days of the symbiotic interaction. Given the significant reduction in alfalfa root colonization ability shown by both *rhbA* and *rhtA* mutants, and the important role that an efficient host colonization plays in the outcome of different bacteria-host interactions, we presumed that the *rhbA* and *rhtA* mutants should exhibit some altered symbiotic property.

The nodulation kinetics of 1021rhbA and 2011rhtA on alfalfa plants were determined and compared with those shown by their corresponding parental strains (Rm1021 and Rm2011) (Fig. 4.2). Both mutants were able to induce nitrogen-fixing nodules, confirming the results published by others (Barton et al., 1992; Gill et al., 1991; Lynch et al., 2001). The *rhbA* mutant was only slightly affected in nodule formation efficiency, inducing the development of a lower number of nodules than the Wt during the first days of the interaction, a defect that was recovered in time (Fig. 4.2A). In the case of 2011rhtA, a delay of 2-3 days in the onset of nodulation was observed as well as the induction of a lower number of nodules formed between 4 and 8 dpi compared to Rm2011 (Fig. 4.2B).

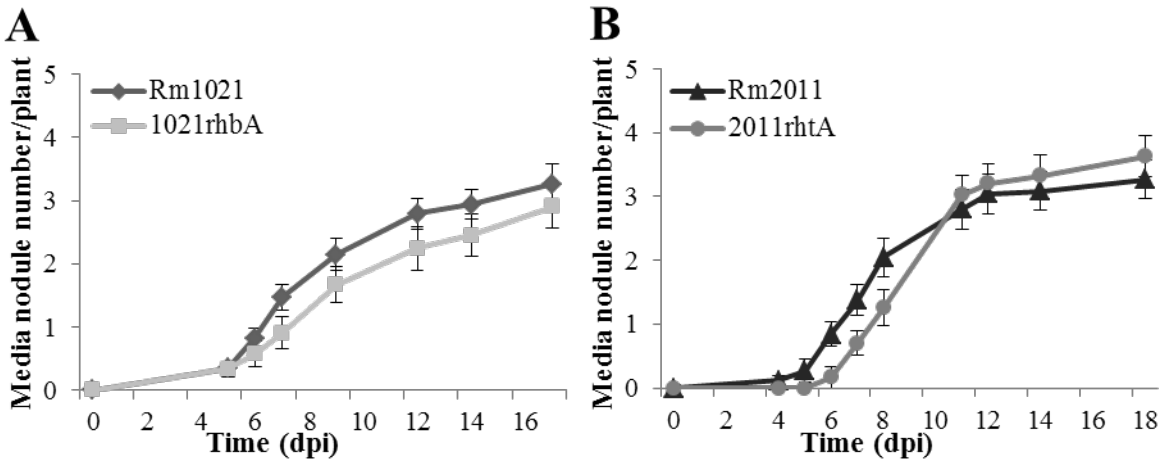

Figure 4.2. Nodulation efficiency test of *S. meliloti* strains. Error bars indicate standard errors. Values on A are the mean of a representative experiment from three independent replicates. Values on B are the mean of a single experiment.

We also evaluated the competitive ability of mutants in *rhbE* (2011rhbE), *rhtA* (2011rhtA) and *rhrA* (2011rhrA). In order to do this, alfalfa seedlings were inoculated with a 1:1 mixture of the mutant strain to be evaluated and Rm2011 harboring the pGus3 plasmid as described in the Materials and Methods section. As shown in Fig. 4.3, the Rhb1021-defective mutants *rhbE* and *rhrA* were able to compete for nodule occupancy as efficiently as the parental strain. However, the the *rhtA* mutant showed a significant reduction (12%) in competitiveness (Fig. 4.3).

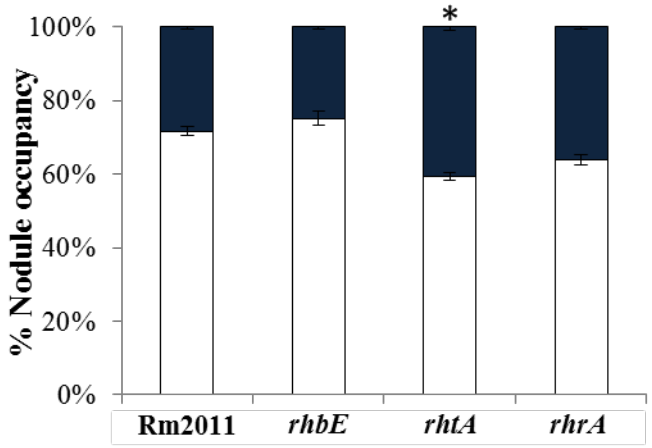

Figure 4.3. Competition nodulation assay of Rhb1021-related mutants. Data represent the percentage of white and blue stained nodules occupied by the different strains after inoculation with 1:1 mixtures of the strain to be evaluated and Rm2011 harboring the pGus3 plasmid: Rm2011 × Rm2011(pGus3), 2011rhbE11 × Rm2011(pGus3), 2011rhtA1 × Rm2011(pGus3), 2011rhrA26 × Rm2011(pGus3). The percentage of nodules occupied by the marked strain is shown with blue bars. Values are the mean of two independent experiments. * Competitive ability of the tested strain is significantly different from that of the parental strain.

Altogether, these results show that although the genes involved in biosynthesis and uptake of Rhb1021 are not essential for nodulation, they can affect some rhizobial symbiotic properties such as nodule formation efficiency or competitiveness. Under our experimental conditions, the defect shown by Rhb1021 defective mutants in nodule formation efficiency was very subtle and transitory, indicating that: i) either the bacteria are not under iron-depleted conditions or they are using alternative mechanisms to obtain iron during the symbiotic interaction, and ii) although the inability to translocate on surfaces reduces the bacterial ability to colonize root surfaces, it is not crucial for triggering nodule formation. Although Rhb1021 is likely to be a factor that

contributes to the competitive ability of free-living *S. meliloti* especially in iron-depleted soils, no differences in competitiveness were observed between the Wt and Rhb1021 defective mutants in our experiments, a result that could be expected if the mutant is being extracellularly complemented by the siderophore produced by the Wt strain. Competition experiments performed in iron-depleted soils and in the presence of natural complex bacterial communities would help to uncover the real biological significance of Rhb1021 production in *S. meliloti*.

On the other hand, under the same experimental conditions, an *rhtA* mutant unable to acquire Rhb1021 which accumulates outside the cell, showed a worse symbiotic performance than the *rhb* mutant, reflected in its nodule formation efficiency and competitive ability. It is tempting to speculate that accumulation of Rhb1021 outside *rhtA* mutant cells is responsible for the increase in surface translocation and that this might be detrimental for optimal root colonization, nodule formation efficiency and competitiveness. Another not excluding possibility is that the inability to acquire Rhb1021 leads to an iron nutritional deficiency in *S. meliloti*.

Symbiotic properties of *S. meliloti rirA* mutant

Studies performed in our group showed that *rirA* plays a role in the control of *S. meliloti* surface motility and biofilm formation (Nogales et al. 2010; Amaya-Gómez et al., submitted). We also demonstrated that a *rirA* mutant overproduces Rhb1021 regardless of iron availability (Amaya-Gómez et al. in preparation), and it is highly impaired in root colonization (Amaya-Gómez et al., submitted). Previous reports described that a *S. meliloti rirA* mutant was as effective as Rm1021 in inducing nitrogen fixing nodules in alfalfa (Chao et al., 2005; Viguier, 2005). However, under our experimental conditions, we found that the G212rirA mutant elicited the formation of ineffective nitrogen fixing nodules on alfalfa. This phenotype was clearly evident at the end of the nodulation experiment, when most of the nodules induced by G212rirA were white and alfalfa plants inoculated with this mutant showed a yellow appearance indicating their ineffectiveness for nitrogen fixation (Fig. 4.4A). It should be mentioned that we detected few pink

nodules in plants inoculated with the *rirA* mutant, but we were unable to isolate viable cells from these nodules. In addition, the *rirA* mutant was highly impaired in nodule formation efficiency (Fig. 4.4B), and exhibited a significant reduction (29%) in competitiveness compared with the Wt strain Rm1021 (Fig. 4.4C). These results indicate that contrary to what has been published, RirA plays an important role in the *Rhizobium*-legume symbiosis.

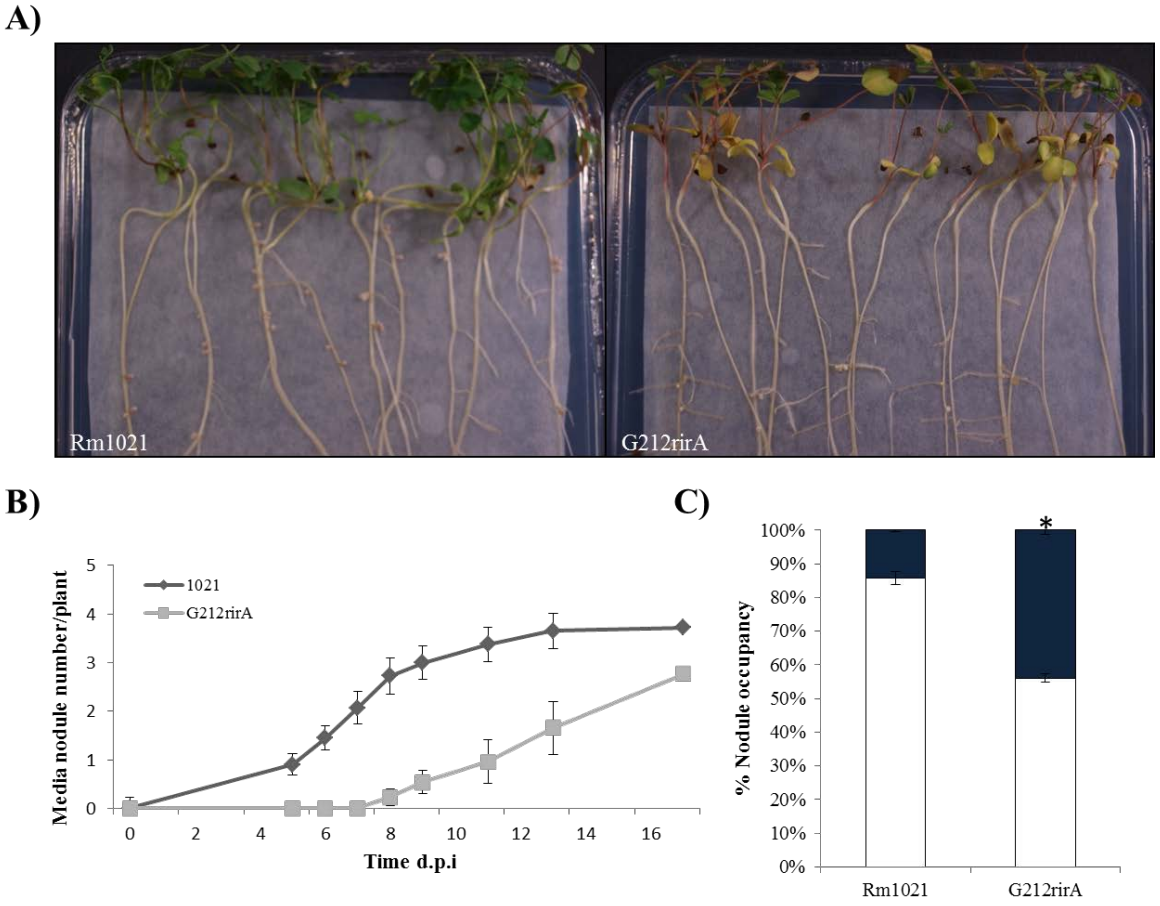

Figure 4.4. Symbiotic phenotype of the *S. meliloti rirA* mutant. A) Physical appearance of plants inoculated with Rm1021 or G212rirA, 20 days after inoculation. B) Nodulation efficiency test of Rm1021 and G212rirA. Error bars indicate standard errors. The experiment was repeated three times. C) Competition nodulation assay of the *rirA* mutant. Data represent the percentage of white and blue nodules occupied by the different strains after inoculation with 1:1 mixtures of Rm1021 or *rirA* mutant and Rm1021 harbouring the pGus3 plasmid. Percentage of nodules occupied by the marked strain is shown with blue bars. Values are the mean of two independent experiments. * indicates that the competitive ability of G212rirA significantly differed from that of Rm1021.

At present, we cannot give an explanation to these contradictory results. Disruption of the *rirA* gene in G212rirA was confirmed by PCR (data not shown), however genetic complementation experiments have not been performed yet to exclude the possibility of additional mutations that could be responsible for the observed phenotypes. It should also be mentioned that the iron sources and concentrations used in the plant mineral solution employed in our experiments and those performed by Chao et al. (2005) and Viguier et al., (2005) were different. While our plant mineral solution contained 68 μM of ethylenediaminetetraacetic acid iron (III) sodium salt (EDTA-Fe), that used by Chao et al. (2005) contained 5, 10 and 15 μM of $FeSO_4$. On the other hand, Viguier et al. (2005) used free-nitrogen Jensen's solution, which contains $FeCl_3$ to a final concentration of 431 μM. If under our conditions there is higher iron availability for the bacteria, the derepressed iron uptake exhibited by the *rirA* mutant, would lead to toxic intracellular iron levels and oxidative stress (Chao et al., 2005), affecting cell viability and establishment of symbiosis. Additional experiments are required to solve the contradictory data as well as to investigate if the symbiotic phenotype shown by the *rirA* mutant could be due to alterations in surface motility and/or biofilm formation or to deregulated iron homeostasis.

4.5. References

Amaya-Gómez., C. V. 2009. Identificación de determinantes genéticos del swarming en *S. meliloti*. Trabajo de Investigación Tutelada, Universidad de Granada, Trabajo de Investigación Tutelada.

Barton, L. L., F. A. Fekete, C. R. Vester, P. R. Gill, and J. B. Neilands. 1992. Physiological characteristics of *Rhizobium meliloti* 1021 Tn5 mutants with altered rhizobactin activities. Journal of Plant Nutrition 15: 2145–2156.

Beringer, J. E. 1974. R factor transfer in *Rhizobium Leguminosarum* Journal of General Microbiology 84: 188-198.

Casse, F., C. Boucher, J. S. Julliot, M. Michel, and J. Denarie. 1979. Identification and characterization of large plasmids in *Rhizobium meliloti* using agarose gel electrophoresis. Journal of General Microbiology 113: 229–242.

Chao, T.-C., J. Buhrmester, N. Hansmeier, A. Pühler, and S. Weidner. 2005. Role of theregulatory gene *rirA* in the transcriptional response of *Sinorhizobium meliloti* to iron limitation. Applied and Environmental Microbiology 71: 5969-5982.

Daniels, R., J. Vanderleyden, and J. Michiels. 2004. Quorum sensing and swarming migration in bacteria. Fems Microbiology Reviews 28: 261-289.

Davey, M. E., and G. A. O'toole. 2000. Microbial Biofilms: from Ecology to Molecular Genetics. Microbiol. Mol. Biol. Rev. 64: 847-867.

Fujishige, N. A., N. N. Kapadia, P. L. De Hoff, and A. M. Hirsch. 2006. Investigations of *Rhizobium* biofilm formation. FEMS Microbiology Ecology 56: 195-206.

Garcia-Rodriguez, F. M., and N. Toro. 2000. *Sinorhizobium meliloti nfe* (nodulation formation efficiency) genes exhibit temporal and spatial expression patterns similar to those of genes involved in symbiotic nitrogen fixation. Mol Plant Microbe Interact 13: 583–591.

Gill, P. R., L. L. Barton, M. D. Scoble, and J. B. Neilands. 1991. A high-affinity iron transport system of *Rhizobium meliloti* may be required for efficient nitrogen fixation in planta. Plant and Soil 130: 211–217.

Kearns, D. B. 2010. A field guide to bacterial swarming motility. Nat Rev Micro 8: 634-644.

Leonard, L. T. 1943. A simple assembly for use in the testing of cultures of rhizobia. Journal of Bacteriology 45: 523–527.

Lynch, D. et al. 2001. Genetic organization of the region encoding regulation, biosynthesis, and transport of rhizobactin 1021, a siderophore produced by *Sinorhizobium meliloti*. Journal of Bacteriology 183: 2576-2585.

Meade, H. M., and E. R. Signer. 1977. Genetic mapping of *Rhizobium meliloti*. Proceedings of the National Academy of Sciences of the United States of America 74: 2076-2078.

Nogales, J., L. Bernabéu-Roda, V. Cuéllar, and M. J. Soto. 2012. ExpR is not required for swarming but promotes sliding in *Sinorhizobium meliloti*. Journal of Bacteriology 194: 2027–2035.

Nogales, J. et al. 2010. Transcriptome profiling of a *Sinorhizobium meliloti fadD* mutant reveals the role of rhizobactin 1021 biosynthesis and regulation genes in the control of swarming. BMC Genomics 11: 157.

Ó Cuív, P., P. Clarke, D. Lynch, and M. O'Connell. 2004. Identification of *rhtX* and *fptX*, novel genes encoding proteins that show homology and function in the utilization of the siderophores rhizobactin 1021 by *Sinorhizobium meliloti* and pyochelin by *Pseudomonas aeruginosa*, Respectively. Journal of Bacteriology 186: 2996–3005.

Olivares, J., J. Casadesús, and E. J. Bedmar. 1980. Method for testing degree of infectivity of *Rhizobium melioti* strains. Applied and Environmental Microbiology 39: 967-970.

Osterås, M., B. T. Driscoll, and T. M. Finan. 1995. Molecular and expression analysis of the *Rhizobium meliloti* phosphoenolpyruvate carboxykinase (pckA) gene. Journal of Bacteriology 177: 1452-1460.

Persmark, M. et al. 1993. Isolation and structure of rhizobactin 1021, a siderophore from the alfalfa symbiont *Rhizobium meliloti* 1021. Journal of the American Chemical Society 115: 3950–3956.

Rigaud, J., and A. Puppo. 1975. Indole-3-acetic acid catabolism by soybean bacteroids. Journal of General Microbiology 88: 223–228.

Rinaudi, L. V., and J. E. González. 2009. The low-molecular-weight fraction of exopolysaccharide II from *Sinorhizobium meliloti* is a crucial determinant of biofilm formation. Journal of Bacteriology 191: 7216-7224.

Soto, M. J., M. Fernández-Pascual, J. Sanjuan, and J. Olivares. 2002. A *fadD* mutant of *Sinorhizobium meliloti* shows multicellular swarming migration

and is impaired in nodulation efficiency on alfalfa roots. Molecular Microbiology 43: 371-382.

Verstraeten, N. et al. 2008. Living on a surface: swarming and biofilm formation. Trends in Microbiology 16: 496-506.

Viguier, C., P. Ó Cuív, P. Clarke, and M. O'Connell. 2005. RirA is the iron response regulator of the rhizobactin 1021 biosynthesis and transport genes in *Sinorhizobium meliloti* 2011. FEMS microbiology letters 246: 235-242.

Conclusiones

1. El análisis transcriptómico de células de *Sinorhizobium meliloti* crecidas en medio sólido y semisólido ha puesto de manifiesto el cambio drástico que sufre la fisiología de esta bacteria en respuesta al crecimiento sobre una superficie con respecto a la mostrada en cultivo líquido. Dicho cambio queda reflejado en la expresión diferencial de más de mil genes implicados en distintas actividades metabólicas, captación y metabolismo de hierro, motilidad, quimiotaxis, y genes de respuesta a estrés.

2. El crecimiento de un mutante *fadD* de *S. meliloti* en condiciones ambientales que favorecen la aparición de la motilidad swarming en esta bacteria, provoca fundamentalmente inducción de la expresión génica, destacando sobre todo la de genes relacionados con captación y metabolismo de hierro.

3. Al igual que los flagelos, genes esenciales en la biosíntesis del sideróforo rizobactina 1021 desempeñan un papel clave en el movimiento en superficie y el desarrollo de biopelículas maduras de la cepa Rm1021 de *S. meliloti*. La función de estos genes en los dos fenotipos asociados a superficie no está exclusivamente ligada al mantenimiento de la homeostasis intracelular de hierro.

4. Una mutación en el gen *fadD* libera el requerimiento de producción de rizobactina 1021 para el desplazamiento en superficie de *S. meliloti* Rm1021, por un mecanismo aún desconocido.

5. Los niveles de hierro en el medio constituyen una señal medioambiental que controla la capacidad de movimiento en superficie y la capacidad de formar biopelículas de *S. meliloti*. Altas concentraciones de hierro inhiben específicamente la translocación en superficie de una cepa silvestre, al mismo tiempo que inducen la formación de biopelículas altamente estructuradas que se desarrollan más rápido que aquellas formadas en presencia de bajos niveles de hierro.

6. Junto con el hierro, los genes *fadD* y *rirA* forman parte de los mecanismos que co-regulan de manera inversa motilidad en superficie y desarrollo de biopelículas en *S. meliloti*. Una mutación que provoque pérdida de función en cualquiera de estos genes induce translocación en superficie, incluso en condiciones desfavorables como es la presencia de altos niveles de hierro, e interfiere negativamente con el desarrollo normal de biopelículas. El control sobre la producción de rizobactina 1021 podría ser la causa final responsable

del efecto del hierro y una mutación *rirA* en los dos fenotipos asociados a superficie.

7. La cepa GR4, incapaz de producir el sideróforo rizobactina 1021 y poco propensa a mostrar desplazamiento en superficie en condiciones de laboratorio, es mejor formadora de biopelículas que la cepa Rm1021 tanto en una superficie abiótica como el vidrio como sobre la superficie de raíces de alfalfa, pudiendo ser ésta al menos una de las razones del mejor comportamiento simbiótico de la cepa GR4.

8. El sideróforo rizobactina 1021 tiene propiedades surfactantes que podrían ser, al menos en parte, responsables de su función en translocación en superficie y formación de biopelículas en *S. meliloti*.

9. El producto del gen *rhbG* (*SMa2339*) no es responsable de incorporar la porción lipídica constituida por ác. 2-decenoico a la molécula de rizobactina 1021. A diferencia del resto de genes *rhb*, *rhbG* no es esencial ni para la síntesis del sideróforo ni para el desplazamiento en superficie de *S. meliloti*. No obstante, la acción de este gen tiene efectos tanto en los niveles de sideróforo producidos por la bacteria, como en los dos fenotipos asociados a superficie analizados en este estudio. La pérdida de función de *rhbG* promueve movimiento bacteriano en superficie independiente de la acción flagelar e interfiere negativamente con el desarrollo de biopelículas de modo casi idéntico al causado por mutaciones en *rhbA* y *rhbD*.

10. El análisis de distintas propiedades simbióticas de mutantes afectados en motilidad en superficie y formación de biopelículas (*fadD, rhb, rirA*) ha puesto de manifiesto que aunque estos mutantes son capaces de desarrollar nódulos fijadores de N en plantas de alfalfa, la mayoría exhiben algún defecto simbiótico en mayor o menor grado, encontrándose los fenotipos más acusados en mutantes hipermóviles en superficie. Estos resultados validan la estrategia consistente en caracterizar las bases moleculares que rigen el movimiento en superficie de *S. meliloti* para la identificación de nuevos genes bacterianos importantes en la colonización de plantas.

Appendix 1: Published article

BMC Genomics

RESEARCH ARTICLE Open Access

Transcriptome profiling of a *Sinorhizobium meliloti fadD* mutant reveals the role of rhizobactin 1021 biosynthesis and regulation genes in the control of swarming

Joaquina Nogales, Ana Domínguez-Ferreras, Carol V Amaya-Gómez, Pieter van Dillewijn, Virginia Cuéllar, Juan Sanjuán, José Olivares, María J Soto*

Abstract

Background: Swarming is a multicellular phenomenom characterized by the coordinated and rapid movement of bacteria across semisolid surfaces. In *Sinorhizobium meliloti* this type of motility has been described in a *fadD* mutant. To gain insights into the mechanisms underlying the process of swarming in rhizobia, we compared the transcriptome of a *S. meliloti fadD* mutant grown under swarming inducing conditions (semisolid medium) to those of cells grown under non-swarming conditions (broth and solid medium).

Results: More than a thousand genes were identified as differentially expressed in response to growth on agar surfaces including genes for several metabolic activities, iron uptake, chemotaxis, motility and stress-related genes. Under swarming-specific conditions, the most remarkable response was the up-regulation of iron-related genes. We demonstrate that the pSymA plasmid and specifically genes required for the biosynthesis of the siderophore rhizobactin 1021 are essential for swarming of a *S. meliloti* wild-type strain but not in a *fadD* mutant. Moreover, high iron conditions inhibit swarming of the wild-type strain but not in mutants lacking either the iron limitation response regulator RirA or FadD.

Conclusions: The present work represents the first transcriptomic study of rhizobium growth on surfaces including swarming inducing conditions. The results have revealed major changes in the physiology of *S. meliloti* cells grown on a surface relative to liquid cultures. Moreover, analysis of genes responding to swarming inducing conditions led to the demonstration that iron and genes involved in rhizobactin 1021 synthesis play a role in the surface motility shown by *S. meliloti* which can be circumvented in a *fadD* mutant. This work opens a way to the identification of new traits and regulatory networks involved in swarming by rhizobia.

Background

Swarming is a type of bacterial motility generally dependent on flagella and is characterized by a rapid and coordinated population migration across solid surfaces. In contrast to other modes of bacterial surface translocation, swarming involves a complex process of differentiation in which cells usually become hyperflagellated and elongated [1]. Signals and signalling pathways controlling swarm cell differentiation are largely unknown. Extracellular chemical signals such as N-acyl-homoserine lactones (AHL), peptides and amino acids, fatty acids, polyamines, etc, as well as physiological parameters, surface contact and wetness provide stimuli to trigger swarm cell differentiation (reviewed in [1-4]). It is generally believed that the different environmental, cell-to-cell, and intracellular signals may be sensed and transduced by two-component regulatory systems and cytosolic regulators, leading to a complex regulatory network.

Classical genetic studies performed in different bacteria have allowed the identification of several genes essential for swarming. Interestingly, recent genome-scale

* Correspondence: mariajose.soto@eez.csic.es
Departamento de Microbiología del Suelo y Sistemas Simbióticos, Estación Experimental del Zaidín, CSIC, Profesor Albareda, 1, 18008 Granada, Spain

approaches performed in model bacteria such as *Salmonella typhimurium*, *Escherichia coli* and *Pseudomonas aeruginosa*, indicate that swarmer differentiation represents much more than a motility phenotype as substantial alterations in metabolic pathways and gene expression have been observed [5-9]. In *E. coli*, up to one-fifth of the genes on the genome seem to be involved in swarming [7]. Besides flagellar functions, a large number of genes involved in several metabolic activities, iron acquisition, regulatory proteins, chaperones, and biosynthesis of cell surface components have been demonstrated to be important for this multicellular migration [7,8].

In several pathogenic bacteria, swarming is associated with virulence [1,2]. This could be partially due to the fact that the expression of some virulence determinants seems to be coregulated with swarmer differentiation. Urease, metalloprotease and haemolysin are up-regulated during swarming in the uropathogenic *Proteus mirabilis* [3], whereas phospholipase is induced in the opportunistic pathogen *Serratia liquefaciens* [10]. Global gene expression analysis performed on swarmer cells has revealed the up-regulation of a large number of virulence-related genes in *S. typhimurium* and *P. aeruginosa* such as genes encoding components of a type III secretion system, its effectors, extracellular proteases, and proteins involved in iron transport [6,9]. An interesting aspect related to virulence is the fact that swarmer cells, like biofilm communities, display increased resistance to several antimicrobials when compared to planktonic cells [9,11].

Although swarming has been extensively studied in pathogenic bacteria, this type of surface motility has also been described in beneficial bacteria such as rhizobia. These soil bacteria are known for their ability to establish a mutualistic symbiosis with legume plants. A remarkable feature of this interaction is the formation of a new organ, the root nodule, within which endosymbiotic differentiated bacteria fix atmospheric nitrogen to generate nitrogen sources usable by the plant, thus conferring a nutritional advantage to the host. The formation of a nitrogen-fixing nodule is a complex process requiring the coordination of bacterial infection with a root developmental program (for a review see [12,13]). Accumulating evidence suggests that in order to colonize, invade and establish a chronic infection within the host, rhizobia use similar strategies as pathogenic bacteria (reviewed in [14,15]).

The first report of swarming by rhizobia was described for a *fadD* mutant of the alfalfa symbiont *Sinorhizobium meliloti* [16]. In this bacterium, the lack of the *fadD* gene (encoding a long-chain fatty acyl-coenzyme A ligase), results in multicellular swarming behaviour but also defects in nodulation, thereby suggesting that fatty acid-related compounds may act as signals controlling motility and symbiosis. More recently, it has been reported that a wild type strain of *Rhizobium etli*, the bacterial symbiotic partner of common bean plants, can swarm [17]. The finding that mutants in the *cinIR* quorum sensing system of this bacterium were no longer able to move over semisolid surfaces, led to the discovery that AHL carrying a long-chain fatty acid moiety have a dual role in swarming in this rhizobium: as quorum sensing signals and as biosurfactants which promote surface translocation [18]. The characterization of several *R. etli* mutants defective in swarming has allowed the identification of additional genetic determinants which seem to play a role in this multicellular behaviour, including genes involved in polysaccharide synthesis or export, motility and amino acid and polyamines metabolism [19]. Interestingly, half of the mutants with an altered swarming pattern showed deficiencies in either nodulation or nitrogen fixation. The biological role of swarming in rhizobia remains to be elucidated. However, the fact that some mutations which alter swarming behaviour in *S. meliloti* and *R. etli* result in an impairment in the establishment of the symbiosis, suggests either that components essential for this multicellular motility and/or factors which are co-regulated during swarmer cell differentiation may play a role in the interaction with the host plant.

To gain insights into the adaptation process involved in multicellular swarming motility in rhizobia, global gene expression profiles of *S. meliloti fadD* cells under swarming inducing conditions were determined and compared with the profiles obtained during growth in liquid media as well as on non-swarming hard agar.

Results and Discussion

Construction and characterization of a *S. meliloti* Rm1021 *fadD* mutant

In *S. meliloti*, swarming motility has been reported for a *fadD* mutant (QS77) of the GR4 strain. Under the same swarming inducing conditions, the wild type strain GR4 has never shown this surface motility [16,20]. In order to identify *S. meliloti* genes whose expression is altered under swarming inducing conditions, we performed a transcriptomic analysis of a *fadD* mutant using the Sm6kOligo microarrays [21]. Since these arrays are based on the genome of *S. meliloti* strain Rm1021 [22], we constructed a *fadD* mutant in this genetic background by site-directed mutagenesis as described in Methods. The mutant obtained was named 1021FDC5. In contrast to the wild type strains GR4 and Rm1021, 1021FDC5 like QS77 could not grow on minimal medium (MM) plates containing oleate as sole carbon source (data not shown), a phenotype that was restored after introduction of the pBBRD4 construct harbouring

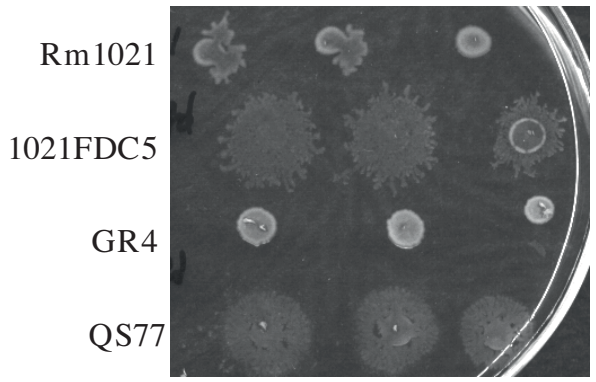

Figure 1 Swarming behaviour of *S. meliloti* strains. The swarming motility phenotype of *S. meliloti* wild-type strains Rm1021 and GR4 and their corresponding *fadD*-derivative mutants 1021FDC5 and QS77 was analyzed by inoculating aliquots (2 μl) of each strain prepared as described in Materials and Methods onto semisolid MM plates containing 0.6% purified agar. Replicates corresponding to the same strain were placed in a row. The photograph was taken 48 hours after inoculation and is a representative of at least three independent experiments.

a wild type *fadD* gene. Furthermore, as reported for QS77, 1021FDC5 showed conditional swarming motility on semisolid MM plates (Fig. 1). It is worth mentioning that whereas GR4 has never shown surface motility under our swarming inducing conditions, in approximately 70% of the experiments performed, Rm1021 cells spread over the surface of the plate resembling the movement displayed by the *fadD* mutants (Fig. 1). A similar behaviour was observed for the closely related strain Rm2011 (see below). This suggests that the control of swarming may be different in GR4 and Rm1021/Rm2011, although in all three *S. meliloti* strains a mutation in *fadD* promotes multicellular surface motility (Fig. 1; see below). This result was particularly intriguing as it has been published that in *S. meliloti*, ExpR is required for swarming but not for swimming [23,24], and it is well known that Rm1021 and Rm2011 are *expR*-deficient strains [25]. We have tried to reproduce swarming in different *S. meliloti* strains under the conditions described by Bahlawane *et al.* [24] without success. In any case, we show here that *expR*-defective strains (Rm1021, Rm2011 and their *fadD*-derivative mutants) can swarm on semisolid MM which suggests that the role of ExpR in swarming needs to be re-evaluated.

Transcriptome profiling of *S. meliloti* 1021FDC5 in broth and on agar surfaces

In order to identify genes whose expression is altered during swarming in *S. meliloti*, the transcriptome of 1021FDC5 growing on swarming inducing media (semisolid MM containing 0.6% agar) was compared with that of cells growing under non-swarming conditions (solid MM containing 1.3% hard agar and MM broth). We also compared the transcriptomes of 1021FDC5 after growth in broth and on solid MM to identify genes which are not specific for swarming but responsive to growth on surfaces. This analysis required, as a first step, the determination of bacterial growth curves in liquid, semisolid and solid MM to ensure that the respective transcriptomes were obtained in the same growth phase. Fig. 2 shows that the growth profiles were very similar for all three conditions tested, with cells entering stationary phase at 24 h. We studied the different expression profiles at early exponential phase (7 hours) and mid exponential phase (14 hours). In our standard swarming assays, 7 hours is the minimum time required to macroscopically observe surface motility whereas after 14 hours, swarming diminishes as recognized by slower cell migration and increased mucoidy. The macroscopic appearance of 1021FDC5 cells growing on solid and semisolid MM is shown in Fig. 3. After 14 h on solid MM (1.3% agar), 1021FDC5 grows as a homogenous lawn on the plate, indistinguishable from the non-swarming strain GR4. On the other hand, on semisolid MM (0.6%), growth of both GR4 and 1021FDC5 is not homogenous on the surface of the plate with visible uncolonized areas. However, whereas the borders of colonized areas by GR4 are smooth, in the case of 1021FDC5 these borders show a dendritic morphology indicating that these cells were actively swarming. Therefore, we conclude that this experimental setup is adequate for a transcriptomic study of swarming.

An internal control experiment in which Cy3- and Cy5- labelled cDNAs were synthesized from total RNA extracted from liquid cultures of 1021FDC5, allowed us to consider as differentially expressed only genes showing an M value of ≥ 1 or ≤ -1. A total of 1166 genes

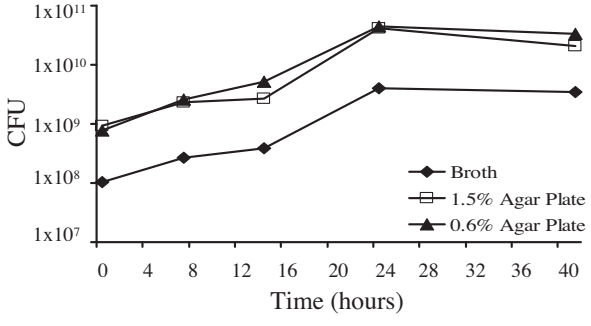

Figure 2 Growth curves of *S. meliloti* 1021FDC5 in broth and agar surfaces. Bacterial growth curves were determined in liquid, semisolid (0.6% purified agar) and solid (1.3% purified agar) MM. CFU refers to colony forming units/ml of broth or per plate. Data are representative of at least two replicate experiments.

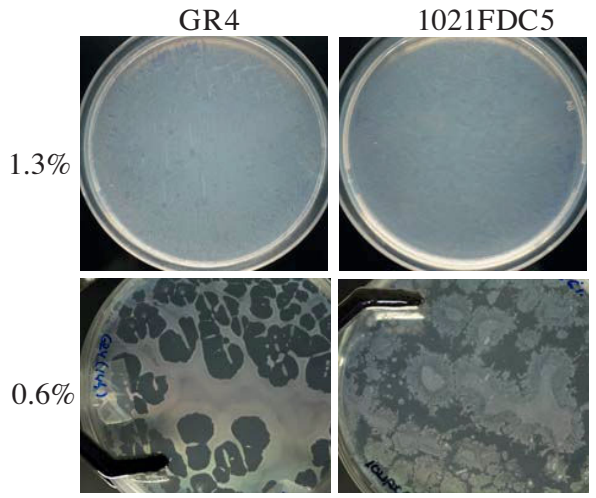

Figure 3 Macroscopic appearance of 1021FDC5 cells growing on solid and semisolid MM plates. 100 μl of a suspension containing approximately 10^9 cells of either *S. meliloti* 1021FDC5 (*fadD* mutant) or GR4 (wild type strain which does not show swarming) were evenly spread over the surface of solid (1.3% agar) and semisolid (0.6% agar) MM plates. The photographs were taken 14 hours after incubation at 30°C.

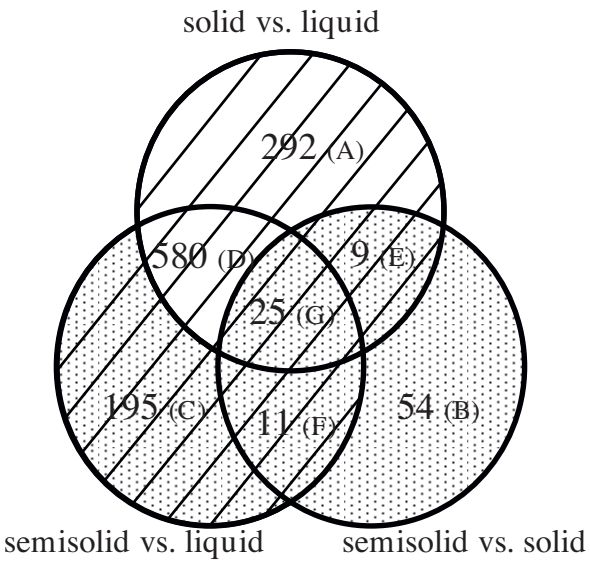

Figure 4 Venn diagram of *S. meliloti* differentially regulated genes identified in microarray experiments. The diagram represents the number of differentially expressed genes obtained in six different microarray experiments (based on additional file 1). The transcriptomes of *S. meliloti* 1021FDC5 cells obtained after growth in liquid, solid or semisolid MM were compared. For each of the three combinations, changes in the mRNA levels were monitored after 7 and 14 hours of growth. The different subsets have been assigned with letters (A-G). Surface responsive genes are indicated with stripes and swarming responsive genes with dots.

(19% of the annotated genes in the *S. meliloti* Rm1021 genome) appeared as differentially expressed in any of the six conditions studied (see additional file 1 and Table 1). More than 35% of the 1166 genes formed part of presumed operons where two or more genes appeared as differentially expressed under our experimental conditions. To facilitate the analysis, genes showing up- or down-regulation in any of the six different comparisons were plotted in a Venn diagram (Fig. 4). Most of the genes identified in our study (1112) showed differential expression in response to growth on a surface (i.e. differentially expressed in cells grown on solid or semisolid media vs. broth; striped area in Fig. 4) and only 54 genes appeared exclusively in the comparison of the transcriptome of cells grown on semisolid MM with that of cells grown on solid MM. Within the group of surface-responsive genes, more than 50% of the genes (580 + 25) showed differential expression regardless of the concentration of agar used, whereas a smaller number of genes showed differential expression after growth

Table 1 Number of genes differentially expressed in *S. meliloti* 1021FDC5 in response to different growth conditions

	Up-regulated		Down-regulated	
Comparison	7 hours	14 hours	7 hours	14 hours
Semisolid vs liquid	35	580	8	217
Semisolid vs solid	38	18	39	9
Solid vs liquid	7	542	10	354

specifically on hard agar or semisolid medium, (292 and 195, respectively). On the other hand, a total of 294 genes were found to be differentially expressed specifically under swarming inducing conditions (dotted area in Fig. 4 comprising genes which appeared differentially expressed in the comparison of cells grown on semisolid vs. solid media (99 genes), plus 195 genes which exclusively appeared differentially expressed in cells grown on semisolid vs. liquid media). It is noteworthy that 45 out of the 294 genes differentially expressed under swarming inducing conditions were also found differentially expressed in response to surface growth (subsets E, F, and G of 9, 11, and 25 genes, respectively; Fig. 4). This might suggest that a significant portion of swarming-responsive genes are regulated in response to contact with a surface, a known signal for swarming in other bacteria [1,4].

Surface responsive genes

The comparison of the transcriptome of cells grown in liquid MM with that of cells grown on solid or semisolid MM sampled at two different time points, led to the identification of 1112 differentially expressed genes (Table 1 and striped area in Fig. 4): 705 genes were up-regulated in response to surface growth, 384 were

down-regulated, and 23 genes showed variable responses (up- or down-regulated depending on the time point or agar concentration). Most of the surface responsive genes identified in our study (96%) showed a late response, appearing as differentially expressed after 14 hours growth (Table 1).

Many of the down-regulated genes (31%) encoded proteins of unknown or hypothetical function, which hindered drawing conclusions from down-regulated processes. Most noteworthy of the remaining down-regulated genes is that several are involved in nitrogen metabolism and exopolysaccharide production. Among the former are the regulatory genes *glnK* and *ntrBC*, glutamine synthetase genes (*glnII*, *glnT*, SMc01594 and SMc02352), putative glutamate synthase genes (*glxBCD* and *gltD*), the *nirB* nitrite reductase gene, and genes coding for transporters for ammonium (*amtB*), nitrate (*nrtABC* and SMb21114), and amino acids (*aap* genes). The lower expression observed for most of these genes could be explained by the down-regulation of the *ntrC* gene coding for the key transcriptional activator of nitrogen catabolic operons [26]. Likewise, the expression of some *nif* (*nifA, nifB, nifX*) and *fix* (*fixB, fixI*$_2$, *fixQP*$_3$) genes was diminished in cells grown on solid and semi-solid media compared to liquid culture. This could also be a consequence of the lower abundance of the NtrC activator and/or of the higher oxygen concentration in agar-solidified media. The other conspicuous group of down-regulated genes in response to growth in agar surfaces included several *exo* genes involved in exopolysaccharide (EPS) production (*exoA*, *exoM*, *exoN*, *exoP*, *exoN2*).

In contrast with the down-regulated genes, the majority (85%) of the genes up-regulated in response to surface growth have known or putative functions. Below is a description of the most relevant ones:

1) Carbon and energy metabolism

The induction of genes involved in the uptake (*smoEFGK*) and metabolism (*smoS*, *mtlK*, *xylA*) of mannitol as well as those involved in glutamate degradation (*glmS*, *gsh1*, *carA*, *gabT*, *nodM*), the carbon and nitrogen sources provided in our experiments, indicated a higher metabolic rate in response to surface growth. This is in agreement with the up-regulation of genes of the tricarboxylic acid cycle (*lpdA2*, *acnA*, *icd*, *sdhBCD*, *mdh*, *sucABCD*, *pckA*), the Calvin cycle (SMb20194, *ppe*, *cbbXSLAT*), glycolysis (*cbbA2*, *gap*, *glk*, *pgk*, *eno*, *pdhAa*, *pgi*), and of the different complexes in the respiratory chain and associated functions: *nuoA1B1C1D1-G1IJK1LMN*, *cyoBC*, *fixN1Q1*, *ndh*, *ctaBCDE*, *rrpP*, *ppa*, *ppk*, *atpABDEFF2GHI* and SMc00410. The higher metabolic rate could also be the cause of the observed induction of phosphate transport systems (*phoTEDC*, *phoU*, *pstABC* and SMc02146).

2) Protein metabolism

As many as 54 genes coding for ribosomal proteins were found to be induced during surface growth. We also observed up-regulation of different genes involved in the ribosome assembly and maturation (*rbfA* and *rhlE*), genes involved in the processing of mRNA, rRNA and tRNA (*rne*, *rnc*, *rnr*, *rnpA* and *pnp*), and different genes related to the translation process (*infB*, *tufA, tufB, fusA1, tsf*, *pth* and *prfB*). Due to the general induction of protein synthesis it was not a surprise to find induction of other related processes such as tRNA and amino acid biosynthesis (16 tRNA synthetases and 46 genes involved in the synthesis of different amino acids showed increased expression during surface growth).

3) Macromolecule synthesis

In agreement with the above mentioned increase in protein synthesis, the induction of several functions related to the transcription process was also observed, including the induction of RNA polymerase genes (*rpoA*, *rpoB*, *rpoC* and *rpoZ*), several sigma factors (*rpoH1*, *rpoE4* and *sigA*) and the transcription terminator factor (*rho*). On the other hand, we also detected induction of genes involved in DNA synthesis (*dnaN*, *dnaX*, *topA*, and *gyrA*) and related functions (*purA*, *purM*, *purQ*, *guaA*, *guaB*, *pyrB*, SMc01361, *pyrC-pyrE-frk*, *pyrF*, *cyaC*, SMa2357, *ndk, prsA*, SMc02218,*typA*).

Our microarray data suggest that during growth on agar surfaces, *S. meliloti* cells stimulate fatty acid biosynthesis over degradation. Thus, genes involved in the initiation (*accA*, *accBC*, *accD*) and elongation (*fabABI2*, *fabF*, *fabG*, *plsX-fabH*, *fabI1*, *fabZ*, SMc04273) of fatty acids and the acyl carrier protein AcpP were up-regulated during growth on agar media compared to broth, whereas the *fadB* and SMc02229 genes, putatively involved in degradation of fatty acids were down-regulated.

As previously mentioned, we observed repression of several *exo* genes suggesting that in response to growth on agar surfaces, *S. meliloti* produces less succinoglycan. On the contrary, several genes with a role in the synthesis of different surface polysaccharides were found to be up-regulated. This was the case for the *kdsA*, *kdsB* and *kdtA* genes, involved in the synthesis and transfer of Kdo (3-deoxy-D-manno-2-octulosonic acid), a component present in capsular polysaccharides (KPS) and lipopolysaccharides (LPS); the *rkpA* gene involved in the biosynthesis of a specific lipid carrier required for KPS synthesis; and the *acpXL* and *lpxD* genes involved in the biosynthesis of the lipid A of LPS [27]. Genes involved in the transport and modification of cyclic β-glucans such as *ndvA* and *opgC* as well as genes involved in the synthesis of peptidoglycan (*murA*) and lipoproteins (*lgt*) were also up-regulated under surface growth conditions.

4) Motility and chemotaxis

No less than thirty seven genes of the flagellar regulon were up-regulated during growth on a surface, whereas only two chemotaxis genes (*cheW3* and *mcpT*) showed lower expression under these conditions compared to growth in liquid medium. Up-regulated genes included those for chemotaxis (*cheABR* and *mcpEUX*), the flagellar structure (*flaCD, fliEFLGM, fliK, flgABCDEFGHIKL*), the flagellar motor (*motABC*), the chaperone-encoding gene *motE*, related genes of yet unknown function (SMc03013, SMc03017, SMc03023, and SMc03045), as well as genes coding for regulatory proteins (*flaF*, *flbT*, *visN* and *rem*) [28,29]. Motility genes were generally more induced than chemotaxis genes in response to growth on a surface. Five genes belonging to the four different classes of the *S. meliloti* flagellar regulon were chosen to validate our microarray data (see below).

5) Iron uptake and metabolism

19 genes up-regulated in response to growth on surfaces belong to this functional category, including genes involved in the synthesis (*rhbBCDEF* and SMa2339) and transport (*rhtA, rhtX*) of the siderophore rhizobactin 1021 [30-32]; several genes coding for proteins involved in the uptake of haem and hydroxamate siderophores (*hmuPS, hmuT, shmR, fhuA1, fhuA2, fhuP*) [33-35]; the *exbB-exbD* genes putatively coding for the inner membrane components of the TonB energy transduction complex required for Fe^{3+}-siderophore acquisition systems [36]; the *fhuF* gene coding for ferrioxamine B reductase [35]; and the putative iron regulator *irr*. Induction of these genes may be related to increased difficulty for iron acquisition during growth on a solid surface due to a slower diffusion of nutrients than in broth.

6) Stress-related genes

Up-regulation of genes related to oxidative stress was detected in response to surface growth including *sodB*, *katA*, peroxidases (SMb20964 and *cpo*), and glutathione transferases (*gst4* and *gst8*). Noticeable was also the induction of genes related to thermal stress such as those coding for cold shock proteins (*cspA1*, *cspA4*, *cspA2* and *cspA6*) and heat shock proteins (*grpE*, *hslU*, *hslV*, *hslO*, *ibpA*, SMb21295 and SMc01106). The up-regulation of genes involved in DNA repair processes (*radA*, *recF*, *recN* and *ligA*) could be linked to the induction of genes involved in DNA synthesis (see above), whereas the induction of chaperone genes (*groESL1, groESL2, tig, ibpA*, *lon*) could be the consequence of the observed increase in protein synthesis and/or the existence of stress conditions during surface growth. Also noteworthy was the induction of several genes involved in resistance to different toxic compounds. This was the case for *mrcA1*, a gene coding for a probable penicillin-binding 1A transmembrane protein, the *fsr* gene which encodes a putative fosmidomycin resistance transmembrane protein, the *uppP* gene coding for a putative undecaprenyl-diphosphatase which could confer resistance to bacitracin, putative components of a multidrug efflux system (SMc02867 and SMc02868), and the *aqpS-arsC* genes involved in arsenic detoxification.

All together these data suggest the existence of striking differences in the physiology of *S. meliloti* growing in broth compared with agar surfaces and more specifically that cells growing on agar surfaces have a higher metabolic rate than those grown in broth. Similar results were obtained in a transcriptomic study performed in *Salmonella* [6]. As suggested in the work by Wang *et al.* [6], this could be explained if agar surfaces represent a more aerobic environment than liquid cultures. This could also explain the down-regulation we have observed for several low oxygen responsive genes (*nif* and *fix*) during growth on agar-solidified media when compared to broth. On the other hand, the up-regulation of several genes related to oxidative stress, chaperone functions, or genes involved in resistance to different toxic compounds, could indicate that cells growing on solid agar surfaces are subject to stress. However, the observed induction of chemotaxis and motility genes together with the down-regulation of several *exo* genes under surface growth contrast with the response of *S. meliloti* to several environmental stresses (osmotic stress, phosphate and iron starvation, or acidic pH), in which motility genes are down-regulated while at the same time *exo* genes are up-regulated [21,37,38]. The identification of several regulatory genes in *S. meliloti* which simultaneously affect EPS production and cellular motility, indicates that regulation of these two rhizobial traits are coupled [24,39-41]. In addition to environmental stresses, the results obtained in this work suggest that contact with a surface might be another signal recognized by *S. meliloti* to co-ordinate the regulation of EPS production and motility.

Regulation of genes in response to swarming-specific conditions

In contrast to surface growth, our microarray data revealed that the response of *S. meliloti* to swarming-specific conditions is characterized by the differential expression of a smaller number of genes (294) (dotted area in Fig. 4; additional file 2): 99 of these were identified in the comparison semisolid vs. solid, 36 of which also appeared in the comparison semisolid vs. broth, plus 195 genes which exclusively appeared in semisolid vs. broth. This result is comparable to that found in a similar transcriptomic study performed in *Salmonella* in which a small number of genes (97) were found to show swarming-specific regulation, in contrast with more than a thousand genes found to respond to surface growth

[6]. In our study, most of the genes (73%) responding to swarming-specific conditions identified in the comparison semisolid vs. solid showed an early response (7 hours after incubation) (Table 1). On the contrary, the majority of genes (89%) identified in the semisolid vs. broth comparison, appeared after 14 hours of growth.

207 genes out of the 294 genes were up-regulated under swarming-inducing conditions, only 78 were found to be down-regulated and the remaining 9 showed variable responses. No informative conclusions could be reached from down-regulated functions as, firstly, approximately one fourth of the genes code for hypothetical proteins of unknown function and secondly the remaining down-regulated genes belong to diverse functional categories. Similarly, many of the up-regulated genes have unknown functions or display partial or global homology to genes deposited in databases (66 genes). This suggests that bacterial components with a putative role in swarming in *S. meliloti* have yet to be thoroughly studied. However, a subset (25 genes) of the up-regulated genes induced under swarming inducing conditions could be assigned to iron uptake and metabolism, including the transcriptional regulator of the iron limitation response *rirA* [42,43], and the putative iron response regulator *irr*. It is also interesting that swarming conditions induced in *S. meliloti* 1021FDC5 a slight up-regulation of genes involved in the resistance to toxic compounds (*mrcA2, uppP, aqpS-arsC*). Increased resistance to antibiotics and to other antimicrobials has been observed in swarmer cells of different bacteria [9,11]. Whether this is also the case for *S. meliloti* swarmer cells will be the subject of future studies.

To gain further insight into some of the genes responding to swarming specific conditions, we focused on the subset of 36 genes (from now on S36) which were identified as differentially expressed in both semisolid vs. solid and semisolid vs. broth (subsets F and G of 11 and 25 genes, respectively in Fig. 4) (Table 2). Five genes of S36 were chosen to validate our microarray data (see below). The majority of the genes within S36 (27 genes) were up-regulated under swarming inducing conditions compared to growth in either broth or on hard agar, whereas only one gene (SMb21284) was found to be down-regulated. 36% of the genes belonging to S36 were located on megaplasmid pSymA, a percentage which is significantly higher than the 21% expected for an even distribution among *S. meliloti* replicons, suggesting a putative role of this megaplasmid in *S. meliloti* swarming. Interestingly, up to 17 genes present in S36 are related with iron uptake and metabolism. They include SMb21431 and SMb21432 which code for putative components of iron uptake ABC transporters, and 15 out of the 19 iron-related genes identified as up-regulated in response to surface growth (only *rhbD, rhtX, fhuA1, fhuA2* and *irr* were not present in S36). 13 out of the 15 surface-responsive genes related to iron uptake and metabolism were also significantly induced on solid MM versus broth after 14 hours of growth (see additional file 1). Although the induction of these genes could be explained by the increased difficulty for iron acquisition during growth on agar containing media, it is surprising that up to 8 of these iron-related genes show higher expression in 0.6% swarm agar than in the harder 1.3% agar. This suggests that lower diffusion of iron is not the only factor controlling the expression of genes involved in iron uptake and metabolism, and furthermore that a specific connection may exist between swarming and iron-related genes. In *S. typhimurium* and *P. aeruginosa* induction of genes related to iron uptake and metabolism has also been detected in the transcriptomic analysis of swarmer cells [6,9]. Moreover, mutants of *E. coli* and *P. putida* affected in different systems of iron acquisition show defects in swarming [7,44]. These and our results suggest that different bacteria have acquired similar adaptation processes for swarming with iron acquisition systems playing an important role.

Validation of the results from the microarray experiments by RT-qPCR

To validate our microarray data we performed reverse transcription-quantitative PCR on several selected surface responsive genes as well as on genes showing response to swarming-specific conditions. Among surface responsive genes, we analyzed the expression of several motility genes belonging to different classes of the *S. meliloti* flagellar regulon [28,29] on solid, semisolid and in liquid MM after 14 h of growth: the *visN* and *rem* genes coding for master regulators of class IA and class IB, respectively; the *flgB* gene as a representative of class II genes, encoding a flagellar basal-body rod protein; and the class III genes *flaA* and *flaC*, encoding the principal and secondary flagellins, respectively. In our transcriptomic study *flaA* was not present in the list of differentially expressed genes. Since many motility genes were up-regulated in response to surface growth and FlaA is the main component of the flagellum, we hypothesized that the fact that this gene does not show differential expression in our study, could be due to the limitations inherent to the microarray approaches. Therefore, we decided to include *flaA* in the RT-qPCR studies. All five of the motility genes analyzed showed surface specific induction (Fig. 5A), thereby confirming the microarray results. Interestingly, the RT-qPCR analyses revealed that, except for *rem*, the motility genes analyzed showed higher induction values on semisolid than on solid media, which is in agreement with the existence of a higher motility activity under swarming inducing conditions.

Table 2 Subset S36[a] of *S. meliloti* 1021FDC5 genes differentially expressed under swarming-specific conditions

Gene	Descriptions	M value[b]			
		SS/L 7 h	SS/L 14 h	SS/S 7 h	SS/S 14 h
SMa0520	Transcriptional regulator, RpiR family	**1,45**	**1,90**	**1,73**	**1,55**
SMa0564	Putative dehydrogenase	-0,45	**-1,12**	-0,83	**2,78**
SMa1052	Conserved hypothetical protein	**1,01**	**1,24**	0,51	**1,56**
SMa1077 (*nex18*)[c]	Nex18 Symbiotically induced conserved protein	**1,16**	0,81	0,44	**2,76**
SMa1078	Conserved hypothetical protein	**1,89**	**1,74**	0,28	**1,93**
SMa1079 (*tspO*)	TspO Tryptophan rich sensory protein	**1,36**	0,31	0,59	**1,91**
SMa1100	Conserved hypothetical protein	**1,31**	**1,61**	0,52	**1,57**
SMa2339	Siderophore biosynthesis protein	0,80	**1,33**	**1,55**	-0,17
SMa2402 (*rhbB*)[c]	L-2,4-diaminobutyrate decarboxylase	**1,84**	0,75	**2,58**	-0,19
SMa2404 (*rhbC*)	RhbC rhizobactin biosynthesis protein	1,49	**1,19**	**2,65**	0,00
SMa2408 (*rhbE*)	RhbE rhizobactin biosynthesis protein	**2,38**	**2,23**	**3,83**	0,03
SMa2410 (*rhbF*)	RhbF rhizobactin biosynthesis protein	**2,36**	**1,34**	**3,76**	-0,11
SMa2414 (*rhtA*)[c]	RhtA rhizobactin transporter	**1,43**	**1,64**	**2,68**	0,05
SMb20005	Putative glutathione S-transferase	**2,34**	-0,08	0,31	**-1,38**
SMb20604	ABC transporter, permease	0,18	**-4,84**	0,20	**1,14**
SMb20605	ABC transporter, periplasmic solute-binding protein	0,01	**-5,55**	0,09	**1,34**
SMb21284	Putative polysaccharide deacetylase	-0,21	**-1,55**	-0,15	**-1,15**
SMb21431	Hypothetical protein, possibly C terminus of iron ABC transporter periplasmatic solute-binding protein	-0,34	**1,75**	**1,44**	-0,14
SMb21432	Putative iron uptake ABC transporter periplasmic solute-binding protein precursor	**-1,07**	**1,63**	**2,15**	-0,40
SMb21676	Hypothetical protein	0,17	**1,92**	-0,58	**1,96**
SMc00402	Hypothetical signal peptide protein	-0,03	**1,91**	**1,42**	-0,23
SMc00592	Hypothetical, transmembrane protein	-0,44	**1,47**	**1,30**	-0,23
SMc01242	Conserved hypothetical signal peptide protein	0,29	**-1,35**	0,13	**1,04**
SMc01417	Hypothetical protein	**1,26**	0,14	**1,12**	-0,05
SMc01510 (*hmuV*)	Putative hemin transport system ATP-binding ABC transporter	-0,06	**1,48**	**1,53**	-0,12
SMc01512 (*hmuT*)	Putative hemin binding periplasmic transmembrane protein	-0,34	**1,49**	**1,39**	0,09
SMc01513 (*hmuS*)[c]	Putative hemin transport protein	-0,93	**1,34**	**2,60**	-0,07
SMc01514	Conserved hypothetical protein	**-1,14**	**1,50**	**2,37**	-0,09
SMc01658 (*fhuF*)	Siderophore reductase	-0,39	**1,28**	**2,03**	-0,06
SMc01659 (*fhuP*)	Periplasmic component of ferrichrome and ferrioxamine B ABC transporter	-0,41	**1,85**	**2,60**	0,12
SMc01747 (*hmuP*)	Hypothetical protein, hemin uptake protein	-0,78	**1,29**	**2,23**	0,04
SMc01917 (*nuoE1*)	NADH dehydrogenase I chain E	0,03	**1,21**	**-1,13**	-0,14
SMc02084 (*exbD*)	Probable biopolymer transport transmembrane protein	-0,68	**1,48**	**1,16**	-0,03
SMc02085 (*exbB*)[c]	Probable biopolymer transport transmembrane protein	-0,54	**1,82**	**1,55**	-0,01
SMc02726 (*shmR*)	Hemin-binding outer membrane receptor	-0,11	**2,02**	**2,84**	0,30
SMc03167	MFS-type transport protein	**1,09**	0,62	**1,27**	0,38

[a]The subset S36 comprises 36 genes showing differential expression in the two transcriptome comparisons aimed to identify swarming responsive genes (i.e. semisolid vs. solid and semisolid vs. broth); [b]$\log_2$ (experiment signal/control signal). Values in bold face indicate that they meet both M and p criteria; [c]Genes validated by RT-qPCR (see Fig. 5B). SS, growth in semisolid MM (0.6% agar); S, growth in solid MM (1.3% agar); L, growth in liquid MM.

To confirm the differential expression of genes showing response to swarming-specific conditions, we selected: four genes related to iron uptake and metabolism (*rhbB, rhtA, hmuS* and *exbB*) which showed early induction (7 h) in semisolid vs. solid; *nex18*, a symbiotically induced gene showing late (14 h) up-regulation in semisolid vs. solid; and *exsF*, a gene coding for a putative two-component response regulator with sequence similarity to CheY, and found as an early down-regulated gene in swarm cells compared to cells grown on solid MM. The expression of these six genes was determined on solid and semisolid MM after 7 and 14 hours of growth. As shown in Fig. 5B, once more, the RT-qPCR results confirmed the microarrays data.

As detailed above, we have macroscopic evidence that under our experimental conditions (spread plating on semisolid MM) cells of 1021FDC5 show swarming (Fig. 3). However, to test whether the genes differentially

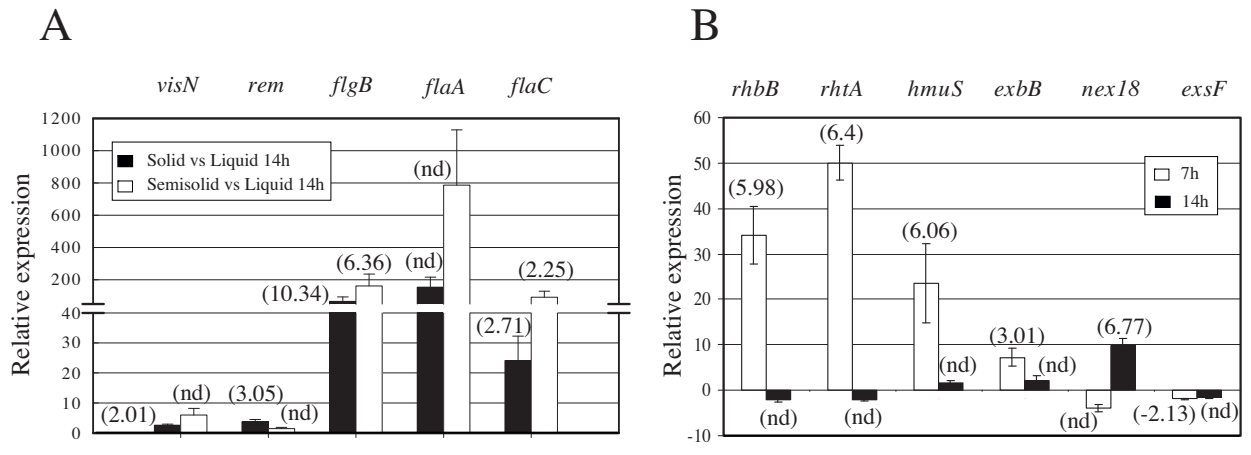

Figure 5 Confirmation of the differential expression of selected genes in a *fadD* mutant of *S. meliloti* in response to different growth conditions as determined by quantitative real-time PCR. A) The relative expression of surface responsive genes was calculated as the fold change between growth on solid MM (black bars) or semisolid MM (white bars) compared to growth in liquid MM after 14 hours of incubation. B) The relative expression of genes responding specifically to swarming inducing conditions was calculated as the fold change between growth on semisolid MM compared to growth on hard agar MM at 7 hours (white bars) or at 14 hours (black bars). For comparisons, fold changes in gene expression obtained in the microarray experiments (calculated as 2^M) are shown in parenthesis. Results are averages from at least two independent biological experiments with three technical replicates. Error bars indicate standard error at 95% confidence. nd, not detected in the microarray experiments

expressed under these conditions could truly be considered swarming-specific, we analyzed and compared the expression of *rhbB*, *rhtA* and *hmuS* by RT-qPCR from cells present in the border of swarming colonies obtained in standard swarming assays and cells from a colony grown on solid MM. The results confirmed the up-regulation of these genes in swarming cells vs non-swarming cells with relative expression values of 5.72 ± 0.54 for *rhbB*, 4.61 ± 0.38 for *rhtA* and 4.41 ± 0.69 for *hmuS*. The differences in the induction values found for these genes between cells spread plated on semisolid MM (Fig. 5B) and cells from the border of a typical swarming colony could be explained by differences in the growth phase of the two samples. Nevertheless, these data indicate that our experimental approach is adequate for the identification of swarming-specific genes.

Role of pSymA, rhizobactin-related genes and iron in *S. meliloti* swarming

Since the proportion of genes belonging to pSymA present in the subset S36 of swarming-responsive genes was higher than expected, we investigated whether this megaplasmid played any role in surface translocation. The swarming ability of SmA818, a *S. meliloti* strain cured of pSymA, was tested. In contrast to the parental strain Rm2011, SmA818 did not show swarming in any of the numerous assays performed (Fig. 6A). Mutagenesis-based approaches have revealed that a wide variety of genes are involved in swarming [7,8,19]. Since pSymA harbours more than one-fifth of the genes present in the *S. meliloti* genome, the finding that loss of this megaplasmid results in loss of swarming, might be not surprising. However, this result prompted us to investigate which genes of pSymA could play a role in triggering conditional swarming in *S. meliloti*.

Among the pSymA swarming-specific induced genes were those involved in the biosynthesis and transport of the siderophore rhizobactin 1021 [30]. In *E. coli*, mutations in most of the genes involved in the utilization of the siderophore enterobactin strongly inhibit swarming [7]. Likewise, in *P. putida*, mutants either in the siderophore pyoverdine or in the FpvA siderophore receptor have been shown to be defective in surface motility [44]. Hence, the swarming-defective phenotype observed in SmA818 could be due to the lack of rhizobactin-related genes. To test this, swarming assays were performed with mutants affected in either of the two different rhizobactin 1021 biosynthesis genes (*rhbA* and *rhbE*), a mutant lacking the RhtA outer membrane receptor for the siderophore, and with a *rhrA* mutant strain lacking the AraC-like regulator which positively regulates the production and transport of rhizobactin 1021. Additionally, we also looked at the swarming phenotype of a *rirA* mutant. RirA has been demonstrated to be the general regulator of the iron response in *S. meliloti*, including genes involved in the biosynthesis and transport of rhizobactin 1021 [42,43]. In our microarrays, *rirA* appeared to be induced 2-fold in growth on semisolid vs. solid media after 14 hours of incubation (see additional file 2). As shown in Fig. 6B, neither the mutants in the

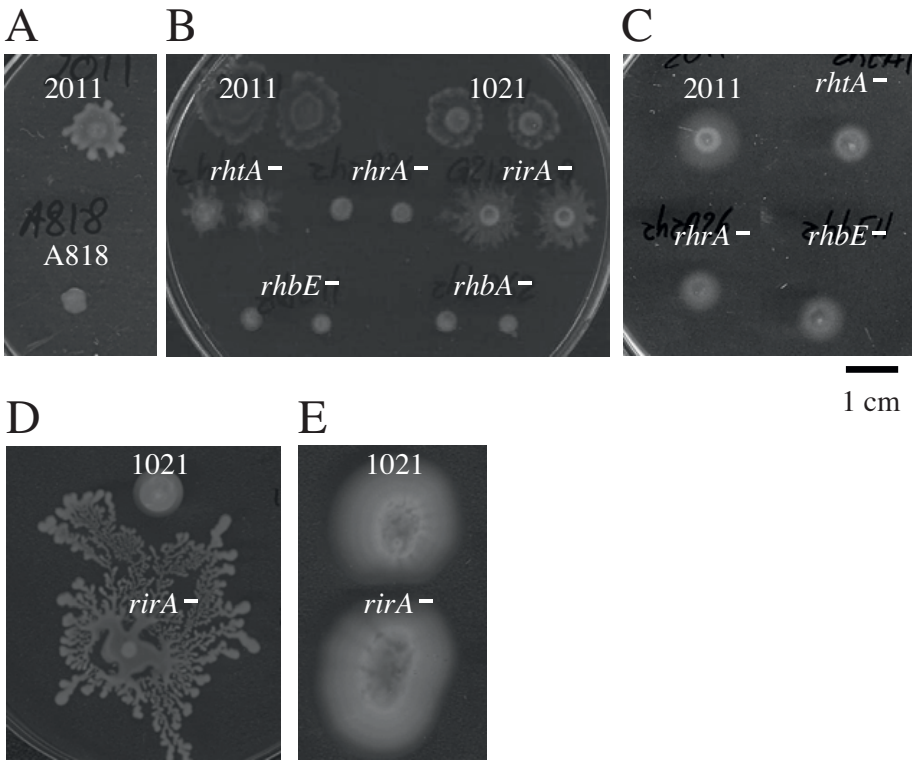

Figure 6 Effect of pSymA, rhizobactin-related genes, and iron concentration on the motility of *S. meliloti*. A) Swarming test of wild type Rm2011 and a pSymA-cured derivative strain (SmA818). B) Swarming assay of mutants in the biosynthesis and transport of rhizobactin 1021 and in the rhizobial iron regulator *rirA*. C) Swimming test of Rm2011 and rhizobactin 1021-related mutants in Bromfield (0.3% agar). D) Swarming and E) swimming tests of Rm1021 and the *rirA* mutant in MM containing high iron concentration (220 μM). Photographs were taken either at 48 hours (A, B, and C) or 5 days (D and E) after inoculation and are representative of three replicates from at least three different experiments.

rhizobactin biosynthesis genes (*rhb*) nor the *rhrA* mutant were able to swarm, while the absence of either the RhtA siderophore receptor or the RirA regulator did not prevent swarming. The motility defect shown by the *rhb* and *rhrA* mutants was specific for swarming since assays performed in Bromfield and MM (0.3% agar) showed that these strains were able to swim (Fig. 6C). Thus, the motility phenotypes shown by the *rhb* and *rhrA* mutants suggest that either rhizobactin-mediated iron uptake or rhizobactin *per se* play a role during swarming in *S. meliloti* Rm2011. In *P. putida*, the defect in swarming shown by mutants unable to synthesize the siderophore pyoverdine could be restored by adding different sources of iron, suggesting that the intracellular iron level rather than the siderophore is the functional signal for swarming in this bacterium [44]. To test whether the lack of surface motility in the *rhb* and *rhrA* mutants could be due to iron deficiency, increasing concentrations (22, 220, and 2200 μM) of either $FeCl_3$ or the iron chelate ferric citrate, whose uptake is independent on siderophore, were added to the media. None of these conditions could restore surface translocation in the mutants (data not shown), with the highest concentration used being inhibitory of cell growth. This result indicated that low intracellular iron levels were not responsible for the swarming deficiency of the *rhb* and *rhrA* mutants, and that the presence of rhizobactin 1021 is important for triggering swarming in *S. meliloti*. Furthermore, the fact that the *rhtA* mutant which is defective in rhizobactin 1021 utilization [30], still swarms (Fig. 6B) suggests that the function played by rhizobactin 1021 in swarming is exerted outside the cell. Rhizobactin 1021 is a citrate-based dihydroxamate siderophore structurally similar to schizokinen with the only but important difference that rhizobactin 1021 contains a long-chain fatty acid ((E)-2-decenoic acid) that gives the siderophore an asymmetric structure and amphiphilic properties [45]. The role of the decenoic acid residue in rhizobactin 1021 function has not been studied, although it has been proposed to be important during the membrane translocation of the ferric complex by making the molecule more mobile. Considering our results, it is tempting to speculate that the surfactant properties of rhizobactin 1021 may promote surface translocation in *S. meliloti*. Similarly, the

biosurfactant activity associated to long-chain AHLs produced by *R. etli* has been proved to play a direct role in surface movement of swarmer cells, adding a new function to these well known signalling molecules [18]. Curiously and in support of our hypothesis, *S. meliloti* GR4 which is not able to swarm on semisolid MM, does not produce siderophores in liquid MM as determined by the CAS assay (data not shown).

The restoration of surface motility of the rhizobactin-defective mutants was attempted by adding concentrated supernatants containing rhizobactin 1021. Although the addition of these supernatants functioned in iron nutrition bioassays restoring the growth of *rhb* mutants, they failed to promote swarming of the mutants and even hampered this surface motility of the wild type and *fadD* mutant strains (data not shown). This result might be due to the negative effect on swarming of supraoptimal concentrations of nutrients or compounds excreted by Rm2011.

To further confirm that the presence of rhizobactin 1021 is important for triggering swarming in *S. meliloti*, the motility phenotypes of Rm1021 and the *rirA* mutant were tested under iron-replete conditions as it has been reported that these conditions inhibit rhizobactin 1021 production in the wild type but not in the mutant [43]. CAS assays were performed to determine siderophore concentrations in the supernatants of these two strains under different growth conditions. We found that the wild type and the *rirA* mutant produced similar amounts of siderophore when cells were cultivated in MM containing 22 μM of $FeCl_3$ (data not shown). The presence of 220 μM of $FeCl_3$ abolished siderophore production in Rm1021 but not in the *rirA* mutant (data not shown). Hence, swimming and swarming assays were performed in MM containing 220 μM of $FeCl_3$. No differences in swimming were observed between the two strains (Fig. 6E). However, swarming by Rm1021 was inhibited at this iron concentration but not that by the *rirA* mutant in which swarming seemed even to be enhanced compared to lower iron concentrations (Fig. 6D). This result not only supports that in *S. meliloti* Rm1021 rhizobactin 1021 is required for swarming but also suggests that iron and *rirA* play a role in the control of this multicellular phenotype. The concentration of iron in the medium has been shown to be decisive for swarming in several bacteria [44,46,47]. In *S. meliloti* strain Rm1021, like in *Pseudomonas* spp., an excess of iron inhibits swarming, an effect that in *S. meliloti* could be due at least in part to the inhibition of rhizobactin 1021 production. On the other hand, the enhanced motility shown by the *rirA* mutant under high iron conditions suggests that additional genes controlled by this regulator might be involved.

The lack of a functional *fadD* gene restores swarming in pSymA-cured and rhizobactin-defective strains, and allows swarming under high-iron conditions

As described above, pSymA and at least the rhizobactin 1021-related genes *rhb* and *rhrA* are required for swarming in *S. meliloti* Rm1021. To investigate if these genes are also important in the surface motility shown by the *fadD* mutant, swarming assays were performed with the pSymA-cured strain SmA818 in which the *fadD* was inactivated as well as with double mutants *rhbfadD* and *rhrAfadD*. As shown in Fig 7A and 7B, the lack of a functional *fadD* gene restored surface motility in all the swarming-deficient strains. Thus, although rhizobactin biosynthesis and regulation genes were found to be up-regulated in the *fadD* mutant under swarming inducing conditions, these genes are not required for this surface motility in this genetic background. A possible explanation for these findings could be that the signal transduction pathway leading to the induction of the rhizobactin genes is not altered in the *fadD* mutant. A recent microarray analysis performed in our group supports this hypothesis. The comparison of the transcriptome of the wild type strain with that of the *fadD* mutant under swarming-inducing conditions after 7 and 14 hours of growth, revealed only 11 differentially expressed genes (including the up-regulation of the *npt* gene in the *fadD* mutant) (data not shown). Neither *rhb* genes nor *rhrA* were amongst them, suggesting that these genes show similar expression levels under swarming inducing conditions in both genetic backgrounds. The finding that rhizobactin-related genes are not essential for swarming in the *fadD* mutant could be explained if the function played by iron/rhizobactin 1021 in the control of swarming in Rm1021 (as a surfactant or signal molecule) could be exerted in the *fadD* mutant by a different and unknown compound which is not present or inactive in the wild-type strain.

We also tested if the presence of high iron concentrations prevents swarming in a *fadD* mutant as it does in 1021. Swarming assays were performed on semisolid MM containing 220 μM of $FeCl_3$ with 1021 and GR4 as wild type strains, and their corresponding *fadD*-derivative mutants. As shown in Fig. 7C, swarming was never observed in GR4 but always in the *fadD* mutant QS77. As already mentioned, in 1021 swarming was observed at a certain frequency on MM containing 22 μM of $FeCl_3$ and never observed under high iron conditions but its corresponding *fadD* mutant showed swarming at both iron concentrations similar to that found for the *rirA* mutant. However, in contrast to the *rirA* mutant, the iron-independent swarming phenotype shown by the *fadD* mutant cannot be explained by differences in the production of rhizobactin 1021 since the *fadD* mutant,

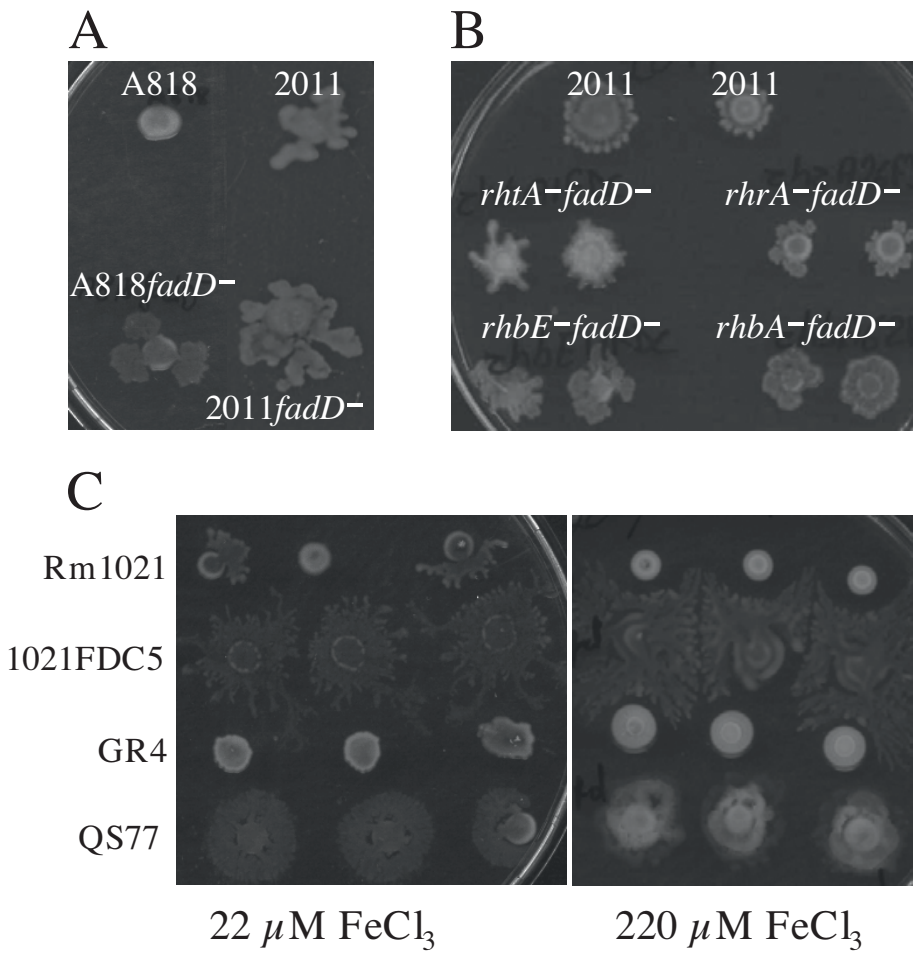

Figure 7 Role of pSymA, rhizobactin-related genes, and iron concentration on *fadD*-dependent swarming of *S. meliloti*. Swarming tests of *fadD*-derivative mutants of Rm2011 and the pSymA-cured strain A818 (A), of double mutants lacking *fadD* and rhizobactin 1021-related genes (B), and wild type and *fadD*-derivative mutants under standard (22 μM $FeCl_3$) and high iron conditions (220 μM $FeCl_3$) (C). Photographs were taken 48 hours after inoculation and are representative of three replicates from at least three different experiments.

like the wild type, inhibits siderophore production under high iron conditions (data not shown). Therefore in *S. meliloti*, the lack of a functional *fadD* gene relieves the control that iron has over swarming as well as the dependence on rhizobactin 1021 for this surface motility. A possibility worth investigating is if fatty acid derivatives, whose concentration is dependent on FadD activity but not iron-responsive, could replace siderophore function during swarming. Likewise, future investigations should address a possible connection between the *rirA* and *fadD* regulatory networks that could explain the iron-insensitivity of swarming shown by the *fadD* and *rirA* mutants.

Conclusions

To the best of our knowledge, the present work represents the first global gene expression analysis of rhizobium growth on surfaces, including swarming inducing conditions. The results reveal that the physiology of *S. meliloti* cells growing on the surface of agar media is significantly different from that of cells growing in broth, with the differential expression of more than a thousand genes. It is tempting to speculate that these major changes in gene expression could also take place in rhizobium during colonization of root surfaces, an important prerequisite for nodule formation. Thus, the approach used in this study may be helpful to identify genes and regulatory mechanisms that could be crucial during the early stages of the rhizobium-legume symbiosis and it could serve as a model for studying gene expression in different plant-associated bacteria.

The surface motility shown by several *expR*-deficient strains in this work indicates that the role played by this LuxR-type regulator in swarming by *S. meliloti* needs to be re-examined. Moreover, the genomic

analysis under swarming-inducing conditions allowed the identification of environmental signals (surface contact and iron concentration) and genes that play important roles in the control of this surface motility in a wild type strain of *S. meliloti*. Furthermore, the results suggest that rhizobactin 1021 plays a role in swarming although the requirement for rhizobactin-related genes and the inhibition of this surface motility by an excess of iron can be circumvented in a *fadD* mutant. Future work should focus on investigating the specific role of rhizobactin 1021 in swarming of *S. meliloti* as well as to identify why the lack of a functional *fadD* gene allows surface translocation of bacterial cells under conditions which negatively influence this type of multicellular migration.

Methods

Bacterial strains and growth conditions

Strains used in this study are listed in Table 3. *E. coli* strains were grown in Luria-Bertani (LB) medium [48] at 37°C; *S. meliloti* strains were grown at 30°C in TY complex medium [49] or in minimal medium (MM) containing glutamate (6.5 mM), mannitol (55 mM), mineral salts (K_2HPO_4, 1.3 mM; KH_2PO_4. $3H_2O$, 2.2 mM; $MgSO_4$ $7H_2O$, 0.6 mM; $CaCl_2$ $2H_2O$, 0.34 mM; $FeCl_3$ $6H_2O$, 0.022 mM; NaCl, 0.86 mM) and vitamins (biotin (0.2 mg/L); calcium pantothenate (0.1 mg/L)) [50]. Standard MM contains 22 μM $FeCl_3$. When a different concentration or source of iron was required, 100-fold concentrated stock solutions of either $FeCl_3$ or ferric citrate were prepared and added to MM without

Table 3 Bacterial strains and plasmids used

Strain or plasmid	Relevant characteristics[a]	Reference or source
Escherichia coli		
DH5α	*supE*44, Δ*lacU*169, *f*80, *lacZ*ΔM, *recA*1, *endA*1, *gyrA*96, *thi*1, *relA*1, *5hsdR*171	Bethesda Research Lab®
S17.1	*thi*, *pro*, *recA*, *hsdR*, *hsdM*, Rp4Tc::Mu, Km::Tn*7*; Tp^r, Sm^r, Sp^r	[57]
Sinorhizobium meliloti		
GR4	Wild type	[58]
QS77	GR4 (*fadD*::Tn*5*), Km^r	[16]
Rm1021	SU47 *expR102*::IS*Rm*2011-1, Sm^r	[59]
1021FDC5	Rm1021 (Δ*fadD*::Km), Sm^r Km^r	This work
1021FDCSS	Rm1021 (Δ*fadD*::SmSp), Sm^r Sp^r	This work
Rm2011	SU47*expR102*::IS*Rm*2011-1, Sm^r	[60]
2011FDC	Rm2011 (Δ*fadD*::SmSp), Sm^r Sp^r	This work
SmA818	Rm2011 pSymA cured, Sm^r	[61]
A818FDC	SmA818 (Δ*fadD*::SmSp), Sm^r Sp^r	This work
2011rhbA62	Rm2011 (*rhbA*::Tn*5lac*), Sm^r Rif^r Nm^r	[30]
2011rhbAFDC	2011rhbA62 (Δ*fadD*::SmSp), Sm^r Sp^r Rif^r Nm^r	This work
2011rhbE11	Rm2011 (*rhbE*::Tn*5lac*), Sm^r Rif^r Nm^r	[30]
2011rhbEFDC	2011rhbE11 (Δ*fadD*::SmSp), Sm^r Sp^r Rif^r Nm^r	This work
2011rhrA26	Rm2011 (*rhrA*::Tn*5lac*), Sm^r Rif^r Nm^r	[30]
2011rhrAFDC	2011rhrA26 (Δ*fadD*::SmSp), Sm^r Sp^r Rif^r Nm^r	This work
2011rhtA1	Rm2011 (*rhtA*::Tn*5*), Sm^r Rif^r Nm^r	[30]
2011rhtAFDC	2011rhtA1 (Δ*fadD*::SmSp), Sm^r Sp^r Rif^r Nm^r	This work
G212rirA	Rm1021 (lac^-, *rirA*::Km), Sm^r Km^r	O'Connell, M.
G212rirAFDC	G212rirA (Δ*fadD*::SmSp), Sm^r Km^r	This work
Plasmids		
pBSKS(+)	Cloning vector; Ap^r	Stratagene
pHP45Ω	Plasmid containing Sm/Sp cassette; Ap^r, Sm^r, Sp^r	[62]
pHP45Ω Km	Plasmid containing Km cassette; Ap^r, Km^r	[63]
pK18*mobsacB*	Suicide plasmid; Km^r	[51]
pBBRD4	pBBR1 MCS-3 derivative containing the *fadD* gene of *S. meliloti* GR4; Tc^r	[16]
pBSDIL12	pBSKS derivative containing the *fadD* gene of *S. meliloti* GR4; Ap^r	This work
pBS12.6Km	pBSDIL12 in which the *fadD* gene has been deleted and interrupted with a Km cassette; Ap^r Km^r	This work
pK18fadDCKm	pK18*mobsacB* carrying the fadD mutated version of pBS12.6Km;	This work
pK18fadDCSS	pK18fadDCKm in which the Km cassette interrupting the *fadD* gene has been substituted by a Sm/Sp cassette	This work

iron. To test the ability to use oleate as sole carbon source, MM was used in which glutamate and mannitol were replaced with 2 mM NH_4Cl and 5 mM oleate, respectively. When required, antibiotics were added at the following final concentrations: for *E. coli*, streptomycin (Sm) 50 μg/ml, spectinomycin (Sp) 100 μg/ml, kanamycin (Km) 50 μg/ml, and ampicillin (Ap) 200 μg/ml; for *S. meliloti*, Sm 200 μg/ml, Km 200 μg/ml, rifampin (Rif) 100 μg/ml, and neomycin sulphate (Nm) 100 μg/ml. To improve reproducibility, all liquid cultures of *S. meliloti* were routinely initiated from glycerol stocks.

Construction of *S. meliloti fadD* mutants

The *fadD*$^-$ strain 1021FDC5 used in the microarray experiments was obtained by allelic exchange. A disrupted version of the *fadD* gene was constructed by deleting an internal fragment and inserting a kanamycin resistance cassette. Firstly, a *Kpn*I/*Xba*I fragment harbouring the *fadD* gene of *S. meliloti* was subcloned from pBBRD4 [16] into pBluescript to give pBSDIL12. After removal of a *Bam*HI site from the polylinker of pBSDIL12, an internal *Bam*HI fragment of 300 bp of the *fadD* gene was replaced with a 2.2 kb *Bam*HI fragment containing the Km^R cassette from pHP45Ω-Km to give pBS12.6Km. This construction was digested with *Kpn*I, treated with T4 DNA polymerase (Roche Biochemicals) to make blunt ends, and then digested with *Xba*I to isolate the Km^R fragment which was then cloned into the suicide vector pK18*mobsacB* previously digested with *Sma*I/*Xba*I, to give pK18fadDCKm. This plasmid was introduced by conjugation into *S. meliloti* 1021 and allele replacement events were selected as described previously [51].

The *fadD*$^-$ strain 1021FDCSS was obtained following the same procedure as for 1021FDC5 with the only difference that the Km^R cassette present in pK18fadDCKm was substituted by the Sm^R/Sp^R cassette from pHP45Ω to give pK18fadDCSS. The *fadD* mutation present in 1021FDCSS was transferred into different strain backgrounds by generalized transduction of 1021FDCSS using phage ôM12 as described previously [52]. All the different *fadD* mutants obtained were confirmed by Southern hybridization with a specific probe.

Swarming and swimming assays

Swarming assays were carried out as described in Soto *et al*. [16]. Briefly, *S. meliloti* cells grown in TY broth to late logarithmic phase (optical density (OD) at 600 nm = 1-1.2) were pelleted, washed twice in MM and resuspended in 0.1 volume of the latter medium. 2 μl aliquots of this bacterial suspension (ca. 2×10^7cells) were dispensed onto the surface of swarm plates and allowed to dry for 10 min. Swarm plates were prepared with 20 ml of MM containing 0.6% purified agar (Pronadisa), and air dried at room temperature for 15 min. Incubation periods of 14 to 20 h at 30°C, were enough to observe swarming. To complement swarming in rhizobactin-defective mutants, a concentrated supernatant containing rhizobactin 1021 was prepared as described by Lynch *et al*. [30] from wild-type strain Rm2011 grown to stationary phase in either TY broth with 200 μM 2, 2'-dipyridyl or MM broth with 2 μM 2, 2'-dipyridyl. Before its use in swarming assays, the presence of siderophore in the supernatants was checked in iron nutrition bioassays as described by Lynch *et al*. [30]. Two complementation approaches were used: 1) a well was cut in the center of a swarm plate and 100 μl of the rhizobactin containing supernatant was added. Aliquots of the wild type strain and rhizobactin-defective mutants prepared as described above were placed onto the surface of the swarm plate surrounding the well; 2) cells of the wild type strain and rhizobactin-defective mutants were grown in TY broth, pelleted, washed twice in MM and resuspended in 0.1 volume of the rhizobactin containing supernatant. Finally, 2 μl aliquots of this bacterial suspension were assayed for surface motility on swarm plates.

Swimming plates were prepared with either Bromfield medium (0.04% tryptone, 0.01% yeast extract, and 0.01% $CaCl_2.2H_2O$) containing 0.3% Bacto agar or with MM containing 0.3% purified agar. Plates were inoculated with 3 μl droplets of rhizobial cultures grown in TY, and incubated at 30°C for 2 to 5 days.

Determination of bacterial growth curves

Bacterial growth curves of *S. meliloti* 1021FDC5 were determined in liquid, semisolid (0.6% purified agar) and solid (1.3% purified agar) MM. A preinoculum was grown in 20 ml of TY broth to late logarithmic phase ($OD_{600\ nm}$ = 1-1.2). After incubation, cells were pelleted, washed twice in MM and resuspended in 2 ml of the latter medium. For growth curves in liquid MM, Erlenmeyer flasks (250 ml) containing 50 ml of liquid MM were inoculated with 0.5 ml of the rhizobial suspension (approximately 10^8 cells/ml) and incubated at 30°C with continuous shaking (190 r.p.m.). For growth curves in plates, aliquots of 0.1 ml of the rhizobial suspension were used to sow MM plates (approximately 10^9 cells/plate). This size of inoculum was used to ensure that on semisolid and solid MM plates, the same density of cells per surface area was applied as in standard swarming assays (10^7 cells per 0.2 cm^2). The rhizobial suspension was evenly spread over the surface of semisolid and solid MM plates, allowed to dry for 10 min and then inverted and incubated at 30°C. This sampling on plates was preferred over inoculation with droplets, to minimize heterogeneity among cells. Samples from liquid cultures and plates were collected at different time

points for cell count determination. Cells grown on plates were harvested by scraping the surface with 2 ml of sterile liquid MM.

RNA isolation and synthesis of labelled cDNA

For RNA isolation, cells from 18 ml of broth culture or grown on the surface of 3 plates were harvested, washed with sarkosyl 0.1% and cell pellets were immediately frozen in liquid nitrogen and conserved at -80°C until RNA isolation. For microarray hybridization and reverse transcription quantitative real-time PCR (RT-qPCR), RNA was isolated using the Qiagen RNeasy RNA purification kit (Qiagen) following the manufacturer's instructions. Residual DNA was removed with RNase-free Dnase I Set (ROCHE). The quality of the RNA was checked on 1.4% agarose gel electrophoresis.

Cy3- and Cy5-labelled cDNAs were prepared according to DeRisi *et al*. [53] from 15 μg of total RNA. Three slide hybridizations were performed using the labelled cDNA synthesized from each of the RNA preparations from three independent bacterial cultures.

Microarray hybridization, image acquisition and data analysis

Sm6koligo microarrays were purchased from A. Becker (University of Bielefeld, Bielefeld, Germany). Hybridizations were performed as described previously [21,37]. For image acquisition a GenePix 4100A Scanner (Axon Instruments, Inc., Foster City, CA, USA) was used. Quantifications of mean signal intensities for each spot were determined using the GenePix Pro 5.0 software (Axon Instruments, Inc.). Normalization and t-statistics were carried out using the EMMA 2.6 microarray data analysis software developed at the Bioinformatics Resource Facility Center for Biotechnology, Bielefeld University http://www.genetik.uni-bielefeld.de/EMMA/ [54]. Three independent biological replicates were performed for each experiment. Genes were regarded as differentially expressed if they showed $p \leq 0.05$, $A \geq 7$ and $M \geq 1$ or $M \leq -1$ (A, average signal to noise; M value is $\log_2$ experiment/control ratio) in any of the experiments performed. Detailed protocols and raw data resulting from the microarray experiments have been deposited in the ArrayExpress database with the accession number E-MEXP-1953.

Reverse transcription quantitative real-time PCR (RT-qPCR)

Total RNA (1 μg) treated with RNase-free Dnase I Set (ROCHE) was reversely transcribed using Superscript II reverse transcriptase (INVITROGEN) and random hexamers (ROCHE) as primers. Quantitative real-time PCR was performed on an iCycler iQ5 (Bio-Rad, Hercules, CA, USA). Each 25 μl reaction contained either 1 μl of the cDNA or a dilution (1:10.000, for amplification of the 16S rRNA gene), 200 nM of each primer and iQ SyBrGreen Supermix (BioRad). Control PCR reactions of the RNA samples not treated with reverse transcriptase were also performed to confirm the absence of contaminating genomic DNA. Samples were initially denatured by heating at 95°C for 3 minutes followed by a 35-cycle amplification and quantification program (95°C for 30 s, 55°C for 45 s, and 72°C for 45 s). A melting curve was conducted to ensure amplification of a single product. The oligonucleotide sequences for qPCR are listed in additional file 3. The efficiency for each primer pair (E) was determined by running 10-fold serial dilutions (4 dilution series) of Rm1021 genomic DNA as template and generating a standard curve by plotting the log of the dilution factor against the C_T value during amplification of each dilution. Amplification efficiency is calculated using the formula ($E = [10^{(1/a)}-1] \times 100$) where a is the slope of the standard curve.

The relative expression of each gene was normalized to that of 16 S rRNA and the analysis of results was done using the comparative critical threshold ($\Delta\Delta C_T$) method [55].

CAS siderophore assay

The determination of siderophores in liquid cultures was performed using the Chrome azurol S (CAS) assay solution described by Schwyn and Neilands [56]. Supernatants of *S. meliloti* cultures grown in MM containing different concentrations of $FeCl_3$ were mixed 1:1 with the CAS assay solution. After reaching equilibrium, the absorbance was measured at 630 nm.

Additional file 1: Genes differentially expressed in response to surface growth and/or swarming-specific conditions in *S. meliloti* 1021FDC5. Tabular data (.xls) list the 1166 genes showing differential expression in any of the six comparisons performed in this study. Only M values above 1 or below -1 with $p \leq 0.05$ are shown. The category in the Venn diagram (A-G in Fig. 4) to which each gene belongs is also indicated. **L**, growth in **l**iquid MM; **S**, growth on **s**olid MM (1.3% agar); **SS**, growth on **s**emi **s**olid MM (0.6% agar). Time of incubation is shown in parenthesis.
Click here for file
[http://www.biomedcentral.com/content/supplementary/1471-2164-11-157-S1.XLS]

Additional file 2: Swarming-responsive genes identified in *S. meliloti* 1021FDC5. Tabular data (.xls) list the 294 genes showing differential expression in response to swarming-specific conditions. Only M values above 1 or below -1 with $p \leq 0.05$ are shown. The category in the Venn diagram (A-G in Fig. 4) to which each gene belongs is also indicated. **L**, growth in **l**iquid MM; **S**, growth on **s**olid MM (1.3% agar); **SS**, growth on **s**emi **s**olid MM (0.6% agar). Time of incubation is shown in parenthesis.
Click here for file
[http://www.biomedcentral.com/content/supplementary/1471-2164-11-157-S2.XLS]

Additional file 3: Sequences of the oligonucleotides used for quantitative real-time PCR. Table of data.
Click here for file
[http://www.biomedcentral.com/content/supplementary/1471-2164-11-157-S3.DOC]

Abbreviations

AHL: N-acyl-homoserine lactones; TTSS: type III secretion system; MM: minimal medium; EPS: exopolysaccharide; RT-qPCR: reverse transcription-quantitative polymerase chain reaction; (Sm): Streptomycin; (Sp): Spectinomycin; (Km): Kanamycin; (Ap): Ampicillin; (Rif): Rifampin; (Nm): Neomycin sulphate; OD: optical density; CAS: Chrome azurol S.

Acknowledgements

We thank Dr M. Hynes and Dr. M. O'Connell for providing several strains used in this work. JN was supported by a postdoctoral contract (Consejería de Innovación, Ciencia y Empresa, Junta de Andalucía). This work was supported by a FPI fellowship from MICINN to CVA-G, and by grants BIO2007-62988 and CVI 03541 to MJS.

Authors' contributions

JN and AD-F performed experiments, analyzed data and participated in the writing of the manuscript. PvD performed experiments and contributed to the writing. CVA-G and VC performed experimental work. JS and JO helped to coordinate the study and contributed to the writing. MJS designed research, analyzed data and wrote the manuscript. All authors have read and approved the final manuscript.

Received: 16 September 2009 Accepted: 8 March 2010
Published: 8 March 2010

References

1. Fraser GM, Hughes C: **Swarming motility.** *Curr Opin Microbiol* 1999, **2**:630-635.
2. Harshey RM: **Bacterial motility on a surface: many ways to a common goal.** *Annu Rev Microbiol* 2003, **57**:249-273.
3. Rather PN: **Swarmer cell differentiation in *Proteus mirabilis* .** *Environ Microbiol* 2005, **7**:1065-1073.
4. Verstraeten N, Braeken K, Debkumari B, Fauvart M, Fransaer J, Vermant J, Michiels J: **Living on a surface: swarming and biofilm formation.** *Trends Microbiol* 2008, **16**:496-506.
5. Kim W, Surette MG: **Metabolic differentiation in actively swarming *Salmonella*.** *Mol Microbiol* 2004, **54**:702-714.
6. Wang Q, Frye JG, McClelland M, Harshey RM: **Gene expression patterns during swarming in *Salmonella typhimurium* : genes specific to surface growth and putative new motility and pathogenicity genes.** *Mol Microbiol* 2004, **52**:169-187.
7. Inoue T, Shingaki R, Hirose S, Waki K, Mori H, Fukui K: **Genome-wide screening of genes required for swarming motility in *Escherichia coli* K-12.** *J Bacteriol* 2007, **189**:950-957.
8. Overhage J, Lewenza S, Marr AK, Hancock RE: **Identification of genes involved in swarming motility using a *Pseudomonas aeruginosa* PAO1 mini-Tn *5* - *lux* mutant library.** *J Bacteriol* 2007, **189**:2164-2169.
9. Overhage J, Bains M, Brazas MD, Hancock REW: **Swarming of *Pseudomonas aeruginosa* is a complex adaptation leading to increased production of virulence factors and antibiotic resistance.** *J Bacteriol* 2008, **190**:2671-2679.
10. Eberl L, Christiansen G, Molin S, Givskov M: **Differentiation of *Serratia liquefaciens* into swarm cells is controlled by the expression of the *flhD* master operon.** *J Bacteriol* 1996, **178**:554-559.
11. Lai S, Tremblay J, Déziel E: **Swarming motility: a multicellular behaviour conferring antimicrobial resistance.** *Environ Microbiol* 2009, **11**:126-136.
12. Gibson KE, Kobayashi H, Walker GC: **Molecular determinants of a symbiotic chronic infection.** *Annu Rev Genet* 2008, **42**:413-441.
13. Oldroyd GED, Downie JA: **Coordinating nodule morphogenesis with rhizobial infection in legumes.** *Annu Rev Plant Biol* 2008, **59**:519-546.
14. Soto MJ, Sanjuán J, Olivares J: **Rhizobia and plant-pathogenic bacteria: common infection weapons.** *Microbiology* 2006, **152**:3167-3174.
15. Soto MJ, Domínguez-Ferreras A, Pérez-Mendoza D, Sanjuán J, Olivares J: **Mutualism *versus* pathogenesis: the give-and-take in plant-bacteria interactions.** *Cell Microbiol* 2009, **11**:381-388.
16. Soto MJ, Fernández-Pascual M, Sanjuán J, Olivares J: **A *fadD* mutant of *Sinorhizobium meliloti* shows multicellular swarming migration and is impaired in nodulation efficiency on alfalfa roots.** *Mol Microbiol* 2002, **43**:371-382.
17. Daniels R, Vanderleyden J, Michiels J: **Quorum sensing and swarming migration in bacteria.** *FEMS Microbiol Rev* 2004, **28**:261-289.
18. Daniels R, Reynaert S, Hoekstra H, Verreth C, Janssens J, Braeken K, Fauvart M, Beullens S, Heusdens C, Lambrichts I, De Vos DE, Vanderleyden J, Vermant J, Michiels J: **Quorum signals molecules as biosurfactants affecting swarming in *Rhizobium etli*.** *Proc Natl Acad Sci USA* 2006, **103**:14965-14970.
19. Braeken K, Daniels R, Vos K, Fauvart M, Bachaspatimayum D, Vanderleyden J, Michiels J: **Genetic determinants of swarming in *Rhizobium etli*.** *Microbial Ecol* 2008, **55**:54-64.
20. van Dillewijn P, Sanjuán J, Olivares J, Soto MJ: **The *tep1* gene of *Sinorhizobium meliloti* coding for a putative transmembrane efflux protein and N-acetyl glucosamine affect *nod* gene expression and nodulation of alfalfa plants.** *BMC Microbiol* 2009, **9**:17.
21. Krol E, Becker A: **Global transcriptional analysis of the phosphate starvation response in *Sinorhizobium meliloti* strains 1021 and 2011.** *Mol Genet Genomics* 2004, **272**:1-17.
22. Galibert F, *et al*: **The composite genome of the legume symbiont *Sinorhizobium meliloti*.** *Science* 2001, **293**:668-672.
23. Gao M, Chen H, Eberhard A, Gronquist MR, Robinson JB, Rolfe BG, Bauer WD: ***sinI* - and *expR* -dependent quorum sensing in *Sinorhizobium meliloti*.** *J Bacteriol* 2005, **187**:7931-7944.
24. Bahlawane C, McIntosh M, Krol E, Becker A: ***Sinorhizobium meliloti* regulator MucR couples exopolysaccharide synthesis and motility.** *Mol Plant Microbe Interact* 2008, **21**:1498-1509.
25. Pellock BJ, Teplitski M, Boinay RP, Bauer WD, Walker GC: **A LuxR homolog controls production of symbiotically active extracellular polysaccharide II by *Sinorhizobium meliloti*.** *J Bacteriol* 2002, **184**:5067-5076.
26. Davalos M, Fourment J, Lucas A, Bergès H, Kahn D: **Nitrogen regulation in *Sinorhizobium meliloti* probed with whole genome arrays.** *FEMS Microbiol Lett* 2004, **241**:33-40.
27. Becker A, Fraysse N, Sharypova L: **Recent advances in studies on structure and symbiosis-related function of rhizobial K-antigens and lipopolysaccharides.** *Mol Plant-Microbe Interact* 2005, **18**:899-905.
28. Sourjik V, Muschler P, Scharf B, Schmitt R: **VisN and VisR are global regulators of chemotaxis, flagellar, and motility genes in *Sinorhizobium* (*Rhizobium*) *meliloti* .** *J Bacteriol* 2000, **182**:782-788.
29. Rotter C, Mühlbacher S, Salamon D, Schmitt R, Scharf B: **Rem, a new transcriptional activator of motility and chemotaxis in *Sinorhizobium meliloti* .** *J Bacteriol* 2006, **188**:6932-6942.
30. Lynch D, O'Brien J, Welch T, Clarke P, Cuiv PO, Crosa JH, O'Connell M: **Genetic organization of the region encoding regulation, biosynthesis, and transport of rhizobactin 1021, a siderophore produced by *Sinorhizobium meliloti*.** *J Bacteriol* 2001, **183**:2576-2585.
31. Ó Cuív P, Clarke P, Lynch D, O'Connell M: **Identification of *rhtX* and *fptX*, novel genes encoding proteins that show homology and function in the utilization of the siderophores rhizobactin 1021 by *Sinorhizobium meliloti* and pyochelin by *Pseudomonas aeruginosa*, respectively.** *J Bacteriol* 2004, **186**:2996-3005.
32. Challis GL: **A widely distributed bacterial pathway for siderophore biosynthesis independent of nonribosomal peptide synthetases.** *ChemBioChem* 2005, **6**:601-611.
33. Wexler M, Yeoman KH, Stevens JB, de Luca NG, Sawers G, Johnston AWB: **The *Rhizobium leguminosarum tonB* gene is required for the uptake of siderophore and haem as sources of iron.** *Mol Microbiol* 2001, **41**:801-816.
34. Battistoni F, Platero R, Duran R, Cerveñansky C, Battistoni J, Arias A, Fabiano E: **Identification of an iron-regulated, hemin-binding outer membrane protein in *Sinorhizobium meliloti*.** *Appl Environ Microbiol* 2002, **68**:5877-5881.
35. Ó Cuív P, Keogh D, Clarke P, O'Connell M: **The *hmuUV* genes of *Sinorhizobium meliloti* 2011 encode the permease and ATPase components of an ABC transport system for the utilization of both haem and the hydoxamate siderophores, ferrichrome and ferrioxamine B.** *Mol Microbiol* 2008, **70**:1261-1273.

36. Wandersman C, Delepelaire P: **Bacterial iron sources: from siderophores to hemophores.** *Annu Rev Microbiol* 2004, **58**:611-647.
37. Domínguez-Ferreras A, Pérez-Arnedo R, Becker A, Olivares J, Soto MJ, Sanjuán J: **Transcriptome profiling reveals the importance of plasmid pSymB for osmoadaptation of *Sinorhizobium meliloti*.** *J Bacteriol* 2006, **188**:7617-7625.
38. Hellweg C, Pühler A, Weidner S: **The time course of the transcriptomic response of *Sinorhizobium meliloti* 1021 following a shift to acidic pH.** *BMC Microbiol* 2009, **9**:37.
39. Yao SY, Luo L, Har KJ, Becker A, Rüberg S, Yu GQ, Zhu JB, Cheng HP: ***Sinorhizobium meliloti* ExoR and ExoS proteins regulate both succinoglycan and flagellum production.** *J Bacteriol* 2004, **186**:6042-6049.
40. Gibson KE, Barnett MJ, Toman CJ, Long SR, Walker GC: **The symbiosis regulator CbrA modulates a complex regulatory network affecting the flagellar apparatus and cell envelope proteins.** *J Bacteriol* 2007, **189**:3591-3602.
41. Hoang HH, Gurich N, González JE: **Regulation of motility by the ExpR/Sin quorum sensing system in *Sinorhizobium meliloti*.** *J Bacteriol* 2008, **190**:861-871.
42. Chao TC, Buhrmester J, Hansmeier N, Pühler A, Weidner S: **Role of the regulatory gene *rirA* in the transcriptional response of *Sinorhizobium meliloti* to iron limitation.** *Appl Environ Microbiol* 2005, **71**:5969-5982.
43. Viguier C, Ó Cuív P, Clarke P, O'Connell M: **RirA is the iron response regulator of the rhizobactin 1021 biosynthesis and transport genes in *Sinorhizobium meliloti* 2011.** *FEMS Microbiol Lett* 2005, **246**:235-242.
44. Matilla MA, Ramos JL, Duque E, Alché JD, Espinosa-Urgel M, Ramos-González MI: **Temperature and pyoverdine-mediated iron acquisition control surface motility of *Pseudomonas putida*.** *Environ Microbiol* 2007, **9**:1842-1850.
45. Persmark M, Pittman P, Buyer JS, Schwyn B, Gill PR Jr, Neilands JB: **Isolation and structure of rhizobactin 1021, a siderophore from the alfalfa symbiont *Rhizobium meliloti* 1021.** *J Am Chem Soc* 1993, **115**:3950-3956.
46. McCarter L, Silverman M: **Iron regulation of swarmer cell differentiation of *Vibrio parahaemolyticus*.** *J Bacteriol* 1989, **171**:731-736.
47. Déziel E, Lépine F, Milot S, Villemur R: ***rhlA* is required for the production of a novel biosurfactant promoting swarming motility in *Pseudomonas aeruginosa* :3-(3-hydroxyalkanoylosy) alkanoic acids (HAAs), the precursors of rhamnolipids.** *Microbiology* 2003, **149**:2005-2013.
48. Sambrook J, Fritsch EF, Maniatis T: *Molecular cloning: A laboratory manual* Cold Spring Harbor Laboratory Press, Cold Spring Harbor N. Y, 2 1989.
49. Beringer JE: **R factor transfer in *Rhizobium leguminosarum*.** *J Gen Microbiol* 1974, **84**:188-198.
50. Robertsen BK, Aiman P, Darwill AG, Mcneil M, Albersheim P: **The structure of acidic extracellular polysaccharides secreted by *Rhizobium leguminosarum* and *Rhizobium trifolii* .** *Plant Physiol* 1981, **67**:389-400.
51. Schäfer A, Tauch A, Jäger W, Kalinowski J, Thierbach G, Pühler A: **Small mobilizable multi-purpose cloning vectors derived from the *Escherichia coli* plasmids pK18 and pK19: selection of defined deletions in the chromosome of *Corynebacterium glutamicum*.** *Gene* 1994, **145**:69-73.
52. Finan TM, Hartwieg E, LeMieux K, Bergman K, Walker GC, Signer ER: **General transduction in *Rhizobium meliloti*.** *J Bacteriol* 1984, **159**:120-124.
53. DeRisi JL, Iyer VR, Brown PO: **Exploring the metabolic and genetic control of gene expression on a genomic scale.** *Science* 1997, **278**:680-686.
54. Dondrup M, Goesmann A, Bartels D, Kalinowski J, Krause L, Linke B, Rupp O, Sczyrba A, Pühler A, Meyer F: **EMMA: a platform for consistent storage and efficient analysis of microarray data.** *J Biotechnol* 2003, **106**:135-146.
55. Pfaffl MW: **A new mathematical model for relative quantification in real-time RT-PCR.** *Nucleic Acids Res* 2001, **29**:e45.
56. Schwyn B, Neilands JB: **Universal chemical assay for the detection and determination of siderophores.** *Anal Biochem* 1987, **160**:47-56.
57. Simon R, Priefer U, Pühler A: **A broad host range mobilization system for *in vivo* genetic-engineering: transposon mutagenesis in Gram-negative bacteria.** *Biotech* 1983, **1**:784-791.
58. Casadesús J, Olivares J: **Rough and fine linkage mapping of the *Rhizobium meliloti* chromosome.** *Mol Gen Genet* 1979, **174**:203-209.
59. Meade HM, Signer ER: **Genetic mapping of *Rhizobium meliloti*.** *Proc Natl Acad Sci USA* 1977, **74**:2076-2078.
60. Casse F, Boucher C, Julliot JS, Michel M, Denarié J: **Identification and characterization of large plasmids in *Rhizobium meliloti* using agarose-gel electrophoresis.** *J Gen Microbiol* 1979, **113**:229-242.
61. Oresnik IJ, Liu SL, Yost CK, Hynes MF: **Megaplasmid pRme2011a of *Sinorhizobium meliloti* is not required for viability.** *J Bacteriol* 2000, **182**:3582-3586.
62. Prentki P, Krisch HM: ***In vitro* insertional mutagenesis with a selectable DNA fragment.** *Gene* 1984, **29**:303-312.
63. Fellay R, Frey J, Krisch H: **Interposon mutagenesis of soil and water bacteria: A family of DNA fragments designed for in vitro insertional mutagenesis of Gram negative bacteria.** *Gene* 1987, **52**:147-154.

doi:10.1186/1471-2164-11-157
Cite this article as: Nogales *et al.*: Transcriptome profiling of a *Sinorhizobium meliloti fadD* mutant reveals the role of rhizobactin 1021 biosynthesis and regulation genes in the control of swarming. *BMC Genomics* 2010 **11**:157.